Interspecific behavioural interference and range dynamics: genomic analysis of rubyspot damselflies

CHRISTOPHE WILLIAM PATTERSON

Interspecific behavioural interference and range dynamics: genomic analysis of rubyspot damselflies

Christophe William Patterson

Submitted for the degree of Doctor of Philosophy

Department of Biosciences

Durham University

2024

Authors declaration

The material contained within this thesis has not previously been submitted for a degree at Durham University or any other university. The research reported within this thesis has been conducted by the author unless indicated otherwise.

Chapter 2 has already been published in full as Patterson, C.W. & Drury, J.P. (2023) Interspecific behavioural interference and range dynamics: current insights and future directions. *Biological Reviews* **98**, 2012–2027.

Chapter 3 has already been published in full as Patterson, C.W., Bonillas-Monge, E., Brennan, A., Grether, G.F., Mendoza-Cuenca, L., Tucker, R., Vega-Sánchez, Y.M. & Drury, J. (2023) A chromosome-level genome assembly for the smoky rubyspot damselfly (Hetaerina titia). *Journal of Heredity*, esad070.

Christophe William Patterson

May 2024

Thesis abstract

The ongoing reshuffle of Earth's biota, particularly from climate change, has increased the necessity to understand and predict how the spatial distribution of species can shift. In this thesis, I further our knowledge of the processes that influences the ranges of species by conducting novel research into the how interspecific behavioural interference affects range dynamics. Interspecific behavioural interference is any aggressive or mating behaviour by one species that is directed towards and has a negative impact on the fitness of another. I primarily using next-generation sequence data to conduct phylogenetic, phylogeographic, and population genetic analysis on rubyspot damselflies (*Hetaerina).* The research focuses on smoky rubyspot damselflies (*Hetaerina titia*) which exhibit a striking seasonal polyphenism in wing colouration which influences the degree of interspecific behavioural interference seen between individuals and populations. Chapter 2 provides a synthesis of past research into how interspecific behavioural interference affects range dynamics across taxa and then outlines potential future avenues of research. Chapter 3 presents a de-novo chromosome level draft genome of *H. titia* which is the first chromosome level draft genome for a broad winged damselfly (Calopterygidae). Chapter 4 determines the spatiotemporal dynamics of the speciation cycle across several species of *Hetaerina* supporting the hypothesis that time since divergence predicts the stage of the non-ecological speciation cycle. Genetic sequencing identifies a region of secondary contact between two lineages of *H. titia* separated by an estimated 3.6 million years. One individual is identified as an F_1 hybrid, suggesting that reproductive isolation exists between Pacific and Atlantic lineages of smoky rubyspot. Chapter 5 uses multivariate models of trait evolution to test for co-evolution between the peak and off-peak seasonal phenotype of *H. titia.* Models do not support co-evolution but do support different selective regimes in different geographic regions. Finally, Chapter 6, uses population genetics and species distribution models to show that populations of *H. titia* that reside in higher latitudes likely originate from a range expansion from Florida since the last glacial maximum (LGM). Consequently, the loss of polyphenism in high latitude populations may be an adaptation to novel species assemblies that arose since the LGM. Collectively, this thesis provides novel research into the ecological and evolutionary consequences of interspecific behavioural interference, particularly into spatial and temporal dynamics of species distributions.

Table of Contents

Acknowledgements

This thesis would not have been possible without the support of my friends, family, and colleagues. First and foremost, I need to thank my primary supervisor Dr Jonathan Drury who has provided me with continuous support and guidance throughout my doctoral studies. I am immensely grateful to have had such a supportive, kind, and knowledgeable mentor and I hope to far into the future. I am also lucky to have had the support of my co-supervisor Dr Adrian Brennan whose expertise and advice were invaluable throughout. I have also had the kind support and mentorship of many other academics especially Dr Wayne Dawson and Dr Regan Early.

I am also very grateful to my examiners Dr. Andreanna Welch and Dr. Lesley Lancaster who made my viva an enriching and enjoyable experience.

During my time as a PhD candidate, I have had the joy of meeting and working with many *many* talented, hard-working, and supportive peers. I am particularly grateful to the cohort of PhD candidates who started their studies with me during the depths of the covid-19 pandemic. Ellie Ward, Tom Smart, Beth Gillie, Laura Campbell, Matt Quin, and Rachel McConnell provided me friendship and sanity during such an uncertain and difficult time. My time working towards my PhD was made immeasurably better by many others, including Alex Goodridge, Katy Ivison, Bethany Jetson, Dan Nesbit, Alice Oswald, Cam Goodhead, Alison Copeland, Charlotte Sharpe, Lucy, Eladio, Pierre Tichit, Madda Aase-Remedios, Rachel Dobson, Kieran Lawrence, Sian Green, Jonathan Rees, Ariane Dellavalle and everyone else who was a friend along the way however briefly.

Many people work behind the scenes supporting PhD research. I'd like to thank Emma Robinson who provides invaluable help on a daily basis to PhD candidates across the department. Karen Bower, at ARC, without whom I would not have got multiple computer programs working and the research in this thesis would be considerably reduced. The training provided to me by the NEOF team, especially Gavin Horsburgh, was also crucial for getting to grips with the laboratory and bioinformatics skills required to conduct this research.

I am lucky to have the continued support of my old friends, Jamie Macintosh, Victoria Hoare, Rowen Hawkes, Natalie Barron, Hebe Carmichael, Rachel Haynes, Emma Smith, Dr. Ben Holt and many more.

My ability to undertake a PhD was not possible without my Mum and Dad who instilled in me the value of education from when I was little and have supported my curiosity all my life. My two sisters Hannah and Katrina are awesome and are doing equally amazing things out in the "real" world.

For the second time, the acknowledgements of my thesis must end by thanking the endless support of my partner, Holly. I am infinitely thankful for the fact that you moved across the country to support me. We moved during a pandemic, and we had all our possessions stolen along the way, it was a hard time for us both. I could not have had the resilience to keep working towards this thesis without you. Thank you.

Chapter 1 General Introduction

A smoky rubyspot damselfly, *Hetaerina titia,* from Tuxtla Gutiérrez, Chiapas, Mexico. (16°39'10.2"N, 93°09'22.6"W). Rubyspot damselflies (*Hetaerina*) have mostly clear wings, but males exhibit red basal spots. Smoky rubyspots, like this individual, can have varying degrees of melanisation across their wings.

Introduction

Ecosystems comprise complex networks of interactions between and within different species. Interactions between species are a driving force for shaping the world's biodiversity. Research into the ecological and evolutionary consequences of interspecific biotic interactions has predominantly focused on trophic interactions or exploitative competition between species of similar ecological niches. [e.g. the evolution of predator defences (Reimchen, 1994), the never-ending evolutionary race between hosts and parasites (Decaestecker *et al.*, 2007), and the partitioning of foraging niches (MacArthur, 1958)]. Separately, studies on intraspecific biotic interactions have shown clear evolutionary consequences of courtship and territoriality (Wiley, 1978; Andersson, 1989; Ah-King, Kvarnemo & Tullberg, 2005). However, courtship and territoriality are not limited to intraspecific interactions (Gröning *et al.*, 2007; Peiman & Robinson, 2010; Grether *et al.*, 2017). Interspecific courtship, mating, and territoriality occurs across a wide range of taxa and have both evolutionary and ecological consequences (Grether *et al.*, 2017).

During speciation, intraspecific social signals are often evolutionary constrained or under stabilising selection (de Kort & ten Cate, 2001; Gröning *et al.*, 2007; Grether *et al.*, 2017). Consequently, closely related species often have similar social signals and engage in behavioural interactions, such as interspecific courtship and territoriality (Gröning *et al.*, 2007; Grether *et al.*, 2017; Patterson & Drury, 2023). Any aggressive or mating behaviour by one species that is directed towards and has a negative impact on the fitness of another species is referred to as *interspecific behavioural interference* (Grether *et al.*, 2017).

Interspecific behavioural interference has direct consequences on the evolution and distribution of Earth's biodiversity, such as causing reproductive and antagonistic character displacement (Gröning & Hochkirch, 2008; Grether *et al.*, 2009; Pfennig & Pfennig, 2012). However, for a number of reasons, interspecific behavioural interference can persist over long evolutionary timescales (Grether *et al.*, 2017). For instance, increased mate discrimination can decrease both intraspecific and interspecific mating attempts, reducing an individual's total number of successful copulations (Takakura, Nishida & Iwao, 2015) Additionally, poor species recognition means heterospecific share the same pool of potential mates, which drives selection for interspecific territoriality, meaning similar antagonistic signals can be maintained or

converge (Drury *et al.*, 2015b). Thus, many species engage in interspecific behavioural interference, and this includes species that stably coexist

Although interspecific behavioural interference can occur in stably coexisting species, interspecific behavioural interference can also prevent species co-existence and alter population dynamics (Iritani & Noriyuki, 2021; Grether & Okamoto, 2022; Irwin & Schluter, 2022). Theory is now backed up by several empirical studies. On the Isle of Öland in Baltic Sea, pied flycatchers, *Ficedula hypoleuca*, are driven to use sub-optimal habitat by the high aggression of collared flycatchers, *Ficedula albicollis* (Vallin *et al.*, 2012). In Highlands of Thailand, white-handed gibbons (*Hylobates lar*) and pileated gibbons (*Hylobates pileatus*) have a parapatric range boundary. Interspecific territoriality between the species of gibbon reinforces the range boundary by limiting dispersal and, possibly, decreases the frequency of hybridisation (Asensio *et al.*, 2017). Thus, interspecific behavioural interference is likely to have important impacts on range dynamics.

In recent decades, understanding the causes and drivers of species distribution has shifted from a purely scientific pursuit to an urgent practical necessity. Anthropogenic emissions of greenhouse gases are shifting the Earth's climate and having significant consequences for global distribution of biodiversity. Evidence for the distribution of species tracking with the changing climate first appeared in the late 1990's (Parmesan *et al.*, 1999; Parmesan & Yohe, 2003) and is now observed across terrestrial (Mair *et al.*, 2014; Auld *et al.*, 2022) and marine ecosystems (Hawkins *et al.*, 2008; Yamano, Sugihara & Nomura, 2011; Burrows *et al.*, 2020). However, climate is not the only factor that influences species ranges and recent research has focused on understanding how biotic interactions limit or facilitate range dynamics (Blois *et al.*, 2013; Ockendon *et al.*, 2014; Alexander, Diez & Levine, 2015; Early & Keith, 2019). However, research has focused on inter trophic interactions of exploitative competition (Svenning *et al.*, 2014; Louthan, Doak & Angert, 2015; Early & Keith, 2019; Legault *et al.*, 2020; Ortego & Knowles, 2020; Sirén & Morelli, 2020). The notion that interspecific behavioural interference can influence range dynamics remains less widely studied known and understood (Grether *et al.*, 2017).

The research presented within this thesis focuses on how interspecific behavioural interference has been a mechanism for shaping the spatial distribution of biodiversity on Earth. Specifically, I investigate whether varying levels of interspecific

behavioural interference has influenced the geographic distribution and range dynamics of *Hetaerina* or the rubyspot damselflies.

Hetaerina damselflies

The genus *Hetaerina* consists of around 39 species of damselflies (Garrison, 1990; Standring *et al.*, 2022). *Hetaerina* are known as rubyspot damselflies because of the characteristic basal red spot on males' wings. Species of *Hetaerina* occur in North, South, and Central America from Southern Canada to Argentina. Standring *et al.*, (2022) estimated that crown age for *Hetaerina* is 36 million years ago and that the genera of *Ormenophlebia* and *Mnesarete* are nested, polyphyletically, within the same clade.

Many species of *Hetaerina* co-occur with other *Hetaerina* species and interspecific reproductive interference and interspecific territoriality are widespread. Across all species of *Hetaerina*, adult males compete for mating territories which typically cover 1-2m^2 of fast flowing river. Female *Hetaerina* are phenotypically similar and, where species are found in sympatry, interspecific mating attempts are frequent (Drury *et al.*, 2019a). Female *Hetaerina* likely incur a substantial cost due to the wasted time and energy engaging with heterospecific males. However, *Hetaerina* males are unable to discriminate between conspecific and heterospecific females so are likely to miss conspecific mating opportunities if they do not respond to *Hetaerina* females entering their territory. The indiscriminate mating attempts by *Hetaerina* males means heterospecific males are in competition for the same pool of potential mates. Reproductive character displacement does not occur because any change to the female phenotype or male mate recognition reduces the number of conspecific mating successes in addition to a reduction in congener mating attempts. Male mate recognition does not evolve before the female phenotype and the female phenotype does not evolve before male mate recognition (Drury *et al.*, 2019a). Consequently, interspecific territorially is an adaptive response to reproductive interference (Drury *et al.*, 2015b, 2019a; Grether *et al.*, 2020). Male wing colouration plays a major role in male competitor recognition and, as a result, species pairs show varying levels of interspecific aggression (Anderson & Grether, 2010b).

Smoky rubyspots (*Hetaerina titia*)

The majority of *Hetaerina* damselflies have transparent wings, with males exhibiting a basal red spot on their wings. Smoky rubyspots (*Hetaerina titia*) exhibit a striking seasonal polyphenism in wing colouration (Drury *et al.*, 2019b) Throughout the

year, *H. titia* vary in wing colouration (Drury *et al.*, 2019b). *H. titia* that emerge during the peak breeding season have a higher proportion of black wing pigmentation (Figure 1:1a) than individuals that emerge later or earlier in the year (Figure 1:1b). Yet populations from Pacific drainages and the highest latitudes of North America have a much reduced seasonal variation, with overall lower levels of melanisation than seen in other populations (Drury *et al.*, 2019b). The adult life stage of *H. titia* lives for a few weeks so over the year the population of *H. titia* is repeatedly replaced by newly emerging individuals. As the degree of melanisation laid down at emergence changes, there is a marked shift in the average phenotype of the population (Figure 1:2).

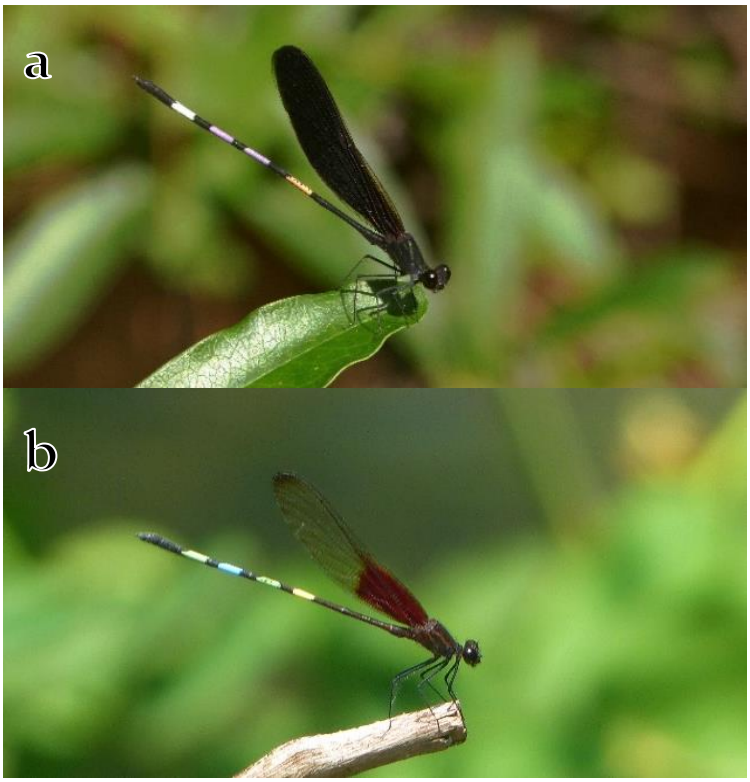

Figure 1:1: Two perched smoky rubyspots, *Hetaerina titia,* showing the striking variation in wing pigmentation. **(a)** A male *H. titia* with high levels of wing melanisation that are found in river basins that drain into the Gulf of Mexico and Caribbean during the peak breeding season. **(b)** A male *H. titia* with low levels of wing melanisation which are found throughout the species range. (Photo credit with permission J.P. Drury).

Individuals of *H. titia* with a higher proportion of black wing pigmentation are less likely to engage in interspecific conflict (Anderson & Grether, 2011; Drury, Anderson & Grether, 2015a) It is, therefore, proposed that the pigmentation of *H. titia* is an adaptation that reduces the level of interspecific interference from male *Hetaerina* heterospecifics (Drury *et al.*, 2015a). The benefits of reduced interspecific interference

potentially outweigh the risk of predation and metabolic costs of producing and displaying melanin wings during the peak breeding season.

Smoky rubyspot and other *Hetaerina* damselflies provide an opportunity to investigate in depth how varying levels of interspecific behavioural interference between species, and varying levels of interspecific behavioural interference seen between populations of the same species, can impact the range dynamics. Due to lower levels of behavioural interference, melanised *H. titia* should be able to establish in novel stream systems at a low density and subsequently increase in number more rapidly than non-melanised *H. titia* and other *Hetaerina* damselflies. Populations of congeners and low-level-melanised *H. titia*, however, are likely unable to propagate across the landscape at low densities because of the higher levels of interspecific interference, owing to the phenotypic similarity and consequent behavioural interference of other *Hetaerina* damselflies.

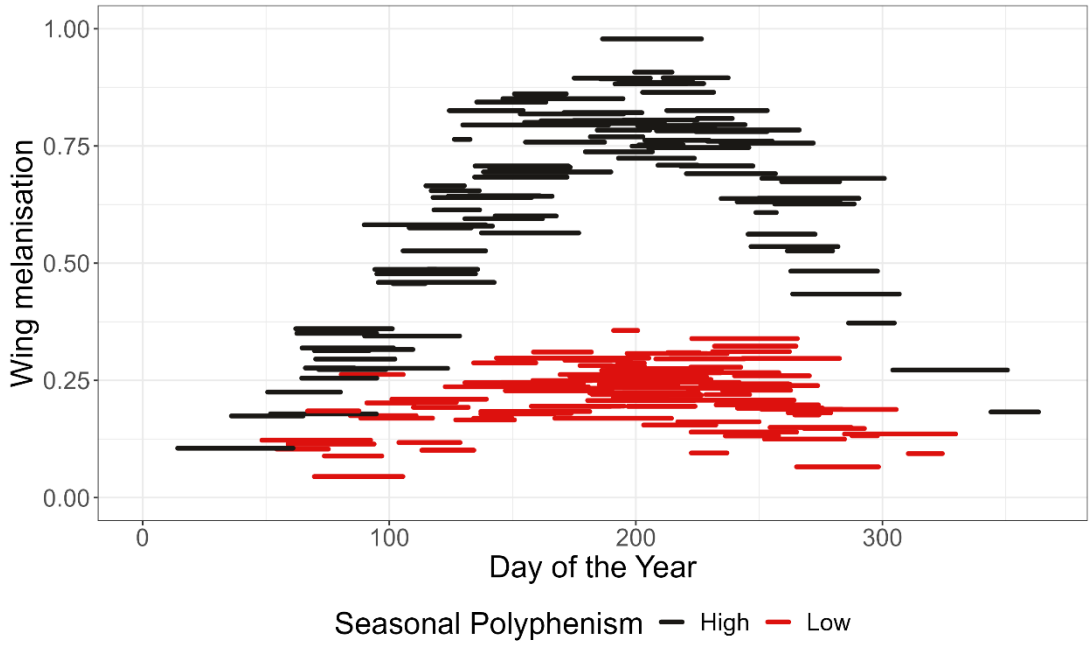

Figure 1:2: An illustrative example of distribution of wing melanisation seen in individuals across the year in two different populations of smoky rubyspot (*Hetaerina titia*). One population with a high degree of seasonal polyphenism (black) and another population with a low degree of seasonal polyphenism (red). Each line segment marks the life span of an adult *H. titia* and the degree of melanisation for that specific individual. Adult wing melanisation does not change after emergence but over the year the average phenotype of the population changes.

Overview

This thesis consists of five research chapters: one systematic literature review and four empirical research papers.

In Chapter 2, I undertake a systematic literature review to outline the theoretical and empirical research into where interspecific behavioural interference has been shown to influence the spatial distribution of species. The factors that affect ranges of species are of significant interest due to ongoing anthropogenic reshuffling of the Earth's biota. Biotic interactions are one such factor of interest but interspecific behavioural interference, despite being prevalent across taxa (Gröning *et al.*, 2007; Grether *et al.*, 2017), is often missing from macroecological studies on species ranges. Here, I present the theory and empirical evidence that interspecific behavioural interference can be an important factor in influencing the spatial extent of a species, and consequently should be included within research investigating how biotic interactions limit species distributions.

In later chapters, I undertake empirical research to understand the evolution and range dynamics of *Hetaerina* damselflies, with a particular focus on smoky rubyspots (*H. titia*). The main body of research uses genomic sequence data from double digest restriction enzyme associated DNA – ddRAD (Peterson *et al.*, 2012; Franchini *et al.*, 2017). To support and enhance my own, and future, genomic research, in Chapter 3, I assemble a chromosome-scale draft genome of *H. titia.* In later chapters, the draft genome directly enables greater inference by enabling the mapping of sequences to specific regions of the genome - specially by allowing distinction between SNPs on autosomal and sex chromosomes.

In Chapter 4, I investigate the spatial and temporal dynamics of divergence among *Hetaerina* damselflies. Damselflies are a noted example of non-ecological radiations where lineages become reproductively isolated but differ little in ecology even when in sympatry (Wellenreuther & Sánchez-Guillén, 2016). Using genomic data from hundreds of individuals across three currently recognised species (*H. titia*, *H. americana*, and *H. calverti*), we determine the spatiotemporal dynamics of speciation within and between lineages of a non-adaptive radiation. At a site of secondary contact, we identify an F_1 hybrid between two highly diverged lineages of *H. titia* which suggests some degree of reproductive isolation between these lineages.

In Chapter 5, I focus on the evolution of the seasonal polyphenism seen across populations of smoky rubyspot. Building on species phylogeny constructed in Chapter 4, I construct a population level phylogeny of *H. titia*. I combine the phylogeny of *H. titia* with an unparalleled dataset of phenotypic measurements of wing melanisation collected both across the year and across the species range. I determine if the level of wing melanisation seen in different seasons has co-evolved due to evolutionary constraints to the environmental-phenotypic reaction norm. I also determine if the difference in polyphenism seen between regions represents a quantitative shift in the evolution of the trait, allowing for insights into how the polyphenism arose.

Finally, in Chapter 6, I hypothesis that the loss of polyphenism seen in higher latitude population of *H. titia*, identified in early chapters, has arisen since the last glacial maximum (LGM). Many high latitude populations of *H. titia,* reside in regions that would have been directly covered by ice sheets during the LGM suggesting that the loss of seasonal polyphenism in *H. titia* has occurred since the populations became established after the glacial retreat. Using a combination of species distribution models (SDMs) and population genetics I determine the provenance of these high latitude populations of both *H. titia* and *H. americana.*

Collectively, the chapters of this thesis provide deeper insights into how interspecific behavioural interference can influence range dynamics. I summarise past research and point to the directions research could undertake in the future. I then conduct empirical research into the spatiotemporal dynamics of *Hetaerina* damselflies for which interspecific behavioural interference is a key influencing factor in their ecology and evolution.

Chapter 2 Interspecific behavioural interference and range dynamics: current insights and future directions

Christophe W. Patterson and Jonathan P. Drury

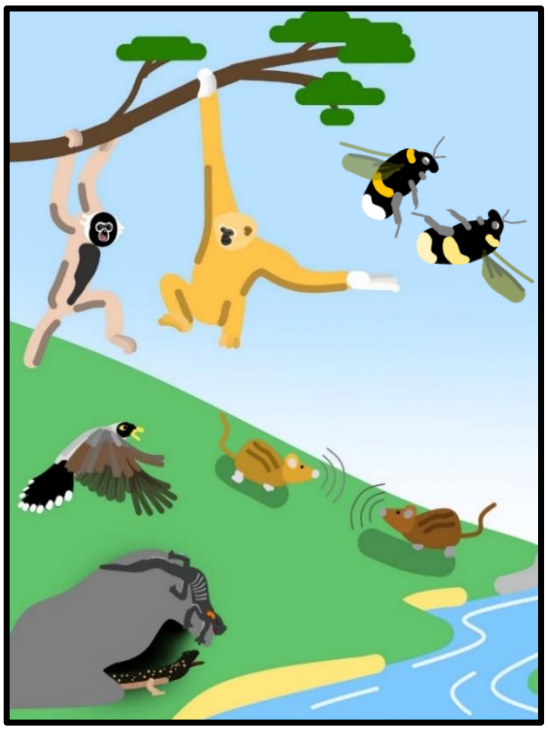

Territorial aggression between white-handed and pileated gibbons prevents the two species from dispersing into each other ranges (Asensio *et al.*, 2017). Copulation between *B. terrestris* and *B. hypocrita sapporoensis* results in unviable eggs being laid the following spring, driving local extinction (Tsuchida *et al.*, 2019). In neo-tropical singing mice, higher elevation species are dominant and exclude range intrusions from lower elevation species (Pasch, Bolker & Phelps, 2013).) Indiscriminate hyperaggression of noisy miners (Manorina melanocephala) has led to shift in the structure of avian communities (Mac Nally et al., 2012). Aggression between *Plethodon* salamanders limits their small and large scale distribution (Lyons, Shepard & Kozak, 2016).

Chapter 2

This Chapter has already been published in full as Patterson, C.W. & Drury, J.P. (2023) Interspecific behavioural interference and range dynamics: current insights and future directions. *Biological Reviews* **98**, 2012–2027.

Available at: https://doi.org/10.1111/brv.12993. It is reproduced here in full, with some minor formatting changes.

Abstract

Novel biotic interactions in shifting communities play a key role in determining the ability of species' ranges to track suitable habitat. To date, the impact of biotic interactions on range dynamics have predominantly been studied in the context of interactions between different trophic levels or, to a lesser extent, exploitative competition between species of the same trophic level. Yet, both theory and a growing number of empirical studies show that interspecific behavioural interference, such as interspecific territorial and mating interactions, can slow down range expansions, preclude coexistence, or drive local extinction, even in the absence of resource competition. We conducted a systematic review of the current empirical research into the consequences of interspecific behavioural interference on range dynamics. Our findings demonstrate there is abundant evidence that behavioural interference by one species can impact the spatial distribution of another. Furthermore, we identify several gaps where more empirical work is needed to test predictions from theory robustly. Finally, we outline several avenues for future research, providing suggestions for how interspecific behavioural interference could be incorporated into existing scientific frameworks for understanding how biotic interactions influence range expansions, such as species distribution models, to build a stronger understanding of the potential consequences of behavioural interference on the outcome of future range dynamics.

Introduction

As anthropogenic changes continue to alter the availability and distribution of habitats, the spatial distribution of species' niches will shift, in turn driving shifts in species' ranges (Parmesan & Yohe, 2003). Given that species vary in their niches and in their responses to environmental change, communities will not shift in concert, resulting in a global reshuffling of diversity and the formation of novel species assemblages. Similarly, invasions due to anthropogenic factors can have disruptive effects on species assemblages. Interactions between species – whether between previously coexisting species or between newly co-occurring species in shifting communities – play key roles in determining the ability of species' ranges to track suitable habitats (Blois *et al.*, 2013; Ockendon *et al.*, 2014; Alexander *et al.*, 2015; Early & Keith, 2019). For instance, the arrival of novel predators can drive prey species to extinction (e.g. brown tree snakes *Boiga irregularis* drove the local extinction of several bird species after they were introduced to Guam; Savidge 1987); conversely, the local extinction of one species can destabilise interaction networks, driving secondary extinctions [e.g. experimental removal of a keystone predator (*Pisaster ochraceus*) led to a decline in diversity in the marine intertidal zone; Paine 1966]. By and large, studies on the impacts of biotic interactions on population and range dynamics have predominantly focused on interactions across trophic levels or, to a lesser extent, on exploitative competition between species of the same trophic level (Svenning *et al.*, 2014; Louthan *et al.*, 2015; Early & Keith, 2019; Legault *et al.*, 2020; Ortego & Knowles, 2020; Sirén & Morelli, 2020).

Yet an important type of competition between closely related animal species is often overlooked: interspecific behavioural interference (Grether *et al.*, 2017). Behavioural interference encompasses any aggressive or mating behaviour by one species that is directed towards and has a negative impact on the fitness of another species (Gröning & Hochkirch, 2008; Burdfield-Steel & Shuker, 2011; Grether *et al.*, 2017). For instance, both territorial aggression between individuals of different species and courtship displays directed by males of one species towards females of another species fall under the umbrella of behavioural interference. Behavioural interference has been documented across a wide range of taxa (Gröning & Hochkirch, 2008; Peiman & Robinson, 2010), and in general, such aggressive and sexual interactions arise between species that are phenotypically and ecologically similar owing to recent shared ancestry

(e.g. species with similar sexual signals and/or perceptual systems), although in some cases, behavioural interference may occur across large phylogenetic distances (e.g. indiscriminate aggression from noisy miners *Manorina melanocephala* towards a broad range of bird species throughout much of Australia; (Mac Nally *et al.*, 2012); Figure 2:1C). Such interactions are costly and lead to decreased fitness as individuals waste energy, are driven to use suboptimal habitat, or miss out on mating opportunities with conspecifics. Consequently, behavioural interference can decrease population growth rates, cause exclusion from adequate habitat, and reduce or prevent dispersal into novel areas (Grether *et al.*, 2017). Thus, interspecific behavioural interference is likely to have important impacts on range dynamics.

Several theoretical investigations of behavioural interference have modelled the factors that promote or preclude coexistence (Case & Gilpin, 1974; Kuno, 1992; Liou & Price, 1994; Amarasekare, 2002; Mikami & Kawata, 2004; Kishi & Nakazawa, 2013; Kyogoku & Sota, 2017; Iritani & Noriyuki, 2021; Grether & Okamoto, 2022; Irwin & Schluter, 2022) and a handful have even explicitly analysed how processes affecting coexistence locally scale up to influence the outcome of movement across landscapes (Ribeiro & Spielman, 1986; Crowder *et al.*, 2011; Nishida, Takakura & Iwao, 2015; Ruokolainen & Hanski, 2016; Legault *et al.*, 2020). One key insight from these models is that the impact of interspecific behavioural interference will be highest on rarer species, and the magnitude of this impact increases as the asymmetry in frequency increases (e.g., Amarasekare 2002; Kuno 1992), i.e. as interactions between the rarer species and heterospecifics become increasingly more common than interactions with conspecifics. Consequently, Allee effects resulting from behavioural interference may make it very difficult for viable populations to become established in novel geographic areas (Grether *et al.*, 2017) or may drive precipitous local extinction once population densities fall below a certain threshold. A common result in models incorporating behavioural interference is the formation and maintenance of abutting (parapatric) range limits, which may move according to the magnitude of and degree of asymmetry in interference (Ribeiro & Spielman, 1986; Nishida *et al.*, 2015). Another insight from these models relates to the interactive effect of resource competition and behavioural interference – several models show that the dynamics of systems with both resource competition and behavioural interference are markedly different than systems with resource competition alone (Ribeiro & Spielman, 1986; Amarasekare, 2002; Crowder *et*

al., 2011), which underscores the importance of further research into behavioural interference in attempts to predict species responses to shifting assemblages.

Insights derived from theory about the impact of behavioural interference on range dynamics are now backed up by a growing body of empirical research. Interspecific behavioural interference has been shown to impact a range of spatial dynamics, ranging from local-scale habitat use (Vallin *et al.*, 2012)to large-scale range limit shifts (Duckworth & Badyaev, 2007). Here we present the results of the first synthesis of this body of work through a systematic literature review, and, in light of the widespread evidence that behavioural interference impacts range dynamics, we discuss patterns emerging from existing studies, highlight key gaps in the literature, and suggest several avenues for future research.

Systematic Literature Review

Methods

To identify examples of interspecific behavioural interference influencing the spatial distribution of a species, we conducted a literature search using the "all databases" option in *Web of Science* (https://www.webofscience.com/). We used the search term "*TS=(((behaviour* OR behavior*) NEAR/6 interference) OR (reproduct* NEAR/6 interference) OR (interspecific NEAR/6 (behaviour* OR behavior*) NEAR/6 competition) OR ((interspecific OR heterospecific) NEAR/6 aggress*) OR ((interspecific OR heterospecific) NEAR/6 dominan*) OR ((interspecific OR heterospecific) NEAR/6 territor*) OR ((interspecific OR heterospecific) NEAR/6 interference) OR (sister AND (taxa OR species) AND (competition OR aggress* OR territor*OR dominan* OR interference))) AND TS= ((range* NEAR/6 shift*) OR (species NEAR/6 distribution*) OR (range* NEAR/6 expansion*) OR (range* NEAR/6 dynamic*) OR (species NEAR/6 displace*) OR (species NEAR/6 replace*) OR (Altitud* NEAR/6 (zonat* OR zone)))*" (*NEAR/6* returns search results that contain the first phrase within six words of the later phrase). While we designed this set of search terms to focus on behavioural interference, we note that hybridisation falls under the general umbrella term of 'reproductive interference'. There is a large, related literature covering the spatial dynamics of hybrid zones (Barton, 1979; Barton & Hewitt, 1989; Buggs, 2007) which focuses on the way that clines form in the presence of selection acting on hybrid genotypes. Here, however, we focus on the outcome of reproductive behavioural interactions *per se*, regardless of whether those interactions

result in the formation of hybrids. We note that, although some treatments of reproductive interference include aggression in the context of access to mates (e.g. Gröning & Hochkirch, 2008) we follow recent literature on behavioural interference in classifying all agonistic interactions directed towards heterospecifics as agonistic interference (Grether *et al.*, 2017)

As of the search date (13 October 2022), we obtained a database of 338 unique peer-reviewed articles, which both authors contributed to reading and extracting data from. To reduce bias in data extraction between readers, the first 37 papers (10%) were independently read by both of us and data extraction compared. Across all 37 papers, the interpretation of the paper and data extracted was concordant. We only included cases for which there are direct observations of interspecific behavioural interference and an explicit link between that interference and spatial dynamics, which totalled 72 papers in our final set. For instance, in cases where species have abutting boundaries (e.g. parapatric range limits), we only included cases where behavioural interference has been documented and this boundary does not also coincide with clear shifts in habitat types. Similarly, for instances of microhabitat segregation or mosaic distribution patterns, we required the study to demonstrate that shifts in habitat use result directly from behavioural interference. While reading these papers, we also noted papers that the authors cited as further evidence for behavioural interference and/or range dynamics within their own or other study systems, which added 26 additional papers to our final set. Of the 98 studies in our final set, 62 studies provided clear evidence that interspecific behavioural interference impacts the spatial distribution of a species, with 19 additional studies providing corroborating evidence in combination with other papers. The remaining papers either found no effect (N = 15) or were inconclusive (N = 2). The 81 papers that either provide evidence directly or in collaboration with other studies found clear evidence in favour of interspecific behavioural interference impacting the spatial distribution of a species and were sorted into 54 unique study systems (Fig. 1A, Table 2:1; see Supplementary Table 2:1 for additional information for each of the 54 study systems.

Reproductive interference versus interspecific aggression

Our search terms returned more study systems where aggressive interference (N = 44) influenced range dynamics than reproductive interference (N = 17) (Figure 2:1A, Table 2:1, Table S1). At face value, these figures suggest that competitive exclusion *via*

aggressive interference is more widespread than sexual exclusion. Yet, this conclusion may be premature. For one thing, we avoided searching for cases of hybrid tension zones (see Section II.1), and hybridisation is among the more highly studied forms of reproductive interference. Moreover, reproductive interference also includes behaviours such as misdirected courtship, signal jamming, and heterospecific mating (Gröning & Hochkirch, 2008), all of which are difficult to detect, especially in species where these processes occur rapidly.

Seven study systems found that both reproductive interference and aggression influence range dynamics. For instance, where collared (*Ficedula albicollis*) and pied (*Ficedula hypoleuca*) flycatchers have recently (150 years ago) come into sympatry (Figure 2:1F), collared flycatchers are more aggressive, which shifts the nest occupancy of pied flycatchers into suboptimal habitat. However, pied flycatchers that nest in suboptimal habitat are less likely to hybridise with collared flycatchers, which reinforces the habitat segregation of the two species (Vallin *et al.*, 2012). Given that interspecific aggression often arises as an adaptive response to reproductive interference (Payne, 1980; Drury *et al.*, 2015b; Drury, Cowen & Grether, 2020; Grether *et al.*, 2020), the abundance of examples of aggressive interference influencing spatial dynamics in vertebrates may be indicative of undetected reproductive interference. Further empirical and theoretical work would help clarify the relative importance as well as the interactive, potentially non-additive, impacts of different types of behavioural interference on spatial dynamics.

The taxonomic distribution of case studies was the most apparent difference among the factors associated with different types of behavioural interference (Figure 2:1A). Most examples of reproductive interference influencing range dynamics were conducted on arthropods (9 out of 10). This contrasts with studies of aggressive interference which were dominated by vertebrates (30 out of 37), especially birds ($N = 17$). Empirical examples of reproductive interference are taxonomically widespread (Gröning & Hochkirch, 2008) so it is surprising to find that evidence of reproductive interference influencing the spatial dynamics of a species comes predominantly from insects and arachnids. One potential explanation for this apparent bias is that it reflects a biological reality about the costs of reproductive interference in arthropods; the fitness cost of reproductive interference may be especially high in arthropods because of females' short reproductive lifespans, and, because in some species, females produce no viable offspring after interspecific mating (Ribeiro & Spielman, 1986) which makes a species particularly vulnerable to local extinction (Irwin & Schluter, 2022). Alternatively, the

bias may reflect the methodological convenience of working with invertebrates – reproductive interference may be hard to measure in the field without experimental mating trials, making larger scale field research of the sort necessary to build a link between reproductive interference and range dynamics more feasible on arthropods.

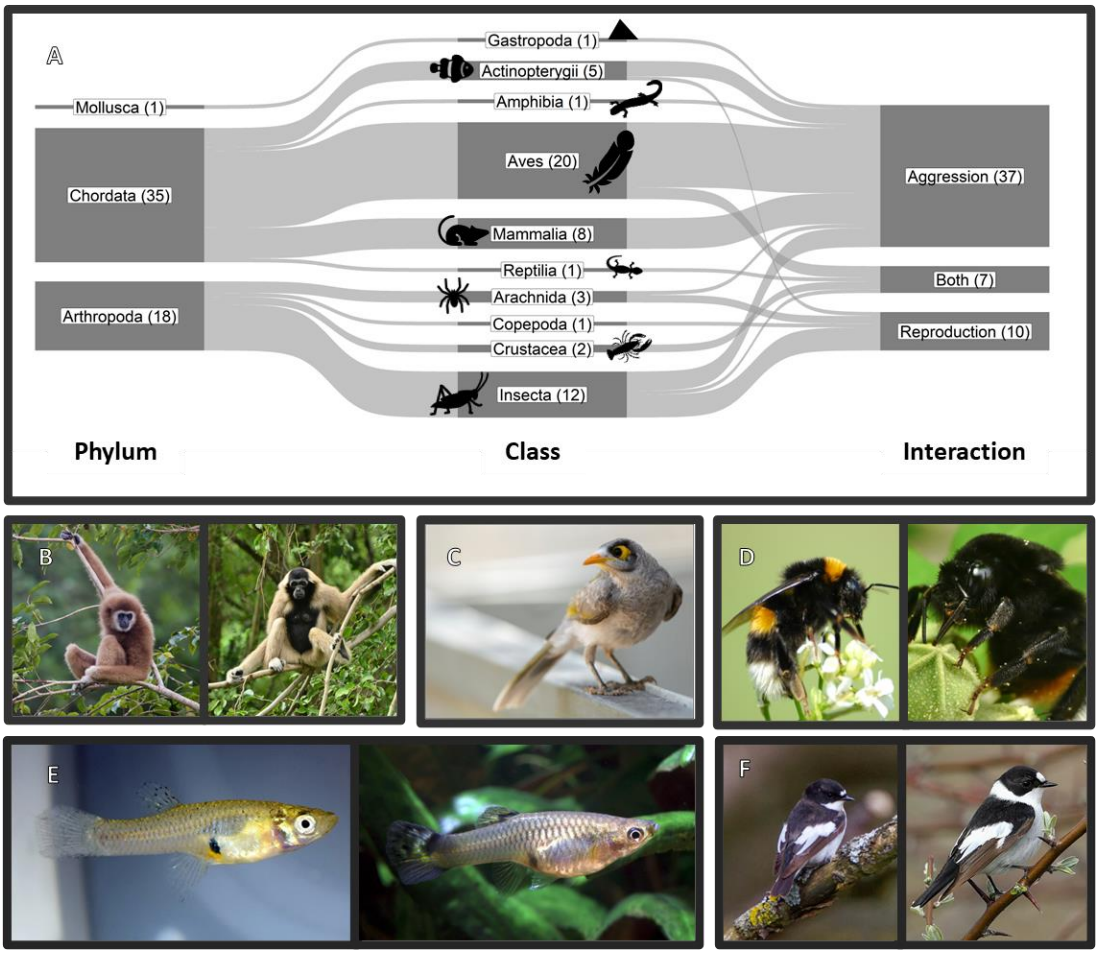

Figure 2:1: There is widespread evidence that behavioural interference (costly aggressive or reproductive interactions between species) influences spatial dynamics in animals. (A) Study systems that directly measured the impact of interspecific behavioural interference on the spatial distribution of one of more species by phylum, class, and whether the study covered aggressive or reproductive behavioural interference, or both. All study systems investigated the impact of intraclass behavioural interference, except for one case of interphylum behavioural interference between a crustacean and actinopterygians (Bubb et al., 2009). The interphylum system is counted here in Crustacea as the crustacean was the more aggressive species. Sankey diagram created using the R package ggsankey (https://github.com/davidsjoberg/ggsankey). (B) In Thailand, white-handed gibbons (Hylobates lar) (left) and pileated gibbons (Hylobates pileatus) (right) are interspecifically territorial at their parapatric range boundary,

reinforcing that boundary and, likely, decreasing the frequency of hybridisation (Asensio *et al.*, 2017). (C) Indiscriminate hyperaggression of noisy miners (Manorina melanocephala) has led to shift in the structure of avian communities (Mac Nally et al., 2012). (D) In Japan, the invasive bumblebee Bombus terrestris (left) engages in reproductive interference with two species of native bumblebee species, driving rapid declines in B. ignities (right) and B. h. sapporeenis (Tsuchida *et al.*, 2019). (E) The accidental introduction of guppies (Poecilia reticulata) (left) led to the eradication of invasive mosquitofish (Gambusia affinis) (right) in Okinawa owing to reproductive interference, and consequently guppies have been proposed as a potential control agent for mosquitofish elsewhere (Tsurui-Sato *et al.*, 2019). (F) Pied flycatchers (Ficedula hypoleuca) (left) are driven to use sub-optimal habitat by the high aggression of collared flycatchers (Ficedula albicollis) (right) (Vallin *et al.*, 2012; Rybinski et al., 2016). All photographs reproduced under creative commons by Wikimedia-user:Kongkham6211, JJ Harrison, flickr-user:coniferconifer, Vera Buhl, Rex Boggs, Andrej Chudý, Ron Knight, Holger Krisp, and Wikimedia-user:Fredlyfish4.

Table 2:1: All 54 study systems identified during the literature review that found clear evidence that interspecific behavioural interference (IBI) impacts the spatial distribution of a species. An expanded table which includes a description of each study system can be found in Supplementary Table 2:1. The elevational column indicates whether the study investigated range dynamics across an elevational gradient. The invasion column indicates whether the study contained a species outside of its native range. The comparative column indicates whether the study examined variation in behavioural interference across many species and/or environments.

Interacting Species	**IBI Type**	**Elevational (Y/N)**	**Invasion (Y/N)**	**Comparative (Y/N)**	**References**
Aves					
Great reed warblers (Acrocephalus arundinaceus) & marsh warblers (Acrocephalus palustris)	Aggression	N	N	N	(Rolando & Palestrini, 1989)
Bicknell's thrushes (*Catharus bicknelli*) & Swainson's thrushes (*Catharus ustulatus*)	Aggression	Y	N	N	(Freeman & Montgomery, 2015)
Black-headed nightingale thrushes (*Catharus mexicanus*) & ruddy-capped nightingale-thrushes (*Catharus frantzii*)	Aggression	Y	N	N	(Jones *et al.*, 2020)
Collared (Ficedula albicollis) & pied (Ficedula hypoleuca) flycatchers	Aggression	N	N	N	(Vallin *et al.*, 2012; Rybinski *et al.*, 2016)

Several species of wood wrens (*Henicorhina leucophrys* & *Henicorhina leucosticta*) and thrushes (*Catharus mexicanus & Catharus aurantiirostris*) along an elevational gradient in Costa Rica.	Aggression	Y	N	N	(Jankowski, Robinson & Levey, 2010)
Narrow-billed woodcreepers (*Lepidocolaptes angustirostris*) & scaled woodcreepers (*Lepidocolaptes squamatus*)	Aggression	N	N	N	(Maldonado-Coelho *et al.*, 2017)
Common nightingales (*Luscinia megarhynchos*) & thrush nightingales (*Luscinia luscinia*)	Aggression	N	N	N	(Sorjonen, 1986; Reif *et al.*, 2015, 2018)
Noisy miners (*Manorina melanocephala*) & local bird assemblages	Aggression	N	N	N	(Mac Nally *et al.*, 2012; Lill & Muscat, 2015)
Flame robins (Petroica phoenicea) & Norfolk robins (Petroica multicolor)	Aggression	N	N	N	(Robinson, 1992)
Carolina chickadees (*Poecile carolinensis*) and black-capped chickadees (*Poecile atricapillus*)	Aggression and Reproductive Interference	N	N	N	(Bronson *et al.*, 2003; McQuillan & Rice, 2015)
Invasive ring-necked *parakeets (Psittacula krameri*) and native communities	Aggression	N	Y	N	(Hernández-Brito *et al.*, 2014)

Townsend's warblers (*Setophaga townsendi*) and hermit warblers (*Setophaga occidentalis*)	Aggression and Reproductive Interference	N	N	N	(Pearson, 2000; Pearson & Rohwer, 2000)
Western bluebirds (*Sialia mexicana*) & mountain bluebirds (*Sialia currucoides*)	Aggression	N	N	N	(Duckworth & Badyaev, 2007; Duckworth, 2013; Duckworth, Belloni & Anderson, 2015)
Spotted owls (*Strix occidentalis*) & barred owls (*Strix varia*)	Aggression	N	Y	N	(Gutiérrez *et al.*, 2007; Van Lanen *et al.*, 2011; Wiens, Anthony & Forsman, 2014)
Dominant and subordinate congeneric birds in urban environments	Aggression	N	N	Y	(Martin & Bonier, 2018; Martin, Burke & Bonier, 2021)
Dominant and subordinate birds from North America	Aggression	N	N	Y	(Freshwater, Ghalambor & Martin, 2014)
Birds along an elevational gradient in Borneo	Aggression	Y	N	Y	(Boyce & Martin, 2019)
North American perching birds (passerines)	Aggression and Reproductive Interference	N	N	Y	(Cowen, Drury & Grether, 2020)

Birds along an elevational gradient in Papua New Guinea	Aggression	Y	N	Y	(Freeman, Class Freeman & Hochachka, 2016)
Amphibia					
Southern Appalachian salamander (*Plethodon teyahalee*) & red-cheeked salamanders (*Plethodon jordani*)	Aggression	Y	N	N	(Hairston, Nishikawa & Stenhouse, 1987; Gifford & Kozak, 2012)
Actinopterygii					
Damselfish (*Dischistodus* spp.) in the Great Barrier Reef	Aggression	N	N	N	(Bay, Jones & McCormick, 2001)
Guppies (Poecilia reticulata) & mosquitofish (Gambusia affinis)	Reproductive Interference	N	Y	N	(Tsurui-Sato *et al.*, 2019)
Obscure damselfish (*Pomacentrus adelus*) & speckled damselfish (*Pomacentrus bankanensis)*	Aggression	N	N	N	(Eurich, McCormick & Jones, 2018)
Invasive brown trout (*Salmo trutta*) & white-spotted charr (*Salvelinus leucomaenis*) in Japan	Aggression	N	Y	N	(Takami *et al.*, 2002; Hasegawa *et al.*, 2004; Hasegawa & Maekawa, 2009)
Gopher rockfish (*Sebastes carnatus*) & Black-and-yellow rockfish (*Sebastes chrysomelas*)	Aggression	N	N	N	(Larson, 1980)

Arachnida					
Invasive sheet-web spiders (*Linyphia triangularis*) & bowl-and-doily spiders (*Frontinella communis*)	Aggression	N	Y	N	(Houser, Ginsberg & Jakob, 2014)
Copepoda					
Skistodiaptomus copepods	Reproductive Interference	N	N	N	(Thum, 2007)
Crustacea					
Invasive rusty crayfish (*Orconectes rusticus*) and native Sanborn crayfish (*Orconectes sanborni*)	Aggression and Reproductive Interference	N	Y	N	(Butler & Stein, 1985)
Invasive signal crayfish (*Pacifastacus leniusculus)* in Europe & native communities. This includes an example interphylum behavioural interference: aggression by signal crayfish toward native bullhead fish (*Cottus gobio*).	Aggression and Reproductive Interference	N	Y	N	(Svärdson, Fürst & Fjälling, 1991; Söderbäck, 1994, 1995; Westman & Savolainen, 2001; Westman, Savolainen & Julkunen, 2002; Bubb *et al.*, 2009)
Gastropoda					
Keyhole limpets (*Siphonaria lessonii*) & pulmonate limpets (*Fissurella crassa*)	Aggression	N	N	N	(Aguilera & Navarrete, 2012)

Insecta					
Aedes mosquitos (Ae. albopictus & Ae. aegypti)	Reproductive Interference	N	Y	N	(Nasci, Hare & Willis, 1989; Bargielowski, Lounibos & Carrasquilla, 2013; Bargielowski & Lounibos, 2016; Lounibos & Juliano, 2018; Zhou *et al.*, 2022)
Two tick species (Amblyomma variegatum & Amblyomma hebraeum)	Reproductive Interference	N	N	N	(Bournez *et al.*, 2015)
Whiteflies (*Bemisia tabaci* spp.)	Reproductive Interference	N	Y	N	(Liu *et al.*, 2007; Crowder *et al.*, 2011; Wang, Crowder & Liu, 2012)
Invasive buff-tailed bumblebees (*Bombus terrestris*) & native bumblebees *(Bombus h. sapporoensis* & *Bombus ignitus*) in Japan	Reproductive Interference	N	Y	N	(Tsuchida *et al.*, 2019)
Rubyspot damselflies (*Hetaerina* spp.)	Aggression	N	N	Y	(McEachin *et al.*, 2022)
Two ant species (*Iridomyrmex* spp.)	Aggression	N	N	N	(Haering & Fox, 1987)
Arboreal termite species in Papua New Guinea (Microcerotermes biroi, Nasutitermes novarumhebridiarum, & Nasutitermes princeps)	Aggression	N	N	Y	(Leponce, Roisin & Pasteels, 1997)

White-crossed seed bugs (*Neacoryphus bicrurus*) and co-occurring insect communities	Aggression and Reproductive Interference	N	N	N	(McLain & Shure, 1987)
Invasive southern green stink bugs (*Nezara viridula*) & native green stink bugs (*Nezara antennata*)	Reproductive Interference	N	Y	N	(Kiritani, 2011)
Alpine dark bush-crickets (*Pholidoptera aptera*) & Transylvanian dark bush-crickets (*Pholidoptera transsylvanica*)	Reproductive Interference	N	N	N	(Dorková *et al.*, 2020)
Eastern subterranean termites (*Reticulitermes flavipes*) & Western subterranean termites (*Reticulitermes grassei*)	Aggression	N	Y	N	(Perdereau *et al.*, 2011)
Invasive Asian blue ticks (Rhipicephalus [Boophilus] microplus) & African blue ticks (Rhipicephalus [Boophilus] decoloratus) in South Africa	Reproductive Interference	N	Y	N	(Sutherst, 1987; Tønnesen *et al.*, 2004)
Cepero's groundhoppers (*Tetrix ceperoi*) & slender groundhoppers (*Tetrix subulata*)	Reproductive Interference	N	N	N	(Gröning *et al.*, 2007; Hochkirch, Gröning & Bücker, 2007; Hochkirch & Gröning, 2012)
Arboreal ant species in Papua New Guinea	Aggression	N	N	Y	(Mottl *et al.*, 2021)
Mammalia					

Fallow deer (Dama dama) & roe deer (Capreolus capreolus)	Aggression	N	Y	N	(Ferretti & Mori, 2020)
White-handed gibbons (*Hylobates lar*) & Pileated gibbons (*Hylobates pileatus*)	Aggression	N	N	N	(Suwanvecho & Brockelman, 2012; Asensio *et al.*, 2017)
Least chipmunks (*Neotamias minimus*) & yellow-pine chipmunks (*Neotamias amoenus*)	Aggression	Y	N	N	(Heller, 1971; Chappell, 1978)
Townsend's chipmunks (*Neotamias townsendii*) & yellow-pine chipmunks (*Neotamias amoenus*)	Aggression	N	N	N	(Trombulak, 1985)
Uinta chipmunks (Neotamias umbrinus) & Colorado chipmunks (Neotamias quadrivittatus)	Aggression	Y	N	N	(Bergstrom, 1992)
Stoats (Mustela erminea) & least weasels (Mustela nivalis)	Aggression	N	N	N	(Erlinge & Sandell, 1988)
Pied tamarins (*Saguinus bicolor*) & Golden-handed tamarins (*Saguinus midas*)	Aggression	N	N	N	(Sobroza *et al.*, 2021)
Chiriquí singing mice (*Scotinomys xerampelinus*) & Alston's singing mice (*Scotinomys teguina*)	Aggression	Y	N	N	(Pasch *et al.*, 2013)
Reptilia					

Invasive house geckos (*Hemidactylus frenatus*) & native communities	Aggression and Reproductive Interference	N	Y	N	(Bolger & Case, 1992; Petren, Bolger & Case, 1993; Case, Bolger & Petren, 1994; Dame & Petren, 2006)

Elevational gradients

Range dynamics along elevational gradients have long been of interest to ecologists and evolutionary biologists. For instance, a classic hypothesis posits that abiotic factors are likely to play a more important role than biotic factors at high-elevation range limits (Louthan *et al.*, 2015). As a result, there may be an increased risk of extinction in montane ecosystems caused by the 'escalator to extinction' (Sekercioglu *et al.*, 2008; Freeman *et al.*, 2018) in which warming conditions cause the climate niches of high-elevation species to disappear. Given the interest in biotic interactions along elevational gradients, it is not surprising that we identified multiple examples of interspecific behavioural interference of one species influencing the elevational distribution of another species (17% of cases documenting an impact of behavioural interference on range dynamics). Due to rapid habitat turnover with altitude, range boundaries across an elevational gradient are often sharply defined, making studies of range limits inherently simpler along an elevational gradient (Pasch *et al.*, 2013; Žagar *et al.*, 2015; Jones *et al.*, 2020), so it would be premature to draw conclusions on the relative importance of behavioural interference on elevational range limits in comparison to range boundaries across landscape scales.

Several key patterns emerge from studies along elevational gradients. First, interspecific territoriality plays a key role in creating and maintaining elevational range limits. Comparative analyses, for instance, have shown that bird species have wider elevational ranges in mountains without competitors (Burner *et al.*, 2020). Additionally, the response of several species of montane birds to heterospecific songs decreases with distance from their parapatric boundary, indicating a learned response to the presence of an aggressive congener (Jankowski *et al.*, 2010; Freeman & Montgomery, 2015; Freeman *et al.*, 2016; Boyce & Martin, 2019; Jones *et al.*, 2020). Secondly, asymmetries in dominance are not consistently biased in favour of low-elevation species, as there are examples of species pairs with subordinate high-elevation species (e.g. *Catharus* thrushes; Freeman and Montgomery 2015) and of pairs in which the lower elevation species is subordinate [e.g. *Scotinomys* singing mice (Pasch *et al.*, 2013), *Neotamias* chipmunks (Bergstrom, 1992) and, if aquatic depth gradients are comparable to elevational gradients, *Pomacentrus* damselfish (Eurich *et al.*, 2018)] (see also Freeman 2020). These examples demonstrate the varied and often unpredictable role that behavioural interference can play in influencing elevational range limits, thereby challenging the

hypothesis that abiotic factors are likely to play a more important role than biotic factors at high-elevation range limits (Louthan *et al.*, 2015). Finally, we also note a bias in the geographic locations of studies investigating behavioural interference across elevational gradients, with two exceptions in Borneo and Papua New Guinea, all study systems were located in northern and Central America (Figure 2:2). Studies across landscapes were found across a wider area, but still with noted gaps in Africa and Asia, likely due to an underlying geographic bias in scientific research (Culumber *et al.*, 2019).

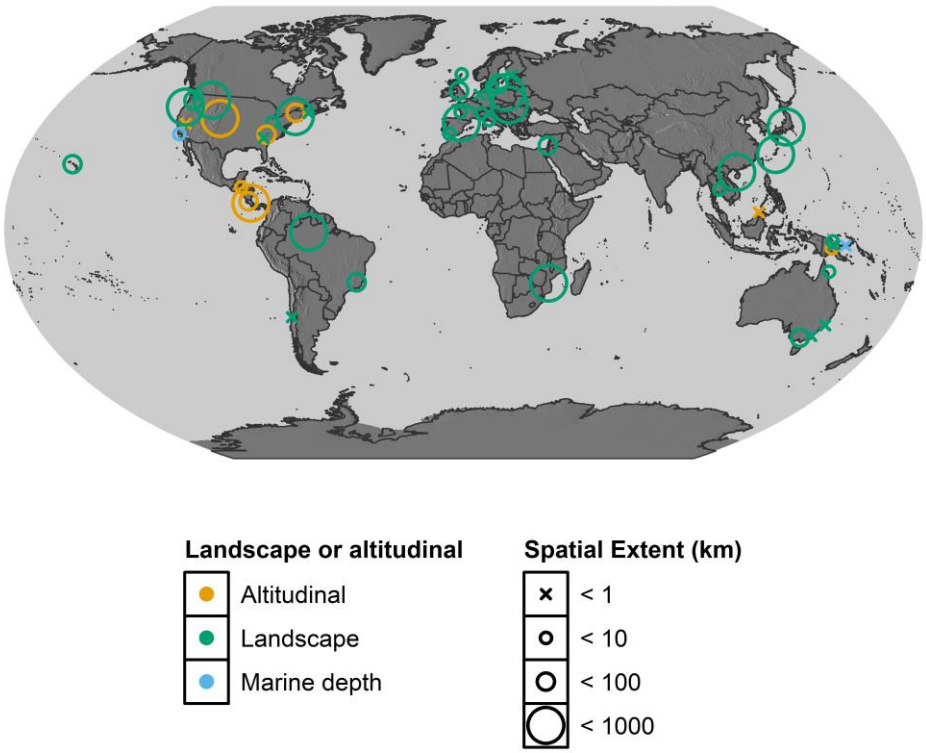

Figure 2:2: The global distribution of field studies that found an effect of interspecific behavioural interference on the spatial distribution of one or more species. Colour denotes whether the study investigated the spatial distributions across a landscape (i.e. latitude and longitude), across an elevational gradient (altitudinal), or across a sea-depth gradient (marine depth). Size indicates the maximum spatial extent for where data was collected for study but is not to scale, excluding comparative studies that had a greater than 1000 km global distribution (N = 7).

Across landscapes, we found examples of behavioural interference influencing the spatial distributions of species in studies ranging in spatial scope from local (<1 km) scales [e.g. Hochkirch & Gröning, (2012) found that, within a single nature reserve, reproductive interference causes two groundhopper species to exhibit a mosaic of small-scale habitat use] to continental (<1000 km) scales [e.g. Reif *et al.*, (2015, 2018) found that across Eastern Europe, aggression drives shifts in habitat preferences in sympatry compared to allopatric populations of common *Luscinia megarhynchos*, and thrush nightingales, *Luscinia luscinia*).

Invasion biology

Anthropogenic influences have led to a dramatic rise in the number of non-native species that become invasive after being translocated to novel regions (Blackburn *et al.*, 2011). As the ranges of invasive species expand they may engage in interspecific behavioural interference, driving displacement of native species (Rowles & O'Dowd, 2007; Kyogoku & Sota, 2017; Lounibos & Juliano, 2018; Pereira, Lourenço & Mota, 2020). The systematic review identified multiple examples of invasive species engaging in reproductive interference (Westman *et al.*, 2002; Tønnesen *et al.*, 2004; Lounibos & Juliano, 2018; Tsuchida *et al.*, 2019; Tsurui-Sato *et al.*, 2019) and aggressive interference (Westman *et al.*, 2002; Rowles & O'Dowd, 2007; Bubb *et al.*, 2009; Houser *et al.*, 2014) with native species (15/54 = 28% of cases). For instance, invading Argentine ants in Australia outcompete native ant species through direct aggressive interactions (Rowles & O'Dowd 2007). Similarly, in Japan, invasive buff-tailed bumblebees (*Bombus terrestris*) engage in reproductive interference with two species of native bumblebee species (Figure 2:1D). Copulation between male *B. terrestris* and female *Bombus hypocrita sapporoensis* or *Bombus ignitus* results in unviable eggs being laid the following spring when there are no further intraspecific mating opportunities. Consequently, *B. ignitus* and *B. h. sapporoensis* have declined rapidly in areas with *B. terrestris*, and further declines could lead to the extinction of the native bumblebee species (Tsuchida *et al.*, 2019). Other well-established cases where invading lineages quickly replace previously established lineages include the replacement of asexual gecko lineages throughout the Pacific due to interference from invasive Asian house geckos, *Hemidactylus frenatus,* geckos (Bolger & Case, 1992; Petren *et al.*, 1993; Dame & Petren, 2006), and the replacement of *Aedes aegypti* by *Ae. albopictus* both throughout the southern USA . (Nasci *et al.*, 1989) and in China (Zhou *et al.*, 2022).

Yet, behavioural interference is not always beneficial to invasive species and detrimental to native species. Invasive species may be unable to establish in areas that contain a more aggressive congener, and higher levels of aggressive or reproductive interference could allow native species to tolerate the presence of the invading species (Crowder *et al.*, 2011), or even prevent its spread. For instance Australian house geckos, *Gehyra dubia*, are more aggressive than the globally invasive Asian house gecko, *Hemidactylus frenatus* which could prevent the invasive species replacing the native (Cisterne, Schwarzkopf & Pike, 2019). Additionally, conservation efforts towards the critically endangered Nashville crayfish, *Orconectes shoupi*, may be aided by its higher aggression toward the invasive bigclaw crayfish, *Orconectes placid* (Bizwell & Mattingly, 2010). Whether asymmetries in behavioural interference generally influence the outcome of translocations of animal species is, therefore, an important open question.

In addition to being a potentially accelerating factor in biological invasions, behavioural interference has also been suggested as a management tool for invasive species. On Okinawa, for instance, the accidental introduction of guppies (*Poecilia reticulata*) led to the eradication of invasive mosquitofish (*Gambusia affinis*) (Figure 2:1E; Tsurui-Sato *et al.*, (2019). Laboratory experiments indicate that male guppies attempt to mate with female mosquitofish, thereby reducing their reproductive output. Introduced guppies also have negative impacts on native taxa, but by introducing only males, or mixed populations into environments with lethal winter temperatures, guppies could be used to eradicate mosquito fish from other river systems (Tsurui-Sato *et al.*, 2019). Similarly, a study on aggression between invasive brown trout (*Salmo trutta*) and native white-spotted charr (*Salvelinus leucomaenis*) demonstrated that habitat modifications in the form of visual barriers could reduce observed levels of interspecific aggression (Hasegawa & Maekawa, 2009).

Empirical validation of theoretical predictions

The formation of parapatric ranges, where two species have adjacent ranges with little or no overlap, is a key prediction of the theoretical models of how interspecific behavioural interference impacts range dynamics when the impacts of behavioural interference are symmetrical (Ribeiro & Spielman, 1986). In line with this prediction, we found that, where the impact of behavioural interference is equal, the ranges of interacting species pairs are stable (Bull & Burzacott, 1994; Thum, 2007; Asensio *et al.*, 2017). For instance, in Thailand, two species of gibbon, white-handed

gibbons (*Hylobates lar*) and pileated gibbons (*Hylobates pileatus*), have a parapatric distribution with only a small (<1 km wide) boundary where the species are found in sympatry. Both *H. lar* and *H. pileatus* hold territories that are controlled exclusively by monogamous pairs. Detailed mapping of territories and observations of conflict events show that, where the two species are found in sympatry, pairs of both species defend territories against both conspecifics and heterospecifics (Figure 2:1B; (Asensio *et al.*, 2017)). If the impact of behavioural interference is asymmetrical, however, replacement of one species by the other commonly results (Tønnesen *et al.*, 2004; Duckworth & Badyaev, 2007; Vallin *et al.*, 2012; Tsuchida *et al.*, 2019; Tsurui-Sato *et al.*, 2019; Sobroza *et al.*, 2021). Some studies found that the ranges of the two species were stable even in the presence of asymmetrical behavioural interference because the more dominant species was limited by an abiotic or a different biotic factor (Bergstrom, 1992; Pasch *et al.*, 2013).

Although Allee effects are common in theoretical models of behavioural interference, relatively few case studies identified by our literature review explicitly tested for Allee effects, although several investigators of these studies suggest that Allee effects generate range turnovers (Söderbäck, 1994; Tønnesen *et al.*, 2004; Thum, 2007; Kiritani, 2011). The paucity of direct evidence for Allee effects was surprising, given documented Allee effects in laboratory studies [e.g. Kyogoku & Nishida, (2012)] and frequency- and/or density-dependent impacts of interspecific interference in the field (Svensson *et al.*, 2018; Gómez-Llano *et al.*, 2023). Future research, therefore, should aim to understand the importance of Allee effects in determining the outcome of spatial dynamics. For instance, a key test of the impact of behavioural interference on range dynamics would be to induce an Allee effect artificially in field systems known to engage in behavioural interference, by heightening or inversing the densities and/or frequencies of two species that engage in behavioural interference.

Similarly, although several models incorporate both behavioural interference and resource competition (Ribeiro & Spielman, 1986; Amarasekare, 2002; Crowder *et al.*, 2011), our literature search found few explicit analyses disentangling the relative impacts of behavioural interference and resource competition, or the predicted interactive dynamics of both, on range dynamics [but see Duckworth, (2013); Cowen, Drury and Grether, (2020)].

Future Directions

Our systematic literature review demonstrated that there are now many studies that show varied impacts of behavioural interference on range expansion, but it also highlighted several gaps in our understanding. Here, we argue that further research is needed in several key areas, including the role that behavioural interference has played in shaping historical patterns of range dynamics, the impacts of behavioural interference on future range dynamics under climate change, and the extent to which evolution influences outcomes.

Identifying the impact of behavioural interference on historical spatial processes

There are several existing approaches for studying historical range dynamics that would be useful to develop further to understand outcomes of behavioural interference across a range of timescales. For instance, at a deep evolutionary timescale, models of ancestral biogeography have proved to be useful tools for making inferences about the pace and trajectory of range evolution within independently evolving lineages (Ronquist, 2011). Recently, there have been calls to extend these methods to incorporate ecological factors such as species interactions (Sukumaran & Knowles, 2018), and for the development of tools to identify the signature of competitive exclusion in range data (Quintero, Landis & Hahn, 2020). Incorporating the possibility that the presence and/or magnitude of behavioural interference could modulate the impacts of competition on range dynamics into these models, similar to advances already developed for trait-mediated dispersal (Klaus & Matzke, 2020), could provide a novel tool that would make it possible to test a range of hypotheses that cannot be tested with current methods (Figure 2:3A).

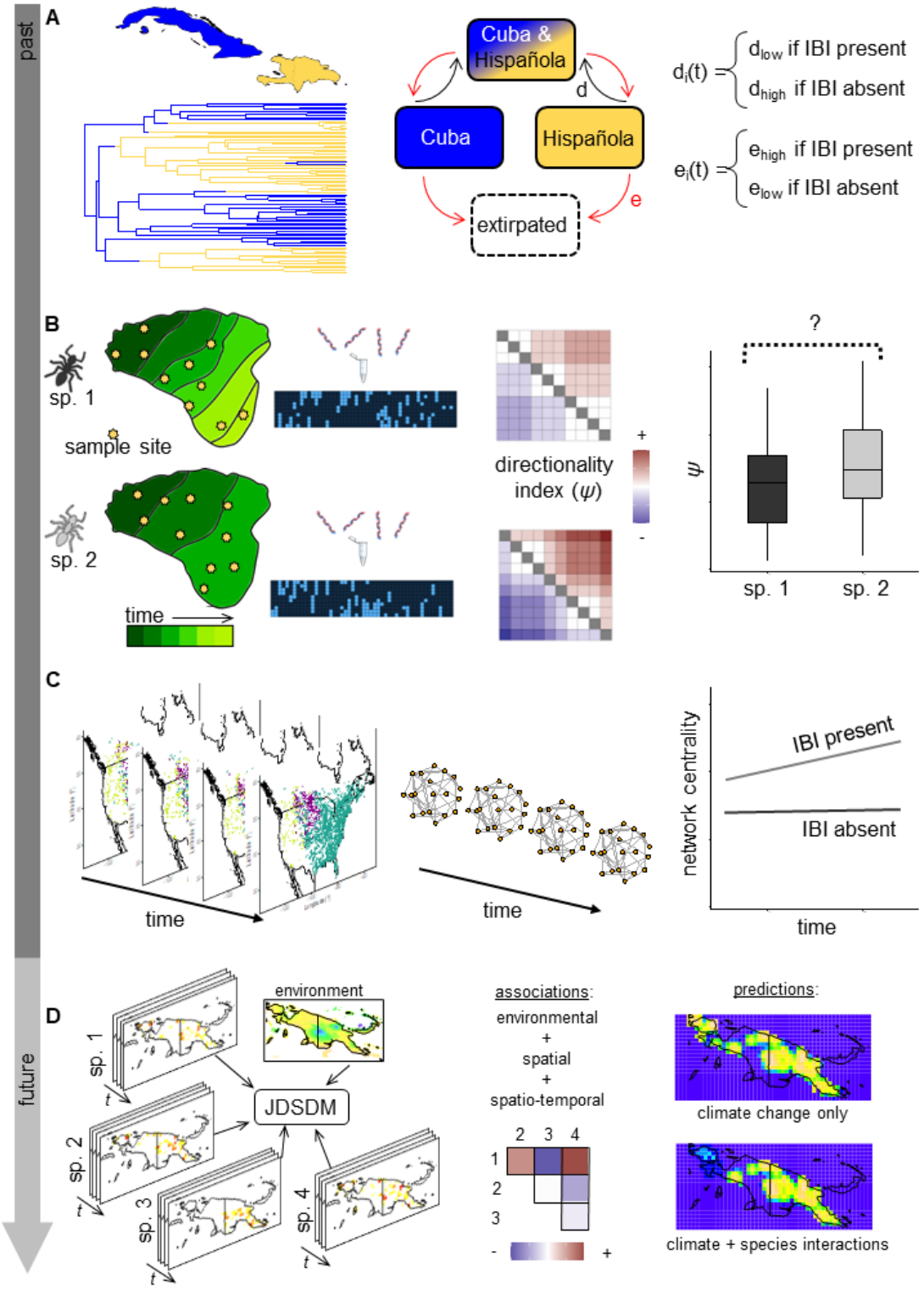

Figure 2:3: Possible directions for future research into the historical (A–C) and potential future (D) impacts of interspecific behavioural interference (IBI) on range dynamics. Approaches to test for historical impacts of IBI include (A) extending models of ancestral biogeography to include separate parameters for species that engage in IBI and

those that do not; (B) deploying genomic tools to test whether the historical dynamics of range expansion differ between species that engage in IBI (sp. 2, in this example) and species that do not by calculating pairwise indices of directional movement such as the ψ index (Peter & Slatkin, 2013); and (C) using long-term census data to analyse how IBI has impacted the dynamics of species co-occurrence through time using tools from network analysis (e.g. indices of network centrality). Developments for forecasting and mitigating the impacts of IBI on global change-induced range shifts might include (D) fitting joint dynamic species distribution models (JDSDMs) and using model inferences to compare future ranges under pure climate-tracking scenarios to scenarios that incorporate species interactions inferred from JDSDMs.

At shallower evolutionary scales, existing population genomic techniques leverage the signatures of historical processes preserved in genomes to test hypotheses about spatial (Peter & Slatkin, 2013; Petkova, Novembre & Stephens, 2015; He, Prado & Knowles, 2017; Al-Asadi *et al.*, 2019) and demographic (Gutenkunst *et al.*, 2009; Gronau *et al.*, 2011; Excoffier *et al.*, 2021) dynamics that have unfolded over scales of thousands to millions of years. Largely, these developments have been designed to examine dynamics within independently evolving lineages. Within this constraint, one way forward would be to conduct comparative analyses to test the hypothesis that lineages (e.g. populations, species) experiencing higher levels of behavioural interference expand their ranges at different rates than lineages experiencing little or no behavioural interference (Figure 2:3B). Recently, Ortego and Knowles, (2020) developed an analytical pipeline that explicitly tests for the impact of facilitation and/or competition between species on generating contemporary geographic patterns of genomic diversity. Extending these models to test explicitly for impacts of behavioural interference is an exciting possibility that would generate new insights.

On a more contemporary scale, long-term census data have proved to be a useful tool for monitoring dynamics of species assemblages over the past century (Rosenberg *et al.*, 2019; Saunders *et al.*, 2022). Such data sets contain interacting species, and understanding how those interactions impact temporal dynamics is one way forward. One recent attempt has shown that stably coexisting species pairs that are interspecifically territorial have increased their fine-scale habitat overlap more than non-interspecifically territorial pairs, suggesting that interspecific territoriality may actually stabilise coexistence in species that would otherwise engage in high levels of exploitative competition (Nesbit *et al.*, 2023). Future applications could use tools developed for

network analyses (Blonder *et al.*, 2012) to examine how behavioural interference influences dynamics within assemblages (Figure 2:3C).

Predicting the impact of behavioural interference in novel assemblages

Insights generated from investigations of the impacts of behavioural interference on historical range dynamics will be essential for generating predictions about the future impacts of behavioural interference on climate change-driven range dynamics. At the heart of attempts to predict how species' ranges will shift in response to global changes are species distribution models (SDMs). SDMs use measures of abiotic factors and presence–absence data to predict species' future ranges under different climate scenarios (Elith & Leathwick, 2009; Titley *et al.*, 2021).

Attempts to incorporate biotic factors into species distribution models have given rise to joint species distribution models (JSDMs) (Tikhonov *et al.*, 2017; Wilkinson *et al.*, 2019). Yet implementing and validating JSDMs is fraught with difficulties because positive and negative occurrence patterns often correlate with abiotic factors (Poggiato *et al.*, 2021). Consequently, although some attempts to implement behavioural interference into SDMs/JSDMs have been conducted (Engler *et al.*, 2013; Bastianelli *et al.*, 2017), many examples of interspecific behavioural interference limiting the spatial distribution of species would not be detected using JSDMs. Despite challenges, joint species distribution modelling remains an active area of research with many promising recent developments (Pichler & Hartig, 2021; Escamilla Molgora *et al.*, 2022). For instance, joint dynamic species distribution models (JDSDMs) use time-series data on abundance to examine the impact of concurrent changes in abundance across assemblages more directly (Thorson, Pinsky & Ward, 2016; Elo *et al.*, 2023). Consequently, we imagine that these tools will be useful for generating predictive models of future range dynamics in the presence of behavioural interference (Figure 2:3D), for instance by comparing the marginal predictions of such models (i.e. the effects of environmental variables only), to conditional predictions that also incorporate impacts of changing species interactions (Wilkinson *et al.*, 2019, 2021). Recently, for instance, Novella-Fernandez *et al.*, (2021) devised an index of 'geographic avoidance' by comparing species suitable ranges (calculated from SDMs) to their observed ranges. Using this index, they found that two pairs of cryptic species of bats in Europe exhibited spatial partitioning consistent with interspecific competition driving exclusion.

They then examined range overlap under future climate projections, demonstrating that some predicted range shifts may not be possible due to predicted range overlap with competitors [Novella-Fernandez *et al.*, (2021), see also Engler *et al.*, (2013); McQuillan & Rice, (2015) for a similar approach]. Future attempts to generate predictions of range dynamics in the presence of behavioural interference could also be used to disentangle and quantify the differing impacts of behavioural interference *versus* resource competition.

The preceding approaches largely rely on metrics of co-occurrence to make inferences about the impacts of behavioural interference, under the assumption that co-occurring lineages are likely to interact. Yet, range overlap *per se* is not robust evidence that interactions occur. One way forward is to use measurements of fine-scale range overlap (i.e. 'syntopy'), which may be more indicative of the opportunity for species interactions (Drury *et al.*, 2020). Still, there is no substitute for direct observations of behaviour across large spatiotemporal scales. For instance, a large-scale study of spatiotemporal variation in agonistic behaviour in damselfish (genus Chaetodon) shows that interactions between individuals of different species increase after coral bleaching events (Keith *et al.*, 2023). Future studies should directly observe behaviours to demonstrate concrete links between behavioural interference and range dynamics.

The role of evolution in mediating responses to behavioural interference

Historically, empirical research into behavioural interference has largely focused on understanding factors that lead to behavioural interference (e.g., Drury, Cowen, & Grether 2020; Leighton et al. 2023) and its evolutionary consequences, such as its impact on trait evolution (Grether *et al.*, 2009; Pfennig & Pfennig, 2009) or other aspects of the speciation cycle (Tobias, Ottenburghs & Pigot, 2020). This work has shown that the likelihood of behavioural interference decreases with increasing divergence time (e.g., Drury, Cowen, & Grether 2020; Barley et al. 2022) likely owing to the relative similarity in perceptual systems and agonistic and/or mating signals used in closely related species (Orians & Willson, 1964; Grether *et al.*, 2009). Consequently, behavioural interference is thought to have a strong impact on the rate of speciation by limiting the rate at which two recently diverged allopatric lineages can coexist in secondary sympatry (Tobias *et al.*, 2020). One possible evolutionary outcome of behavioural interference is divergent reproductive or agonistic character displacement,

in which selection acts on mating or agonistic signals or perceptual systems to prevent or reduce the occurrence of behavioural interference (Grether *et al.*, 2009; Pfennig & Pfennig, 2009). Yet, the benefits of diverging in signals and/or perceptual systems do not always outweigh the costs--for instance, because of the continued pressure of stabilising selection for intraspecific mate recognition (Drury *et al.*, 2019a) or because interspecific competitor recognition may be an adaptive pathway to interspecific resource partitioning (Grether & Okamoto, 2022) -- and consequently, selection may preclude divergence or even drive convergence between interacting lineages.

The evolutionary responses to behavioural interference in shifting ranges should, therefore, play an important role in determining the outcome of range dynamics. For instance, in the case of *Aedes* mosquitoes, reproductive character displacement appears to have slowed down the invasion of *Ae. albopictus* in Florida (Bargielowski *et al.*, 2013; Bargielowski, Blosser & Lounibos, 2015). Similarly, native bumblebees in Japan have evolved polyandrous mating systems in response to reproductive interference from invasive buff-tailed bumblebees (Tsuchida *et al.*, 2019). Yet it is unknown under which circumstances, and to what extent, evolutionary changes might mediate the impact of behavioural interference on range dynamics. Future long-term studies of zones where behavioural interference occurs, in addition to comparisons between sympatric and allopatric populations, could shed further light on these questions.

Conclusions

(1) Multiple lines of evidence now demonstrate that interspecific behavioural interference can limit the spatial distribution of species. Case studies demonstrate that this is true across a wide range of animal taxa, and that both reproductive interference and interspecific aggression can influence spatial dynamics.

(2) In line with predictions derived from theoretical models of behavioural interference, the case studies we compiled demonstrate that symmetry (or lack thereof) in behavioural interference determines the spatial outcome of interactions. Further work is necessary to test other key predictions of theoretical models, such as the presence of Allee effects and interactive impacts of behavioural interference and exploitative competition for resources.

(3) We identified several other gaps that remain in our broad-scale understanding of the impacts of behavioural interference on spatial dynamics. For instance, which factors (e.g. phylogenetic distance, life history, climate niche, etc.) explain variation in the presence or magnitude of the effect of behavioural interference on range dynamics?

(4) Several recent developments have paved the way for modelling the impacts of species interactions on both historical and future spatial dynamics, and future work adapting these methods to explore further the links between behavioural interference and range dynamics will be an important way forward.

(5) In addition to modelling approaches, further work aimed at quantifying the interactive effects of evolutionary change and spatial movement will be crucial for predicting the outcome of range dynamics in the presence of behavioural interference.

(6) The spatial distribution of species has implications for conservation, human health, and agriculture. Alongside other abiotic and biotic factors, our study highlights the need to include interspecific behavioural interference in predicting and managing the current and future distribution of species.

Acknowledgements

We thank Erandi Bonillas-Monge, Greg Grether, Sal Keith, and Dan Nesbit for helpful comments, and Durham University librarians for assistance. We also thank Darren Irwin and an anonymous reviewer for their additional helpful comments. C.W.P. was funded by a Durham Doctoral Studentship, and J.P.D. was funded by NSFDEB-NERC-2040883.

Supporting information

Additional supporting information may be found in Appendix Chapter 2.

Chapter 3 A chromosome-level genome assembly for the smoky rubyspot damselfly (*Hetaerina titia*)

Christophe W Patterson, Erandi Bonillas-Monge, Adrian Brennan, Gregory F Grether, Luis Mendoza-Cuenca, Rachel Tucker, Yesenia M Vega-Sánchez, Jonathan P. Drury

HXRCb13 collected from María Huatulco, Oaxaca, Mexico (15°44'24.00"N, 96°17'52.80"W) in June 2021 and provided the genetic material to assemble the draft genome of smoky rubyspots, *Hetaerina titia*.

This Chapter has already been published in full as Patterson, C.W., Bonillas-Monge, E., Brennan, A., Grether, G.F., Mendoza-Cuenca, L., Tucker, R., Vega-Sánchez, Y.M. & Drury, J. (2023) A chromosome-level genome assembly for the smoky rubyspot damselfly (Hetaerina titia). *Journal of Heredity*, esad070. Available at: https://doi.org/10.1093/jhered/esad070. It is reproduced here in full, with some minor formatting changes.

Abstract

Smoky rubyspot damselflies (*Hetaerina titia,* Drury, 1773) are one of the most commonly encountered odonates along streams and rivers on both slopes of Central America and the Atlantic drainages in the US and southern Canada. Owing to their highly variable wing pigmentation, they have become a model system for studying sexual selection and interspecific behavioural interference. Here, we sequence and assemble the genome of a female smoky rubyspot. Of the primary assembly (i.e., the principal pseudohaplotype), 98.8% is made up of 12 chromosomal pseudomolecules (2N = 22A + X). There are 75 scaffolds in total, an N50 of 120 Mbp, a contig-N50 of 0.64 Mbp, and a high arthropod BUSCO score (C:97.6% [S:97.3%, D:0.3%], F:0.8%, M:1.6%). We then compare our assembly to that of the blue-tailed damselfly genome (*Ischnura elegans*), the most complete damselfly assembly to date, and a recently published assembly for an American rubyspot damselfly (*H. americana*). Collectively, these resources make *Hetaerina* a genome-enabled genus for further studies of the ecological and evolutionary forces shaping biological diversity.

Introduction

Given their easily observable behaviour during adult life stages, odonates (Order Odonata, containing both dragonflies and damselflies) have emerged as model systems for many questions in ecology and evolutionary biology (Corbet, 1999; Cordoba-Aguilar, Beatty & Bried, 2022). Yet, genomic resources for aquatic insects are underrepresented relative to resources for other terrestrial insects (Hotaling, Kelley & Frandsen, 2020). There are currently only 10 odonate species with de novo assemblies present on GenBank, of which six are classified as chromosome-level assemblies and four are scaffolds.

Rubyspot damselflies (genus *Hetaerina*), in particular, have been widely studied among investigators interested in sexual selection (e.g. Grether, 1996; Córdoba-Aguilar *et al.*, 2009), as well as in understanding the causes and consequences of behavioural interference between species (Anderson & Grether, 2010a; Drury *et al.*, 2019a; Grether *et al.*, 2020). Recently, a genome assembly of *H. americana* was published (Grether *et al.*, 2023), enabling genomic research on this group of charismatic insects. However, because the best estimate for the crown age for the *Hetaerina* is 36.2 million years ago (Mya) and phylogenetic analyses demonstrate that the clade is paraphyletic and requires taxonomic revision (Standring *et al.*, 2022), more genomic resources beyond *H. americana* are needed to fully resolve species relationships and support genomic research on this taxon. Moreover, although the *H. americana* assembly provides a high-quality set of genomic resources, the scaffolds are not fully resolved into chromosomes; estimates from *Calopteryx* spp. suggest that members of Calopterygidae have 12 pairs of autosomes and an XO sex-determination system: females carry two X chromosomes, and male carry a single X chromosome (Kuznetsova & Golub, 2020; Kuznetsova *et al.*, 2021), but the *H. americana* assembly comprises over 1500 scaffolds.

One of the most widely studied *Hetaerina* species, smoky rubyspot damselflies (*Hetaerina titia*), currently lacks genomic resources. Smoky rubyspots damselflies are the most phenotypically distinct of rubyspot damselflies–both males and females possess melanin pigment in their wings (Figure 3:1) that distinguish them from the relatively transparent wings typical of other rubyspot damselflies. However, the extent of dark pigmentation varies both seasonally and geographically (Drury *et al.*, 2019b). Based on this extensive variation, *H. titia* was once divided into two species, *H. titia* and *H. tricolor*

(Johnson, 1963), though current taxonomic consensus treats *H. titia* as one highly variable lineage (Garrison, 1990; Drury *et al.*, 2015a).

Like other rubyspot damselflies, *H. titia* occurs along streams and rivers, with males defending mating territories along the banks and females descending from higher hunting perches to the river generally only to mate and oviposit. However, territorial males tend to perch higher and in slower parts of streams than sympatric congeners (McEachin *et al.*, 2022). Moreover, *H. titia* exhibits the largest latitudinal range of any *Hetaerina* species, stretching from Panama in the south to Canada in the north.

Here, we report the first genome assembly for *H. titia*, based on long-read sequence data from a female collected in Oaxaca, Mexico and Omni-C sequencing from a female collected in Chiapas, Mexico. We also present analyses comparing our assembly to the recently published genome of *H. americana* (Grether *et al.*, 2023) and to the highest quality zygopteran (damselfly) genome assembly of *Ischnura elegans* (Price, Winter & Brooks, 2022).

Methods

Biological Materials

A wild female *H. titia* (Figure 3:1B,C) was collected from Santa María Huatulco, Oaxaca, Mexico (15.74, -96.298) in June 2021 and submerged in RNAlater (Invitrogen) for Hifi sequencing. Another female *H. titia* was collected from Nuevo Milenio Santa Cruz la Central, Chiapas, Mexico (15.76,-93.30) in April 2023 and submerged in RNAlater for Omni-C scaffolding. We note that, given the XO sex determination system of Calopterygidae, all regions of the genome are sequenced by choosing female specimens. Specimen collection was conducted under permit SGPA/DGVS/04421/21, issued by the Mexican Secretaría de Medio Ambiente y Recursos Naturales (SEMARNAT).

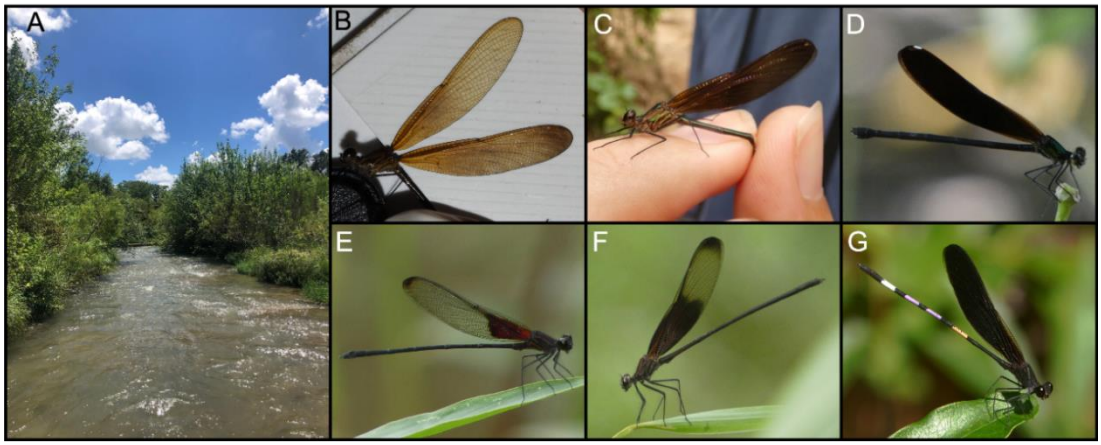

Figure 3:1: (a) An example photograph of a typical habitat where smoky rubyspot damselflies (*Hetaerina titia*) are found (Medina River in Castroville, Texas, U.S.A.). (b-c) The female H. titia individual collected in Santa María Huatulco, Oaxaca, Mexico that was used to construct the draft genome. (d-g) Examples of variation of wing pigmentation in (d) a highly melanised female (cf. panel c), and (e-g) males. All photos by Jonathan Drury.

Nucleic Acid Library Preparation

High Molecular Weight (HMW) DNA extraction was carried out at the Natural Environmental Research Council (NERC) environmental 'omics facility in Sheffield, UK. Upon receipt, the tissue samples were immediately removed from RNAlater and stored in SET buffer (75mM NaCl, 25mM EDTA pH8, 20mM Tris-HCl pH7.5) at -80°C. Fresh lysis buffer and Proteinase K solution were prepared as described in "10 x Genomics DNA Extraction from Single Insects" (https://support.10xgenomics.com/de-novo-assembly/sample-prep/doc/demonstrated-protocol-dna-extraction-from-single-insects 10 x Genomics) with modifications. Briefly, the whole damselfly was added to a lysis buffer of 10 mM Tris-HCl, 400 mM NaCl, 100 mM EDTA (pH 8.0), 10% SDS, and supplemented with 10 nM dithiothreitol (DTT). A Proteinase K solution containing 2 mg/ml of Proteinase K, 1% SDS, and 4 mM EDTA (pH 8.0) was added, and the sample was then homogenised in the lysis buffer by a pestle. The sample was left to digest overnight at 37° C.

The DNA was precipitated by adding 5 M NaCl and 100% ethanol, and, following centrifugation, the resulting pellet was washed twice with 70% ethanol. The

DNA was resuspended in elution buffer (Pacific Biosciences [PacBio], Cat #101-633-500) and left to elute at room temperature for 48 hours. The DNA was purified and concentrated twice with 0.45× AMPure beads (PacBio, Cat #100-265-900), to ensure samples were not contaminated with RNA, which can inhibit sequencing. To remove degraded DNA fragments (<9 kbp), and contamination such as pigment present in the tissue, the DNA sample was loaded onto the Blue pippin (Sage Science), using a 0.75% Agarose Cassette (Sage Science, Cat. #BLF7510) and 0.75 % DF Marker S1 high-pass 6-10 kb v3 cassette definition file. Fragments larger than 9 kb were collected, and smaller fragments were discarded. The size selected DNA sample was purified using 0.45× AMPure beads.

Purified DNA was quantified using a Qubit™ 3 Fluorometer (Invitrogen™ Q33216), its purity assessed using 260/280 and 260/230 ratios determined using a NanoDrop 8000 Spectrophotometer (Thermo Scientific™ ND-8000-GL), and finally analysed on a Femtopulse system to accurately size the fragments present within the sample (Agilent Technologies, Santa Clara, CA).

DNA Sequencing

HiFi Library Preparation and Sequencing was completed at the NERC environmental 'omics facility in Liverpool, UK. A HiFi SMRTbell library was constructed using the SMRTbell Express Template Prep Kit v2.0 with Low DNA Input (PacBio Cat. #100-938-900) according to the manufacturer's instructions. The HiFi SMRTbell library was sequenced using one SMRT Cell 8M, Sequel II sequencing chemistry 2.0, and 10-hr movies on a PacBio Sequel II sequencer.

Nuclear Genome Assembly

Circular consensus sequencing (CCS) reads with a quality score lower than 20QV were removed. PacBio Hifi adapters were screened and removed using HifiAdapterFilt v2.0 (Sim *et al.*, 2022). To estimate genome size and sequencing error rate, we used *jellyfish v2.3.0* (Marçais & Kingsford, 2011) to count k-mers using k=21 and then ported the data into *genomescope v2* (Ranallo-Benavidez, Jaron & Schatz, 2020). The *genomescope* genome size estimate was used to establish the most appropriate parameters for genome assembly. Genome assembly was then conducted using the program *Hifiasm v.0.16* (Cheng *et al.*, 2021, 2022) using default parameters. *Hifiasm* outputs two assemblies: a primary and alternative assembly consisting of each haplotype

of the diploid genome. We ran *purge_dups v1.2.6* (Guan *et al.*, 2020) on the primary assembly to identify duplicated regions of the assembly from either unidentified haplotypes or contig overlaps. We then removed these duplicates from the primary assembly, transferred them to the alternate assembly, and then ran *purge_dups* on the alternate assembly. We then screened the assemblies for contamination using *blastn* and *blobtoolkit2*/3.1.6 (Table 3:1) (Challis *et al.*, 2020).

Table 3:1: Assembly pipeline with software and version, as well as the options chosen where they differ from default of each software.

Assembly Stage	**Software and version**	**Options**
Assembly		
Filtering PacBio HiFi adapters	HiFiAdapterFilt v2.0	-l 34 -t 64 -m 80
K-mer counting	jellyfish v2.3.0	k=21
Estimation of genome size and heterozygosity	GenomeScope v1.0[1]	
De novo assembly (contiging)	HiFiasm v0.16.1	
Remove low-coverage, duplicated contigs	purge_dups v1.2.6	purge_dups -2 -T cutoffs, get_seq -e
Organelle assembly		
Mitochondrial genome	mitohifi v2.2	-c -o 5 -f MK722304.1 -g MK722304.1
	mitos2	
Genome quality assessment		
Genome completeness	BUSCO v5.3.2	-m genome -l insect_obd10/arthropoda_obd10
Contamination	Blastn (blobtoolkit2/3.1.6)	-outfmt "6 qseqid staxids bitscore std" -max_target_seqs 10 -max_hsps 1 -evalue 1e-25
Assembly metrics	quast/5.2.0	

[1]output archived at http://qb.cshl.edu/genomescope/analysis.php?code=JRQJM0S1JoMbmflwyqd1

Dovetail Omni-C Library Preparation and Sequencing

To further increase the contiguity of the assembly, Omni-C sequencing was conducted by Dovetail Genomics (Scotts Valley, US). Omni-C sequencing utilises the proximate physical distance between adjacent stretches of DNA in the nucleus to generate a map of physically linked DNA. Following standard manufacturer's protocol, formaldehyde was used to fix the chromatin within the nucleus and then the chromatin was extracted. DNAse I was used to digest the fixed chromatin and then chromatin ends were repaired and ligated to a biotinylated bridge adapter followed by proximity ligation of adapter containing ends. After proximity ligation, crosslinks were reversed, and the DNA purified. Purified DNA was treated to remove biotin that was not internal to ligated fragments. Sequencing libraries were generated using NEBNext Ultra enzymes and Illumina-compatible adapters. Biotin-containing fragments were isolated using streptavidin beads before PCR enrichment of each library. The library was sequenced on an Illumina HiSeqX platform to produce approximately 30x sequence genome coverage. Scaffolds were constructed using HiRise with MQ>50 reads (Putnam *et al.*, 2016).

To construct a scaffolded genome assembly, we used the un-contaminated primary contig assembly and Dovetail OmniC library reads as input data for HiRise (Putnam *et al.*, 2016). Dovetail OmniC library sequences were aligned to the draft input assembly using *bwa* (Li & Durbin, 2009). The separations of Dovetail OmniC read pairs mapped within draft scaffolds were analysed by HiRise to produce a likelihood model for genomic distance between read pairs, and the model was used to identify and break putative misjoins, to score prospective joins, and make joins above a threshold.

Quality assessment and assembly metrics

To estimate genome completeness and accuracy, we calculated the BUSCO v5.3.2 (Manni *et al.*, 2021) score of our assemblies using the lineage datasets *insecta_odb10* and *arthropoda_odb10*. Basic genome assembly metrics were calculated using *quast/5.2.0* (Mikheenko *et al.*, 2018). To compare our assembly's completeness and contiguity in relation to other available odonate assemblies, we calculated BUSCO scores (using insecta_ob10 and arthropoda_ob10) and NGX metrics for 10 odonate genomes on Genbank. We excluded assemblies where there was an obvious higher quality genome present for the same species.

Mitochondrial Genome Assembly

We assembled the mitochondrial genome of *Hetaerina titia* using the *mitohifi v2.2* (Uliano-Silva *et al.*, 2023) pipeline, which identified the mitochondrial genome of the confamilial species *Matrona basilaris* (genbank: MK722304.1) as a reference - the closest annotated mitogenome to *H. titia* available on NCBI. The mitochondrial annotation was conducted using *mitos2* (Donath *et al.*, 2019). Any identified contigs from the draft nuclear genome that were smaller than the draft mitochondrial genome and had a >99% match to the mitochondrial genome, using BLAST+ (Camacho *et al.*, 2009), were then removed from the primary (n = 1) and alternate (n = 0) assemblies using a custom R script and *blobtools* (Challis *et al.*, 2020).

Comparison with Ischnura elegans and Hetaerina americana

We visualised the synteny between the *H. titia* primary assembly with that of the chromosome level genome of *I. elegans* using a Circos Assembly Conistency plot built using the pipeline JupiterPlot (Chu, 2018), and a custom R script for final visualisation using the *circulize v0.4.15* package (Gu *et al.*, 2014) (Table 2). We also visualised the correspondence between *H. titia* versus the draft genome of *H. americana* (Grether *et al.*, 2023) and the genome of *I. elegans* (Price *et al.*, 2022) versus *H. americana*. We used LASTZ (Harris, 2007) to align each of the genomes and calculated the overall percentage of genomic similarity between *H. titia* and *I. elegans*, *H. americana* and *I. elegans,* and *H. titia* and *H. americana* using the total aligned length divided by the total number of mismatches.

Table 3:2: Genome alignment pipeline with software, version and options chosen (when non-default options used).

Purpose	Software version	Options
Genome data visualisation, Karyotype construction, and scaffold and bundle filtering	JupiterPlot-1.0 circulize v0.4.15	ref= HetTit1.0 scaf=HetAmer1.0 m=4000000 ng=95 t=24 ref=ioIscEleg1.2 scaf=HetTit1.0 m=100000 ng=80 minBundleSize=2500 maxGap=1000000 ref=ioIscEleg1.2 scaf=HetAmer1.0 m=100000 ng=80 minBundleSize=2500 maxGap=1000000
Pairwise scoring of alignment to calculate percentage of identity	LASTZ-1.04.15	lastz_32 --notransition --step=20 --nogapped --progress=1 --gfextend --chain --format=blastn

Results

Sequence Output and Genome Assembly

Sequencing attained 3,268,207 total PacBio Hifi reads spanning 24,472,197,766 bp (17.4x coverage for a genome of 1.4 Gbp, L50 = 8,304, N50 = 1068.5 kb). Omni-C sequencing generated 161,707,092 paired reads spanning 48,512,127,600 bp with an estimated coverage of 34.7x (for a genome of 1.4 Gbp). Analyses in *genomescope* estimated a genome size of 1.33 Gbp, a heterozygosity of 0.50%, and a sequencing error rate of 0.13%. K-mer density plots showed two peaks in coverage at ~8x and ~15x corresponding to the heterozygous and homozygous regions of the diploid genome. *HifiAdapterFilt* v2.0 identified 581 PacBio Hifi reads as adapter contaminated which we removed, and the remaining reads were assembled into contigs using *Hifiasm*. All assembly statistics, as well as NCBI Accession Numbers, are provided in Table 3, and assembly quality is depicted graphically in Figure 3:2A.

The total length of the scaffolded primary assembly was 1.44 Gbp, which is inline with the estimate of 1.33 Gbp from *genomescope*. The majority (98.8%) of the primary assembly was scaffolded into 12 chromosomal pseudomolecules. The final primary assembly consisted of 75 scaffolds, with a maximum scaffold length of 151.5 Mbp, an L50 of 6, and an N50 of 120 Mbp. There were 3798 gaps in the primary scaffolds with a total length of N bases of 0.4 Mbp (0.02% of the total assembled scaffolds' length). The alternative assembly was 1.43 Gbp and consisted of 4054 contigs with a maximum contig length of 3.1 Mb, an L50 of 664, and a N50 of 0.6 Mbps.

BUSCO analyses suggest that both primary and alternate pseudohaplotypes are near-complete genomes, with little duplication or missing data (Table 3). The primary assembly arthropoda BUSCO score was (C:97.6% [S:97.3%, D:0.3%], F:0.8%, M:1.6%).

Our final circular mitochondrial assembly was 17,701 bp long, with a base composition of A = 31.0 %, T = 40.5%, G = 15.7%, and C = 12.8%. Its annotation consisted of 22 transfer RNAs and 13 protein coding genes.

BUSCO and NGx metrics show that our genome is among the most complete and contiguous odonate genomes available (Figure 3:3)

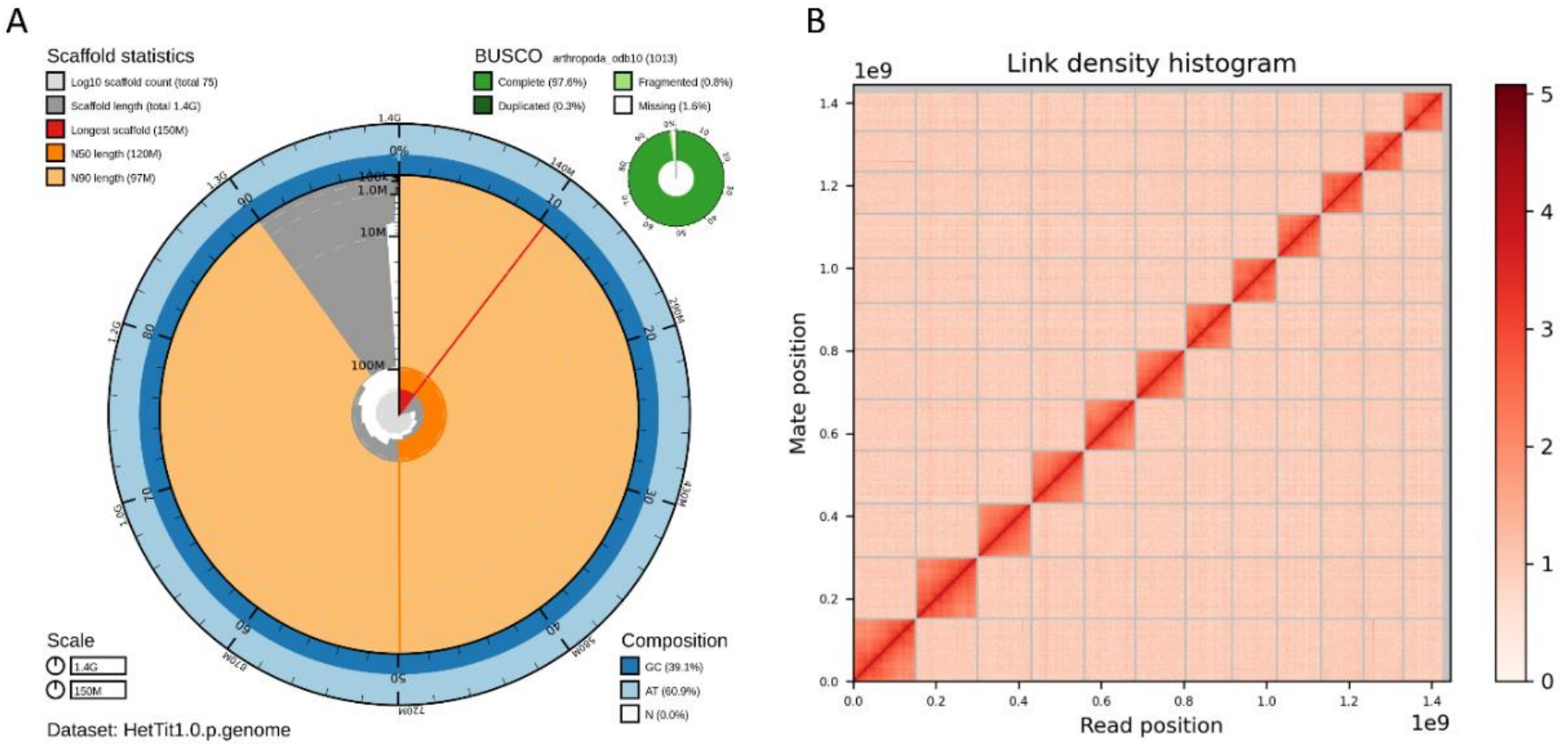

Figure 3:2: (A) The graphical representation of the primary (i.e., principal pseudohaplotype) draft genome assembly produced by blobtools2. The main plot is divided into 1,000 size-ordered bins around the circumference with each bin representing 0.1% of the 1,444,697,970 bp assembly. The distribution of record lengths is shown in dark grey with the plot radius scaled to the longest record present in the assembly (151,479,759 bp, shown

in red). Orange and pale-orange arcs show the N50 and N90 record lengths (120,343,728 and 97,068,442 bp), respectively. The pale grey spiral shows the cumulative record count on a log scale with white scale lines showing successive orders of magnitude. The blue and pale-blue area around the outside of the plot shows the distribution of GC, AT and N percentages in the same bins as the inner plot. A summary of complete, fragmented, duplicated, and missing BUSCO genes in the arthropoda_odb10 set is shown in the top right (see Table 3 for further details). (B) The Hi-C sequencing contact map. The density of the positions of the paired Hi-C sequence reads mapped onto the scaffolds of the primary assembly

Table 3:3: Sequencing and assembly statistics and accession numbers. Including BioPrjects and Vouchers for raw sequence reads and samples, Genome assembly metrics calculated by quast/5.2.0, BUSCO scores calculated using arthropoda_ob10 and insecta_ob10 (C = complete, S = single, D = duplicated, F = fragmented, M = Missing), and the organelle assembly accession number. Sequencing read coverage based on a genome size of 1.4 Gbp. Bp: base pairs. P: primary assembly, A: alternative assembly.

BioProjects & Vouchers	Species NCBI BioProject	PRJNA906955	
	NCBI BioSample	SAMN32641599	
	Specimen ID	HXRCb13	
	NCBI Genome Accessions	Primary	Alternate
	Genome sequences	GCA_037158775.1	GCA_037158765.1
Genome Sequencing	PacBio HiFi reads	Run	1 PACBIO_SMRT (Sequel II) run: 8M spots, 24.4G bases, 17.05Gb
		Accession	SRR23023424
	Omni-C data	Accession	SAMN35765994
Genome Assembly Quality Metrics	Assembly identifier	HetTit1.0	
	HiFi read coverage	17.4x	
	Omic-C read coverage	34.7x	
		Primary	Alternate

	No. contigs	4094			4054		
	Contig N50 (bp)	638359			664		
	Contig L50	639			631942		
	Longest contig	4037799			3160621		
	Number of scaffolds	75			NA		
	Scaffold N50	120343728			NA		
	Scaffold L50	6			NA		
	Largest scaffold	151479759			NA		
	Size of final assembly (bp)	1444296070			1429703052		
	BUSCO completeness (insect_odb10) n=1367		**C**	**S**	**D**	**F**	**M**
		P	97.0%	96.0%	1.0%	1.6%	1.4%
		A	95.9%	94.9%	1.0%	2.0%	2.1%
	BUSCO completeness (arthropoda_odb10) n= 1013		C	S	D	F	M
		P	97.6%	97.3%	0.3%	0.8%	1.6%
		A	96.2%	95.7%	0.5%	1.3%	2.5%
Organelle	Mitochondrion	NCBI Accession Number					OQ363879

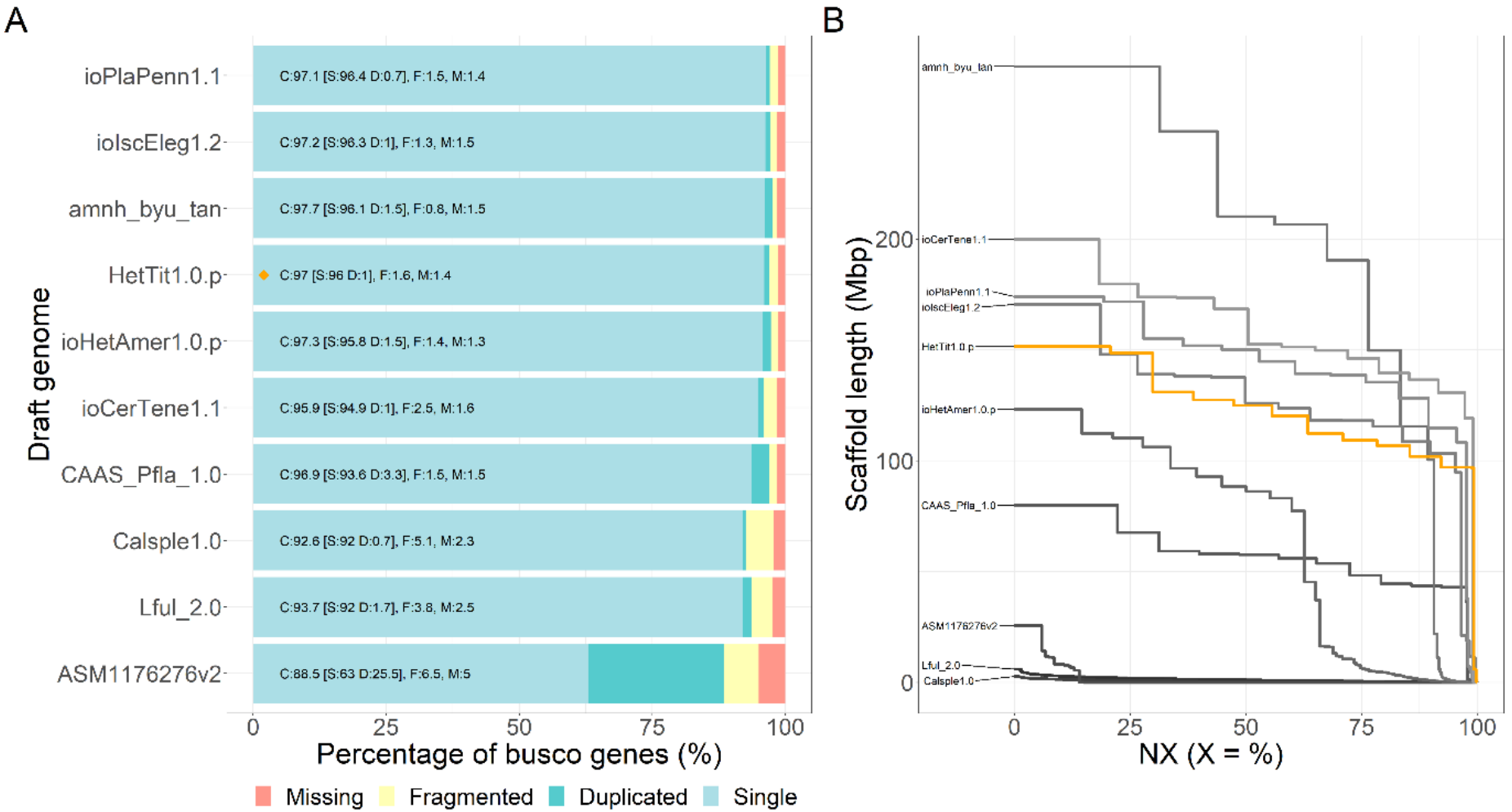
A
ioPlaPenn1.1
ioIscEleg1.2
amnh_byu_tan
HetTit1.0.p
ioHetAmer1.0.p
ioCerTene1.1
CAAS_Pfla_1.0
CalsIple1.0
Lful_2.0
ASM1176276v2
C:97.1 [S:96.4 D:0.7], F:1.5, M:1.4
C:97.2 [S:96.3 D:1], F:1.3, M:1.5
C:97.7 [S:96.1 D:1.5], F:0.8, M:1.5
C:97 [S:96 D:1], F:1.6, M:1.4
C:97.3 [S:95.8 D:1.5], F:1.4, M:1.3
C:95.9 [S:94.9 D:1], F:2.5, M:1.6
C:96.9 [S:93.6 D:3.3], F:1.5, M:1.5
C:92.6 [S:92 D:0.7], F:5.1, M:2.3
C:93.7 [S:92 D:1.7], F:3.8, M:2.5
C:88.5 [S:63 D:25.5], F:6.5, M:5
Draft genome
0
25
50
75
100
Percentage of busco genes (%)
Missing
Fragmented
Duplicated
Single
B
Scaffold length (Mbp)
200
100
0
NX (X = %)

Figure 3:3: Comparison of the genome completeness and contiguity for the 10 odonate genomes available on Genbank, with the primary assembly for Hetaerina titia (HetTit1.0.p) marked in orange. (A) BUSCO scores for each assembly using the insecta_ob10 dataset. (B) NGx plot showing scaffold/contigs of each assembly ordered from largest to smallest and the cumulative percentage of the genome covered. Included genomes are ioPlaPenn1.1, Platycnemis pennipes (Price & Allan, 2023), CAAS_Pfla_1.0, Pantala flavescens (Liu et al., 2022), ioSymStri1.1, Sympetrum striolatum (Crowley et al., 2023), ioCerTene1.1 Ceriagrion tenellum (Genbank: GCA_963169105.1), amnh_byu_tan, Tanypteryx hageni (Tolman et al., 2023), Lful_2.0, Ladona fulva, (Genbank: GCA_000376725.2), ioHetAmer1.0.p, Hetaerina americana, (Grether et al., 2023) Calsple1.0, Calopteryx splendens (Ioannidis et al., 2017), ASM1176276v2, Rhinocypha anisoptera (Genbank: GCA_011762765.2), and ioIscEleg1.2, Ischnura elegans, (Price *et al.*, 2022).

Comparative Analyses

There was a high level of correspondence between *H. titia*, *H. americana*, and *I. elegans* genomes (Figure 3:4A). However, neither *H. titia* or *H. americana* had a corresponding m-chromosome, a comparatively small pair of autosomes found in *I. elegans* and other odonates. In addition, the upper and lower half of the largest scaffold within the *H. titia* and *H. americana* genome (scaffold 1) mapped to two different chromosomes of *I. elegans* (scaffolds 9 and 12).

There is a high level of correspondence with the reference genome of *H. americana* (Figure 3:4B). *H. titia* scaffold 1, which matched two separate chromosomes of the *I. elegans* genome, mapped to a single large scaffold on the *H. americana* draft genome.

We calculated the overall similarity in aligned sequences between *H. titia* and *H. americana* as 88.44%. The overall similarity in aligned sequences between *H. titia* and *I. elegans* was 81.35%. The overall similarity between *H. americana* and *I. elegans* was 80.58%.

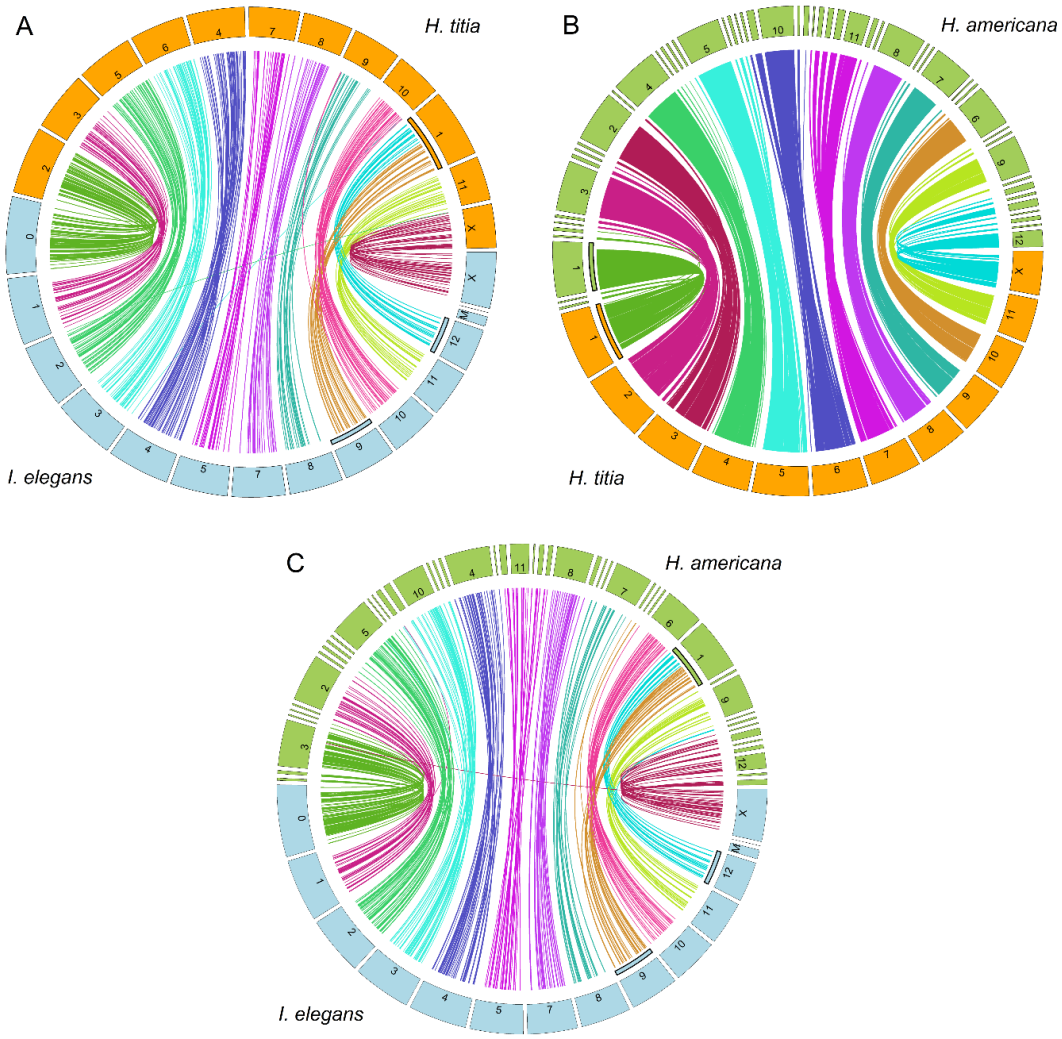

Figure 3:4: Circos assembly consistency plot showing the aligned regions between genome assemblies. Displayed scaffolds are restricted to those larger than 1Mbp **(A)** Scaffolds of *Ischnura elegans* (blue) (Price *et al.*, 2022) and *Hetaerina titia* (orange), **(B)** Scaffolds of *Hetaerina americana* (green) (Grether *et al.*, 2023) and *H. titia* (orange) **(C)** Scaffolds of *H. americana* (green) and *Ischnura elegans* (blue). Internal highlighting of chromosomes indicates a fusion event between chromosomes 9 and 12 of *I. elegans* into chromosome 1 of *H. titia* and *H. americana*. Scaffolds for *H. titia* and *H. americana* are numbered by length, largest to smallest. The *H. titia* X chromosome was identified by mapping to the X chromosome of *I. elegans*. Chromosome numbers for *I. elegans* were retrieved from NCBI. Scaffold and chromosome labels are consistent between plots.

Discussion

We generated a highly complete, high-quality de novo genome assembly from long-read and Omni-C sequence data obtained from two female smoky rubyspot damselfly (*Hetaerina titia*). BUSCO scores for the *H. titia* assembly reveal a more complete genome than many other existing assemblies of odonates. The highest single complete insecta BUSCO score, for another Odonata genome, is 97.4% for *Platycnemis pennipe*s (Price & Allan, 2023) vs. 97.0% for our draft genome of *H. titia* (for further comparison between all available odonate genomes see Figure 3:3A)). The 12 largest scaffolds are longer than 100 Mbps, which is comparable to the lengths of chromosomes of other odonates (Figure 3:3B, Ioannidis *et al.*, 2017; Price *et al.*, 2022, 2023), and comprise 98.8% of the total draft genome. Moreover, our mitochondrial assembly is highly complete and represents the first annotated mitochondrial assembly for *Hetaerina*. Our genome size estimate for *H. titia* (1.44 Gbp) is larger than an earlier estimate based on microscopy (1.1 Gbp - Ardila-Garcia and Gregory, 2009) but smaller than the sequencing-based estimates for *H. americana* (1.63 Gbp - Grether *et al.*, 2023) and *C. splendens* (1.6 Gbp - Price *et al.*, 2022).

Previous estimates of *Hetaerina* karotypes, including *H. americana* and *H. titia,* were 2N = 24A + X (not including the m-chromosomes) (Kuznetsova & Golub, 2020). Our findings suggest that the genome of *H. titia* is 2N = 22A + X, and does not have an m-chromosome, conflicting with previous estimates for the species and most other Calopterygidae genomes, such as *C. splendens,* which are 2N = 24A + X (plus an the additional m-chromosomes) (Kuznetsova & Golub, 2020; Kuznetsova *et al.*, 2021). The scaffold size of the *H. titia* draft genome was comparable to the chromosome-scale scaffolds of *I. elegans* (Price *et al.*, 2022). The *I. elegans* genome was constructed using PacBio Hifi sequencing and scaffolded to Hi-C data similar to that used in our genome assembly for *H. titia*. Each large scaffold of *H. titia* mapped concordantly onto a corresponding chromosome of *I. elegans*, with two exceptions: (1) The upper and lower half of scaffold one mapped onto two separate chromosomes of *I. elegans* and (2) there was no corresponding scaffold mapping to the m-chromosome of *I. elegans*. The linked density histogram of *H. titia* (Figure 3:2A) clearly indicates that *H. titia* has a single large chromosome and contains no evidence of an m-chromosome. The mapping of the *H. titia* and *H. americana* genome to the *I. elegans* genome (Figure 3:3A,C) supports a chromosomal fusion event and the loss of the m-chromosome in the shared ancestry of

H. titia and *H. americana* making the karyotype for these species 2N = 22A + X. Nearly all damselflies have greater than 22 autosomes making a fusion, rather than a fission event, within the ancestry of *H. americana* and *H. titia* the most parsimonious explanation. The loss of the m-chromsome is common within damselflies and its presence is often inconsistent within cytogenetic studies of the same species (Kuznetsova & Golub, 2020).

The relatively low similarity of the compared genomes of *H. titia* vs. *H. americana* (88.44%) likely results from the long-time separating *H. americana* and *H. titia* from their most recent common ancestor (estimated at ~33 Mya by Standring *et al.*, 2022). The considerable phylogenetic distance further supports the value of a high-quality reference genome for *H. titia*. Our de novo assembly for *H. titia* will serve to facilitate resequencing and genotyping of samples from this and other closely related *Hetaerina* species. The *H. titia* draft genome will enable further research into the evolutionary and demographic history of populations of *H. titia* in relation to the highly variable polyphenism of the species. The addition of a new chromosome scale assembly for Odonata will allow for further understanding of genome evolution within this early branching insect lineage (Tolman *et al.*, 2023). Further annotation of the *H. titia* genome would benefit the study of functional sequence evolution compared with *H. americana* and other congeners, opening the way for molecular evolutionary studies. The *H. titia* assembly described here, in combination with the recently assembled *H. americana* genome, make rubyspot damselflies a genome-enabled genus.

Funding

This work was supported by a NERC Environmental Omics Facility Grant (NEOF1274) to JPD, a NERC Cross-disciplinary Research for Discovery Science Grant (NE/X018199/1) to JPD, and funding from Durham University (including a Durham Doctoral Studentship to CP). EBM was supported by NSF DEB-NERC-2040883 to JPD and GFG.

Acknowledgements

Specimen collection was conducted under permit SGPA/DGVS/04421/21, issued by the Mexican Secretaría de Medio Ambiente y Recursos Naturales (SEMARNAT) to LMC. We thank Kelsey Yule for assistance in the field. We thank

Dovetail Genomics for sequencing and logistical support for the Omni-C sequencing and scaffolding.

Data Availability

Data generated for this project have been collated in NCBI BioProject PRJNA906955. The PacBio HiFi reads (with adapter indices and low-quality reads removed) for the sample (NCBI BioSample SAMN32641599) have been submitted to the NCBI Sequence Read Archive (SRR23023424). The Omni-C Illumina HiSeqX reads for the sample (NCBI BioSample SAMN35765994) have been submitted to the NCBI Sequence Read Archive (SRR25489624). The GenBank organelle assembly is submitted under the Accession number OQ363879. GenBank accessions for primary and alternate assemblies are GCA_037158775.1 and GCA_037158765.1, respectively.

Assembly code is available on GitHub at https://github.com/ChristophePatterson/Hetaerina_titia_genome

Chapter 4 Phylogeographic history of *Hetaerina* spp. reveal lineages at multiple stages of the non-ecological speciation cycle.

Typical riparian habitat of *Hetaerina* damselflies with damselfly and researcher in situ. Location: Santa María Huatulco, Oaxaca, Mexico (15°50'11.2"N 96°19'37.3"W) June 2021

Abstract

Non-ecological speciation is a process where allopatric lineages diverge in the absence of pronounced ecological differences, only coming into secondary contact after sufficient time for reproductive isolation to evolve. Many damselfly clades are characterized as non-adaptive radiations (the result of several rounds of non-ecological speciation), but there are few damselfly lineages for which we have a detailed understanding of the spatiotemporal dynamics of divergence. Using genomic data from 222 individuals of rubyspot damselflies (*Hetaerina titia*) across Central and North America, we investigated the phylogeographic history of this wide ranging species, finding strong evidence for a pronounced division between Pacific and Atlantic populations, and between Northern and Southern Atlantic drainages. Unexpectedly, we found evidence that Pacific and Atlantic populations of *H. titia* exhibit reproductive isolation in a point of secondary contact on the Isthmus of Tehuantepec in Mexico, suggesting that the Pacific form of *H. titia* comprises an undescribed species. Across several approaches for estimating the timing of splits, we found that Pacific and Atlantic forms of *H. titia* split more recently (~3.3Ma) than the broadly sympatric sister lineages *Hetaerina. americana* and *Hetaerina calverti* (~5.6Ma). In aggregate, our results support key assumptions of the non-ecological speciation model and demonstrate that these two pairs of sister lineages are at different stages of the non-ecological speciation cycle.

Introduction

The speciation cycle is key to explaining the diversity of life on earth and as such understanding the speciation cycle is a key aim of evolutionary biology (Tobias *et al.*, 2020). Yet many aspects of the process by which one population transitions to two allopatric populations then, upon secondary contact, become two sympatric species remain poorly understood. There are multiple outcomes to the speciation cycle, from two sympatric and reproductively isolated populations, to the admixture and collapse of the two diverging populations back into one (van der Valk *et al.*, 2021; Zou *et al.*, 2022), to parapatric species with hybrid zones (Barton & Hewitt, 1989; Irwin & Schluter, 2022; DeRaad *et al.*, 2022). The outcome of secondary contact is primarily predicted by divergence time but we lack a comprehensive understanding of which mechanisms (pre or post-zygotic barriers) primarily drive reproductive isolation and if this varies between each stage of the speciation cycle, how quickly each mechanism can arise, and if this varies between taxa (Matute & Cooper, 2021).

Moreover, investigations of the speciation cycle have predominantly focused on ecological speciation where the species divergence and reproductive isolation is driven by adaptation to different ecological niches (Schluter, 2000; Rundell & Price, 2009; Czekanski-Moir & Rundell, 2019). A second widely accepted model of speciation is non-ecological speciation, where divergence between species is not primarily driven by the natural selection for niche exploitation (Gittenberger, 1991; Czekanski-Moir & Rundell, 2019). Non-ecological speciation can be driven by several processes. The build-up of genomic incompatibles across the genome through genetic drift or at localized small barrier loci under local selection can build up between populations in allopatry (Ravinet *et al.*, 2017; Dion-Côté & Barbash, 2017; Westram *et al.*, 2022). Behavioural and phenotypic differences can enforce micro-habitat segregation (Vallin *et al.*, 2012; Duckworth *et al.*, 2015; Hood *et al.*, 2020; Patterson & Drury, 2023). And divergence in reproductive and antagonistic signals/apparatus (i.e. pre-zygotic barriers) can reduce the frequency of interspecific mating interactions (Arnegard *et al.*, 2010; Okamoto & Grether, 2013; McEachin *et al.*, 2022). Upon secondary contact, hybrids may be inviable (Tsuchida *et al.*, 2019), sterile (Xiong *et al.*, 2023), or have a lower fitness compared to non-hybrid individuals (Stelkens, Schmid & Seehausen, 2015; Irwin & Schluter, 2022). Non-ecological speciation can lead to a radiation of taxa that differ little in ecology, referred to as a non-adaptive radiation (Gittenberger, 1991; Rundell & Price,

2009; Czekanski-Moir & Rundell, 2019). Interest in non-ecological speciation is increasing because of the growing discovery of cryptic species by DNA sequencing (Eme *et al.*, 2018; Struck *et al.*, 2018). Many populations once assumed to consist entirely of interbreeding individuals with a single ecological niche, actually consists of two, or more, genetically differentiated species with little or no apparent ecological differentiation (Fišer, Robinson & Malard, 2018).

Damselflies (Odonata, suborder Zygoptera) are an iconic example of non-adaptive radiations (Wellenreuther & Sánchez-Guillén, 2016). During allopatry, damselflies undergo little ecological differentiation but undergo changes in morphological characteristics involved in mate recognition – see Wellenreuther and Sánchez-Guillén, (2016) for a review. For example, *Ischnura* have diverged in the morphology of mating appendages but little in ecology (Sánchez-Guillén, Van Gossum & Cordero Rivera, 2005). In *Calopteryx,* shifts in visual signals used in courtship reduce interspecific mating (Svensson *et al.*, 2010, 2014). Sánchez-Guillén *et al.*, (2014) showed a strong correlation between reproductive isolation and genetic differentiation among 30 species pairs of *Ischnura* damselflies. *Enallagma* have also undergone two separate radiations that were not primarily driven by filling available niches (McPeek & Brown, 2000). Having diverged around 200 Mya (Kohli *et al.*, 2021), with over 2942 described species, 309 genera, and 27 families (Suhling *et al.*, 2015), damselflies offer a wide range of opportunities to test the rate at which non-ecological speciation cycles progresses.

Here, we investigate the genus of damselflies, *Hetaerina*, to determine if divergence time predicts the outcome of secondary contact within a non-ecological radiation. *Hetaerina* damselflies have a crown age estimated to be 32 million years ago (Standring *et al.*, 2022) with most species living in sympatry with one or more heterospecific *Hetaerina* damselfly. There are currently around 38 recognised *Hetaerina* species (Garrison, 1990; Standring *et al.*, 2022), but the discovery that *Hetaerina americana* consists of at least two highly diverged and sympatric cryptic species, *H. americana* and *Hetaerina calverti* (Vega-Sánchez, Mendoza-Cuenca & González-Rodríguez, 2020; Vega-Sánchez *et al.*, 2024)*,* suggests the number may be higher. Reproductive clasper morphology is the only way to identify some adult *Hetaerina* species in the field (Vega-Sánchez *et al.*, 2020, 2024). Micro-habitat preferences have been found and are enforced by interspecific aggression (McEachin *et al.*, 2022). However, micro-habitat preference can switch between different sites (Anderson & Grether, 2011), and ecological niche

models have high degrees of overlap (Grether, Finneran & Drury, 2024), indicating *Hetaerina* is an example of a non-ecological radiation.

We investigate two geographically widespread lineages of *Hetaerina* from across North and Central America: the *H. americana* and *H. calverti* species complex and *Hetaerina titia*. Recent genetic analyses reveal that *H. americana* is split into at least three distinct lineages, the newly recognized *H. calverti* and two distinct allopatric clusters that are described as a Northern and a Southern cluster of *H. americana* (Vega-Sánchez *et al.*, 2024). *H. calverti* is found in sympatry at several sites with either the northern or southern lineages of *H. americana.* As of yet, there are no known sites where the northern and southern lineages are found in sympatry and there is little evidence of introgression (Vega-Sánchez *et al.*, 2024). *H. titia* exhibit the largest latitudinal range of any *Hetaerina* species sharing a high proportion of its range with *H. americana,* but the range of *H. titia* extends south beyond Mexico south to Costa Rica (Grether *et al.*, 2024). The phylogenies of *H. titia* constructed using single mitochondrial and nuclear genes suggest some genetic distinction between populations that reside in separate Pacific and Atlantic drainages (Drury & Grether, 2014; Drury *et al.*, 2019a). Given the large-scale phylogenetic distances within *H. americana* and that the range of *H. titia* covers a number of known phylogeographic boundaries, it is likely that *H. titia* also exhibits large scale phylogenetic distances. *H. titia* is of further interest because it exhibits a striking seasonal polyphenism in wing melanisation which has a significant impact on the frequency of interspecific behavioural interference from other *Hetaerina* damselflies (Drury *et al.*, 2015a, 2019b). As such, we also aim to understand the phylogenetic relationship between populations of *H. titia* with varying degrees of seasonal of polyphenism.

Taken together, these taxa represent a novel study system of a non-ecological speciation cycle with various pairs of lineages either existing in allopatry, undergoing secondary contact, or in sympatry. We create several SNP databases built from double digest restriction enzyme associated DNA (ddRAD) sequence data for samples of *H. titia*, *H. americana, H. calverti* from across North and Central America. We determine the number of distinct lineages within these species, and which lineages exist in sympatry, which are in allopatry, and which, if any, are undergoing secondary contact. We then estimate the divergence times between these lineages to understand the timescale for sympatry in a non-ecological radiation.

Methods

DNA extraction

Whole organism samples of *Hetaerina* damselflies were collected between 2006 and 2021 from across North and Central America, immediately placed in >99% ethanol and stored at either -80°C or -20°C in 5ml screwcap vials. DNA extraction was conducted using DNeasy Blood and Tissue Kits with full methodology outlined in the Supplementary Material.

ddRAD libraries

To generate genome wide SNP data for *Hetaerina* damselflies, with a focus on *H. titia* and *H. americana/calverti,* we followed a double digest restriction enzyme associated DNA (ddRAD) protocol (Peterson *et al.*, 2012). Library preparation was conducted twice creating two separate ddRAD libraries. Library One was conducted at the NERC environmental omics facility (NEOF), at the University of Sheffield, using the ddRAD protocol from DaCosta and Sorenson (2014). Library Two was conducted at Durham University Bioscience department following the methodology from Franchini *et al.* (2017). Both libraries used the same restriction enzymes PstI and EcoRI and both sets of adapters contained a region of four random nucleotides for PCR clone removal. After demultiplexing and clone filtering, sequence data from both libraries were analysed together. For Library One we processed 190 *Hetaerina* samples (183 *H. titia*, 4 *H. occisa*, and 3 *H. americana*) and in Library Two we processed 192 *Hetaerina* samples (112 *H. titia* and 80 *H. americana*). Full details of each library protocol are provided in Appendix Chapter 4.

Re-sequencing of highly heterozygous samples

Preliminary analysis, using the r package SambaR (de Jong *et al.*, 2021), identified five samples as having high levels of heterozygosity - one sample from Library One and four samples from Library Two. The samples with high heterozygosity in Library Two were processed within the same pool and had the same i5 inner barcode and are likely due to a fault in inner barcode ligation or pipette error. The likely cause of the high heterozygosity for the sample from Library One could not be determined. To determine whether laboratory error or hybridisation between divergent lineages was the cause for the high heterozygosity, we re-extracted DNA from tissue for the five identified

samples and re-sequenced them in line with the methodology described in Library Two. All four samples from Library Two did not show high levels of heterozygosity after re-sequencing. The sample from Library One retained high levels of heterozygosity. Further field collection was conducted at the same location as the sample that retained high levels of heterozygosity to collect 22 samples that were sequenced in line with the methodology described in Library Two.

SNP Calling

The demultiplexed sequence files were mapped to draft genomes using Burrow-Wheeler aligner (bwa) *mem* alignment algorithm (Li & Durbin, 2009). All sequences were separately mapped to a *H. americana* draft genome (Grether et al, 2023) and to a *H. titia* draft genome (Patterson *et al.*, 2023, Chapter 2). The full bioinformatics pipeline is outlined in Supplementary Figure 4:1 and all scripts can be found on GitHub (https://github.com/ChristophePatterson/Thesis-Phylogeographic-Hetaerina).

Increased phylogenetic distance decreases the probably that both samples will retain the same restriction enzyme sites, as such multiple SNP libraries were constructed with varying combination of species to avoid losing inference due to lack of share ddRAD loci between species. Firstly, two SNP libraries were produced that contained all *Hetaerina* samples (*H. americana/calverti, H. occisa, and H. titia*) and were mapped to either the *H. americana* or the *H. titia* draft genome. A further four different SNP libraries were constructed, again using both draft genomes, for all *H. americana* and *H. calverti* samples and, separately, all *H. titia* samples.

The filtered vcf files were imported into R using the package vcfR (Knaus & Grünwald, 2017). Further SNP and sample filtering, and conversion of vcf into compatible formats for each analysis software was done using the r package ape (Paradis & Schliep, 2019), adegenet (Jombart, 2008), and poppr (Kamvar, Tabima & Grünwald, 2014).

Hetaerina *species delimitation and population structure.*

To determine the population structure of *H. titia* and *H. americana/calverti,* we used the r package LEA (Frichot & François, 2015) to conduct principal component analysis (PCA) and non-negative matrix factorization algorithms (sNMF) for least-squares estimates of ancestry proportions for each sample (Frichot *et al.*, 2014). sNMF analysis produces comparable estimates of ancestry estimates as structure (Hubisz *et al.*,

2009) and admixture (Alexander, Novembre & Lange, 2009) but with faster computation time (Frichot *et al.*, 2014). We ran sNMF analysis on all SNP libraries. We restricted the SNPs to those that were biallelic and removed samples that had more than 20% missing data. To maintain equal level of ploidy we removed SNPs mapped to the single sex chromosome found in *Hetaerina*. In sNMF, we tested for a range of ancestral populations (K = 1 to 10) and plotted the mean cross-entropy values for 100 repetitions. We used *hierfstat* (Goudet, 2005) to calculate Fst between each identified cluster. To avoid recent introgression (<2 generations) violating the assumption of the phylogeny and demographic analysis, we excluded samples CUAJa02 and all other samples from sample sites CUAJ01 and CUAJ02 from later analysis. Although other samples from site CUAJ01/02, did not show any evidence of high levels of heterozygosity or introgression, we removed samples site from our phylogenetic and demographic analysis to ensure model assumptions were met.

Phylogenetic inference of Hetaerina

We constructed a maximum likelihood phylogenetic tree of *H. titia*, *H. calverti*, and *H. americana* using RAxML/8.2.12 (Stamatakis, 2014). We limited the SNP libraries generated by bcftools (Danecek *et al.*, 2021) to only homozygous sites (heterozygous sites coded as missing), then removed samples with greater than 20% missing data, and then excluded invariant sites. We ran RAxML on all six SNP datasets produced by mapping ddRAD sequence reads to either *H. titia* or *H. americana* draft genome (Supplementary Table 2). In RAxML we used a general time reversible model (GTR), a gamma distribution of rate heterogeneity, and a Lewis ascertainment correction due to the exclusion of invariant sites (-m = ASC_GTRGAMMA) based upon the RAxML manual recommendation and similar studies (Lozier *et al.*, 2016; Devitt *et al.*, 2019). In addition, phylogenetic inference was also conducted using SVDquartets (Chifman & Kubatko, 2014) within the programme PAUP* (Wilgenbusch & Swofford, 2003). The dataset generated for SVDquartet was the same as that used in RAxML but heterozygous sites, which are compatible with SVDquartet analysis, were retained. We calculated the SVD score of 100,000 unrooted 4-'taxa' trees (quartets) to infer the optimal phylogenetic relationship between the samples for each quartet. We then constructed a consensus tree across all samples from the quartets using the Quartet FM method (Reaz, Bayzid & Rahman, 2014). We repeated this process 100 times to produce

bootstrap support values for each tree node determined by the percentage of times the node was part of the consensus topology of the trees.

Species/lineage delimitation

To build a more detailed understanding of the process by which each lineage of *H. titia* and *H. americana* arose, we used the R package *delimitR* (Smith & Carstens, 2020). *delimitR* uses site frequency spectrums (SFS) built from a SNP data set to predict the most likely demographic history for a number of potential populations or species. *delimitR* uses fastsimcoal2 (v2.6) (Excoffier *et al.*, 2013, 2021) to simulate SFS for each specified demographic scenario under a range of priors and then builds a random forest classifier. The random forest classifier is used to estimate the most likely demographic scenario for the observed data. We used *delimitR* to estimate the most likely demographic scenario that gave rise to the population clusters of *H. titia, H. americana*, and *H. calverti* identified by sNMF. Separately for both *H. titia* and for *H. americana* and *H. calverti* we simulated each valid combination of the following demographic scenarios; one to three potential lineages that arose either by pure isolation, isolation with gene flow, isolation with secondary contact, or isolation with constant migration. We used a broad range of uniform priors to simulate each demographic scenario. Effective populations size (N*e*) was set from 100,000 to 2,000,000, divergence time for the first population split (Tdiv1) was 500,000 to 8,000,000 generations, and divergence for the second population split (Tdiv2) was 500,000 to 12,000,000 generations. We set Tdiv1 to be always greater Tdiv2. Migration rates were set from 0.000005 to 0.0005 as a proportion of N*e* per generation.

Input SFS was calculated using the package *easySFS* (https://github.com/isaacovercast/easySFS) which builds off the *dadi.Spectrum* class from the software dadi (Gutenkunst *et al.*, 2009). To take into account un-genotyped SNPs, which are inherent to ddRAD data, we projected down the SFS to maximise the number of segregating sites following (Gutenkunst *et al.*, 2009).

Hetaerina *divergence estimation*

To estimate the divergence time of *H. titia, H. americana, H. calverti*, and any distinct sub-populations of each species identified by LEA, PCA, RAxML and SVDquartet, we ran the Bayesian coalescent analysis SNAPP implemented within the programme Beast v2.7.5 (Bouckaert *et al.*, 2019). Due to computational constraints, we

restricted the analysis to four individuals per cluster (24 individuals in total) with the highest SNP coverage from each distinct ancestral clustering identified by LEA. We removed the SNPs that were no longer polymorphic between the selected samples, that were genotyped in at least one individual from each population, and that mapped to X chromosome. This retained 552 SNPs when using SNPs mapped to the *H. titia* draft genome and 527 SNPs when using the SNPs mapped to the *H. americana* draft genome. We used previous estimate from Stranding et al (2022) to select priors by secondary calibration for divergence time between *H. titia* and *H. americana/calverti* (mean = 33.08 million years ago (mya), sigma = 5.53mya) and for the divergence of *H. americana* and *H. calverti* (mean = 3.76mya, sigma = 1.87mya). We used a starting tree that had the same relationships identified by RAxML and SVDquartets for each of the clusters and ran MCMC for 1,000,000 generations, sampling every 500 iterations. A SNAPP configuration file was created using a custom R script and the ruby script from https://github.com/mmatschiner/snapp_prep. We assessed the convergence using tracer and calculated the maximum clade credibility tree, with a 10% burn in removal, using the *treeannotator* program distributed with Beast.

To further estimate the divergence times using an independent approach, as well as to estimate effective population sizes and asymmetrical post-divergence migration rates between sub-populations of *H. titia, H. americana,* and *H. calverti,* we used *G-Phocs* (Gronau *et al.*, 2011). In comparison to previous analysis which used SNP datasets, G-Phocs uses sequences of whole loci. G-Phocs uses MCMCcoal to estimate divergence times and effective population sizes from multilocus sequence data and allows users to specify migration bands between lineages. We used a custom R script to generate consensus sequences for whole ddRAD loci for each sample from the vcf output of bcftools call command retaining invariant sites. We removed loci that had a sequence length of less than 100 and had greater than 50% missing base calls. Due to computational constraints, we restricted G-Phocs analysis to the three samples with highest loci coverage from each ancestral cluster identified by sNMF and include no more than 2000 randomly selected ddRAD loci, similar to Prates *et al.*, (2018). We used the tree topology generated from RAxML, SVDquartet, and SNAPP and ran G-Phocs with and without migration for all possible migration bands within the tree (with the exception of migration from either of the recently diverged lineages to the older lineage, which is an unresolved issue within G-Phocs: https://github.com/gphocs-dev/G-PhoCS/issues/25). We ran G-Phocs with a range of uninformative priors following

Prates *et al* (2018). The effective population size (theta - Θ) and the divergence times (tau - τ) priors were set using gamma distributions of α=1 and β=20, and α=1 and β=200, respectively. The migration rate prior was set to a gamma distribution with α=1 and β=2e-7. To avoid ascertainment bias in loci mapped to a more closely related draft genome we compared divergence times between lineages of *H. titia* and *H. americana* using loci mapped to the relative heterospecific draft genome.

Each run of G-Phocs was conducted for 1,000,000 iterations with a 10% burn-in and sampled every 100 iterations. We optimised the initial acceptance rate to be 30-40% by running 100 interactions of automatic fine-tuning. Convergence was confirmed by visualising trace plots in R. The R package *coda* was used to calculate the effective sample size (ESS) and the 95% Highest Posterior Density (HPD) from the trace file. We converted mutation rate-scaled parameter estimates of G-Phocs into the number of diploid individuals and the number of years using 2.8e-9 mutations per base pair per generation (Keightley *et al.*, 2014). We converted generations to years using an estimated generation time of one year.

Investigation of a potential secondary contact zone

Preliminary analysis identified at least one individual that had a mix of Pacific and Atlantic ancestry. To determine the number of generations since the potential hybridisation event and see if any other individuals had admixed ancestry, we ran a hybridisation analysis using the R package *introgress* (Gompert & Buerkle, 2010). We subset our data to samples from sites in and around the Isthmus of Tehuantepec. We calculated the allele frequency for each SNP for both Pacific and Atlantic populations, excluding samples from the site where the putative hybrid was identified. We then subset our dataset to 886 autosomal SNPs and 21 sex linked SNPs that had an allele frequency difference greater than 0.8 between the Pacific and Atlantic, in line with DeRaad *et al.* (2022). We then assigned each allele to a "parental" Pacific or Atlantic genotype, calculated the percentage of Pacific and Atlantic alleles carried by each sample (the hybridisation index), and then calculated the average autosomal heterozygosity across all highly divergent SNPs (the multi-allele heterozygosity) for each sample. For recent introgression(~3 generations), *introgress* can provide estimates of the parental history of hybrid individuals, for instance, an F_1 hybrid would have a hybrid index of 0.5 and a multi-allele heterozygosity of 1 (Fitzpatrick, 2012).

Results

For brevity we focus on results from the SNP libraries mapped to higher quality draft genome of *H. titia*. For analysis using the draft genome of *H. americana* see Appendix Chapter 4. For *H. titia,* we retained 222 *H. titia* samples with 3,730 SNPs. The remaining samples had a median percentage of missing genotypes of 2.21% which ranged from 0.21% to 20.61%. We retained 57 *H. americana/calverti* samples with 1,798 SNPs. The remaining samples had a median percentage of missing of 3.84% and ranged from 0.16% to 19.75%.

Hetaerina titia *population structure*

We identified three distinct clusters in *H. titia* (Figure 4:1): the cross-entropy values from sNMF admixture analysis showed a strong inflection at K = 3, with a cross entropy value of 0.22 (Supplementary Figure 4:3). Cross-entropy values decreased to 0.21 at K = 7, but the calculated cross-entropy values overlapped with repeats using K = 3. The cross-entropy values for higher values of K did not increase but rather remained at 0.22.

Our principal component analyses returned similar results with axis one and two grouping samples into three distinct zones (Figure 4:2). Both PCA and sNMF indicated the existence of three distinct groups which segregated into (1) a Pacific Coast cluster, (2) a Caribbean and South Gulf cluster, and (3) a North Gulf and Atlantic cluster (Figure 4:1, Figure 4:2). We refer to these three clusters as the Pacific *H. titia*, the Southern Atlantic *H. titia*, and the Northern Atlantic *H. titia*, respectively. We identified one sample with extensive admixture, between the Pacific and Southern Atlantic clusters, from site CUAJ01 in Cuajinicuil, Oaxaca (16° 47'24.00"N, 95°0'36.00"W) on the Gulf slope of Isthmus of Tehuantepec (Mexico).

The pairwise Fst values between the three identified groups indicate a highly differentiated population structure. Fst was 0.803 between the Pacific and Northern Atlantic, 0.716 between the Pacific and Southern Atlantic, and 0.507 between the Northern and Southern Atlantic. Fst values indicate that the Northern and Southern Atlantic clusters are more closely related to each other than the Pacific populations.

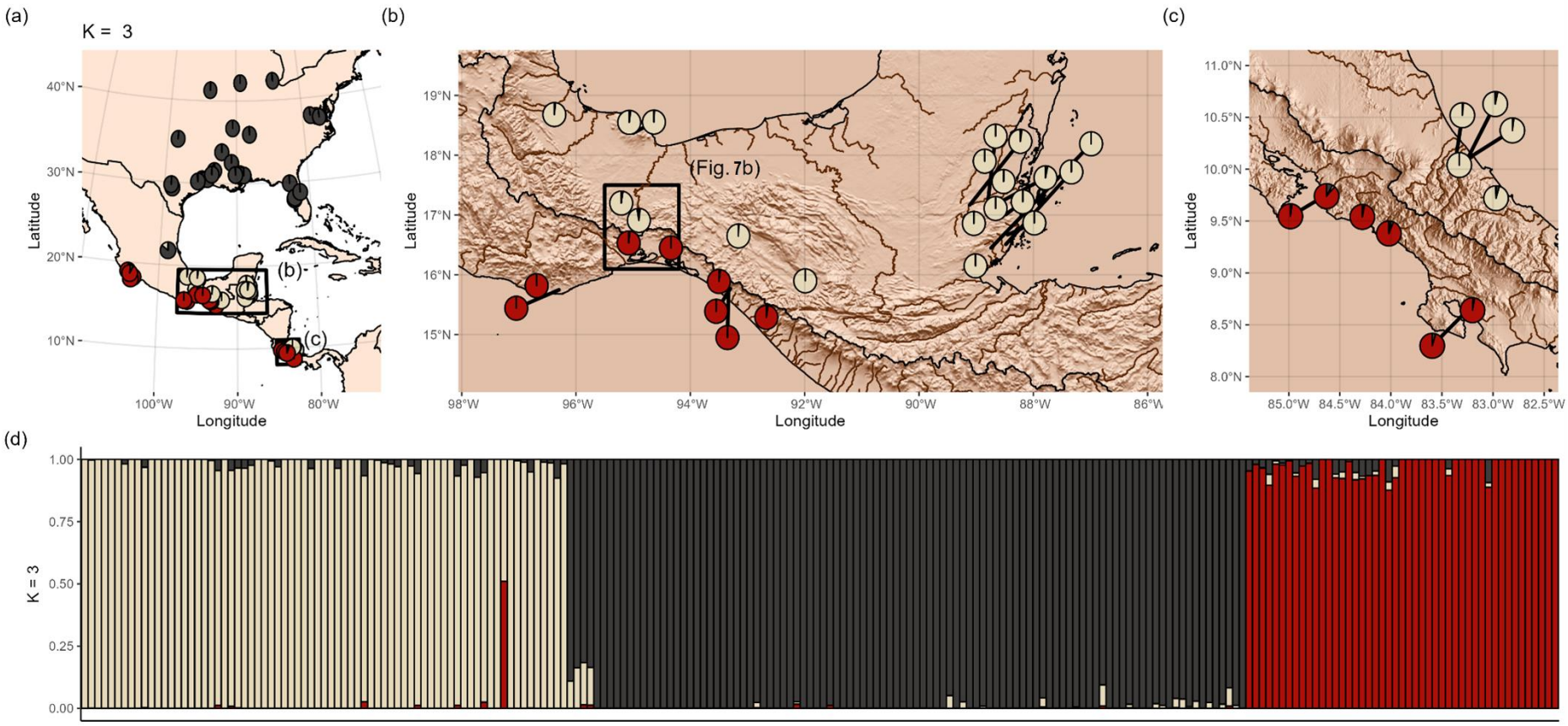

Figure 4:1: Ancestry estimates using three ancestral populations for 222 *Hetaerina titia* with a dataset of 3,815 unlinked biallelic autosomal SNPs. SNPs were generated by mapping ddRAD reads to the draft genome of *H. titia*. sNMF was run for 20 repetitions and an alpha value of 100. **(a)** The mean estimate of ancestry proportion for all samples within each sample site of *Hetaerina titia* across North and Central America, **(b)** Isthmus of

Tehuantepec and Belize, and **(c)** Costa Rica**. (d)** Estimate of ancestry analysis for each individual. Samples are ordered by drainage, then country, and then latitude. Rivers and drainage basins from Hydrosheds. Topography data from the R package *elevatr*. The black boxes shown in panel **(a)** are the bounding areas for facets **(b)** and **(c).** The black box in facet **(b)** is the bounding box for Figure 4:7b.

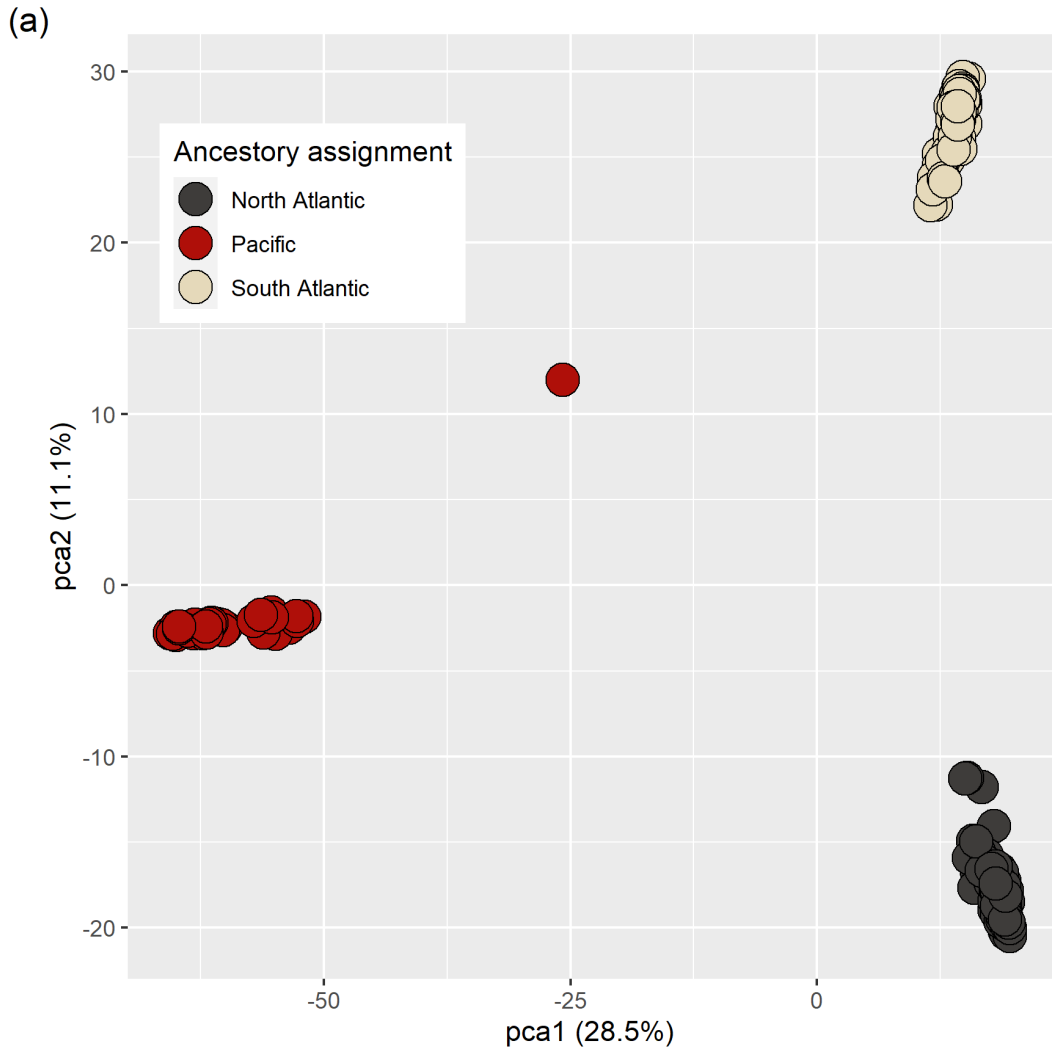

Figure 4:2: **(a)** Principal component analysis of 222 *Hetaerina titia* with a dataset of 3,815 unlinked biallelic autosome SNPs. Percentages indicate how much variation is explained by each component and colour indicates the highest assigned ancestry population from sNMF for each individual. The single point directly between the main Pacific and Atlantic cluster is an F_1 hybrid.

Hetaerina americana and H. calverti population structure

In our analyses of *H. americana* and *H. calverti*, we also found evidence for three distinct clusters. The cross-entropy values for sNMF showed a strong inflection at K = 3, with a cross entropy value of 0.250 that decreased to 0.245 at K = 4, but with a range that overlapped with K = 3. After K = 4 the mean cross-entropy values increased (Supplementary Figure 4:4).

Principal component analyses were concordant with admixture analyses; both PCA and sNMF indicated the existence of three distinct groups which separated *H. calverti* from a Northern and Southern grouping of *H. americana*. We identified three sites where both Southern *H. americana* and *H. calverti* were found in sympatry with no evidence of admixture. Our ancestry analysis indicates *H. americana* is split into two different populations - a Northern population, that resides in the continental United States and a Southern population, found on both the Gulf and Pacific slopes of Mexico (Figure 4:3). *H. calverti* is also present in both the Gulf and Pacific slopes of Mexico. We refer to these lineages as Northern *H. americana* and Southern *H. americana* going forward. Pairwise F*st* values between the identified groups were 0.815 (*H. calverti* vs Northern *H. americana*), 0.772 (*H. calverti* vs Southern *H. americana*), and 0.674 (Northern vs Southern *H. americana*).

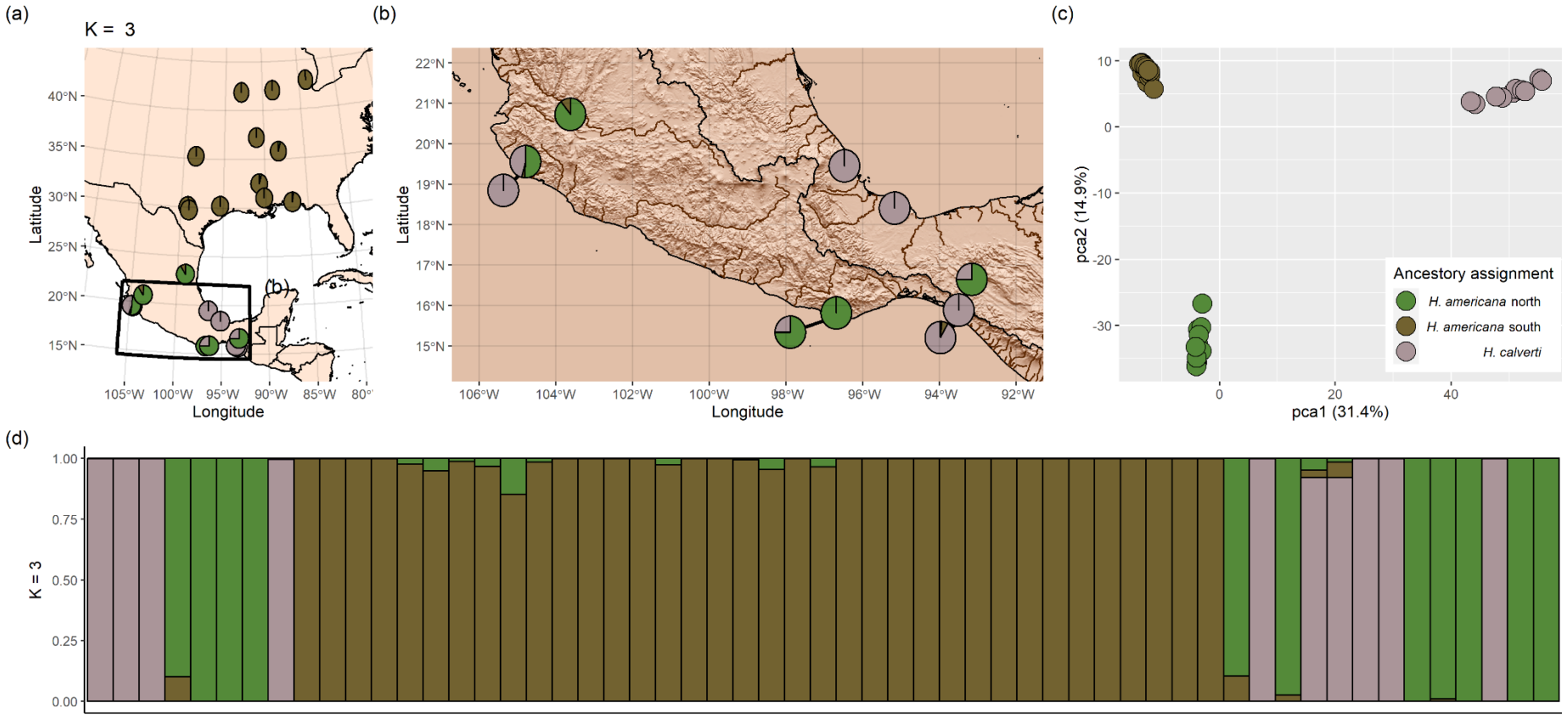

Figure 4:3: Ancestry estimates using three ancestral populations for 58 *Hetaerina americana/calverti* with a dataset of 1,798 unlinked biallelic autosomal SNPs, 20 repetitions and an alpha value of 100. **(a, b)** The mean estimate of ancestry proportion for all samples within each sample site of *H. americana/calverti*. . **(c)** Principal component analysis of the same dataset with sample colour indicating the highest assigned ancestry population

from sNMF for each individual. **(d)** Estimate of ancestry analysis for each sample. Samples are ordered by drainage, then country, and then latitude. Rivers and drainage basins from Hydrosheds. Topography data downloaded using R package *elevatr*.

Phylogenetic inference of Hetaerina

The maximum likelihood multi-species tree separated samples into species and several distinct sub-species groups. In agreement with population structure analyses, populations of *Hetaerina titia* that reside in drainages that flow into the Atlantic, including the Gulf of Mexico and the Caribbean, are more closely related to each other than populations that reside in drainages that flow into the Pacific. The Atlantic lineage is split into two groups, (1) samples that originated from the continental United States and the most Northern sample site in Mexico, and (2) the remaining samples from Mexico, Belize, and Costa Rica. Within the Pacific *H. titia* lineage there are three distinct groups, one group from Costa Rica and two separate Northern and Southern lineages in Mexico. The RAxML tree generated from a larger SNP library that only contained *H. titia* identified the same groups as the multi-species tree but with the additional separation of samples from the Caribbean slope of Costa Rica from samples from Mexico and Belize (Figure 4:4). The tree containing only *H. titia* also indicates that populations of *H. titia* from Florida are closely related to those at higher latitudes in Virginia and Michigan.

A high number of samples that were originally collected as *H. americana* are identified as being on a separate, highly diverged lineage. The separate lineage corresponds to the recently identified *H. calverti* (Vega-Sánchez *et al.*, 2020). Based off our genetic analysis, many newly identified *H. calverti* were collected from sites that also contained samples identified as *H. americana*. Within the *H. americana* lineage there is a distinct split between population in continental United States and populations in Mexico. Unlike *H titia*, neither *H. americana* nor *H. calverti* split into Pacific and Atlantic drainages. For *H. americana* and *H. calverti*, the same groups were identified by RAxML when using just *H. americana* and *H. calverti* samples (Supplementary Figure 4:14). All inference from SVDquartet analysis was in concordance with results from RAxML (Supplementary Figure 4:15).

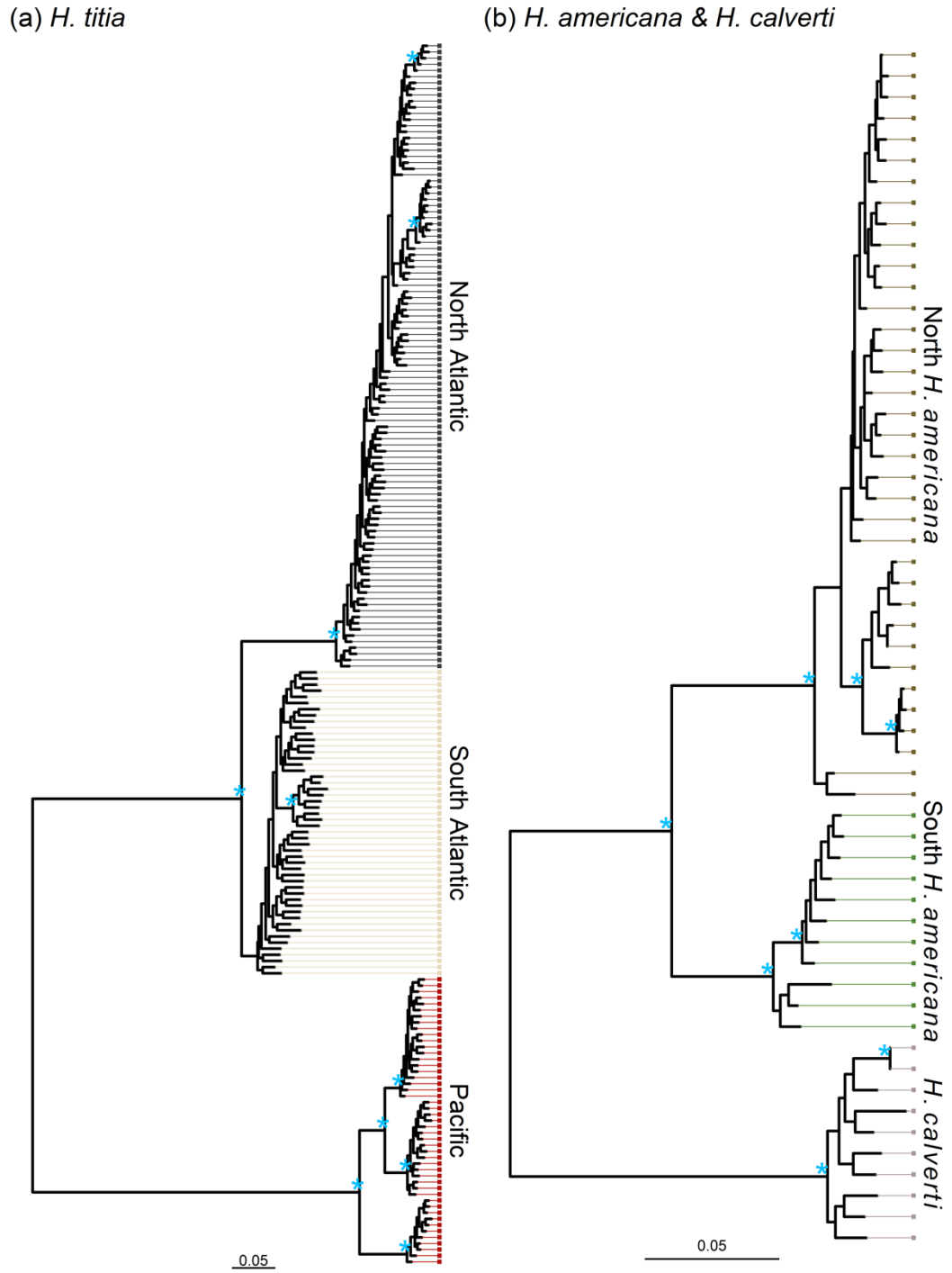

Figure 4:4: The maximum likelihood tree for (a) *Hetaerina titia* and (b) *Hetaerina calverti* and *Hetaerina americana* calculated by RAxML. 3,002 SNPs for *H. titia* and 1,381 SNPs for *H. americana* and *H. calverti* and mapped onto the genome of *H. titia*. Scale bar indicates number of substitutions per SNP site. The node marked with a blue star "*" indicate a bootstrap support value (out of 100) of greater than 95%. The tree tips are coloured according to the species and the max sNMF ancestry assignment (K=3) shown in Figure 4:1 and Figure 4:3.

Species and population delimitation

The best fit demographic scenarios for *H. titia* were firstly, three separate lineages with isolation with gene flow between the Northern and Southern Atlantic lineages (Model-13, 83.5%), and, secondarily, three separate lineages with no migration (Model-5, 16.4%). The out of the bag error rate varied between different *H. titia* demographic scenarios but was low across all models (<10%) and especially for models 5 and 13 (3.5% and 1.61%). Furthermore, incorrect classifications of models 5 and 13 were limited to the alternative of these two scenarios. When plotting using PCA, the SFS simulation results for models 5 and 13 are distinct from other demographic scenarios. For *H. americana/calverti*, the favoured model was, firstly, three separate lineages with no migration (Model-5, 64.1%) and, secondarily, three lineages with isolation with migration between the Northern and Southern lineages of *H. americana* (Model-13, 24.3%). The out of the bag error rate for *H. americana* and *H. calverti* demographic scenarios varied but were again low for models 5 and 13 (5.71% and 1.9%, respectively) and incorrect classifications limited to the alternative of these two scenarios. No other demographic scenarios for either *H. titia* or *H. americana/calverti*, received more than 10% support. Model selection using delimitR suggests little historical secondary contact between any lineages within *H. titia* or between *H. americana,* and *H. calverti*. The exception being there may have been isolation with migration between the Northern and Southern Atlantic lineages of *H. titia*.

Divergence times

All SNAPP runs constructed a basic tree topology that was identical to that of RAxML and SVDquartets (Figure 4:5), all runs converged (ESS>1000), and all nodes had a posterior probably of one. SNAPP analysis using the SNPs mapped to the *H. americana* genome and the *H. titia* genome converged on the same tree and estimates of divergence times between each species and sub-population overlapped. Using the SNP data mapped to the *H. titia* genome, the divergence time between *H. titia* and *H. americana/calverti* was estimated to be 28.6 mya (95% highest posterior density (HPD) 18.4-37.8mya). The divergence between *H. calverti* and *H. americana* was estimated to be 5.6mya (HPD 3.5-7.7mya) and show in Supplementary Figure 4:16. SNAPP analysis also identified relatively distant dates for the divergence between the sub-populations within *H. titia* and *H. americana*. Populations of *H. titia* that reside in Atlantic drainages

were estimated to have diverged from populations in the Pacific 3.6mya (HPD 2.1-5.1 mya). The two lineages of H. titia that reside within Atlantic drainages separated an estimated 1.0mya (HPD 0.5-1.5mya). The two identified lineages of *H. americana* diverged 2.5mya (HPD 1.2-3.5mya). Across 99.6% of posterior distribution trees, the split between Pacific and Atlantic *H. titia* was younger than the split between *H. americana* and *H. calverti*. The mean difference in ages between the split of *H. americana* and *H. calverti*, and Pacific and Atlantic *H. titia* was 2.0 million years, HPD 0.5-3.6 million years).

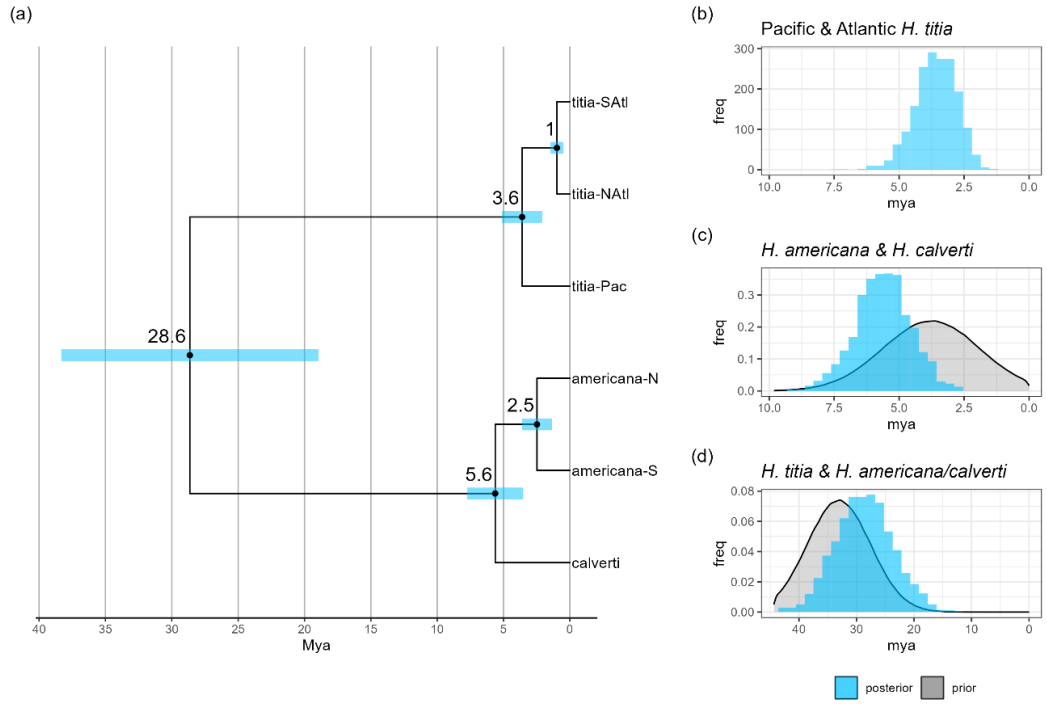

Figure 4:5: **(a)** Estimates of divergence dates (million years ago - mya) between populations of Pacific *Hetaerina titia* (titia-Pac), Atlantic *H. titia* (titia-NAtl and titia-SAtl), *Hetaerina americana* (americana-N and americana-S), and *Hetaerina calverti* (calverti) calculated using SNAPP analysis in Beast. Node labels indicate the mean estimated divergence date with 95% highest posterior density in blue. All branches had a posterior distribution of 1. Tree plotted in R using the packages *treeio* and *ggtree*. Input data was 552 autosomal SNPs mapped to the genome of *Hetaerina titia*. **(b-c)** The prior and posterior distribution (where applicable) of divergence times between the major lineages.

Estimates of the divergence times and effective population size estimated by G-Phocs were broadly consistent with those of SNAPP (Figure 4:6, Supplementary Figure 4:17) but did vary between models that included different migration bands. For brevity, we present the two demographic models that were best supported by delimitR. For G-Phocs models for *H. titia* without migration, the estimated divergence times between Atlantic and Pacific *H. titia* was 3.0 mya (2.8-3.1 mya HPD). For models without migration, the divergence between *H. caverti* and *H. americana* was 4.0 mya (3.8-4.1 mya HPD). Models without migration estimated the most recently diverged lineages of *H. titia* and *H. americana* split 0.9 mya (0.8-0.9mya HPD) and 1.6 mya (1.4-1.9 mya), respectively. For models with migration between the Northern and Southern Atlantic *H. titia*, which was moderately supported by delimitR, the divergence time between Northern and Southern Atlantic *H. titia* was pushed back to 1.7 mya (1.4-1.9 mya HPD) but had little impact on the divergence between any other split in *H. titia* or *H. americana*, or *H. calverti.*

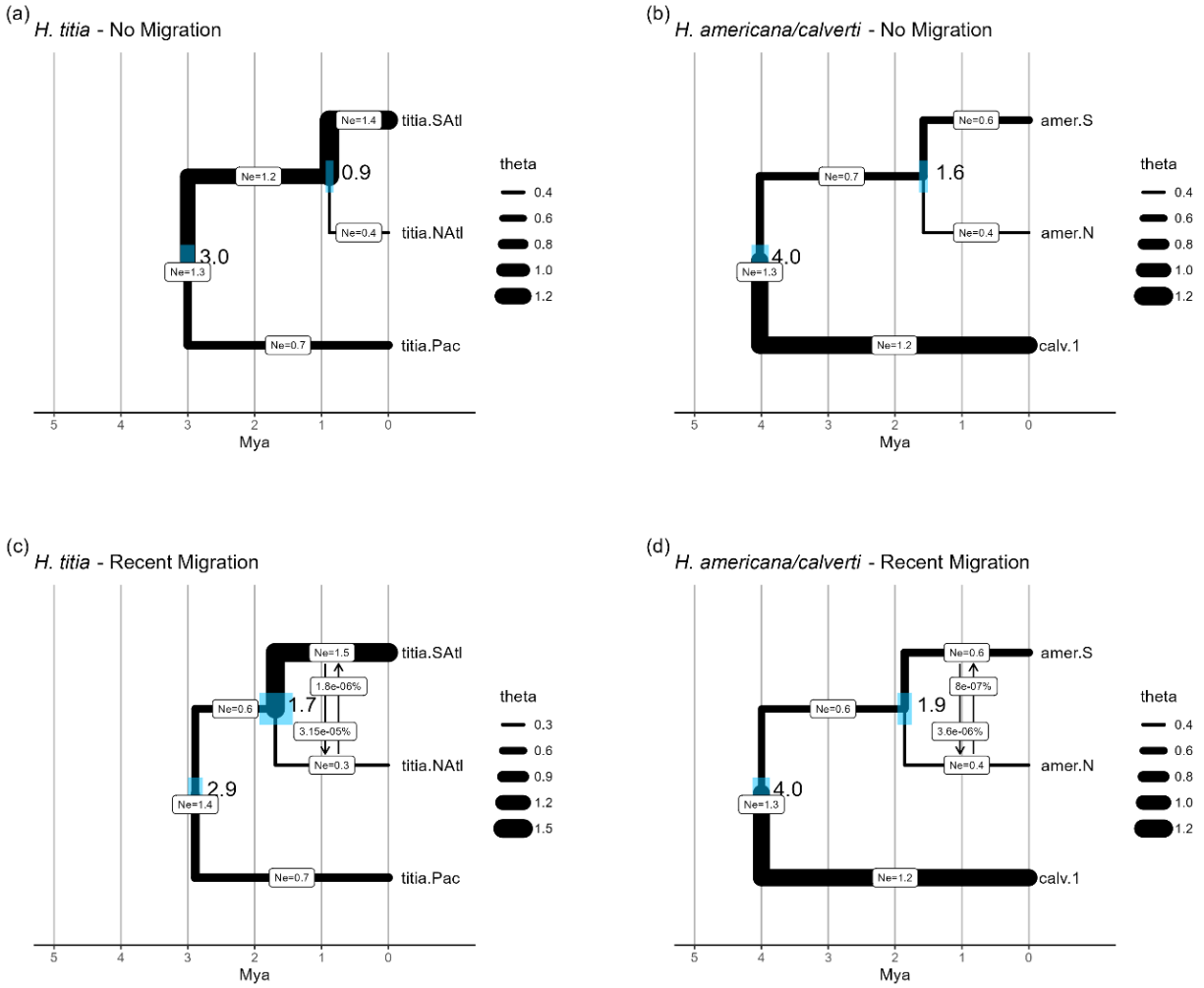
(a)
H. titia - No Migration
Ne=1.4
titia.SAtl
Ne=1.2
0.9
Ne=0.4
titia.NAtl
3.0
Ne=1.3
Ne=0.7
titia.Pac
theta
0.4
0.6
0.8
1.0
1.2
5
4
3
2
1
0
Mya
(b)
H. americana/calverti - No Migration
Ne=0.6
amer.S
Ne=0.7
1.6
Ne=0.4
amer.N
4.0
Ne=1.3
Ne=1.2
calv.1
theta
0.4
0.6
0.8
1.0
1.2
5
4
3
2
1
0
Mya
(c)
H. titia - Recent Migration
Ne=1.5
titia.SAtl
1.8e-06%
Ne=0.6
1.7
3.15e-05%
Ne=0.3
titia.NAtl
2.9
Ne=1.4
Ne=0.7
titia.Pac
theta
0.3
0.6
0.9
1.2
1.5
5
4
3
2
1
0
Mya
(d)
H. americana/calverti - Recent Migration
Ne=0.6
amer.S
8e-07%
Ne=0.6
1.9
3.6e-06%
Ne=0.4
amer.N
4.0
Ne=1.3
Ne=1.2
calv.1
theta
0.4
0.6
0.8
1.0
1.2
5
4
3
2
1
0
Mya

Figure 4:6: The estimated divergence times (million years ago) and effective population size (theta – N*e* in millions of individuals) from G-Phocs analysis of *Hetaerina titia* and *Hetaerina americana*. Migration rate is the number of migrated as a percentage of Ne per generation. All models ran for 1,000,000 interactions with 10% burn in. Blue bars show 95% highest posterior density for each divergence date **(a)** Model estimates for *H. titia* with no migration bands. **(b)** Model estimates for *H. americana* and *H. calverti* with no migration bands. **(c)** Model estimates for *H. titia* demography with migration bands between Northern and Southern Atlantic *H. titia* **(d)** Model estimates for *H. americana* and *H. calverti* with migration bands between North and Southern *H. americana*. G-phocs runs presented here are conducted on the heterospecific draft genome. i.e., *H. titia* loci mapped to the *H. americana* draft genome and the *H. americana* loci mapped to the H. titia draft genome.

The effective population sizes for each lineage of *H. titia* were consistent between models and runs. For *H. titia*, the Southern Atlantic H. titia lineage had the largest effective population size, around 1.8 million individuals, and the Northern Atlantic lineage had the smallest, around 0.4 million individuals. The Pacific lineage's effective population size was estimated to be around 0.7 million individuals. *H. calverti* was estimated to have a much greater effective population size than either lineage of *H. americana*; 1.2 million individuals compared to 0.6 million for the Southern *H. americana* lineage and 0.4 million for the Northern *H. americana* lineage.

Where migration rates were included, the estimated migration rate between populations was low. For all migration bands, the percentage individuals within each population per generation that were estimated to have originated by migration was between $3.2x10^{-5}$% and $8x10^{-7}$%.

An F_1 hybrid at a zone of secondary contact

Calculations of hybrid index and heterozygosity indicated that sample CUAJa02 from site CUAJ01 (an Atlantic drainage near the continental divide) was a F_1 hybrid between Pacific and Atlantic lineages (Figure 4:7). Sample CUAJa02 had an autosome heterozygosity of 92.2% and a hybrid index of 0.514, close to the theoretical level of an F_1 hybrid (100% and 0.5 respectively) and markedly above that of a F_2 hybrid (50% and 0.5, respectively). The X chromosome of sample CUAJa02 was entirely homozygous with one exception. Sample CUAJa02 is a male, and as *Hetaerina* exhibit an XO sex determination system, this means the predicted parents of sample CUAJa02 were a female from the Pacific lineage and a male from the Atlantic lineage. The single sex linked heterozygous site had markedly higher read depth than the other SNPs on the X chromosome suggesting the SNP was autosomal and incorrectly mapped to the X chromosome (Supplementary Figure 4:18). We genotyped 22 other samples from this location which all had Southern Atlantic ancestry and exhibited no evidence of introgression. We have evidence through whole genome resequencing that a second individual, CUAJa03, had an entirely pacific ancestry but did not obtain high quality ddRAD sequence data for this sample.

The rate of heterozygosity, across the highly segregating sites, was close to zero for all other samples collected from CUAJ01 and CUAJ02. All other samples either had nearly entirely Pacific or Atlantic "parental" genotypes.

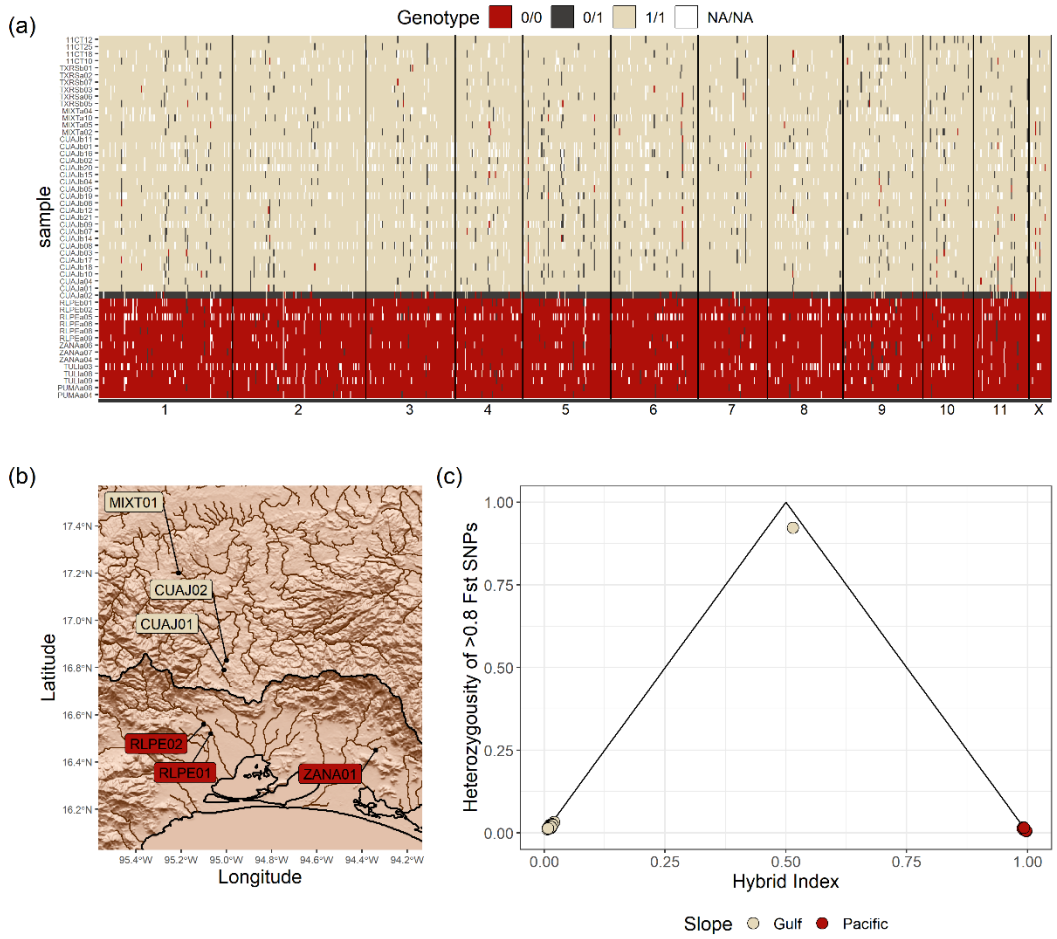

Figure 4:7: Hybrids between Pacific and Southern Atlantic *Hetaerina titia* from site CUAJ01 on the Isthmus of Tehuantepec. **(a)** Genotypes for 886 autosomal SNPs and 21 sex linked SNPs that had a greater than 0.8 allele frequency difference between Pacific and Atlantic individuals (calculations excluded samples from CUAJ01/02). Each sample is position along the y axis each SNP is ordered by the position along each chromosome along the x axis. Each SNP is coloured by whether they were homozygous for the Pacific allele (0/0 –red), homozygous for the Atlantic allele (1/1 –lightbrown), or heterozygous (0/1 – black). **(b)** Sample locations around the Isthmus of Tehuantepec. The continental divide is shown in black. See Figure 4:1b for inset map. **(c)** A triangle plot showing the hybrid index, measuring the percentage of "parental" genotype, and the heterozygosity of each sample. A theoretical F_1 hybrid would be placed at the top corner of the triangle. SNPs on the X chromosome were excluded when calculating the hybrid index and heterozygosity.

Discussion

Our study investigated the phylogeographic structure and phylogeny of several *Hetaerina* damselflies to determine if divergence time predicts the outcome of secondary contact within a non-ecological speciation. We identified three distinct, predominantly allopatric lineages of *H. titia* (Pacific, Northern Atlantic, and Southern Atlantic *H. titia*) but also a single site where Pacific and Southern Atlantic *H. titia* lineages are undergoing secondary contact with limited introgression. We identified a location that the most differentiated lineage of *H. titia* (*H. titia* Pacific) is in secondary contact with the Southern Atlantic *H. titia* lineage but is not widely sympatric. We found that hybridization is possible between Southern Atlantic and Pacific *H. titia* but appears limited, and the lack of wider admixture at the site indicates strong reproductive isolation. We further identified three distinct lineages within the *H. americana* and *H. calverti* species complex, which includes a Northern and a Southern allopatric lineage and a sympatric lineage corresponding to the newly described *H. calverti* -corroborating the work of Vega-Sánchez *et al.*, (2024). Our estimates of divergence dates between these lineages show that it is the most differentiated lineage of *H. americana* (aka *H. calverti*) that has become sympatric with the other two *H. americana* lineages. Divergence estimates, from both SNAPP and G-Phocs, indicate that the Pacific lineage of *H. titia* is estimated to have diverged earlier from other *H. titia* lineages than *H. calverti* has from *H. americana,* backing up the notion that increased divergence times increases the possibility of sympatry (Tobias *et al.*, 2020; Matute & Cooper, 2021).

Taken as a whole, our results show multiple lineages at various stages of the non-ecological speciation cycle. Within *H. americana* and *H. titia,* there are multiple allopatric lineages that have undergone substantial genetic differentiation after diverging over the last one to eight million years. We corroborate that *H. calverti* coexists in sympatry with the southern lineage of *H. americana* (Vega-Sánchez *et al.*, 2020, 2024) and estimate that these lineages diverged somewhere between 4 or 5.6 million years ago. This is older than the divergence time estimated from Standring *et al.*, (2022) of 3.76 million years. Vega-Sánchez *et al.*, (2024), also demonstrated that *H. calverti* lives in sympatry with the northern lineage of *H. americana* at sites within Northwest Mexico where we did not obtain samples.

Our work demonstrates that *H. titia* is split into three highly differentiated allopatric lineages that diverged somewhere between 1 and 5 million years ago, most

likely 3.6 and 1 million years ago, respectively. Our discovery of a single wild F_1 hybrid between the Pacific and Southern Atlantic lineages of *H. titia* in a location of secondary contact suggests that there is strong but incomplete reproductive isolation between the lineages. Unlike *H. americana* and *H. calverti,* the two lineages of *H. titia* have not become sympatric more widely across their range. The mean estimated divergence times from SNAPP suggest that the transition from parapatry to widespread sympatry in this group may take longer at around 3.6 million years. Divergence estimation using G-Phocs places this timing at 3 million years. Our estimated divergence time between *H. americana* and *H. calverti* suggest sympatry can occur within 5.6 million years (SNAPP) or 4.0 million years (G-Phocs). Nearly all combinations of SNAPP and G-Phocs analysis place the divergence between *H. americana* and *H. calverti* as older than the split between Pacific and Atlantic *H. titia*. We suggest that *H. calverti* is sympatric with *H. americana* while the Pacific lineage of *H. titia* is reproductively isolated but not yet widely sympatric with the Southern Atlantic of *H. titia* because of the difference in divergence times between these lineages. Our results fit well with the other studies that have estimated divergence times during non-ecological radiations. Salamanders (Kozak, Weisrock & Larson, 2005), killifish (Lambert, Reichard & Pincheira-Donoso, 2019), and snails (Koch *et al.*, 2020) all have estimates of divergence times in the millions of years.

Our discovery that on the Isthmus of Tehuantepec, Pacific and Southern Atlantic *H. titia* are ongoing secondary contact offers an opportunity to understand an outcome of secondary contact during non-ecological speciation. We did not detect admixture within the Pacific *H. titia* lineage that would suggest a recent history of introgression between the Atlantic and the Pacific *H. titia*. We did detect one individual collected from a site on the Atlantic side of Isthmus of Tehuantepec close to the continental divide that held a high proportion of Pacific and Atlantic ancestry. This site is and only ~27 km from the nearest Pacific site where we have found *H. titia*. We estimate that this hybridisation event took place less than one generation (one year) prior to collection (Figure 4:2). This sample, CUAJa02, had approximately 50/50 Pacific and Atlantic ancestry and autosomes were nearly entirely heterozygous at alleles that were highly differentiated between Atlantic and Pacific populations. The X chromosome for CUAJa02 was homozygous for pacific ancestry. The evidence attained indicate that sample CUAJa02 is a F_1 hybrid between a pure Pacific female and a pure Atlantic male. All other samples from CUAJ01 and CUAJ02, and nearby sites, were assigned to the Atlantic or Pacific lineage with no further evidence of hybridization or

introgression. The single F_1 hybrid indicates that there has been dispersal of Pacific *H. titia* into the Atlantic drainage. We have also obtained whole genome resequencing data for an individual collected at the same site and the same time as CUAJa02 whose genotype is entirely Pacific. This later resequencing means that of the four individuals collected at site CUAJ01 in 2021 two had pure Atlantic ancestry, one was pure Pacific, and one was a F_1 hybrid.

Given that the other 22 ddRAD samples from site CUAJ contained no evidence of introgression, there appears to be strong barriers limiting further admixture at this site. This could be caused by post-zygotic hybrid sterility or reduced fecundity. An alternative may be pre-zygotic selective mating preferences between the two lineages and/or low hybrid fitness related to these traits. Pacific and Atlantic *H. titia* exhibit marked difference in seasonal melanisation which could allow discrimination between Pacific and Atlantic *H. titia* but only during the peak season (Drury *et al.*, 2019b).

We have evidence of only one pure pacific individual collected at these sites meaning they are present at relatively low frequency (<4%). What has prevented Pacific *H. titia* from becoming more widely sympatric with Atlantic *H. titia*? We find it unlikely that our collection of samples coincided with the first contact between Pacific and Atlantic *H. titia* in ~3.6 million years. Our preliminary finding and genotyping of a pure Pacific *H. titia* from within the Atlantic drainage could allow estimates of how long the Pacific *H. titia* population has been established within the range of the Atlantic population. Sympatry can be prevented by the production of low-fitness hybrids as seen in the zone of secondary contact between pacific wrens, *Troglodytes pacificus,* and winter wren ,*T. hiemalis* (Mikkelsen & Irwin, 2021). The high level of melanisation seen in the Atlantic lineages of *H. titia* is beneficial in reducing interspecific behavioural interference (Anderson & Grether, 2011; Drury *et al.*, 2015a). As such, Atlantic *H. titia* may have an advantage within river drainages that contain other species of *Hetaerina,* such as *H. occisa* and *H. americana*, which are found within the river drainage of the hybrid site (personal observation). Interspecific behavioural interference can itself influence the range dynamics of populations (Patterson & Drury, 2023). For instance, in a zone of secondary contact, pied flycatchers use sub-optimal habitat because of the high aggression of collared flycatchers (Rybinski *et al.*, 2016). Reproductive interference by an invasive bumblebee in Japan has extirpated native bumble species (Tsuchida *et al.*, 2019). Consequently, mating and territorial interactions between Pacific and Atlantic *H. titia* may be restricting the dispersal of the Pacific *H. titia*. Further monitoring and

sample collection in and around the zone of secondary contact could shed light on how mating segregation evolves during secondary contact, although we do not currently have a method to differentiate Pacific and Atlantic *H. titia* in the field.

Evolution of seasonal melanisation in Hetaerina titia

H. titia exhibits exceptional temporal polyphenism in wing colouration (Drury *et al.*, 2019b). Our results cast considerable light on the evolutionary history of this polyphenism. The phylogeny of *H. titia* shows that the two lineages with populations exhibiting the highest degree melanisation in the peak breeding season are most closely related. Our species phylogeny of *H. titia* suggest the high degree of seasonal melanisation evolved after the split between Pacific and Atlantic *H. titia*. Some populations of *H. titia* within the Northern Atlantic lineage, particularly at higher latitudes, appear to have become secondarily monophenic (Drury *et al.*, 2019b). It is possible, therefore, that in the highest latitude populations of *H. titia* the balance between reduced interspecific behavioural interference and alternative cost to melanisation, such as predation, contrast with those of the polyphenic southern latitude populations. Intriguingly the closest genetic populations to these high latitude monophenic populations are the polyphenic population from Florida.

Conclusion

We produce estimates for the divergence times of multiple lineages undergoing a non-ecological radiation. Divergence times correlate well with the stage of the speciation cycle of each lineage pair with the most distantly related lineages found in sympatry and the most closely related being in allopatry. We identified a site where there is ongoing limited hybridisation between too highly differentiated lineages of the same (currently recognized) species. Collectively this research provides insight into multiple stages of the non-ecological speciation cycle. The discovery of a site of secondary contact between two lineages, which exhibit a polyphenism that influences species recognition, opens up further research into how biodiversity accumulates in a non-adaptative radiation.

Data Availability

All code for the recreation of this chapter is publicly available on GitHub: https://github.com/ChristophePatterson/Thesis-Phylogeographic-Hetaerina and

includes SNP libraries in vcf format. Raw sequence reads will be made available on NCBI upon publication.

Supplementary material

Supplementary material is provided in Appendix Chapter 4.

Chapter 5 Multivariate trait evolution of a seasonal polyphenism at the continental scale

The variation in wing melanisation seen across smoky rubyspot damselfly (*Hetaerina titia)*. Males, shown in first 4 columns, exhibit red basal spots with vary degrees of melanisation. Females, columns 5 to 8, are mostly clear winged but with varying degrees of melanisation.

Abstract

Biotic and abiotic factors change both spatially and temporally across species' range. Many species exhibit seasonal polyphenism where two or more phenotypes arise with the changing environmental conditions across the year. In many polyphenic species developmental constraints limit the divergence between alternative morphs. For seasonally polyphenic species, selection acting on the phenotype present in one season may constrain the phenotypes present in another season but there has been little empirical research. Smoky rubyspot damselflies (*Hetaerina titia*), exhibit a striking seasonal polyphenism in wing melanisation, but the degree of polyphenism varies between regions. We measured the seasonal polyphenism across the range of *H. titia* using a combination of manual and computer vision measurements. We quantified the wing phenotypes in >5,600 photographs of male smoky rubyspots collected both during our own field research and via a participatory science initiative. We then combined this data with the population-level phylogeny of *H. titia* to model how the seasonal polyphenism has evolved across North and Central America. Using multivariate models of trait evolution, we tested whether the peak and off-peak phenotypes have co-evolved and whether there is geographic variation in the tempo of evolution. We find no significant evidence of co-evolution between seasonal phenotypes, supporting the notion that polyphenism can be an effective evolutionary adaptation to variable environmental conditions. We do find evidence that the seasonal polyphenism is evolving under different selective regimes in different geographic regions, suggesting either melanisation has different trade-offs in different regions or there has been developmental release in certain lineages. To our knowledge, our study presents the first empirical research into the evolution of polyphenism with sufficient data to model the seasonal variation in polyphenism across the entire range of a species.

Introduction

Species inhabit variable environments with biotic and abiotic factors changing both spatially and temporally. Phenotypic plasticity is where two or more phenotypes can arise from the same genotype. Polyphenism is a subset of phenotypic plasticity where the same genotype can develop into discrete phenotypes depending on environmental conditions (Simpson, Sword & Lo, 2011). Seasonal polyphenism is a repeated annual cycle in the ratio of phenotypes within a population in response to changing environmental factors (Shapiro, 1976; Brakefield *et al.*, 1996). Seasonal polyphenism means the whole populations can have an annual shift in phenotype (Gallesi *et al.*, 2016; Halali *et al.*, 2021). Selection can favour polyphenism because different phenotypes have increased fitness across different environmental conditions and, in the case of seasonal polyphenism, when selection favours different phenotypes across the year. For example, many Arctic species, such as snowshoe hares, *Lepus americanus*, shift from white to brown fur, which provides better camouflage and decreased predation with decreasing snow cover (Mills *et al.*, 2013). Individual snowshoe hare, and other artic species, shift in phenotype over the year but many species, predominantly invertebrates, have multigenerational seasonal polyphenism (Simpson *et al.*, 2011). In multigenerational seasonal polyphenism, individuals have set phenotypes but there is distinct differences in the phenotype between generations that emerge at different times of year. Many species of butterfly, such as peacock pansies, *Junonia almanac*, (Brakefield & Larsen, 1984) and squinting bush brown, *Bicyclus anynana*, (Lyytinen *et al.*, 2004), have distinct dry and wet season morphs. In the dry season wing shape and colour resembles a dried leaf which provides increased crypsis therefore reducing predation. In the wet season there is an increase in the number and magnitude of fake eye spots on the wings which acts to deflect damage from predation (Brakefield *et al.*, 1996; Baudach & Vilcinskas, 2021). Seasonal polyphenism allows individuals to exhibit optimal trait values across different adaptive peaks in different seasons. However, the optimal trait value for a specific season could vary geographically across regions with different biotic and abiotic factors.

While many species with seasonal polyphenism appear to track the shifting optimal trait value across seasons, developmental constraints often drive trade-offs in trait evolution leading traits to co-evolve across taxa (Armbruster & Schwaegerle, 1996; Armbruster *et al.*, 2014; Sherratt *et al.*, 2019). Due to pleiotropic effects, it is unlikely that

any single trait does not co-vary with any other traits (Clavel, Escarguel & Merceron, 2015). In addition, the underlying genomic architecture that controls the environmental-phenotypic reaction norm could be constrained leading to a mismatch between the actual seasonal trait value and optimal trait value for the environment. Consequently, the divergence in traits between different seasonal phenotypes may be limited (Murren *et al.*, 2015). Decoupling of pleiotropic effects would allow phenotypes to evolve independently and selection to produce optimal phenotypes across multiple environments. Evidence from transcriptomics and selection experiments suggests full decoupling does not always occur (Snell-Rood *et al.*, 2011). For instance, a multi-generation selection experiment on bulb mites (*Rhizoglyphus echinopus*) showed that selection on the male 'fighting' morph led to a correlated response in the alternate male 'scrambler' morph (Buzatto, Clark & Tomkins, 2018). For seasonal polyphenic species, there has been little empirical research to determine if selection acting on the phenotype present in one season can constrain the phenotype present in another season. Furthermore, there has been little empirical work to investigate spatial variation in the evolution of seasonal polyphenism across a species range.

Unlike monophenic traits, modelling the evolution of a polyphenic trait requires multiple measurement of the trait under varying environmental conditions. Logistical challenges means measuring the variability in polyphenism across a species entire range is a substantial challenge (Relyea, Stephens & Hammond, 2021). To adequately model a seasonal polyphenism, measurements must be attained not only from across the entire spatial distribution of a species but also across all seasons. Regions that lack data from across the season cannot have the polyphenism adequately modelled, similar to problems arising from modelling reaction curves (Goolsby, 2015). Without multiple measurements of phenotypes from across the full environmental gradient, models can fail to determine the phenotype-environmental reaction norm leading to false inferences in evolutionary history, phylogenetic signal, and mode of evolution of the polyphenism. The lack of high resolution spatial and temporal data is likely the reason why such research has not been conducted before. However, the proliferation of citizen science recording schemes is increasing the extent of data researchers can draw from. Recent papers have used citizen science photos to determine phenotypic variation at the continental level, far beyond what a single researcher could collect (Silvertown *et al.*, 2011; Drury *et al.*, 2019b; Lehtinen *et al.*, 2020). Advances in computer vison are also increasing the rate at which phenotypes can be extracted from image data (Zhang *et al.*,

2017; Fernandes, Dórea & Rosa, 2020; Li *et al.*, 2020). Combining citizen science data, computer vision, and standardised measurements for validation opens the possibility of modelling a seasonal polyphenism at the continental scale across the full range of a species. Such a dataset could answer whether there is co-evolution between alternative seasonal morphs and if there is geographic variation in the tempo of evolution of this polyphenism.

The damselfly *Hetaerina titia* (smoky rubyspots) exhibit a striking seasonal polyphenism in wing melanisation (Drury *et al.*, 2019b). For each individual, the degree of wing melanisation is set at emergence of the adult life stage. In general, adult *H. titia* that emerge at the start and end of the breeding season exhibit low levels of melanisation, but during the peak breeding season emerging *H. titia* exhibit a high degree of wing melanisation. Adult *H. titia*, like other calopterygids, rarely live longer than a few weeks (Córdoba-Aguilar, 1994; González-Tokman, González-Santoyo & Córdoba-Aguilar, 2013) meaning over the year the entire adult population of *H. titia* is repeatedly replaced and there is a marked shift in the average phenotype of the population (Drury *et al.*, 2015a).

Not all populations of *H. titia* exhibit the same levels of polyphenism (Drury *et al.*, 2019b). Populations of *H. titia* that reside in rivers that drain into the Caribbean and Gulf of Mexico vary highly in melanisation throughout the year (Drury *et al.*, 2019b). In contrast, *H. titia* that reside on the Pacific slope exhibit lower levels of melanisation throughout the year, though some seasonal variation is still present. Populations of *H. titia* in the higher latitudes of the continental United States, which drain into the Atlantic, also do not exhibit high levels of melanisation (Drury *et al.*, 2019b). The variation in seasonal polyphenism seen in *H. titia* provides the opportunity to study how seasonal polyphenism evolves. We test whether the degree of melanisation during the peak and off-peak season have co-evolved. i.e. whether the level of melanisation in one season is constrained by the level of melanisation in the other season. We also determine whether the shift to having high degrees of melanisation in the Atlantic indicates a qualitative shift in the evolution of the polyphenism.

To distinguish between different hypotheses for the evolution of the seasonal polyphenism, we fit phylogenetic models of multivariate evolution to a range-wide phenotypic dataset of *H. titia*. We model the seasonal polyphenism as a multivariate trait where each lineage is characterized by the mean and standard error of the level of

melanisation at peak and off-peak season. We collate a dataset of phenotypic measurements using citizen science images and standardised images collected by researchers in the field. We then combine the phenotypic data with a population level phylogeny of *H. titia* to model how the seasonal polyphenism has evolved.

Methods

Phylogeny

We constructed phylogeny of *H. titia* using a SNP data from double digest restriction enzyme associated DNA (ddRAD) following DaCosta and Sorenson, (2014) and Franchini *et al.*, (2017). Full laboratory procedures and bioinformatics pipeline is outlined in Chapter 4 and Appendix Chapter 4. Once SNPs were called using bwa and samtools, we used the R packages vcfR (Knaus & Grünwald, 2017), ape (Paradis & Schliep, 2019), adegenet (Jombart, 2008), and poppr (Kamvar *et al.*, 2014) to filter and generate input files.

We used the GPS coordinates of each sample site to allocate samples to 5th level of the hydroBASIN dataset (Lehner & Grill, 2013) using the function *st_intersection* within the R package *sf* (Pebesma, 2018). The hydroBASIN dataset is a global model of river basins consisting of 12 levels of hierarchical nested sub-divisions allowing river catchments to be subdivided into consistently sized basins. Due to computational constraints, we restricted the phylogenetic analysis to a single sample with the highest coverage from each hydroBASIN. We removed the SNPs that were no longer polymorphic between the selected samples and that were genotyped in at least one individual from each population; retaining 3,229 SNPs. To construct the phylogeny, we ran the Bayesian coalescent analysis SNAPP (Bryant *et al.*, 2012) implemented within the programme beast v2.7.5 (Bouckaert *et al.*, 2019). *H. titia* is currently recognised as a single highly variable species, but population genomic analyses suggest that the Pacific and Atlantic populations diverged ~3.6 million years ago and that there is reproductive isolation at a site of secondary contact (Chapter 3). The taxonomic classification of *H. titia* requires further investigation but does not influence our methodology and inference in the evolution of the polyphenism.

We used a previous estimate of the crown ages of *H. titia* to select priors (mean = 3.6 million years ago (mya), standard deviation = 0.5 million years). A SNAPP configuration file was created using a custom R script and the ruby script from

https://github.com/mmatschiner/snapp_prep. We ran SNAPP for 1,000,000 interactions and sampled every 500 iterations. The convergence was assessed using tracer and the maximum clade credibility tree, with a 10% burn in removal, was calculated using the standard settings of the *treeannotator* program distributed with beast.

Phenotype data

Both female and male *H. titia* exhibit variation in wing melanisation. Male *H. titia* have red basal wing spots, similar to other *Hetaerina* damselflies, but the red basal colour can be fully or partially masked in highly melanised individuals. Male *H. titia* defend territories along riverbanks while females spend a high proportion of time foraging in the surrounding canopy. Consequently male *H. titia* are substantially easier to identify, catch, and photograph (82% of iNaturalist photos of *H. titia* are male), and, as such, we limit our analysis to modelling the male phenotype.

We attained phenotypic data from two sources. Firstly, a standardised photographic dataset of *H. titia* was collected between 2004 to 2023 during scientific field work. Standardised photos were collected by placing captured *H. titia* on a level stage with a millimetre scale in the same plane as the wings. Photographs of the fore and hindwing were taken using a using Canon EOS 20D with a 100mm macro lens. Secondarily, to increase the spatial and temporal scale of our dataset, we also attained images from the citizen science recording website iNaturalist (https://www.inaturalist.org). We downloaded all images of *H. titia* submitted to iNaturalist (https://www.inaturalist.org) prior to 2024-01-17. We manually curated these photos to only include perched adult male *H. titia* with the entire wing visible within the photo. We also noted and removed any photographs with defects that could alter the calculation of the wing colouration; if the photo was blurred, had low contrast, was overexposed, or had glare from the sun.

We attained measurements of wing colouration from the standardised and iNaturalist images using two methods. Firstly, a manual methodology using the image analysis software imageJ (Schneider, Rasband & Eliceiri, 2012) and a custom macroscript from Drury *et al.*, (2019). Secondly, we developed an automated image detection and segmentation pipeline which uses Deteron2 (Wu *et al.*, 2019) and OpenCV (Bradski, 2000) outlined in full in Jieyu (2023). The automated image detection software allows for the detection and segmentation of damselfly wings using images collected from both the standardised method (with calculations of wing colouration for

of both hind and forewings) and from photos of perched individual from iNaturalist (with a single estimate of melanisation based on the overlapping hind and forewings).

To ensure standardisation between all four of the wing measurement methods we collected images of the same individual *H. titia* using the standardised method and also photographed while perched, similar to that data from Drury *et al.*, (2019) but with an increased data set from additional field seasons. We thus attained multiple combinations of measurements for individuals that had their wing colouration determined from standardised and iNaturalist style photographs, and measured manually using imageJ and automated image detection software.

We quantified the wing phenotypes in 5,615 photographs of male *H. titia* from across North and Central America: 3,528 standardised manual measurements, 786 standardised automated measurements, 523 iNaturalist manual measurements, and 1,482 automated iNaturalist measurement. We used the standardised manual measurements as the "true" value of melanisation and then used linear models to determine the relationship between the standardised manual wing melanisation and all other alternative measurement methods. We used the r-squared value from each linear model to rank the measurement methodology, with the top rank automatically assigned to the "true" standardised manual measurements. For each individual, we used the top ranked phenotypic measurement methodology that had been attained for that individual and then transformed the data using the linear model parameters for that measurement methodology (Table 5:1).

Table 5:1: Model parameters used to calculate a standardised measurement of wing melanisation from each measurement methodology. Each measurement methodology was modelled in comparison to the standard manual methodology. Measurement types are ranked in comparison to the standard manual methodology based of the R-squared value. The total number of phenotype measurements attained using each methodology. The total number of phenotypic measurements used in the final dataset from each methodology.

Measurement type	**Rank**	**R-squared**	**Slope**	**Intercept**	**Degrees of freedom**	**p-value**	**Total**	**Used**
Standard manual measurements	1	1	1	0	-	-	3528	3526
Standard automated measurements	2	0.98	1.02	0.025	310	< 2.2e-16	786	471
iNaturalist manual measurements	3	0.9724	1.15	-0.106	64	< 2.2e-16	523	454
iNaturalist automated measurements	4	0.91	1.07	-0.005	81	< 2.2e-16	1482	1164

Combing phylogeny with seasonal polyphenism

We aimed to model the evolution of seasonal polyphenism in wing melanisation of *H. titia* at the highest resolution possible. As such, we used the highest resolution phylogeny of *H. titia* which retained adequate numbers of phenotypic measurements to estimate the level of melanisation at both peak and off-peak season. Firstly, we collapsed nodes that were not well resolved (posterior probability <0.9) in the phylogeny (Figure 5:1a). After collapsing the tree, we recorded which samples, and therefore which hydrological basins, had between collapsed into a single tree tip. We assigned each phenotypic measurement to a tree tip if the phenotypic measurement shared a hydrological basin with the samples that were collapsed into each tree tip (Figure 5:1b). For instance, samples from hydrological basins 7050050000 and 7050050930 collapsed into a single tree tip so we assigned all phenotypic measurements from these two hydrological basins to the single retained tip. We repeated this process for hydrological basins levels three, four, and five to cluster phenotypic measurement to the most appropriate tip. One well supported node (splitting populations on the Pacific coast of Mexico at the Isthmus of Tehuantepec) did not contain enough phenotypic

measurements to reliably model the seasonal polyphenism separately in each daughter lineage, so we collapsed this node for subsequent analyses.

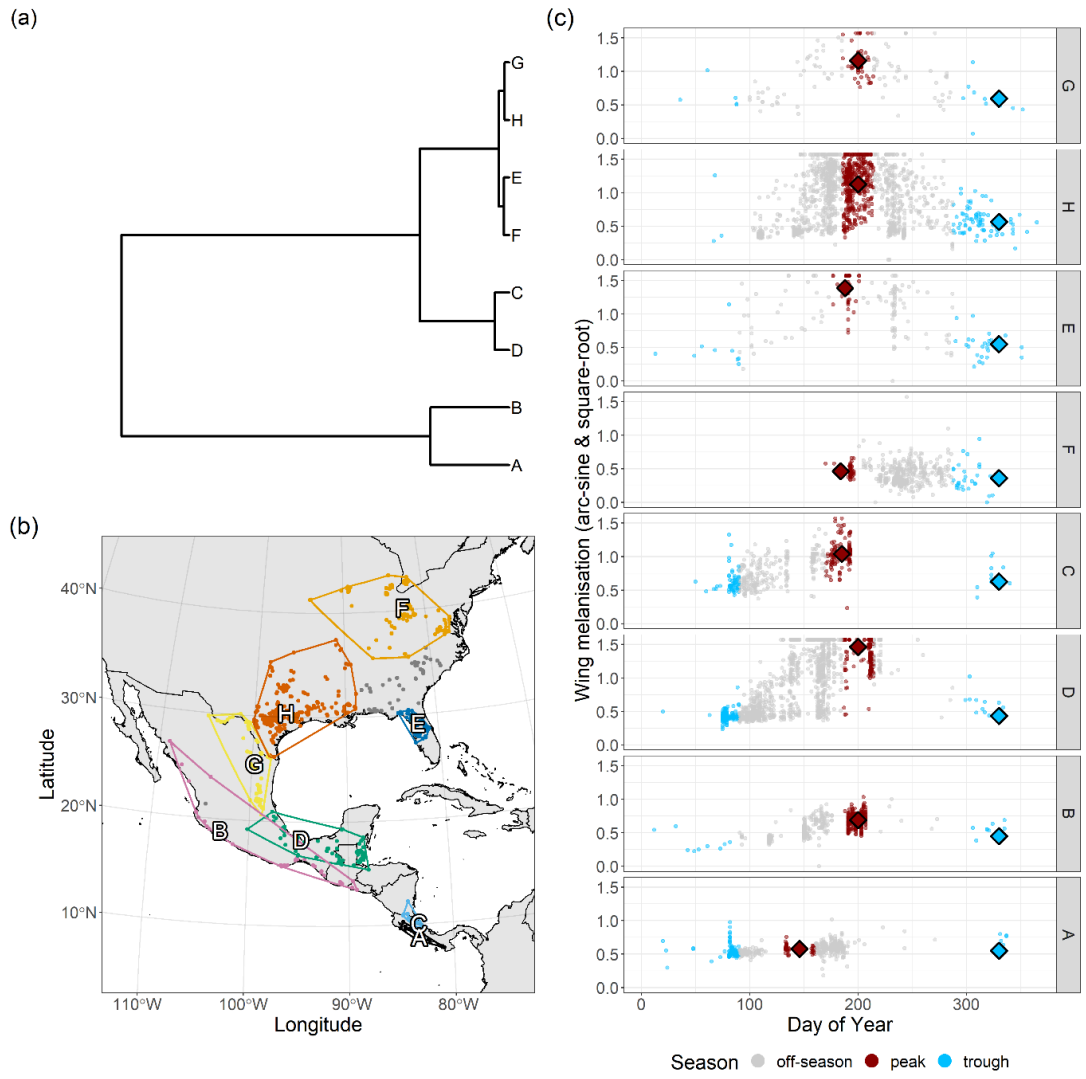

Figure 5:1: Variation in seasonal polyphenism of *Hetaerina titia* across the species phylogeny. (a) The phylogeny of H. titia constructed using SNAPP analysis. All nodes have a posterior probably of 1. (b) Geographic distribution of phenotypic measurements coloured and labelled by the assigned tree tip. Grey points mark phenotypic measurements that could not be assigned to the phylogeny because we did not attain samples for sequencing from the same region. (c) Measurements of wing melanisation from all data sources (iNaturalist and standardised measurements) coloured by the allocated season, with the estimated mean phenotype of the peak and trough of the polyphenism of each tree tip, with mean (diamonds) and standard error.

Calculation of peak and trough

The peak level of melanisation does not occur at the same time of year for all populations of *H. titia*. The first and last emergence of *H. titia* also varies geographically. As such we did not use a specific time window to estimate peak and trough levels of melanisation. We calculated a peak level of melanisation via a smoothed function using the methodology from Mason *et al.*, (2014). From this curve, we calculated the peak date as the date corresponding to the maximum fitted value. We considered all observations within two weeks of the peak date to be 'peak' season observations and calculated the mean and standard deviation of the $asin(sqrt(x))$ transformed wing pigmentation.

There are fewer observations in the off-peak season, which likely reflects generally lower densities in the off-peak season. To calculate a trough value, therefore, we first calculated a 'global' peak season date from all combined observations. Then, we set this peak date as the middle of the 'peak-half' of the year and went on to calculate an 'off-peak half'. Setting a two-week buffer period between the halves, this left an off-peak period from day of the year 287 to 91 (Figure 5:1). As above, we calculated the mean and standard error for all observation in this time period.

Multivariate evolution

We modelled the evolution of the seasonal polyphenism as a multivariate trait using the R package *mvMORPH* (Clavel *et al.*, 2015). Measurements of melanisation for the peak and off-peak season were transformed into an approximate Gaussian distribution using an $asin(sqrt(x))$ transformation. To test for co-evolution between the peak and off-peak wing melanisation we compared models with and without off-diagonal sigma values fixed at zero using Ornstein-Uhlenbeck (OU) models of trait evolution. In single variant trait OU models, sigma denotes the stochastic rate of evolution through the phenotypic landscape. In multivariant trait OU models, off-diagonal sigma values estimate the correlated rate of evolution between two traits. To test if the Atlantic, Pacific, and high latitude lineages of *H. titia* are evolving under different selective regimes, we compared multiple combinations of OU models (Figure 5:2): a single selective regime, different selective regimes between the Pacific and the Atlantic lineages, a different selective regime in the highest latitude lineage, and different selective regimes between Pacific, Atlantic, and highest latitude lineages.

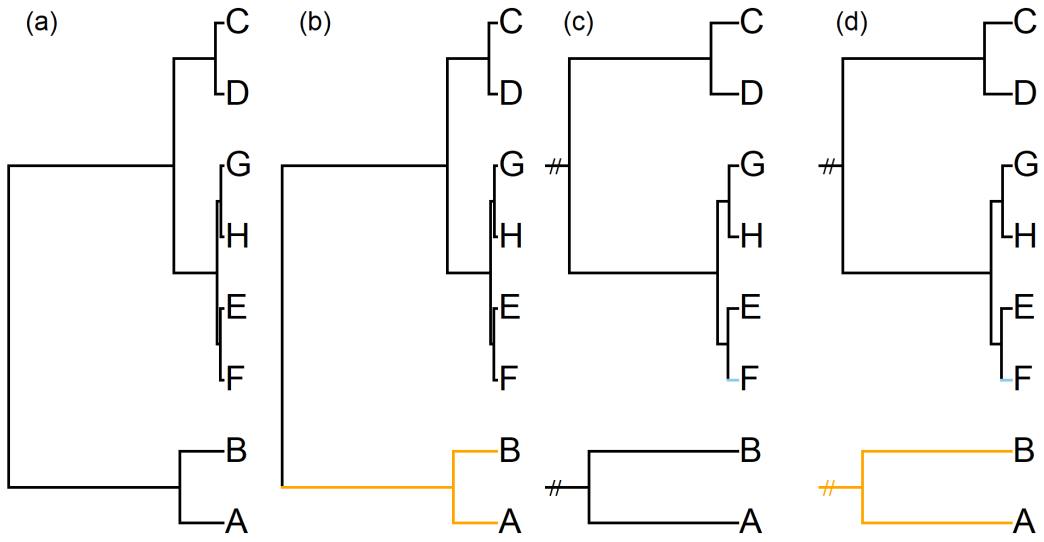

Figure 5:2: Combinations of selection regimes used in Ornstein-Uhlenbeck models. (a) One selective regime, (b) a separate selective regime between the Pacific (orange, tips A and B) and the Atlantic lineages, (c) a separate selective regime in the highest latitude lineage, and (d) a separate selective regime between Pacific, Atlantic, and highest latitude lineages (blue, tip F). Panels (c) and (d) have been cropped to increase visualisation.

To determine which model was favoured, we conducted non-parametric bootstrap likelihood ratio tests (LRT). We used LRT because AIC and AICc are likely inadequate to select between model for a tree with less than 10 tips. The function *mvSIM* was used to run simulations (n = 1000) without co-evolution and with varying combinations of selective regimes. We then calculated the likelihood ratio between the simpler and more complex models for each set of simulated data. We then compared the likelihood ratio generated from the simulated data to that of the models calculated from the observed data. If the likelihood ratio for the observed models falls within the 95% quantile of the distribution of the likelihood for the simulated data, it indicates the simpler model is favoured or that our data would not have the capacity to distinguish between these models.

Values for the transformed proportion of wing melanisation are bounded by 0 and $\pi/2$ (approximately 1.571). The simulations of trait evolution were not bounded, as such, a proportion of the simulated data contained values that were outside of 0 and 1.571. For the simulations with a single selective regime and no co-evolution, 33.8% of simulations had trait values outside of the natural boundaries. Across the simulated data sets 27.7% had a single tip value outside of the natural boundary of 0 and 1.571, 4.9% had two tip values, and 0.5% and three tip values. To assess if our likelihood ratio tests

were not overly influenced by these unrealistic simulated datasets, we, firstly, removed simulations that contained values lower or greater than 0 and 1.571. Secondly, we created pseudo-bounded simulations by forcing all simulated trait values outside of the valid range to be 0 or 1.571, dependent on whether they were lower than 0 or higher than 1.571. We then recalculated the proportion of likelihood ratios that exceeded the observed likelihood ratio using both methods. For all model comparisons, the difference between the likelihood ratios using these alternative methods was less than 1%. As they represent a more realistic dataset, we present the values for the pseudo-bounded simulations going forward. A small number (<0.01%) of model fits for the simulated datasets did not converge and returned negative likelihood ratios, so were excluded. We did not incorporate models of Brownian motion into our analysis because 99.9% of simulation had at least one trait value outside 0 and 1.571.

Results

Consistent with the hypothesis that the seasonal polyphenism within *H. titia* is evolving under separate selective regimes. LRTs comparing model fits on the observed and simulated data favoured three separate selective regimes between the Pacific, the Atlantic, and the highest latitude lineages (Figure 5:3). The observed likelihood ratio for separate selective regimes between the highest latitude lineage, the other Atlantic lineages, and the Pacific lineages was larger than 98.9% of the simulated likelihood ratios using a null model with a single selective regime (Figure 5:3e). Distinction between the Pacific and the Atlantic regimes was only possible when the highest latitude lineage was taken into account. The observed likelihood ratio for separate selective regimes between the Pacific lineages and the Atlantic lineages (without a separate regime for highest latitude lineage) was larger than 73.8% of the single selective regime simulations. The observed likelihood ratio for a separate selective regime for the highest latitude lineage was larger than 97.6% of the simulated likelihood ratios using a null model.

Co-evolution between the peak and off-peak melanisation was not favoured (Figure 5:3f). The observed likelihood ratio for models with co-evolution, that did and did not include the three separate selective regimes, were smaller than 14.0% and 49.3% of the simulated likelihood ratios, respectively (Figure 5:3a). The standardised stationary co-evolution generated under the null models varied from negative to positive one. The observed standardised stationary co-evolution for a single selective regime was positive

(0.32), for a model with three selective regimes the standardised stationary co-evolution was negative (-0.87). The observed standardised stationary co-evolution was smaller than 0.9% of simulated values and greater than 2% of absolute simulated values (Figure 5:3g).

The model parameters for the favoured model, three separate selective regimes and no co-evolution, showed theta, alpha, and sigma values were all higher for the peak phenotype than the off-peak phenotype, with the exception of the highest latitude lineage which and a lower peak theta than off-peak theta (Table 5:1). The stationary variance under this best-fit model is 42x smaller in the off-peak season.

Table 5:2: The Ornstein-Uhlenbeck model parameters for the best selected model; three selective regimes between the Atlantic, the Pacific, and the High Latitude lineages without co-evolution between the peak and off-peak phenotype. Theta (θ) denotes the local optima at which the phenotype is estimated to be drawn towards. The input measurements for wing melanisation were converted into an approximate gaussian distribution by square root arc sine transformation, the value in brackets is the theta value converted back into proportion of wing melanisation (negative values are not convertible). Alpha (α) indicated the strength of the force pulling the phenotype towards that optimum. Sigma (σ) is the stochastic rate of evolution.

Season	**Theta (θ) Atlantic (proportion)**	**Theta (θ) Pacific (proportion)**	**Theta (θ) high latitude (proportion)**	**Alpha (α)**	**Sigma (σ)**	**Stationary variance**
Peak	1.24 (0.89)	0.64 (0.35)	-0.14 (NaN)	10.013	0.33	0.0054
Off-peak	0.55 (0.27)	0.51 (0.24)	0.17 (0.029)	8.10	0.046	0.00013

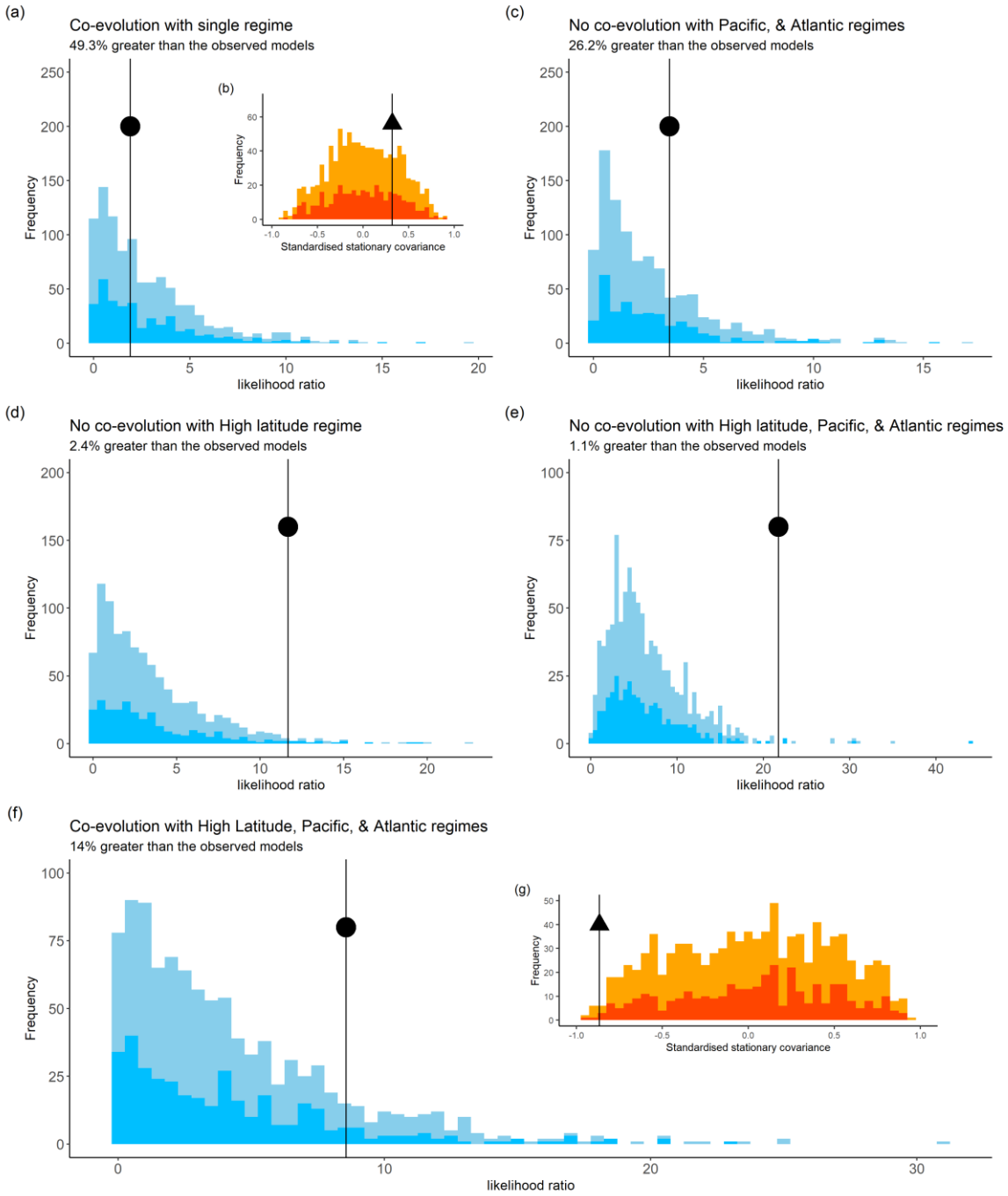

Figure 5:3: Distribution of likelihood ratios produced from a simulation using a null model and the likelihood ratio for models calculated from the observed data. Panel titles denote the model comparison being made and what percentage of simulations (n ≈ 1000) had a greater likelihood ratio than that of the observed model. The lower stacked shaded proportion of the frequency bars indicate the proportion of simulations that had trait values outside of 0 and 1.57. The likelihood ratios are calculated on the pseudo-bounded simulations. The observed likelihood ratio is marked on each plot by the vertical line and circle. The observed standardised stationary covariance is marked by a

vertical line and triangle. **(a)** The likelihood ratios for models without co-evolution, including an inset **(b)** of the distribution of the standardised stationary co-evolution produced for the simulations without co-evolution. All later panels compare models without co-evolution. **(c)** The likelihood ratio of simulations with and without different selective regimes between the Pacific and Atlantic lineages, **(d)** with and without separate selective regimes for the highest latitude lineage, and **(e)** with and without different selective regimes for Pacific, Atlantic, and highest latitude lineage. **(f)** Comparison of simulated likelihood ratios of simulations of with separate regimes for High Latitude, Pacific, and Atlantic lineages, with and without co-evolution. Inset **(g)** shows the distribution of the standardised stationary co-evolution produced for the simulations without co-evolution.

Discussion

This study marks the first attempt to model the evolution of a seasonal polyphenism by fitting multivariate phylogenetic models of phenotypic evolution. We find evidence that the difference in patterns of seasonal wing colouration of smoky rubyspots (*H. titia*) have been driven by distinct selective regimes acting on lineages in different geographical areas rather than all lineages evolving within a single selective regime. The three selective regimes encompass *H. titia* that reside within the Pacific drainage basins, the Atlantic drainage basin, at the highest latitudes of the Atlantic drainage. We did not find significant evidence of co-evolution, suggesting that the degree of melanisation in one peak season does not constrain the degree of melanisation in the off-peak season, or vice versa. No evidence of co-evolution supports the notion that seasonal polyphenism can be an effective strategy for adapting to temporally variable selection pressures.

Our finding that lineages of *H. titia* are evolving under separate selective regimes suggests there is a quantitative shift in the evolutionary dynamics of wing phenotypes between the Atlantic, Pacific, and high latitude populations. Two possibilities emerge from this finding. One, across the range of *H. titia* there are distinct differences in the trade-off in wing melanisation between different geographic regions. Two, since the divergence of the Pacific and Atlantic lineages, there has been a developmental release that previously constrained the divergence in wing melanisation between seasons. We are not able to distinguish between these possible scenarios with our current dataset.

It is possible that all populations of *H. titia* have the capacity to undergo polyphenism, but the environmental trigger is absent or reduced in the Pacific drainage and at the highest latitudes. If this were the case, it would invalidate the interpretations of our phylogenetic analysis. However, for the Pacific lineages we regard a lack of environmental trigger as unlikely for two main reasons. Firstly, the Pacific lineages covers a large latitudinal range and therefore experience a high degree of environmental cues similar to that of the Atlantic lineages. Secondly, there exists highly polyphenic Atlantic lineages living within close proximity (<20km) of Pacific populations with greatly reduced polyphenism. In one river in the Isthmus of Tehuantepec, we have evidence of both lineages coexisting with limited introgression (Chapter 3). Genotyping is currently the only method to distinguish between Pacific and Atlantic individuals, so we have limited phenotypic data positively assigned to each lineage at this site. So far, we have identified one female *H. titia* with a fully Pacific genotype in the Atlantic drainage. If Pacific and Atlantic *H. titia* have distinct phenotypes at the peak of the season at the same site this would rule out a lack of environmental trigger. More pure Pacific individuals from the site are needed to confirm that there are distinct phenotypes between Pacific and Atlantic lineages within the zone of secondary contact.

The distinct selective regime for the highest latitude lineage shows that the seasonal polyphenism in *H. titia* can evolve rapidly. Our phylogeny indicates that the highest latitude *H. titia* are most closely related to those in Florida, which is a highly polyphenic population (facet D in Figure 5:1b). The loss of polyphenism in the highest latitudes suggests that the highest latitude populations have been under strong selective pressure to reduce the level of polyphenism. The low density of heterospecifics at higher latitudes could be the cause for the lack of polyphenism in high latitude *H. titia,* but this requires further investigation. The rapid loss of polyphenism is seen in other species. Snowshoe hares (*L. americanus*) exhibit seasonal polyphenism in coat colouration, but several populations undergone convergent evolution to have year round brown fur as an adaptation to reduced winter snow cover (Mills *et al.*, 2018). The underly genetic cause of the polyphenism in *H. titia* is currently unknown, but further work using whole genome resequencing could investigate the precise genetic cause of the variation in polyphenism across *H. titia*. The loss of polyphenism is more likely to have arisen from genetic variability within *H. titia* rather than introgression because there is currently no evidence of introgression between any species of *Hetaerina* damselflies.

We found that there was no evolutionary correlation between the peak and off-peak phenotype, suggesting that populations of *H. titia* are not strongly influenced by pleiotropic or other effects constraining the divergence in phenotype between seasons. A lack of co-evolution suggests that selection can act to produce an optimal level of melanisation across the year. Our initial hypothesis was that the peak and off-peak phenotypes would be positively correlated as pleiotropic effects would mean an increase in melanisation in one season would act to increase the overall level of melanisation across the year. Although non-significant, our results point towards an alternative evolutionary constraint, a negative correlation between peak and off-peak melanisation (Figure 5:3g). A negative correlation would mean the polyphenism evolves by increasing or decreasing the magnitude of variation between seasons. There would be limited capacity to increase or decrease the degree of melanisation between seasons at the same time. Consequently, selection pressure in one season could lead to changes in trait value in the other season, shifting the trait away from the optimal value. The seasonal polyphenism would evolve at the fastest rate if selection in different seasons was acting in opposing directions.

As expected, the best selected model (Table 5:2) showed that the theta value for peak melanisation is higher than the off-peak melanisation in the Atlantic drainages. The peak theta value was also higher than the off-peak theta value in the Pacific lineages indicates selection for seasonal polyphenism in both Atlantic and Pacific lineages. The theta value for the peak phenotype in the high latitude lineage was negative which does not correspond to a valid level of wing melanisation. Because alpha was constrained across all lineages, the negative peak theta value indicates there is strong selection to reduce the degree melanisation within the high latitude lineage. Models that allow for varying theta and alpha values between different selective regimes could determine more biologically plausible theta value selection in the high latitude lineage, but the model would be overfitted using the phylogenetic tree we attained for our analysis. The value for the stationary variance was 42x smaller in the off-peak than the peak season, suggesting that selection is acting to constrain the off-peak phenotype to a greater degree than the peak phenotype.

Previous research has investigated the evolution of polyphenism by modelling polyphenism as binary presence or absence trait. Binary trait values can indicate when and where polyphenism originated but does not provide information on how polyphenism has evolved once it has arisen (Song *et al.*, 2017; Casasa *et al.*, 2021). Our

methodology of modelling polyphenism, or plasticity, as a multivariate trait could be extended to other study systems. Relyea *et al.*, (2018) investigated the plasticity in the larval development of Anurans in response to predation and increased intraspecific competition and found that there was a notable phylogenetic signal in trait values but little evidence of phylogenetic signal in trait plasticity. Relyea *et al.*, (2018), modelled the evolution of plasticity using the raw difference in trait values between experimental treatments. Our methodology could be used to incorporate trait values from experimental treatments as a multivariant trait to determine the phylogenetic signal of plasticity and have the additional benefit of determining if there is co-evolution between the alternative phenotypes. However, experimental design must ensure that all species are exposed to a gradient that can trigger plasticity in all species, otherwise the reaction norm of the plasticity cannot be adequately modelled (Goolsby, 2015).

In addition, to the peak or off-peak melanisations, there are further aspects of seasonal polyphenism that could be investigated for co-evolution or phylogenetic signal using our methodology. For example, between lineages there is a shift in the timing of peak melanisation that could be evolutionary constrained or co-evolve with the peak melanisation. In addition, due to limitations in data acquisition, we restricted our analysis to the evolution of the male phenotype. Both male and female *H. titia* vary in melanisation throughout the year and both experience lower levels of interspecific behavioural interference when exhibiting higher levels of melanisation (Drury *et al.*, 2015a). The seasonal trade-off in melanisation could be different between the sexes because males and females differ in their behaviour. Differences in predation pressure between males and females is common (Christe, Keller & Roulin, 2006) and seen in Odonata (Rehfeldt, 1992). Male *Hetaerina* spend a significant proportion of time defending territories along riverbanks and are less cryptic than females which could increase predation (Grether & Grey, 1996), although this has not been quantified. It is possible that male and female *H. titia* have divergent optimal trait values but divergence in the environmental reaction norms of males and females could be constrained. Consequently, there may be coevolution between the male and female phenotype causing one or both sexes to exhibit suboptimal phenotypes within specific seasons. Alternatively, the reaction norm of male and female may be decoupled allowing optimal trait values for both sexes across seasons. How sexual conflict influences the evolution of a seasonal polyphenic trait is open question that our methodology could answer if a wider dataset of female phenotypes is attained.

Accumulating the large spatial and temporal scale of wing measurements for our study, was assisted by the fact that we could be treat wing melanisation as the proportion of colour covering a two-dimensional plane. We could extract phenotypic data from any photo that was taken broadly perpendicular to the face of the wing. Our methodology would be equally applicable to measuring the seasonal polyphenism in other winged species, particularly butterflies (Brakefield & Larsen, 1984; Kingsolver & Wiernasz, 1991; Halali *et al.*, 2021; Baudach & Vilcinskas, 2021). Other taxa have colour patterns that occur across a three-dimensional body shape and/or have morphological polyphenism (Moczek, 2010; Simpson *et al.*, 2011). Three-dimensional polyphenism patterns are harder to measure but methods do exist to align photographs from different angles (Van Belleghem *et al.*, 2018; Weller *et al.*, 2024) and advances in computer vision is enabling the construction of three-dimensional objects from a single image (Fu *et al.*, 2021). Thus, expanding our methodology to a wide range other taxa with seasonal polyphenism would be possible.

We modelled the evolution of the seasonal polyphenism in the wing melanisation of *H. titia* by combining a population level phylogeny and a dataset of phenotypes with a high spatial and temporal resolution. Using multivariate models of trait evolution, we find distinct geographic variation in the evolution of the seasonal polyphenism and that the divergence of phenotypes between seasons has not co-evolved. To our knowledge, our study presents the first empirical research into the evolution of polyphenism with sufficient data to phylogenetically model the seasonal variation in polyphenism across the entire range of a species.

Data availability

All code used in the creation of this Chapter can be found on GitHub at https://github.com/ChristophePatterson/Thesis_H_titia_seasonal_polyphenism_evolution

Chapter 6 The loss of seasonal polyphenism in smoky rubyspots is associated with a range expansion since the last glacial maximum.

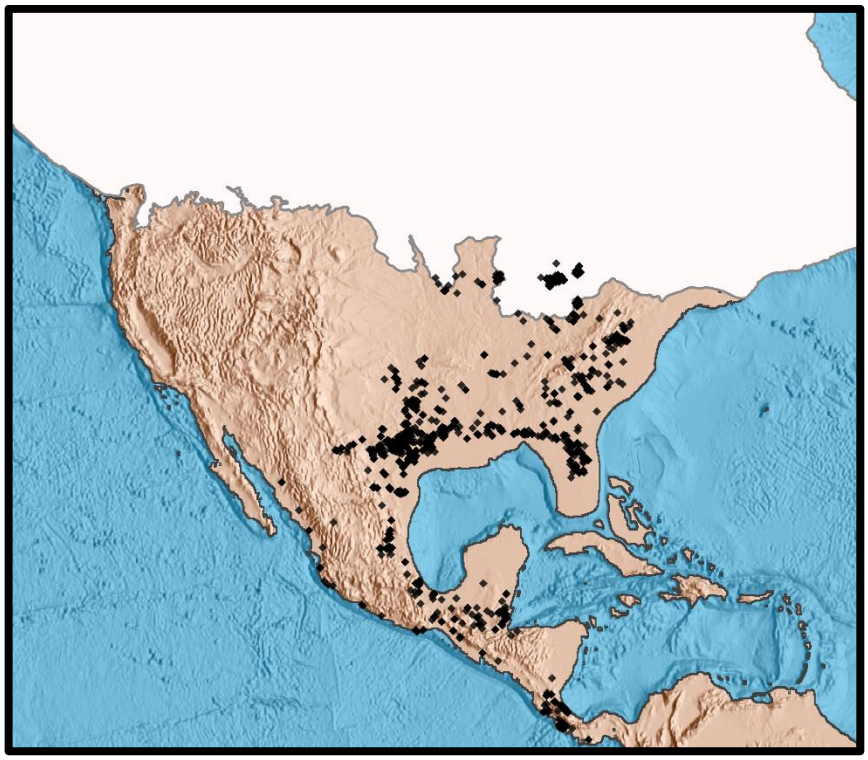

Illustration of North America during the last glacial maximum (21,000 years ago) and the modern-day distribution of records for *Hetaerina titia*. Ice sheet projection from Dalton *et al.*, (2023).

Abstract

Understanding how species responded to past climate change could help predict changes to biodiversity in the future. During the last 115,000 years, there have been repeated cycles of glaciation, and, during colder periods, many high latitude species ranges were restricted to glacial refugia. Here, we use population genetics and species distribution models (SDMs) to examine the historical distribution of two species of *Hetaerina* damselflies in eastern North America during the last glacial maximum (LGM). We focus on smoky rubyspot damselflies (*Hetaerina titia*) because high latitudes population do not exhibit the seasonal polyphenism seen in many lower latitude's populations, potentially as an adaptation to reduced interspecific behavioural interference. We find that populations of *H. titia* at high latitudes are most closely related to those in Florida and that there is significant genetic signal of range expansion from Florida to the higher latitudes. SDMs also predict a region of climatically suitable habitat in Florida during the LGM. Because populations of *H. titia* in Florida exhibit seasonal polyphenism, the loss of the seasonal polyphenism in high latitude populations likely occurred since the LGM. In contrast to *H. titia*, we find that high latitude *Hetaerina americana* are more closely related to populations west of the Mississippi River, in Texas and Northern Mexico. Despite similar dispersal ability and life histories, the Mississippi River is a much greater barrier to geneflow for *H. americana* than *H. titia*. To our knowledge, this research is first to investigate the spatial genetic structure of any Odonate across eastern North America using next-generation sequencing technology, providing novel insights into the genetic diversity and structure across the region.

Introduction

Anthropogenic greenhouse gas emissions are causing a significant shift to the global climate. As the climate changes the spatial distribution of species is changing (Parmesan & Yohe, 2003; Thomas, 2010; Burrows *et al.*, 2014). However, the earth's climate has changed multiple times (Zalasiewicz & Williams, 2021) with corresponding shifts is the spatial distribution of species (Jackson & Blois, 2015). How the distribution of species shifted during past climatic changes could help predict and prepare for the ongoing redistributions of earth's biota (Maguire *et al.*, 2015; Fordham *et al.*, 2020).

Due to variation in dispersal capability, the distributions of species, in response to contemporary climate change, will not change in concert and novel biotic interactions will arise (Williams & Jackson, 2007; Alexander *et al.*, 2015). In addition, if two species with strong biotic interactions shift asynchronously, newly establish populations would no longer be influenced by the presence of the other species (Early & Sax, 2014). The loss of a biotic interaction can greatly influence the demography and the evolutionary trajectory of a population which is clearly seen by invasive species establishing in novel communities (García *et al.*, 2013). Invasive species often have much larger population densities than those in the species native range and can undergo rapid evolution adapting to competitor and predator free environments (Moran & Alexander, 2014). Whether or not the same process will occur during climate induced ranges shifts is an important question to predicting the biological communities of the future (Moran & Alexander, 2014; Alexander *et al.*, 2015).

During the last 115,000 – 11,700 years, there has been repeated cycles of glacial and interglacial periods (Beyer, Krapp & Manica, 2020). During the last glacial maximum (LGM), around 21,000 years ago, much of the highest latitudes of the northern hemisphere were covered by ice sheets and uninhabitable. During the LGM, species ranges shifted to lower latitudes and elevations, referred to as glacial refugia (Maggs *et al.*, 2008; Lyman & Edwards, 2022). Since the LGM many species have undergone range shifts with populations established at higher latitudes and elevations (Maggs *et al.*, 2008; Maguire *et al.*, 2016). During the glacial retreat it is likely that novel communities arose, and many populations underwent release from biotic interactions.

Here, we investigate if the loss of a seasonal polyphenism could be explained as recent evolutionary adaptation to novel biotic communities formed after the LGM.

Smoky rubyspot damselflies (*Hetaerina titia*) exhibit a striking seasonal polyphenism in wing melanisation (Drury *et al.*, 2015a, 2019b). Across large parts of the species range, smoky rubyspots that emerge at the start of the year have low levels of wing melanisation. As the year progresses smoky rubyspots emerge with higher levels of wing melanisation but the average level of melanisation at emergence falls towards the end of the season. Individual wing melanisation does not change after emergence and adult *Hetaerina* have a lifespan typically less than one month. Consequently, the average phenotype of populations shifts throughout the year owing to a shift in wing phenotypes in newly emerging individuals. Because individuals with low melanisation appear phenotypically similar to sympatric congeners, melanised *H. titia* engage in fewer interspecific territorial fights and interspecific mating attempts than non-melanised *H. titia* (Drury *et al.*, 2015a). However, not all populations of *H. titia* exhibit seasonal polyphenism, particularly those at the highest latitudes of the species range (Drury *et al.*, 2019b, Chapter 5). The highest latitude populations of *H. titia* are found in regions that would have been directly covered by ice sheets during the LGM and consequently would not have been suitable habitat. Population genetics suggest that *H. titia* that reside in the highest latitudes of North America are most closely related to those in Florida (Chapter 4). Yet, *H. titia* in Florida exhibit a high degree of seasonal polyphenism suggesting that the loss of polyphenism has arisen since these populations diverged and possibly since the LGM. As wing melanisation is beneficial at higher densities of heterospecific we hypothesis that the loss of seasonal polyphenism is an evolutionary response to the loss of biotic interactions at higher latitudes after a range expansion from a glacial refugia in Florida.

Using a combination of population genetics and species distribution models (SDMs) we determine whether the loss of seasonal polyphenism likely occurred after LGM. We use SDMs to predict the location of the LGM refugia for *H. titia* and, as a comparison, for the congener *Hetaerina americana* (the only other rubyspot damselfly widely distributed in eastern North America). We then use population genetics to determine if the highest latitude populations of *H. titia* and *H. americana* show a signature of range expansion from one or more of the glacial refugia predicted from SDMs. Combined we gain an understanding of how populations of *H. titia* established in the highest latitude of North America and whether this is likely to associate with the loss of melanisation. We also gain a wider understanding of the population genetics of two species of damselflies in the understudied Nearctic (Sanchez-Herrera *et al.*, 2022).

Methodology

Last glacial maximum species distribution models

To estimate the distribution of *H. titia* and *H. americana* since the LGM, thereby identifying plausible locations for glacial refugia, we conducted species distribution models (SDMs) using modern day occurrence records and then projected our models back to LGM. We used climate data from Beyer, Krapp and Manica, (2020) who reconstructed paleoclimate data from the modern period back to the last 120,000 year in time steps of 1,000-20,000 years with a resolution of 0.5 degrees. Beyer, Krapp and Manica, (2020) contains global monthly temperature, precipitation, cloud cover, relative humidity, wind speed, 17 bioclimatic variables, annual net primary productivity, leaf area index and estimated biomes. We limited our analysis to North and Central America using a longitudinal and latitudinal bounding box of (-130°E, 0°N) to (-60°E, 70°N). We also limit our projection of species distributions to the modern day and to 21,000 years ago (LGM).

We focus on the SDMs for *H. titia* and *H. americana* because they are the most numerous and widespread North American species of *Hetaerina*. *H. titia* and *H. americana* are also the only species we attained genetic sequence data for, allowing for comparison between the population genetics and the glacial refugia predicted by SDMs.

We downloaded occurrence records for *Hetaerina* damselflies from the Global Biodiversity Information Facility (GBIF) using the R package *dismo* (https://CRAN.R-project.org/package=dismo). *H. americana* has been recently split into two cryptic species, *H. americana* and *H. calverti* (Vega-Sánchez *et al.*, 2024) consequently we merged records from these two species because we could not positively assign or differentiate records from either species. We excluded records that were not georeferenced, had a latitude and longitude equal to 0, had fewer than 5 decimal points of precision in the georeferenced data, that were for preserved specimens, or were records of species absence. This retained 16,868 occurrence records split across 13,510 records of *H. americana* (of which 39 were records of *H. calverti*) and 3,358 records of *H. titia*. Occurrence data was thinned to one record per grid cell of the climate data retaining 1619 records of *H. americana* and 613 records of *H. titia*. (Derived dataset GBIF.org (30 April 2024) Filtered export of GBIF occurrence data https://doi.org/10.15468/dd.gakazy).

We fit SDMs following the protocol by Bagchi *et al.*, (2013) and developed by Baker *et al.*, (2015). SDMs were trained and tested on multiple spatially disaggregated blocks of climate data with approximately equal mean and variance for each bioclimatic variable allowing for cross validation of our models across multiple data sets for the same species. For each species, SDMs were trained using a leave-one-out approach. Multiple SDMs were trained using occurrence data from all but one of the climate blocks and then cross validated using the data from the excluded block. Model training and cross validation was then repeated for all combination of the leave-one-out climate block sets. We did not restrict our projections to neighbouring biogeographic regions because most other regions were excluded from our analysis by the bounding box of our subset climate data. We do not have accurate range maps or large-scale true absence datasets for *Hetaerina*, as such, we generated pseudo absence data using the function *randomPoints*, from *dismo*, equal to the total number of presence data points for each species.

To select the most appropriate of the 17 bioclimatic variables, we devised all the possible combinations of three to five bioclimatic variables within the Beyer, Krapp and Manica, (2020) dataset. We removed combinations without a single temperature or precipitation variable and that had two variables with spearman's rank correlation greater than 0.7; retaining 231 unique combinations. We ran general additive models for both species, then ranked each combination of bioinformatic variables by how often it appeared in the top 25% of AIC values for each species. The only combination of variables in the top quartile were bioclimatic variables BIO7, BIO10, BIO15, BIO18, and BIO19 (temperature annual range, mean temperature of warmest quarter, precipitation seasonality, precipitation of warmest quarter, and precipitation of coldest quarter, respectively). We used these bioclimatic variables to run an ensemble of SDMs using general addictive models (GAMs), general linear models (GLMs), and random forests (RFs). For each modelling approach we assessed model accuracy using area under the receiver operating characteristic plot (AUC) from Hanley and McNeil (1983).

For the GLMs, we fitted polynomial relationships between the species occurrence records and the selected bioclimatic variables from Beyer, Krapp and Manica, (2020). We modelled the bioclimatic variables as having a combination of either linear, quadratic, and cubic relationships (1-3 polynomial degrees x 5 bioclimatic variables = 243 combinations of bioclimatic variables and polynomial degrees). Model fit was calculated using AUC and the best selected model, for each species, was chosen

using which combination of polynomial degrees that had the highest median AUC across the leave-one-out climate block sets. GAMs were fitted using the *gam()* function of the *mgcv* R package(Wood, 2011). Occurrence records within each climate grid were modelled as a Bernoulli response using a logit link. For the random forest modelling approach we used the *randomForest* R package (Liaw & Wiener, 2002). We initially used a set of 1000 trees and tested the model's performance using the AUC of each omitted climate block. We then iteratively increased the number for trees by 500 until the AUC value did not improve by more than 1%. Full details of all modelling approaches can be found in Bagchi *et al.*, (2013).

To predict the distribution of each *Hetaerina* species at the LGM, we used the best overall modelling approach by determining which modelling method had the highest median AUC across all species. We predicted the distribution of each species using the climate data from 21,000 years ago using the model with the highest AUC for each species from best overall modelling approach. We assigned grid cells with predicted probability of occurrence greater than 0.5 as having suitable climatic habitat. We determined the modern day and LGM latitudinal range of each species using the top and bottom 5% quartiles of climate cells that had a predicted occurrence probability above 0.5. We used a predicted probability of greater than 0.75 as having a high climatic suitability to calculate the difference in the size of climatically suitable habitat.

Population genetics

To characterise the genetic structure of *H. titia* and *H. americana* across North America, and determine if there are genetic signature of range expansion from the glacial refugia identified by the SDMs, we generated genome-wide SNP data following the double digest restriction enzyme (ddRAD) protocol of DaCosta and Sorenson, (2014) and Franchini *et al.*, (2017). Full laboratory protocols are outlined in Chapter 3. Previous population genetic analyses conducted on a similar SNP dataset for *H. titia* and *H. americana* indicate that the populations within North America are distinct from those of Central America (Chapter 4). Generating a new SNP library containing only the North American lineages of *H. titia* and *H. americana* allows for greater inference because SNP libraries that contain other lineages contain a large proportion of SNPs that are fixed between lineages and reduced number of SNPs because of fewer shared restriction sites. We aligned sequence of *H. titia* samples to the draft genome of *H. titia* (Patterson *et al.*, 2023, Chapter 3) using the Burrow-Wheeler aligner (bwa) *mem*

alignment algorithm (Li & Durbin, 2009). We aligned sequences of *H. americana* samples to the draft genome of *H. americana* (Grether *et al.*, 2023) using the same method. We restricted our analysis to samples that have been assigned to the Northern Atlantic lineages of *H. titia* and *H. americana* in previous work (Chapter 4).

Genotype calling was done using *bcftools v1.13* (Li, 2011; Danecek *et al.*, 2021) using the *mpileup* and *call* commands, with a max depth of 10,000 and a prior expected substitution rate of 1e-6. As our samples were collected over a large geographical scale, we did not use Hardy-Weinberg equilibrium calculations for variant calling. After genotyping, variant sites were restricted to SNPs. We filtered to remove all SNP calls with a read depth of less than 10, an average read depth across all samples above 200, and a quality score less than 20. Further filtering removed SNPs that had a minor allele count less than 2, SNPs that were found in less than 80% of samples, and to avoid linkage we randomly selected one SNP from a window of 1000 base pairs using the *prune*+ command in *bcftools* (Danecek *et al.*, 2021).

After initial filtering the vcf files were imported into R using the package vcfR (Knaus & Grünwald, 2017). Further SNP and sample filtering, and conversion of vcf into compatible formats for each analysis software was done using the r packages ape (Paradis & Schliep, 2019), adegenet (Jombart, 2008), and poppr (Kamvar *et al.*, 2014).

We restricted the SNPs to those that were biallelic and autosomal. We then removed samples that had more than 20% missing data. For *H. titia,* we retained 89 *H. titia* samples with autosomal biallelic 5,675 SNPs. We retained 35 *H. americana* samples with 12,639 SNPs. Across both species, the remaining samples had a median percentage of missing data of 2.22% and a range from 0.23% to 18.91%.

To determine the population structure of *H. titia* and *H. americana across* North America we used the r package LEA (Frichot & François, 2015) to conduct principal component analysis (PCA) and non-negative matrix factorization algorithms (sNMF) for least-squares estimates of ancestry proportions for each sample (Frichot *et al.*, 2014). We used sNMF analysis for ancestry analysis, instead of structure (Hubisz *et al.*, 2009) or admixture (Alexander *et al.*, 2009), because it produces comparable estimates of ancestry estimates but with faster computation time (Frichot *et al.*, 2014). In sNMF, we tested for a range of ancestral populations (K = 1 to 10) and plotted the mean cross-entropy values for 20 repetitions.

To reconstruct the historic movement and establishment of populations of *H. titia* and *H. americana,* we used the directional index of genetic drift (φ) introduced by Peter and Slatkin (2013) using the r package *rangeexpansion* (https://github.com/BenjaminPeter/rangeexpansion). The directionally index determines if there is asymmetry in 2D allele frequencies between populations. Under the assumption that range expansions occur as a series of founders' effects where low frequency alleles are likely to be lost, the most likely direction a range expansion between two populations can be inferred. For any two populations, the direction of range expansion can be inferred from whether the calculated value of φ is positive or negative. Calculating φ for multiple population pairs allows the origin of a range expansion to be predicted using time difference of arrival location estimation (TDOA), because the magnitude difference in φ is assumed be equal to the difference in geographic distance from the point of origin. We calculated φ for all population pairs across North America and for each group of populations assigned to different ancestry cluster detected by sNMF.

To further investigate what geographic factors have influenced the population genetics of *H. titia* and *H. americana* we used Estimated Effective Migration Surfaces (EEMS) to model the effective migration rate for both species across North America (Petkova *et al.*, 2015). EEMS allows for the visualization of where (geographically) effective migration differs from that of a strictly isolation-by-distance model, thus revealing barriers to and corridors for gene flow. EEMS has been used to detect genetic signatures of isolation during the LGM (Stiller *et al.*, 2021). We calculated the pairwise difference matrix from the SNP data using a custom R script developed from that of DeRaad *et al.* (2022). We ran EEMS within a custom polygon that encompassed all North American samples of *H. titia* and *H. americana*. The polygon was created using the online tool https://www.keene.edu/campus/maps/tool/. For *H. americana,* we created 500 demes in an offset diagonal grid and ran EMMs for 10,000,000 step MCMC chain with a 5,000,000 step burn-in, and sampled every 9,999 steps. To improve convergence for *H .titia,* we increased the burn in to 10,000,000 and total number of steps to 20,000,000. We also increased the proposal variance for the migration cell effects from 0.1 to 0.2 and increased the proposal variance for the overall migration rate from 0.01 to 0.05. For *H. titia* we also ran five independent MCMC chains to compare convergence across independent chains. We checked runs for convergence and checked

model fit by comparing the observed and the fitted data points. We visualised the results using the R scripts provided with the EEMS package and our own custom R scripts.

To assess overall genetic differentiation between the clusters identified by sNMF we calculated the Fst values (Weir & Cockerham, 1984) between each cluster. We also assessed the overall level of genetic diversity within each cluster by calculating the mean observed heterozygosity for each population and comparing between sNMF clusters. Fst and heterozygosity were calculated using the r package *heirfstat* (Goudet, 2005).

Results

LGM distribution of Hetaerina

Across all modelling approaches, the overall model fit was good with AUCs greater than 0.82 for all model and climate block combinations. The modelling approach with the highest median AUC value for both species was the random forest classifier with the median AUC value for each species higher than 0.86, ranging from a minimum value of 0.84 to 0.87 and a maximum value range of 0.9 to 0.95 (Table 6:1). For brevity, all results refer to the predicted species distribution using the random forest classifier going forward.

Table 6:1: Model cross validation for each species and each modelling approach. Table presents, for each *Hetaerina* species, how many occurrence records (median, minimum, and maximum) were contained within the training and cross validation using each combination of the 10 climate blocks. The median, minimum, and maximum AUC values for each modelling approach, random forest classifier (RF), general linear model (GLM), and general additive model.

Hetaerina species	**Median number of training records (min – max)**	**Median number of Cross validation records (min – max)**	**RF median AUC (min – max)**	**GLM median AUC (min – max)**	**GAM median AUC (min – max)**	**Highest median AUC modelling approach**
H. americana	2839.5 (2746 - 2860)	306.5 (286 - 400)	0.86 (0.84 - 0.9)	0.82 (0.77 - 0.83)	0.83 (0.81 - 0.87)	RF
H. titia	1016.5 (967 - 1042)	107.5 (82 - 157)	0.94 (0.87 - 0.95)	0.89 (0.87 - 0.9)	0.91 (0.81 - 0.93)	RF

The projected latitudinal range of *H. titia* was reduced from 16.8° N - 41.8° N, during the modern day, to 16.2° N - 26.8° N during the LGM. For *H. titia* during the LGM, regions of moderate habitat suitability covered the Gulf coast of the modern United States and Mexico, but with highest predicted habitat suitability in Florida. The total number of cells with a high probably of occurrence of *H. titia* (>0.75) during the LGM fell by around 90% relative to the modern day, from 1137 to 134 cells.

For *H. americana,* the highest predicted habitat suitability during the LGM was in the approximate location of the modern-day border between Texas and northern Mexico. The projected latitudinal distribution of *H. americana* shifted from 24.2°N - 33.8°N, during the LGM, to 28.2°N - 45.2 N in the modern day. *H. americana* also had a projected reduction in suitable habitat of 90%, from 1,303 to 552 cells.

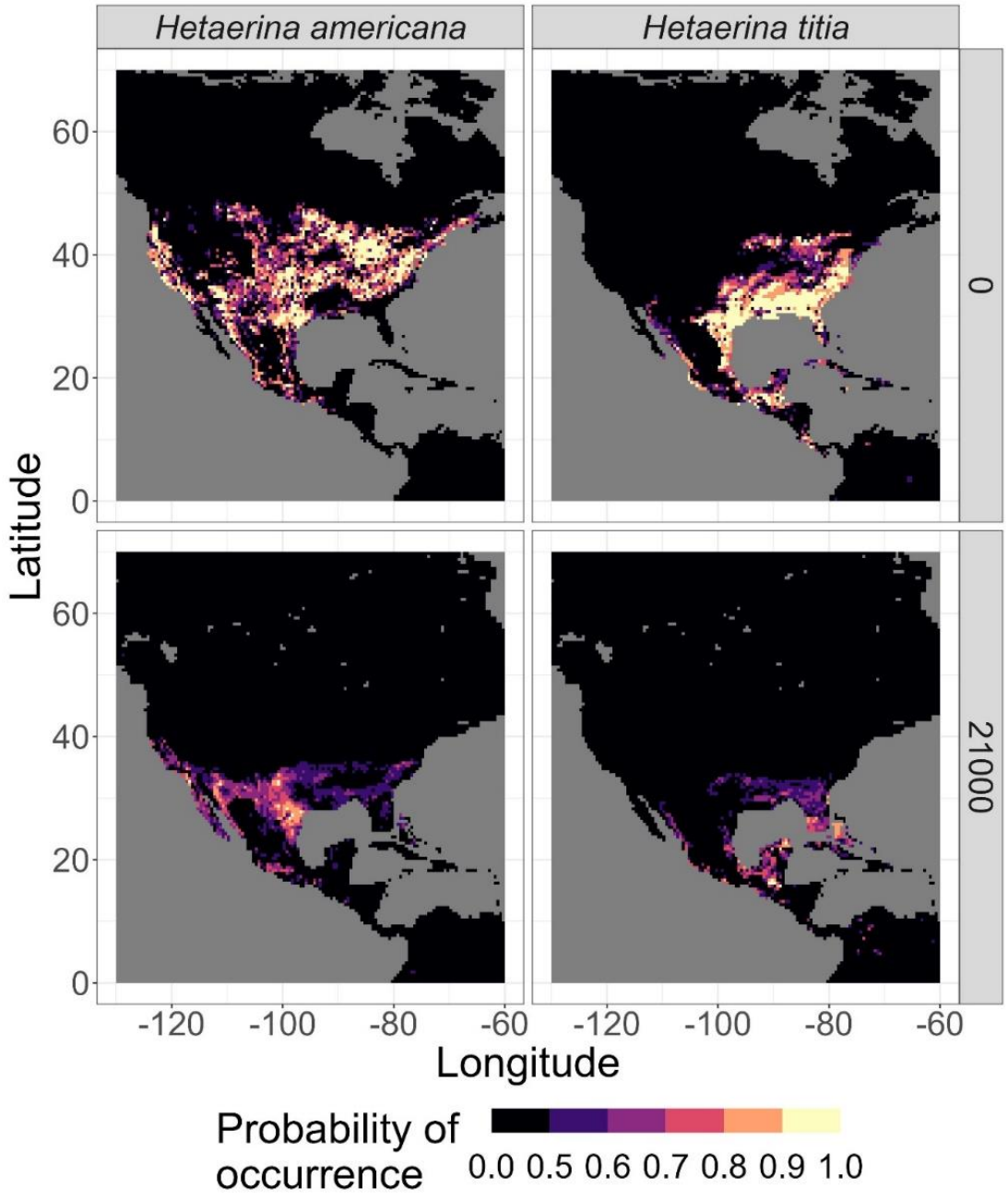

Figure 6:1: The predicted distribution of *Hetaerina americana* and *Hetaerina titia* for modern day, 0 years ago, and at the last glacial maxima (LGM) 21,000 years ago. Predictions are made using the highest AUC random forest model for each species. Predicted probabilities below 0.5 are shown in black.

Population genetics

sNMF and PCA analyses separated both *H. titia* and *H. americana* along an east to west axis of population differentiation (Figure 6:2). For *H. titia*, the cross-entropy values produced by sNMF analysis had a strong inflection at K=3 but with values that overlapped with K=2 (Supplementary Figure 4:1), meaning we used K=2 for all

downstream analysis but present the findings for K=3 in the Appendix Chapter 6. Populations of *H. titia* clustered into two distinct regions with distinct differentiation between the ancestry assignment of populations in Florida and those in Mexico and Texas. Populations of *H. titia* that reside either side of the Mississippi exhibited a mixture of ancestry assignment. The highest latitude populations of *H. titia* shared the majority of ancestry assignment with populations in Florida.

For *H. americana*, the cross-entropy values produced by sNMF analysis had a strong inflection at K=2 (Supplementary Figure 4:1), so we used K=2 for all downstream analysis. For populations of *H. americana* at lower latitudes, close to the Gulf of Mexico, there were two distinct clusters of populations which are separated by the Mississippi river (Figure 6:2b). At higher latitudes, populations of *H. americana* east of the Mississippi clustered with the lower latitude populations on the west side of the Mississippi River. PCA axis 1, clearly segregated populations of *H. americana* east and west of the lower reaches of the Mississippi River.

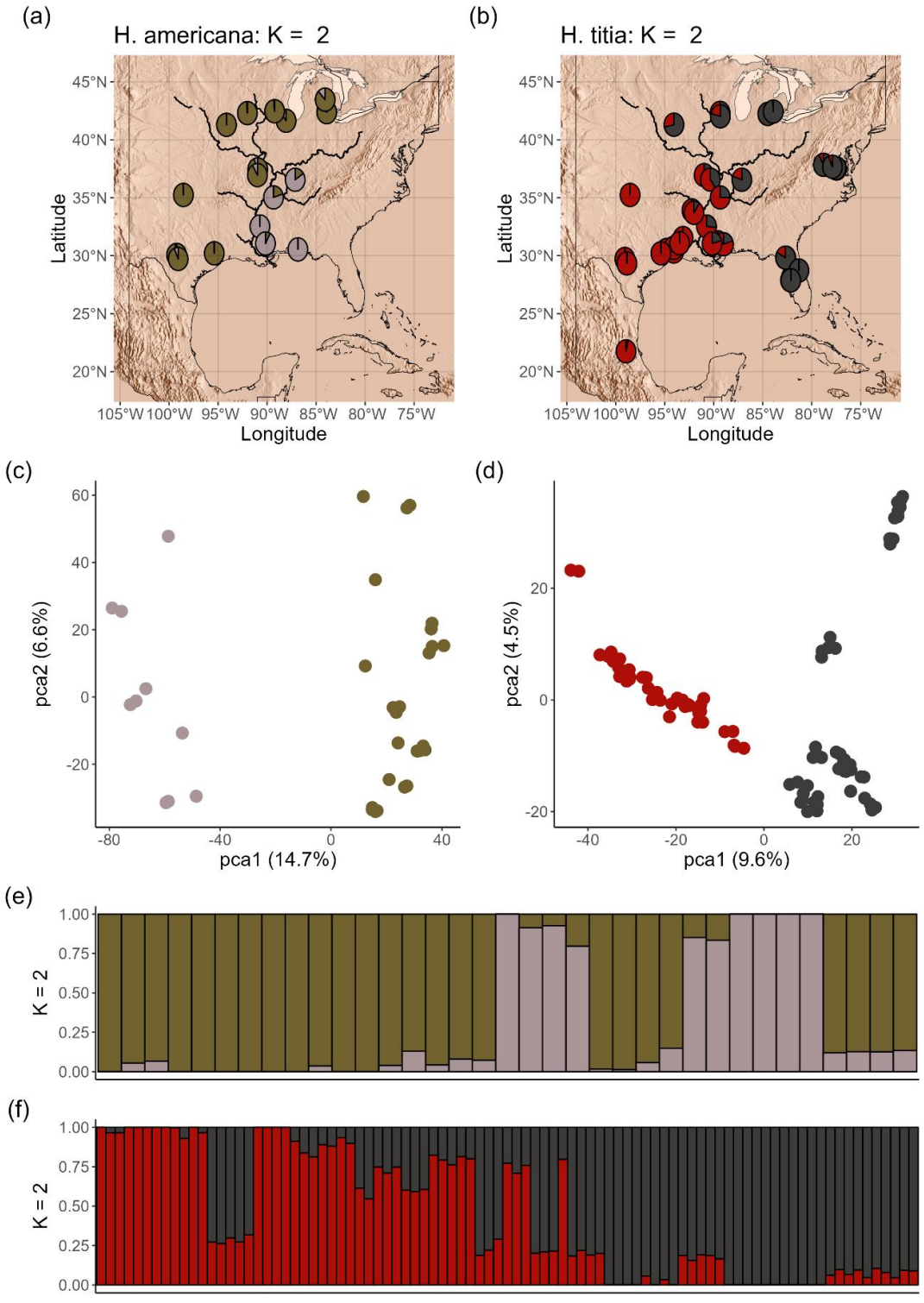

Figure 6:2: Ancestry estimates using two ancestral populations for 89 *Hetaerina titia* and 35 *Hetaerina americana* using a dataset of 5,675 and 12,639 unlinked biallelic autosomal SNPs, respectively. SNPs were generated by mapping ddRAD reads to the draft genome of *H. titia*. LEA was run for 20 repetitions and an alpha value of 100. **(a)** The mean estimate of ancestry proportion for all samples within each sample site of

H. americana across North America, **(b)** The mean estimate of ancestry proportion for all samples within each sample site of *H. titia* across North America. sNMF plots include a shaded relief map using the package elevatoR (Hollister *et al.*, 2023) and the main tributaries of the Mississippi river from the HydroBasins/v2 river dataset (Lehner, Verdin & Jarvis, 2008). Principal component analysis of **(c)** *H. americana* and **(d)** *H. titia*. Percentages in axis labels indicate how much variation is explained by each component and colour indicates the highest assigned ancestry population from sNMF for each individual. Estimate of ancestry analysis for each individual for **(e)** *H. titia* and **(f)** *H. americana*. Samples are ordered by longitude, west (left) to east (right).

Fst calculations between the K=2 clusters were 0.023 for *H. titia* and 0.058 for *H. americana*. On average for both *H. titia* and *H. americana* population in the eastern cluster had higher levels of observed heterozygosity (Supplementary Figure 6:4). Eastern and western *H. titia* had a mean observed heterozygosity 0.192 and 0.134, respectively. In the western populations the observed heterozygosity was lower in populations in central Florida and those at higher latitudes. For *H. americana*, eastern and western a mean observed heterozygosity of 0.165 and 0.111, respectively.

Range expansion

The directionally index of genetic drift (φ) showed a strong signature of range expansion within eastern populations of *H. titia* (Figure 6:3a). The range expansion originated in Florida and radiated out to the highest latitude populations of *H. titia* in the continental United States. There was less evidence of a coherent pattern to φ in the western populations of *H. titia* and from either western or eastern populations of *H. americana* (Figure 6:3b).

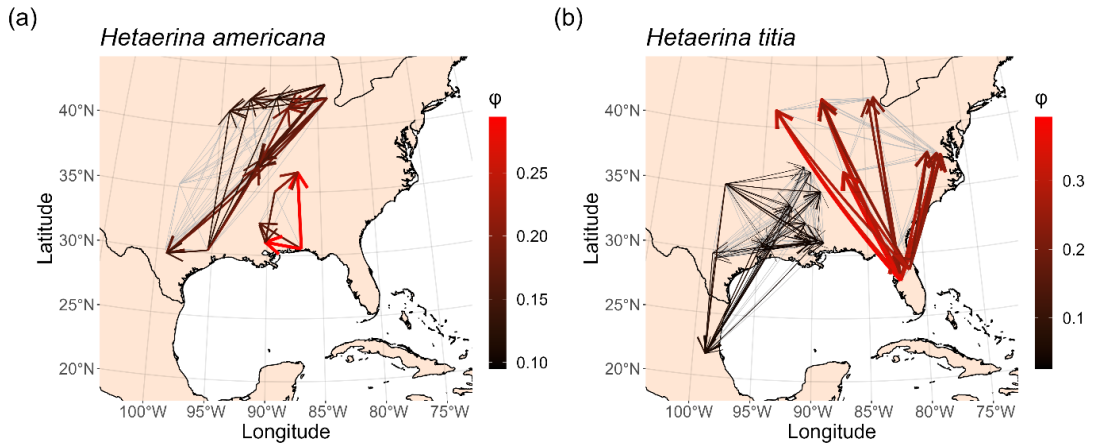

Figure 6:3: Genetic signature of range expansion using the directionally index of genetic drift (φ) for (a) *Hetaerina titia* and (b) *Hetaerina americana*. Calculations of φ were conducted separately for each ancestral cluster identified by sNMF analysis with all population combinates indicated by thin grey lines. For clarity with only plot values φ that have a greater than one standard deviation from the mean value. Arrows are coloured and scaled with φ. The arrows direction marks the signed value of φ pointing towards the site that is further away from the predicted origin of range expansion.

Effective migration estimation

The MCMC chains for EMMS analysis converged for *H. americana*. Two of the trace plots for the independent MCMC chains for *H. titia* showed a continuous trend to MCMC chain so were excluded. The other three MCMC chains for *H. titia* converged on the same parameter values and we present the average values across all converged chains in line with the EEMs manual. As suggested by sNMF analysis, EEMS detected a departure from isolation by distance for populations of *H. americana* across the lower reaches of the Mississippi river. The estimated migration rate for upper reaches of the Mississippi river were above average for *H. americana* (Figure 6:4a). *H. titia* showed a more complex mosaic of effective migration that was not clearly explained by the Mississippi River (Figure 6:4b). The effective diversity was not geographically uniform for either *H. titia* or *H. americana*. For *H. americana,* population close to the Gulf of Mexico had a lower effective diversity than those at higher latitudes (Figure 6:4e). Populations of *H. titia* had much lower average levels of effective diversity in Florida

and in Michigan in comparison to those found across the rest of North America (Figure 6:4d).

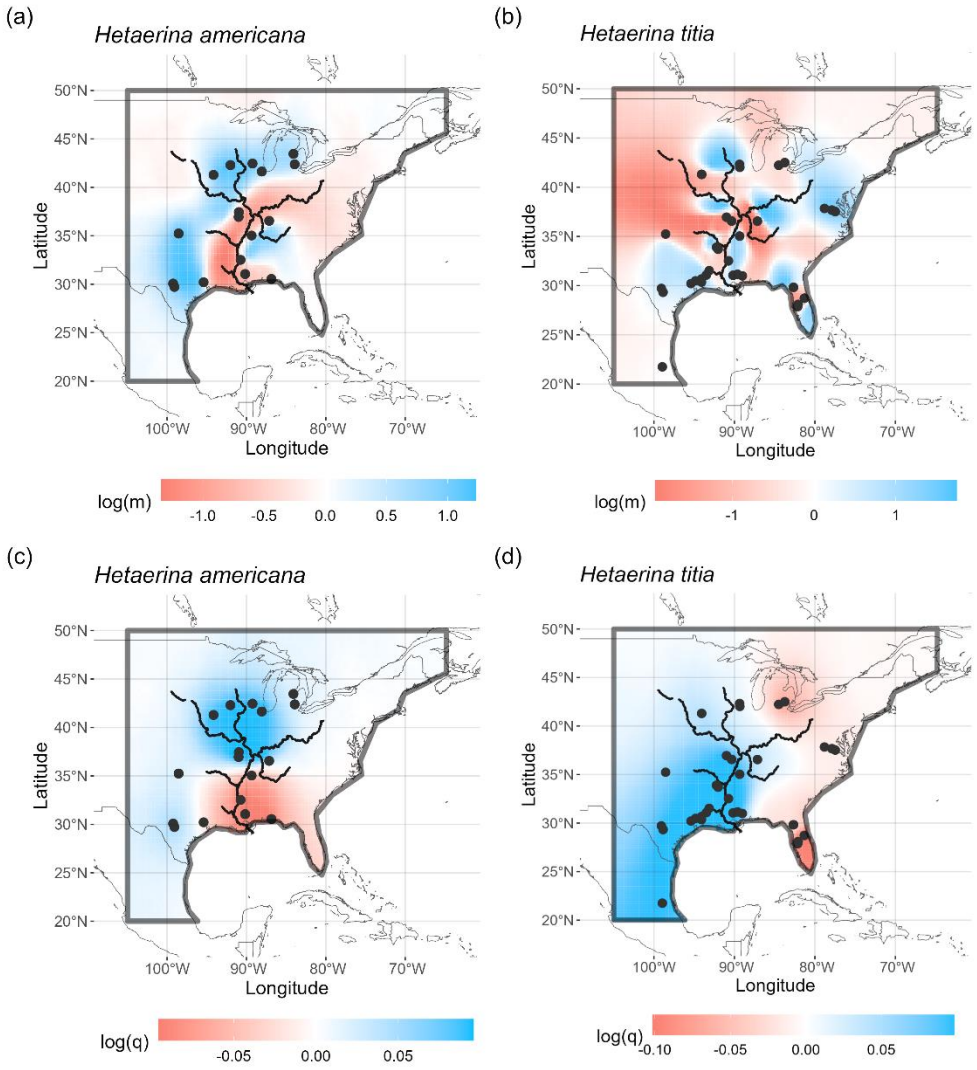

Figure 6:4: The posterior means for the effective migration rate (a, b) and the effective diversity rates (c, d) calculated by EEMS for *Hetaerina americana* and *Hetaerina titia* across North America. *H. titia* results are the mean values for each cell across multiple MCMC chains. Effective migration rate, *m*, indicates how rapidly individuals' relatedness decreases with geographic distance, with low values indicating lower population migration. Effective diversity rates, *q*, indicate how distinct two populations from the same population are likely to be, with lower values indicating higher levels of similarity (lower diversity). Black dots mark sampling location, the thick grey outline shows the geographical limit to EEMS analysis. The main river channel of the Mississippi river is marked by a black line.

Discussion

Our study used species distribution models (SDMs) and spatial population genetics to understand the connectivity and spatial distribution of two *Hetaerina* damselflies across eastern North America since the last glacial maximum (LGM). Our main focus was understanding the geographical origin of the most northly latitudinal populations of *H. titia,* because high latitude *H. titia* do not exhibit the seasonal polyphenism seen in most populations at lower latitudes. We found that the most northly populations of *H. titia* are closely related to those in Florida and that there is a strong genomic signal of range expansion out from Florida towards the northern latitudes. The genetic data corresponds with the SDMs that predict a region of high climatic suitability in Florida during the LGM. In contrast to *H. titia*, the spatial genetic structure of *H. americana* indicates that most northly populations are more closely related to the population west of the Mississippi River and that the region with the highest climatic suitability during the LGM was in the region of modern-day Texas and northern Mexico.

As expected, the SDMs for *H. titia* and *H. americana* projected the ranges of both species to lower the latitudes during the LGM. The projected upper latitudinal limit of both species during the LGM was over 10° lower than the projected upper latitudinal limit for the modern day (Figure 6:1). There was little shift in the minimum latitudinal limit in either species. During the LGM, the total size of predicted suitable climatic habitat for both *H. americana* and *H. titia* fell by around 90%, suggesting there has been a large increase in available climatic niche space since the LGM. The SDMs are consistent with the hypothesis that *H. titia* and *H. americana* in eastern North America were restricted to glacial refugia during the LGM.

For *H. titia*, SDMs suggest a possible glacial refugia in Florida (Figure 6:1c) and ancestral clustering analysis shows that the highest latitudinal populations of *H. titia* are most closely related to those in Florida. Furthermore, the directionally index of genetic drift (Peter & Slatkin, 2013) shows a strong genetic signal of a range expansion that originated in southern Florida and expanded northwards (Figure 6:3a). The genetic data and SDMs suggest that the loss of seasonal polyphenism in northern latitude *H. titia* has occurred since the species expanded its range from a glacial refugia in Florida 21,000 years ago. sNMF analysis and PCA also indicate that there is a distinction between *H. titia* west and east of the Mississippi River, and populations close to either side of

Mississippi River show introgression between these ancestral clusters (Figure 6:2a). The region of admixture along the Mississippi River suggests there was an additional glacial refugia to the west of the Mississippi and that, after the LGM, the populations expanded and mixed with the populations expanding from the east. The approximate location a glacial refugia to the west of the Mississippi River is not clearly indicated by the SDMs but is most likely to be in Mexico. Further analysis of historical demography could shed light effective population size of *H. titia* during and since the LGM allowing inference on the size of the glacial refugia the species resided in.

An alternative to the hypothesis of two glacial refugia (one on either side of the Mississippi River), is that the high latitude population of *H. titia* originated from an additional, separate glacial refugia in northern Florida, Georgia, or Alabama. The cross-entropy values for sNMF analysis had overlapping values for K=2 and K=3 and there is a distinction in PCA axis 2 between populations in northern and central Florida. Using K=3, the sampled population in northern Florida show a high-level admixture between populations in Central Florida and the higher latitudes of North America. SDMs also projected a moderate level of climatic suitability in the region north of the Florida peninsula (Figure 6:1d). Consequently, we find some support for the scenario were during the LGM there were three isolated populations of *H. titia,* one in the south of the Florida peninsula, one in northern Florida, Georgia, or Alabama, and one in Mexico. In the three glacial refugia scenario, the northern Florida refugia contributed the majority of the genetic material to the populations of *H. titia* that expanded into the higher latitudes following the glacial retreat. Further genetic sampling should be conducted in the region of northern Florida, Georgia, or Alabama to determine the proportion of ancestry found within the region.

PCA and sNMF analysis suggest that populations of *H. titia* on both sides of the Appalachian Mountains are closely related and, consequently, likely originated from the same glacial refugia. However, populations either side of the Appalachian Mountains exhibit some genetic distinction and our SDMs indicate the Appalachian Mountains is potential barrier due to the low climatic suitability (Figure 6:1b). *H. titia* on either side of the Appalachian Mountains exhibit low levels of seasonal polyphenism (Chapter 5, Drury *et al.*, 2019b), consequently, there are two different scenarios to how the loss of the polyphenism could have occurred. One, the loss of polyphenism occurred twice either side of the Appalachian Mountains. Two, the loss of polyphenism occurred prior to the populations either side of the Appalachian Mountains diverging. Populations of

H. titia in Georgia and Alabama have low levels of melanisation in comparison to those in Florida which suggests the loss of polyphenism occurred prior to the divergence of populations either side of the Appalachian Mountains.

For *H. americana*, SDM suggest a glacial refugia within the region of the modern-day border of Mexico and the USA. Populations of *H. americana* at higher latitudes are most closely related to populations at lower latitudes west of the Mississippi River. Estimates of the effective migration rate show above average migration between populations to the west of the Mississippi and this connectively extents upwards to the populations at higher latitudes. However, the directionally index of genetic drift indicates that this migration is not associated with the genetic signatures of repeated founder effects. The genomic evidence for *H. americana*, both sNMF, PCA, and EMMs, shows a distinct genetic differentiation with little effective migration across lower reaches of Mississippi river, suggesting some historical divergence between these populations possibly because of two glacial refugia either side of the Mississippi and little admixture since. Populations of *H. americana* on the eastern side of the Mississippi River have lower levels of heterozygosity than those on the western side. The SDMs predicted some climatic suitability on the eastern side of the Mississippi but this was much reduced in comparison to the western side. The low levels of genetic diversity and the low climatic suitability suggest that *H. americana* did reside east of the Mississippi during the LGM but in isolated populations and/or with a small effective population size leading to a loss of genetic diversity. Contrary to *H. titia*, population of *H. americana* east of the Mississippi did not contribute a large proportion of genetic material to the populations that expanded their range into the higher latitudes following the glacial retreat.

Despite similar life history strategies and dispersal abilities, the Mississippi river is a much more distinct phylogeographic boundary for *H. americana* than *H. titia.* The Mississippi river is a known phylogeographic boundary for a range of taxa [reviewed by Lyman and Edwards (2022)], including a freshwater invertebrate (Pessino *et al.*, 2014). We also find evidence that *H. titia* has a phylogeographic boundary between northern and central Florida which is seen in other taxa (Lyman & Edwards, 2022). It is unclear why the Mississippi River appears to prevent dispersal for *H. americana* but not *H. titia.* The flow, size, and course of Mississippi River has varied greatly over the Pleistocene glaciation cycles (Hobbs, 1950). If the expansion of *H. titia* from the glacial refugia occurred more rapidly than in *H. americana*, then *H. titia* may have been able to disperse

over the Mississippi River before the river became a barrier. Further research could investigate the timing of introgression between *H. titia* across the Mississippi to determine if gene flow is ongoing or limited to a historical window when the Mississippi had reduced flow rate. Further research could be conducted to understand the precise mechanism that has caused the reduced gene flow across the Mississippi River which could be explained by either barrier of the river itself or the surrounding habitat.

The phylogeographic structure of Odonata in Nearctic remains understudied in comparison to the Palearctic (Sanchez-Herrera *et al.*, 2022). Lyman and Edwards (2022) conducted a systematic literature review of all phylogeographic research in the eastern North America and did not record any empirical research on Odonata. Consequently, our study is the first to use next-generation sequencing technology to study the phylogeographic structure of an odonate across the eastern North America. Other studies have used phylogenies to investigate the biogeographical variation in the distribution of multiple damselfly species across the Americas (Sánchez-Herrera *et al.*, 2020; Standring *et al.*, 2022), but little work has been done to investigate intraspecific genetic diversity within eastern North America. The Vega-Sánchez *et al.*, (2024), investigated the phylogeographic structure of *H. americana* and *H. calverti* but sampling was focused on Mexico. Other studies have identified that eastern North America contains distinct populations of many Holarctic distributed Odonata, but these large scale global studies do not provide the resolution to investigate within region genetic diversity (Sanchez-Herrera *et al.*, 2022). Prior to the advent of next-generation sequencing, Turgeon and McPeek (2002) showed that the phylogeographic structure of *Enallagma hageni,* in North America, could be explained by the species residing in multiple glacial refugia but did not determine the glacial refugia's location. Further studies on the over 350 species of eastern North American Odonate (Paulson, 2011) should be conducted to understand if the spatial patterns identified in this study are generalisable across Odonata. A notable gap in empirical research is the lack of studies in the population genetics of dragonflies across eastern North America.

There is growing evidence of several cryptic species of *Hetaerina* (Vega-Sánchez *et al.*, 2024, Chapter 4). For instance, *H. americana* was recently revised into two cryptic species (Vega-Sánchez *et al.*, 2020) and there is further evidence of differentiation between *H. americana* in continental USA and those in Mexico (Vega-Sánchez *et al.*, 2024, Chapter 4). Our study also found clear genetic differentiation between *H. americana* east and west of the Mississippi River. *H. titia* also shows high

differentiation between populations in the Pacific drainage and two distinct lineages in the Atlantic drainage, a northern and southern lineage (Chapter 4).

Conclusion

We investigated the phylogeographic structure and historical distribution of suitable climate of two species of *Hetaerina* damselflies in the understudied Nearctic region of eastern North America. We found that population of *H. americana* and *H. titia* that established in the higher latitudes of North America following the glacial retreat originated from different glacial refugia; *H. americana* from Mexico and *H. titia* Florida respectively. The loss of seasonal polyphenism seen in high latitudes population of *H. titia* appears to have occurred since the LGM indicating a rapid adaptation to the novel communities and/or ecosystems that arose over the last 21,000 years.

Chapter 7 General Discussion

Typical river habitat of rubyspot damselflies. Chiapas, Mexico (15°45'59.3"N 93°17'58.0"W)

Overview

This thesis presents novel research into the evolutionary and ecological consequences of interspecific behavioural interference, with a particular focus on the smoky rubyspot damselfly (*Hetaerina titia*). Many populations of *H. titia* exhibit a striking seasonal polyphenism in wing melanisation. The degree of melanisation influences mate and competitor recognition, and consequently there is variation in interspecific behavioural interference seen between populations of *H. titia*. Smoky rubyspots provide an exciting study system to investigate the evolutionary and ecological consequences of aggressive and reproductive interactions between species. Here, I, and the co-authors who have contributed to the already published work, greatly expanded our empirical knowledge of *H. titia* and build basis for further our understanding of the ecological and evolutionary consequences of interspecific behavioural interference.

Chapter 2 presents a synthesis of research showing how interspecific behavioural interference has influenced the spatial distribution of multiple taxa, from crustaceans to primates. Chapter 2 highlights interspecific behavioural interference as an important and often-overlooked biotic interaction to field of macroecology. The research in Chapter 3 provides the most contiguous, and one of the most complete, Odonata genomes assembled to date; a notable addition to the Earth BioGenome Project (Lewin *et al.*, 2018) and a beneficial asset for future genomic research. The draft genome of *H. titia* directly enabled the research and inference in later chapters. Chapter 4 provides an in depth understanding of the phylogeographic structure and phylogeny of *H. titia*, *Hetaerina calverti*, and *Hetaerina americana* across North and Central America. The finding that *H. titia*, *H. calverti*, and *H. americana* consist of six divergent lineages at various stages of the speciation cycle, providing novel insights into non-adaptive radiations.

Chapter 5 combines a higher resolution phylogeny of *H. titia* with a data set of phenotypic measurements from across the species range to study the evolution of seasonal polyphenism. The hypothesis that the level of melanisation seen in one season would be constrained by the level of melanisation in the other season was not supported. Having no constraint in the phenotypes between seasons means that, in the case of *H. titia*, seasonal polyphenism is an effective strategy to adapt to divergent fitness peaks across the year. One finding from Chapter 5, was that the seasonal polyphenism has been lost in high latitude populations of *H. titia* in North America.

Using a combination of population genetics and species distribution models (SDMs), Chapter 6 finds that the high latitude populations of *H. titia* expanded there range from a glacial refugia in the vicinity of the Florida peninsula, suggesting the loss of polyphenism occurred since the last glacial maxima.

In concert, the research presented within this thesis greatly expands our knowledge into rubyspots study system, including key novel research of interest to the wider ecological and evolutionary consequences of interspecific behavioural interference.

Chapter 2

The systematic literature review presented in Chapter 2 is an attempt to bridge the gap between the study of interspecific behavioural interference and the field of macroecology. There is an ongoing and urgent need to understand the processes that will facilitate or prevent the ranges of species from responding to anthropogenic climate change (Thomas, 2010; Travis *et al.*, 2013; Alexander *et al.*, 2015; Poloczanska *et al.*, 2016). Considerable research effort has been conducted into understanding how biotic interactions influence species ranges (Blois *et al.*, 2013; Wisz *et al.*, 2013; Early & Keith, 2019), but research has predominantly focused on interactions between different trophic levels or, to a lesser extent, exploitative competition between species of the same trophic level. The literature review, now published in *Biological Reviews* (Patterson & Drury, 2023), demonstrates clearly that interspecific behavioural interference can influence the spatial distribution of species, in multiple taxa and at large (>1000km) and small (<1km) spatial scales. Consequently, interspecific behavioural interference should not be excluded when predicting future range dynamics, especially those driven by climate change.

Chapter 3

The advent of high quality long-read DNA sequencing has revolutionised the speed and accuracy of genome assemblies (Wenger *et al.*, 2019). Until recently, for evolutionary and ecological researchers working on non-model organisms, constructing a draft genome was an expensive and often inefficient resource to attain (Ellegren, 2014). It is now a realistic goal to sequence the genome of every known eukaryote on Earth (Lewin *et al.*, 2018) with measurable progress already made (Lewin *et al.*, 2022) and with particular progress seen in specific geographic regions, such as the British Isles

(The Darwin Tree of Life Project Consortium, 2022) and California (Shaffer *et al.*, 2022).

Chapter 3, presented the de-novo assembly of a chromosome-level draft genome for a smoky rubyspot damselfly, *H. titia*. The primary and alternate genome assemblies are now publicly available at the National Center for Biotechnology Information (NCBI - GCA_037158775.1) and the chapter is published in the *Journal of Heredity* (Patterson *et al.*, 2023). As *H. titia* is the focal study species for this thesis, the genome assembly was a vital resource for the genomic research in later chapters. However, the genome assembly itself is an important additional genomic resource for the wider study of *Hetaerina* and Odonata. At the time of original publication there were six chromosome scale genome assemblies for Odonata, with one additional genome assembly made available since publication (NCBI – accessed 2024-05-20). Tallying all contig, scaffolded, and chromosome scale assemblies, the total number of Odonate species with genome assemblies on NCBI is now 14. The closest related species with a chromosomal scale genome assembly diverged from *H. titia* at the Jurassic-Cretaceous boundary, 145 million years ago (Figure 7:1).

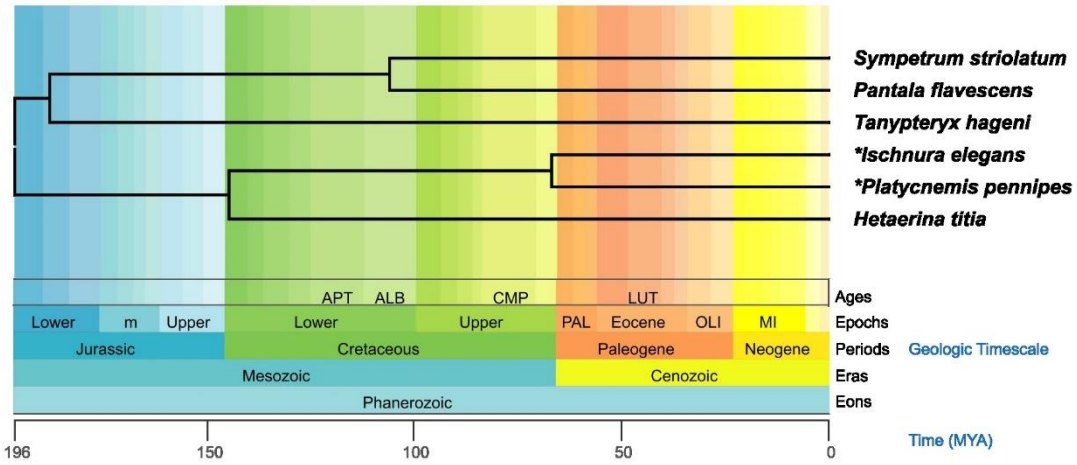

Figure 7:1: The divergence times between species of Odonata with chromosomal scale genome assemblies available on NCBI as of 2024-05-20 with nodes calculated using timetree.org (Kumar et al., 2022) and data from Thomas et al., 2013; Wheat and Wahlberg, 2013; Misof et al., 2014; Rainford et al., 2014. Asterisks indicate where species were not contained with the timetree database and were inferred from closely related taxa. *Ischnura elegans* was replaced with *Ischnura*. *Platycnemis pennipes* was replaced with *Coeliccia cyanomelas*. *Pyrrhosoma nymphula* or *Ceriagrion tenellum* have chromosome level genome assemblies but no substitution from the timetree.org data base was identified.

However, both *P. nymphula* or *C. tenellum* are within the family *Coenagrionidaeare* and consequently are more closely related to as *Ischnura* and *Platycnemis* than *H. titia*.

Consequently, the draft genome of *H. titia* is a distinct genomic resource that will enable a wider understanding of the evolution of Odonata and especially within the superfamily Calopterygoidea for which this is the first chromosome level draft genome. Our brief comparative analysis between the currently available damselfly (Zygoptera) genomes, show that within the *Hetaerina* lineage there has been a chromosomal fusion event and the loss of the micro-chromosome.

The chromosomal scale genome assembly directly enabled greater inference in later chapters of this thesis. For instance, in Chapter 3, the evidence of an F_1 hybrid between Pacific and Atlantic lineages of was greatly improved by showing that the X chromosome was entirely homozygous.

Further research should annotate the genome of *H. titia* to allow for future studies on gene transcription. There have been repeated attempted to sequence the transcriptome of *H. titia* but so far RNA extraction has been inadequate due to the time delay between tropical field collection and attempted RNA extraction. However, tools are available to provide genome annotations without RNA sequence data which could be a further avenue of research (Cantarel *et al.*, 2008; Simão *et al.*, 2015).

The genome assembly presented here, and the scaffolded draft genome of *Hetaerina americana* (Grether *et al.*, 2023), make *Hetaerina* a genome-enabled genus. The draft genome of *H. titia* is already enabling whole genome resequencing to be conducted on *Hetaerina* damselflies and will facilitate many research projects in the future.

Chapter 4

In Chapter 4, using a range of phylogeographic, phylogenetic, and species delimitation tools, I identified several lineages of *Hetaerina* damselflies that are at various stages of the non-ecological speciation cycle. Most notably, the results show that populations of *H. titia* in Atlantic river drainages and Pacific river drainages have been isolated for over 3 million years and there is reasonable support for reproductive isolation at a site of secondary contact. The divergence time between the widely sympatric *H. americana* and *H. calverti* is older than the split between lineages of *H. titia* (around 5.6Mya). We present our findings as evidence of the temporal delay to the non-ecological speciation cycle. The findings fit well with the theory that, due to the slow

rate at with reproductive isolation arises, non-ecological speciation requires a time delay before the widespread sympatry can occur (Matute & Cooper, 2021).

In Chapter 4, I identified a river in the Isthmus of Tehuantepec which contains pure Pacific *H. titia* , pure Atlantic *H. titia*, and an F_1 hybrid between the two lineages of *H. titia*. The identification of a site of secondary contact is an exciting opportunity to test a multitude of evolutionary hypothesises around reproductive interference, non-ecological speciation, hybrid zones, and, reproductive and antagonistic character displacement (Brown & Wilson, 1956; Burdfield-Steel & Shuker, 2011; Grether *et al.*, 2017). The current theory is that the seasonal polyphenism in wing melanisation seen in *H. titia* is an adaptation to reduce interspecific behavioural interference from other *Hetaerina* damselflies (Anderson & Grether, 2010a; Drury *et al.*, 2015a). Both Pacific and Atlantic lineages of *H. titia* exhibit seasonal polyphenism, but with reduced polyphenism in Pacific populations (Chapter 5).

Does interspecific behavioural interference occur between Pacific and Atlantic *H. titia*? In the peak breeding season, when the two lineages would have divergent phenotypes, does interspecific behavioural interference decrease? If so, will selection act to reduce or increase the level of melanisation in either lineage? Will one lineage outcompete the other? Work is ongoing to determine if Atlantic and Pacific *H. titia* can be distinguished in the field, which would be essential for conducting behavioural experiments in the future. There is healthy ecosystem of research into mating behaviour of damselflies (Cordoba-Aguilar *et al.*, 2022), including *Hetaerina* (Córdoba-Aguilar *et al.*, 2009), and, if discrimination is possible, experimentation and monitoring could further our understanding of mating interactions and character displacement between populations in secondary contact.

The F_1 hybrid shows that reproductive interactions do occur between Pacific and Atlantic lineages, however, we predict that interbreeding should be selected against due to low hybrid fitness; assuming that the lack of wide spread introgression is because hybrids are either infertile or have reduced fitness (Irwin & Schluter, 2022).

Although taxonomic revision is beyond the scope of this thesis, the results from Chapter 4 suggest that *H. titia* could be divided into at least two species, a Atlantic and Pacific species. Preliminary measurements of the inferior caudal appendages of Pacific and Atlantic *H. titia* show distinct morphological differentiation, which further supports the case for taxonomic revision.

Chapter 5

Chapter 5 applies the theory and tools of studying the evolution of reaction norms and co-varying traits to studying the evolution of a seasonal polyphenism (Gomez-Mestre & Buchholz, 2006; Bartoszek *et al.*, 2012; Goolsby, 2015). To the best of my knowledge, Chapter 5 is the first attempt to model the evolution of a seasonal polyphenism within a phylogenetic framework with sufficient resolution to model the dynamics of trait evolution across a species' entire range. The research conducted in Chapter 5 is the accumulation of multiple technological advances (next-generation sequencing, large-scale citizen science data collection, and computer vision) without which the scale and resolution of data would have been insufficient to model the traits evolution at this scale. The methodology and application of various technology presented in Chapter 5 could be expanded to answer further research questions on *Hetaerina* damselflies and other taxa. For instance, colour, morphology, resources utilisation, and behaviour all have spatiotemporal variation within species and could be investigated within a phylogenetic framework. Is there a phylogenetic signal and co-evolution in sexual dimorphism across different populations? Is there co-evolution between breeding and non-breeding morphology/colouration? The collection of biological records by the general public will likely provide a wealth of data to answer ecological and evolutionary questions going forward and combined with advances in machine learning allow for easier data acquisition and curation.

For *Hetaerina titia,* the hypothesis that there would be a constraint between peak and off-peak levels of wing melanisation was not supported by the multivariate models of trait evolution. Having no trade-off between seasonal phenotypes suggest that populations of *H. titia* can adapt to the optimal trait values across the year. Further research should work to attain more phenotypic data from regions with a low number of records, particularly along the Pacific coast of Mexico where two well-supported lineages had to be merged in our analyses due to the lack of phenotypic data.

Chapter 6

Chapter 6 uses species distribution models (SDMs) and population genetics to investigate the post-glacial range dynamics of two *Hetaerina* damselflies. There has been surprisingly little research into the phylogeographic structure of Odonata in eastern North America (Lyman & Edwards, 2022; Sanchez-Herrera *et al.*, 2022). As such,

Chapter 6 greatly expands our knowledge of the genetic diversity across the United States. In general, both *H. titia* and *H. americana* have similar patterns to geneflow to other taxa in the region. The largest barrier to geneflow between populations is the Mississippi River a common boundary across taxa Nearctic taxa(Lyman & Edwards, 2022).

The investigation into *H. titia* was of particular interest because of the loss of polyphenism in high latitude populations identified by Drury *et al.*, (2019) and corroborated in Chapter 5. Research presented in the preceding chapter (Chapter 6) indicated that the seasonal polyphenism is evolving under a separate selective regime with the high latitude lineage of *H. titia*. Chapter 6 laid the groundwork for determining how the polyphenism was lost by revealing that the high latitude populations are closely related to those in Florida. The relationship between high latitude *H. titia* and those in Florida is largely supported by the research conducted in Chapter 6. However, there is some introgression between the different lineages of *H. titia* in North America.

Introgression could influence the evolution of the seasonal polyphenism and the results of Chapter 5 should be reassessed considering the evidence for introgression. For instance, future work should calculate the estimates of the peak and off-peak melanisation used in the multivariate analysis conducted in Chapter 5, with and without records from the region where introgression was identified.

Since the advent of low-cost genome wide sequencing, our knowledge of how introgression has influenced evolution has greatly increased (Pereira, Martínez-Solano & Buckley, 2016; Edelman & Mallet, 2021; Rocha *et al.*, 2023; Enbody *et al.*, 2023). Most phylogenetic models of trait evolution assume a bifurcating tree with complete lineage sorting. However, methods are being produced that can incorporate introgression into models of trait evolution (Wang *et al.*, 2021; Hibbins & Hahn, 2021). This is an exciting avenue for future research that could expanded our ability to measure trait evolution at lower taxonomic levels, such as the populations rather than species.

By itself, Chapter 6 expands our understanding of the phylogeographic structure of two widespread damselflies in eastern North America. Finding notable differences between the structure of *H. titia* and *H. americana*. It provides insight into the seemly rapid evolutionary loss of a seasonal polyphenism which could have been an adaptation to novel ecological communities formed after the glacial retreat.

Conclusion

This thesis synthesises and expands our knowledge of how interspecific behavioural interference affects range dynamics. I highlight that interspecific behavioural interference does affect range dynamics and should not be omitted from biogeographical research. The empirical research presented here greatly expands our knowledge of rubyspot damselflies and, specifically, smoky rubyspot damselflies. I determine the phylogenetic and phylogeographic structure of several *Hetaerina* species which provides estimates for spatiotemporal dynamics of the non-ecological speciation cycle. I produce the first evolutionary models of seasonal polyphenism with enough spatial and temporal resolution to estimate rates of evolution across a species range. I provide novel insights into the range dynamics of two *Hetaerina* damselflies since the LGM.

Hetaerina damselflies continue to be a valuable study system for ecological and evolutionary research. This thesis greatly enhances our understanding of the causes and consequences of interspecific behavioural interference and provides a diverse array of avenues for future research.

Appendences

Appendix Chapter 2.

Supplementary Table 2:1: The 54 study systems identified during the literature review that found clear evidence that interspecific behavioural interference (IBI) impacts the spatial distribution of a species. The 'Elevational' column indicates whether the study investigated range dynamics across an elevational gradient. The 'Invasion' column indicates whether the study contained a species outside of its native range. The 'Comparative' column indicates whether the study derived inference from comparing species pairs that engage in behavioural interference with species pairs that do not engage in behavioural interference

Interacting species	IBI.type	Elevational (Y/N)	Invasion (Y/N)	Comparative (Y/N)	Impacts of IBI on spatial dynamics	References	Additional explanations?
Aves							
Great reed warblers (*Acrocephalus arundinaceus*) & marsh warblers (*Acrocephalus palustris*)	Aggression	N	N	N	Territorial mapping and behavioural observations demonstrate that great reed warblers and marsh warblers are interspecifically territorial, with great reed warblers dominating interactions. In areas where both species occur, marsh warblers use habitat further from reed habitats than sites where great reed warblers are absent.	(Rolando & Palestrini, 1989)	

Bicknell's thrushes (*Catharus bicknelli*) & Swainson's thrushes (*Catharus ustulatus*)	Aggression	Y	N	N	Playback experiments between two parapatric thrush species. Lower elevation Swainson's thrushes respond aggressively to the calls of higher elevation Bicknell's thrushes, but not *vice versa*. The aggressive responses of Swainson's thrush toward heterospecifics increases with altitude (i.e. closer to range boundary).	(Freeman & Montgomery, 2015)	
Black-headed nightingale thrushes (*Catharus mexicanus*) & ruddy-capped nightingale-thrushes (*Catharus frantzii*)	Aggression	Y	N	N	Playback experiments showed that lower elevation black-capped nightingale-thrushes respond aggressively to the ruddy-capped nightingale-thrush, but not *vice versa*.	(Jones *et al.*, 2020)	Habitat segregation
Collared (*Ficedula albicollis*) & pied (*Ficedula hypoleuca*) flycatchers	Aggression	N	N	N	Collared (*Ficedula albicollis*) & pied (*Ficedula hypoleuca*) flycatchers have recently (150 years ago) come into sympatry. Collared flycatchers are more aggressive, which shifts the nest occupancy of pied flycatchers into suboptimal habitat. However, pied flycatchers that nest in suboptimal habitat are less likely to hybridise with collared flycatchers, which reinforces the habitat segregation of the two species.	(Vallin *et al.*, 2012; Rybinski *et al.*, 2016)	Exploitative competition for nestboxes (but nestbox access mediated by aggression)

Several species of wood wrens (*Henicorhina leucophrys* & *Henicorhina leucosticta*) and thrushes (*Catharus mexicanus* & *Catharus aurantiirostris*) along an elevational gradient in Costa Rica	Aggression	Y	N	N	Playback experiments show aggressive responses to heterospecific congeners, with the magnitude of such responses increasing towards contact zones.	(Jankowski, Robinson & Levey, 2010)	Habitat turnover
Narrow-billed woodcreepers (*Lepidocolaptes angustirostris*) & scaled woodcreepers (*Lepidocolaptes squamatus*)	Aggression	N	N	N	Fragmentation of the Atlantic Forest in Brazil has facilitated range expansion of narrow-billed woodcreepers. Scaled woodcreepers have been forced to recede into the remaining fragments of forest. However, narrow-billed woodcreepers regularly join mixed-species flocks within the forest and aggressively exclude scaled woodcreepers from joining flocks.	(Maldonado-Coelho *et al.*, 2017)	
Common nightingales (*Luscinia megarhynchos*) & thrush nightingales (*Luscinia luscinia*)	Aggression	N	N	N	Common and thrush nightingales are interspecifically territorial and exhibit evidence of song convergence in sympatry. This aggression drives shifts in habitat preferences in sympatry compared to allopatric populations.	(Sorjonen, 1986; Reif *et al.*, 2015, 2018)	

Noisy miners (*Manorina melanocephala*) & local bird assemblages	Aggression	N	N	N	Noisy miners are extremely aggressive towards nearly all heterospecific birds, even those with little overlap in diet and foraging behaviour, and their presence shapes the structure of entire avian assemblages.	(Mac Nally *et al.*, 2012; Lill & Muscat, 2015)
Flame robins (*Petroica phoenicea*) & Norfolk robins (*Petroica multicolor*)	Aggression	N	N	N	Both species are interspecifically territorial. Migratory flame robins displace the less aggressive Norfolk robin upon returning to breeding habitat, likely displacing Norfolk robins into suboptimal habitat.	(Robinson, 1992)
Carolina chickadees (*Poecile carolinensis*) and black-capped chickadees (*Poecile atricapillus*)	Aggression and Reproductive interference	N	N	N	Carolina chickadees are more aggressive (dominant) than black-capped chickadees, and dominant chickadees are preferred by females of both species in mate choice trials. Species distribution models (SDMs) show that Carolina chickadees' distribution limit largely matches climatic predictors, whereas black-capped chickadee distribution does nor, suggesting that it is limited instead by interactions with Carolina chickadees.	(Bronson *et al.*, 2003; McQuillan & Rice, 2015)
Invasive ring-necked *parakeets (Psittacula krameri*) and native communities	Aggression	N	Y	N	Invasive ring-necked parakeets tend to be dominant in aggressive interactions, and consequently the parakeets exclude other species that use tree cavities, including greater noctules (*Nyctalus lasiopterus*), a threatened bat species. Although many birds currently appear to benefit from parakeet aggression towards predators, greater noctules decline where parakeets occur.	(Hernández-Brito *et al.*, 2014)

Townsend's warblers (*Setophaga townsendi*) and hermit warblers (*Setophaga occidentalis*)	Aggression and Reproductive interference	N	N	N	Moving hybrid zone attributed to asymmetries in behavioural interference. Both species defend mutually exclusive territories, though Townsend's warblers are likely to be more aggressive towards hermit warblers than *vice versa*. Similarly, although mating is largely assortative, exceptions are more likely with Townsend's males mating with hermit females (not *vice versa*).	(Pearson, 2000; Pearson & Rohwer, 2000)	
Western bluebirds (*Sialia mexicana*) & mountain bluebirds (*Sialia currucoides*)	Aggression	N	N	N	As western bluebird range shifts into mountain bluebird range, mountain bluebird populations are going locally extinct due to aggression from western bluebirds limiting nesting opportunities.	(Duckworth & Badyaev, 2007; Duckworth, 2013; Duckworth, Belloni & Anderson, 2015)	Exploitative competition for nestboxes (but nestbox access mediated by aggression)
Spotted owls (*Strix occidentalis*) & barred owls (*Strix varia*)	Aggression	N	Y	N	Barred owls are invading spotted owls' range and driving declines in spotted owls. Playback experiments with decoy mounts demonstrate asymmetric aggression from barred owls towards spotted owls, and tracking data suggest they exclude spotted owls from breeding territories.	(Gutiérrez *et al.*, 2007; Van Lanen *et al.*, 2011; Wiens, Anthony & Forsman, 2014)	Habitat loss, exploitative competition
Dominant and subordinate congeneric birds in urban environments	Aggression	N	N	Y	Subordinate species are less likely to occur and are less abundant in cities where dominant species are widespread breeders (compared to in cities where the sub-dominant species is found in allopatry).	(Martin & Bonier, 2018; Martin, Burke & Bonier, 2021)	Exploitative competition for resources not ruled out
Dominant and subordinate birds from North America	Aggression	N	N	Y	Subordinate species migrate further distances than dominant species	(Freshwater, Ghalambor & Martin, 2014)	

Birds along an elevational gradient in Borneo	Aggression	Y	N	Y	Experiments used simulated territorial intrusion, by song playback, to test whether interspecific aggression drives parapatric ranges along an elevational gradient for different pairs of birds. They found support for this hypothesis in bulbuls: ochraceus bulbuls (*Alophoixus ochraceus*) respond aggressively to pale-faced bulbuls (*Pycnonotus leucops*). However, they did not find evidence that parapatric white-eyes (*Zosterops* sp.) are aggressive to congeners.	(Boyce & Martin, 2019)
North American perching birds (passerines)	Aggression and Reproductive interference	N	N	Y	Analyses of sister taxa show that transitions from allopatry to secondary sympatry are best predicted by the interactive effect of interspecific territoriality and hybridisation.	(Cowen, Drury & Grether, 2020)
Birds along an elevational gradient in Papua New Guinea	Aggression	Y	N	Y	Playback experiments on five species pairs demonstrate that lower elevation species are more aggressive towards heterospecifics than upper elevation confamilial counterparts, and that species only engaged in aggression towards heterospecifics at the range boundary, for three of the five species pairs.	(Freeman, Class Freeman & Hochachka, 2016)
Amphibia						

Southern Appalachian salamander (*Plethodon teyahalee*) & red-cheeked salamanders (*Plethodon jordani*)	Aggression	Y	N	N	Extensive observational and experimental data (from removal experiments and behavioural experiments) demonstrate that aggressive interference is the cause of the species' parapatric elevational ranges in the Great Smokey Mountains. Later modelling suggested interspecific interactions prevent the low-elevation southern Appalachian salamander from expanding into higher elevations.	(Hairston, Nishikawa & Stenhouse, 1987; Gifford & Kozak, 2012)	
Actinopterygii							
Damselfish (*Dischistodus* spp.) in the Great Barrier Reef	Aggression	N	N	N	Four species of damselfish have non overlapping habitat use within reef. Aquarium studies show the damselfish have wider habitat use than seen in the field and simulated intruder experiments in the field reveal high levels of interspecific aggression between species that use adjacent habitat.	(Bay, Jones & McCormick, 2001)	Habitat segregation
Guppies (*Poecilia reticulata*) & mosquitofish (*Gambusia affinis*)	Reproductive interference	N	Y	N	Mosquitofish decline upon introduction of guppies, and experimental evidence shows that reproductive interference occurs asymetrically, with negative fitness impacts on mosquitofish, but not guppies.	(Tsurui-Sato *et al.*, 2019)	
Obscure damselfish (*Pomacentrus adelus*) & speckled damselfish (*Pomacentrus bankanensis)*	Aggression	N	N	N	Species are interspecifically territorial, and upon removal of obscure damsels, speckled damsels expand territories to occupy vacant space, with knock-on effects for habitat use of other reef fish.	(Eurich, McCormick & Jones, 2018)	

Invasive brown trout (*Salmo trutta*) & white-spotted charr (*Salvelinus leucomaenis*) in Japan	Aggression	N	Y	N	Introduced brown trout have expanded throughout drainage, except upstream of weirs where white-spotted charr are more abundant. Experimental data shows that brown trout are dominant in behavioural trials.	(Takami *et al.*, 2002; Hasegawa *et al.*, 2004; Hasegawa & Maekawa, 2009)	
Gopher rockfish (*Sebastes carnatus*) & black-and-yellow rockfish (*Sebastes chrysomelas*)	Aggression	N	N	N	Laboratory experiments show interspecific aggression for territories and removal experiments in the field show that the removal of either species allows the other to expand its depth range.	(Larson, 1980)	
Arachnida							
Invasive sheet-web spiders (*Linyphia triangularis*) & bowl-and-doily spiders (*Frontinella communis*)	Aggression	N	Y	N	An invasive species of spider displaces a native species from their constructed web. Furthermore, field experiments demonstrate that bowl-and-doily spiders are less likely to settle in plots where the invasive species is present and that introducing the invasive species leads to declines in bowl-and-doily spiders.	(Houser, Ginsberg & Jakob, 2014)	Exploitative competition for resources ruled out
Copepoda							
***Skistodiaptomus* copepods**	Reproductive interference	N	N	N	*S. oregonensis* and *S. pygmaeus* exhibit a parapatric boundary. Laboratory studies demonstrate high levels of reproductive interference (although no evidence of introgression), suggesting that Allee effects generated by reproductive interference maintain this parapatric boundary.	(Thum, 2007)	Ecological gradients ruled out as possible explanation
Crustacea							

Invasive rusty crayfish (*Orconectes rusticus*) and native Sanborn crayfish (*Orconectes sanborni*)	Aggression and Reproductive interference	N	Y	N	An invasive crayfish (*O. rusticus*) that replaces native crayfish (*O. sanborni*) tends to be dominant, and because females of the invasive species are larger, males of the native species prefer to mate with invasive females, reducing native female fitness.	(Butler & Stein, 1985)	Juvenile susceptibility to predation of native species
Invasive signal crayfish (*Pacifastacus leniusculus)* in Europe & native communities	Aggression and Reproductive interference	N	Y	N	Signal crayfish have been introduced in many locations throughout Europe, and in several instances, have coincided with decline of native species. In Finland & Sweden, longitudinal data show replacement of native *Astacus astacus*, with experimental evidence for both reproductive interference and aggression implicated in the decline. Agonistic interactions with bullhead (*Cottus gobio*) drive bullhead out of shelters, which may explain pattern where density of signal crayfish is negatively correlated with that of bullhead.	(Söderbäck, 1994, 1995; Westman & Savolainen, 2001; Svärdson Fürst, and Fjälling . 1991, Westman, Savolainen & Julkunen, 2002; Bubb *et al.*, 2009)	Signal crayfish are resistant to crayfish plague that contributes to decline of native crayfish species; life history traits (e.g. developmental time)
Gastropoda							
Keyhole limpets (*Siphonaria lessonii*) & pulmonate limpets (*Fissurella crassa*)	Aggression	N	N	N	Mesocosm experiments demonstrate that large keyhole limpets aggressively displace smaller pulmonate limpets from crevices, and that displacement has fitness consequences not related to exploitative competition.	(Aguilera & Navarrete, 2012)	
Insecta							

***Aedes* mosquitos (*Ae. albopictus* & *Ae. aegypti*)**	Reproductive interference	N	Y	N	In places where *Ae. aegypti* is established, males in invading populations of *Ae. albopictus* mate with *Ae. aegypti* females, greatly reducing their fitness and leading to replacement of *Ae. aegypti* by *Ae. albopictus*.	(Nasci, Hare & Willis, 1989; Bargielowski, Lounibos & Carrasquilla, 2013; Bargielowski & Lounibos, 2016; Lounibos & Juliano, 2018; Zhou *et al.*, 2022)	Larval resource competition
Two tick species (*Amblyomma variegatum* & *Amblyomma hebraeum*)	Reproductive interference	N	N	N	Two species of tick are largely parapatric. In sympatry, interspecific copulations are commonly observed, with little geographic overlap suggesting symmetric reproductive interference may maintain parapatric boundary.	(Bournez *et al.*, 2015)	
Whiteflies (*Bemisia tabaci* spp.)	Reproductive interference	Y	N	N	Invading whitefly species have replaced native strains in several locations owing to asymmetric reproductive interference, in which matings from invading males reduce fitness of native females.	(Liu *et al.*, 2007; Crowder *et al.*, 2011; Wang, Crowder & Liu, 2012)	Life history traits (e.g. developmental time, relative fecundity; although not sufficient without asymmetric reproductive interference to explain rapid replacement)

Invasive buff-tailed bumblebees (*Bombus terrestris*) & native bumblebees *(Bombus hypocrita sapporoensis* & *Bombus ignitus*) in Japan	Reproductive interference	N	Y	N	The invasive bumblebee species *Bombus terrestris* engages in reproductive interference with two species of native bumblebee. Copulation between *B. terrestris* and *B. h. sapporoensis* or *B. ignitus* results in unviable eggs being laid the following spring, driving declines native bumblebee species.	(Tsuchida *et al.*, 2019)	Exploitative competition for nectar and nest sites
Rubyspot damselflies (*Hetaerina* spp.)	Aggression	N	N	Y	Rubyspot damselflies, which engage in high levels of reproductive interference and interspecific territoriality, have diverged in microhabitat use in a way that reduces the effects of behavioural interference.	(McEachin *et al.*, 2022)	
Two ant species (*Iridomyrmex* spp.)	Aggression	N	N	N	Removal experiments showed that these two species hold mutually exclusive territories and compete for space to build colonies. Over a short period of time (11 months), one species ("C") replaced by another ("A"), in part due to asymmetric competition.	(Haering & Fox, 1987)	Habitational succession
Arboreal termite species in Papua New Guinea (*Microcerotermes biroi*, *Nasutitermes novarumhebridiarum*, & *Nasutitermes princeps*)	Aggression	N	N	Y	Long-term mapping of arboreal termite nests and their territories in combination with behavioural observations shows that species defend mutually exclusive territories. Removal of *N. princeps* drives concomitant increase in *M. biroi* home range.	(Leponce, Roisin & Pasteels, 1997)	

White-crossed seed bugs (*Neacoryphus bicrurus*) and co-occurring insect communities	Aggression and Reproductive interference	N	N	N	White-crossed seed bugs engage in asymmetrical reproductive interference (misdirected courtship) and aggression towards many species, and removal experiments demonstrate that several other species increase in density when white-crossed seed bugs are removed.	(McLain & Shure, 1987)	
Invasive southern green stink bugs (*Nezara viridula*) & native green stink bugs (*Nezara antennata*)	Reproductive interference	N	Y	N	Invasive southern green stink bugs are expanding in Japan into the range of and replacing native green stink bugs. In regions of coexistence, heterospecific copulations are commonly observed, and reproductive interference is suspected to drive declines of native species.	(Kiritani, 2011)	Shifting climatic suitability
Alpine dark bush-crickets (*Pholidoptera aptera*) & Transylvanian dark bush-crickets (*Pholidoptera transsylvanica*)	Reproductive interference	N	N	N	Bush-crickets exhibit a 'mosaic' pattern of distribution, where the two species are rarely found in syntopy. Experiments demonstrate that heterospecific matings resulting in transfer of spermatophores are common.	(Dorková *et al.*, 2020)	Habitat segregation ruled out
Eastern subterranean termites (*Reticulitermes flavipes*) & Western subterranean termits (*Reticulitermes grassei*)	Aggression	N	Y	N	Invasive eastern subterranean termites are dominant in aggressive interactions over native western subterranean termites; success of invasion is attributed to this asymmetry.	(Perdereau *et al.*, 2011)	Lack of intraspecific aggression in invasive species; demographic factors (large colony size)

Invasive Asian blue ticks (*Rhipicephalus [Boophilus] microplus*) & African blue ticks (*Rhipicephalus [Boophilus] decoloratus*) in South Africa	Reproductive interference	N	Y	N	Invasive Asian blue ticks have replaced African blue ticks in South Africa. Interspecific matings lead to sterile hybrids, so rapid demographic increases in invader populations lead to Allee effects driving local extinction of native species.	(Sutherst, 1987; Tønnesen *et al.*, 2004, 2004)	Life-history traits (e.g. developmental time); host resistance
Cepero's groundhoppers (*Tetrix ceperoi*) & slender groundhoppers (*Tetrix subulata*)	Reproductive interference	N	N	N	Groundhoppers exhibit a mosaic pattern of distribution, where the two species are rarely found in syntopy. Laboratory and field experiments demonstrate that extensive reproductive interference is likely responsible for this spatial distribution.	(Gröning *et al.*, 2007; Hochkirch, Gröning & Bücker, 2007; Hochkirch & Gröning, 2012)	Habitat segregation ruled out
Arboreal ant species in Papua New Guinea	Aggression	N	N	Y	Colony mapping and behavioural experiments demonstrate that interspecific aggression is the key factor shaping the spatial distribution of ant species in a 9-hectare plot	(Mottl *et al.*, 2021)	Habitat segregation ruled out
Mammalia							
Fallow deer (*Dama dama*) & roe deer (*Capreolus capreolus*)	Aggression	N	Y	N	Fallow deer displace roe deer but not *vice versa*, and habitat use by roe deer is affected by presence of fallow dear. Together, these suggest behavioural interference has led to decline in roe deer populations as fallow deer populations have increased.	(Ferretti & Mori, 2020)	Exploitative competition for resources not ruled out
White-handed gibbons (*Hylobates lar*) & Pileated gibbons (*Hylobates pileatus*)	Aggression	N	N	N	Two species of gibbon are largely parapatric, with a small contact zone that is maintained by interspecific territorial aggression.	(Suwanvecho & Brockelman, 2012; Asensio *et al.*, 2017)	Niche partitioning (via habitat segregation or diet divergence) ruled out.

Least chipmunks (*Neotamias minimus*) & yellow-pine chipmunks (*Neotamias amoenus*)	Aggression	Y	N	N	Removal experiments of two species of chipmunk that engage in aggressive interference. When yellow-pine chipmunks were removed, least chipmunk captures increased; the converse did not occur.	(Chappell, 1978; Heller, 1971)	
Townsend's chipmunks (*Neotamias townsendii*) & yellow-pine chipmunks (*Neotamias amoenus*)	Aggression	N	N	N	Removal experiments of two species of chipmunk that engage in aggressive interactions with one another show that when heterospecifics are removed, the range size of the retained species and juvenile recruitment increases.	(Trombulak, 1985)	Habitat segregation ruled out
Uinta chipmunks (*Neotamias umbrinus*) & Colorado chipmunks (*Neotamias quadrivittatus*)	Aggression	Y	N	N	Colorado chipmunks cannot move into higher elevations because of aggressive interactions with Uinta chipmunks. Uinta chipmunks hypothesised to be restricted to higher elevations because of the high parasitic load of a bot fly found at lower elevations.	(Bergstrom, 1992)	
Stoats (*Mustela erminea*) & least weasels (*Mustela nivalis*)	Aggression	N	N	N	Experimental data demonstrate that stoats are dominant over weasels, and observational data show that weasels are very rarely found in preferred habitat when a stoat held a territory in that area. Distributional data collected over several years shows that when stoats declined, weasels increased locally.	(Erlinge & Sandell, 1988)	

Pied tamarins (*Saguinus bicolor*) & golden-handed tamarins (*Saguinus midas*)	Aggression	N	N	N	Playback experiment of two species of tamarin, in allopatry and sympatry. Pied tamarins are critically endangered and experiencing range fragmentation, while golden-handed tamarins have expanded their range into the range of pied tamarins. Playback experiments show that golden-handed tamarins respond more aggressively than pied tamarins.	(Sobroza *et al.*, 2021)	
Chiriquí singing mice (*Scotinomys xerampelinus*) & Alston's singing mice (*Scotinomys teguina*)	Aggression	Y	N	N	Playback experiments, laboratory experiments, and removal experiments all demonstrate that the higher elevation species (*Scotinomys xerampelinus*) is dominant and prevents range intrusions from lower elevation species. In removal experiments, *Scotinomys xerampelinus* did not descend to occupy areas where *Scotinomys teguina* was removed, but *Scotinomys teguina* did invade higher elevation areas when *Scotinomys xerampelinus* was removed.	(Pasch, Bolker & Phelps, 2013)	
Reptilia							
Invasive house geckos (*Hemidactylus frenatus*) & native communities	Aggression and Reproductive interference	N	Y	N	Comprehensive longitudinal data, in combination with laboratory and field experiments, show that introduced house geckos are aggressive to and avoided by native species, leading to the decline of native species across many different locations. Reproductive interference has also been demonstrated in some locations.	(Bolger & Case, 1992; Petren, Bolger & Case, 1993; Case, Bolger & Petren, 1994; Dame & Petren, 2006)	Competitive exclusion due to differential resource acquisition (though this results from interference competition)

Appendix Chapter 4.

Supplementary Methods

DNA extraction

Approximately 2mm^2 of wing muscle tissue was removed from the thorax and placed in a 1.5 ml Eppendorf tube. 180µl of a tissue lysis buffer (Buffer ATL) and 20µl of proteinase K (600 mAU/ml) were added to each Eppendorf tube and incubated overnight (~15 hours) at 56°C in a water bath. Sample tubes were removed from the water bath and 200µl of Buffer AL was added to each Eppendorf tube before vortexing for 5 seconds. 200µl of >99% ethanol was added before vortexing for 5 seconds. The supernatant, along with any precipitate, was transferred to a DNeasy Mini spin column, placed inside a 2ml collection tube, and centrifuged for 60 seconds at 6000g. The 2ml collection tube was discarded along with the supernatant and the spin column was transferred to a new 2ml collection tube. 500µl of Buffer AW1 was added to the spin column and centrifuged for 60 seconds at 6000g. The 2ml collection tube and supernatant were discarded, and the spin column placed in a new 2ml collection tube. 500µl of Buffer AW2 was added to the spin column and centrifuged for 3 minutes at 6000g. The 2ml collection tube and supernatant were discarded, and the spin column placed in a new 1.5ml Eppendorf tube. 50µl of buffer AE was added to the centre of the spin column before incubating at room temperature for one minute. The Eppendorf tubes with the spin column inserted inside was centrifuged for one minute at 6000g. The spin column was discarded and the 1.5ml Eppendorf tube with the extracted DNA was stored at -20°C for later ddRAD library preparation. Samples extracted for ddRAD library One were initially resuspended using 200µl of buffer AE, and then were desiccated and resuspended in 50µl of buffer AE. Samples extracted for ddRAD library Two were resuspended in 50µl of buffer AE. DNA degradation was visualised via gel electrophoresis and the concentration calculated on a Qubit 2.0 Fluorometer broad range (BR). DNA concentration ranged from 0.47 ng/µl to 26.8 ng/µl with a mean of 4.44 ng/µl. For each sample, this totalled a range 5361ng to 95.4ng of DNA with an average of 888.32ng.

ddRAD libraries

In order to gather genetic information of *Hetaerina* damselflies, with a focus on *Hetaerina titia* and *Hetaerina americana/calverti* double digest restriction enzyme associated DNA (ddRAD) was created. ddRAD library preparation was conducted twice creating two separate ddRAD libraries. Both libraries used the same restriction enzymes PstI and EcoRI and after demultiplexing were analysed together.

Library One

Double digest restriction enzyme association DNA (ddRAD) was created for 190 *Hetaerina* samples (183 *H. titia*, 4 *H. occisa*, and 3 *H. americana*) using two six base restriction enzymes, PstI and EcoRI. Library preparation was done using custom Illumina adapters; 92 barcoded P1 adapters and two P2 adapters with 192 unique barcode combinations. P2 adapters contained 8 bases of random nucleotides for the detection of PCR duplication.

25µl of extracted DNA product (~400ng) was mixed with 1µl of EcoRI-HF, 1µl PstI-HF, and 2µl of 10xNEBuffer2. Samples were digested at 37°C for 3 hours and 65°C for 20 minutes in a thermocycler. Each sample was assigned a unique combination of P1 and P2 illumina adapters. Adapters were ligated to each sample by mixing 30µl of digested DNA with 1µl of 10xNEBuffer2, 0.3µl rATP, 2µl P1 adapters (50nM), 6µl of P2 adapters (50nM), 0.2µl water, and 0.5µl T4 ligase. Ligation was undertaken in thermocycler at 24°C for 30 minutes and 65°C for 20 mins.

The size range of digested and ligated DNA was reduced by manual gel extraction. 3µl of custom internal standards (300 and 450bp) were added to each sample along with 4µl of blue loading buffer. Samples were run in individual wells for 3 hours at 110 volts in 1x Lithium borate gel. For each sample, the upper and lower bands of the internal standards were used to select for DNA between 300 and 450bp my manually cutting out the gel between the two internal standard bands. To avoid over representation of shorter fragments in downstream PCR amplification, a proportion of shorter fragments were removed by cutting a wedge of gel away from the extracted block. The remaining gel piece was placed in a 1.5ml Eppendorf tube for storage.

The size selected sample DNA was extracted from the gel using QIAquick Gel Extraction Kit. 100µl of Buffer QC was added for each 100mg of extracted gel. Samples were incubated at room temperature until completely dissolved. 100µl of isopropanol was added for every 100mg of extracted gel and mixed by tube inversion. 700µl of sample volume was added to a MinElute column and centrifuged for one minute at

10,000rpm and the flow through discarded. This was repeated until the complete sample volume had been passed through the MinElute tube. 500µl of Buffer QC was added to each sample and centrifuged to one minute at 10,000rpm and the flow through discarded. 700µl of Buffer PE was added to each MinElute tube and incubated at room temperature for 2-4 minutes before being centrifuged for one minute at 10,000rpm and the flow through discarded. An additional centrifuge was carried out for one minute at 10,000rpm and the remaining flow through discarded. The MinElute tubes were transferred to a 1.5ml Eppendorf tube and 20µl of low TE applied directly to the filter. Samples were incubated for one minute and then centrifuged for one minute at 10,000rpm.

DNA was amplified by PCR. Template DNA was added to a mix of 30µl Phusion Mix, 14µl water, 10µl of forward RAD1 primer (10µM), and 10µl of forward RAD2 primer (10µM). PCR was conducted with an initial denaturation of 30 seconds mins at 98°C, followed by 12 annealing cycles of 10 seconds at 98 °C, 30 seconds at 60 °C, and 40 seconds at 72°C. Then held for five minutes at 72°C.

PCR product was purified using AMPure beads. 48µl of AMPpure XP solution was added to each PCR reaction, mixed by pipette, and incubated at room temperature for five minutes. Magnetic plates were used to separate AMPure beads with the DNA attached and remaining supernatant removed. Beads were washed twice in 100µl of 80% ethanol and incubated for 30 seconds. Ethanol was removed by gentle centrifugation and pipetted out. Beads were dried for 2-3 minutes. DNA was resuspended in 40µl of Buffer EB by mixing with pipette and incubated for five minutes. Beads were removed by a magnetic plate and the remaining eluent, containing purified DNA, transferred to a new 1.5ml Eppendorf tube.

DNA concentration was calculated by fluorometer and ranged from 84.4ng/µl to 2.99ng/µl, with an average of 30.1ng/µl. 40ng of 16 samples were pooled into separate libraries and then quantified by qPCR. Separate libraries were then pooled into a single library for sequencing.

Bioinformatics

Sequencing was conducted on a NovaSeq 6000 (Illumina) within a single lane. Raw sequence files were demultiplex into one of the two P2 adapters (BC1 and BC2) and processed separately. Initially 212.1×10^6 BC1 paired read files and 189.1×10^6 BC2 paired read files were identified. Trimming was conducted using *trimomatic 0.39* to

remove low quality bases using a sliding window of 4 and an average base quality of 20. Reads shorter than 15 bases were removed. After filtering 169.9 $x10^6$ (80.1%) BC1 paired sequences and $153.6x10^6$ (81.2%) BC2 paired sequences remained.

Sequences were processed with *STACKS v2.60* (Catchen *et al.*, 2013). *clone_filter* identified 15.12% of BC1 reads to be PCR clones and were removed, retaining $144.2x10^6$ paired reads. *pcr_filter* identified 19.66% of BC2 reads to be PCR clones and removed retaining $123.4x10^6$ paired reads.

Reads were demultiplexed using process_radtags using the 8 base unique barcodes on the P1 adapters. 268,996,468 (93.3%) of BC1 reads were retained and assigned to a specific sample, 6.4% of reads did not contain an identifiable barcode and 0.3% could not identify the RAD cut site. 229,259,030 (92.9%) of BC2 reads were retained and assigned to a specific sample, 6.8% did not contain an identifiable barcode and 0.4% could not identify a RAD cut site. All remaining sequence were processed through *cutadapt* to remove both the remaining adapter regions. For all samples the total number of identified paired sequences was 496,388,354. The mean number of reads per sample was 1,292,678±824,724 SD and ranged from 256 to 4,174,260.

Library Two

Double digest restriction enzyme association DNA (ddRAD) was created for 192 *Hetaerina* samples (112 *H. titia* and 80 *H. americana*) using two six base restriction enzymes, PstI and EcoRI. Library preparation was done using custom Illumina adapters; three inner i5 barcoded adapters and four inner i7 adapters plus four outer i5 primers and four outer i7 primers creating 192 unique barcode combinations. Both inner i5 and i7 adapters contained a sequence of 4 bases of random nucleotides for the detection of PCR duplication. This protocol follows

Samples were divided into groups of 16 with similar concentration of DNA and then, within each group, each sample was assigned a unique combination of inner i5 and inner i7 adapters. 400ng of extracted DNA for each sample product (400ng) was mixed with 0.75µl of EcoRI-HF, 0.75µl PstI-HF, and 4µl of 10xNEBuffer2, 4µl of 10mM ATP, 1µl of T4 DNA ligase (400U.µl), 0.75µl of inner i5 adapter (10µM), 0.75µl of inner i7 adapter (10µM) and then ddH_2O to bring the total reaction volume up to 40µl. Samples were digested at 30°C for 3 hours and then mixed with 10µl of EDTA to prevent further enzyme activity.

Each group of digested products was pooled and DNA concentration quantified using qubit (BR). 150ng of digested and pooled product was purified using AMPure beads. 2.4x of AMPpure XP solution was added to each PCR reaction, mixed by pipette, and incubated at room temperature for five minutes. Magnetic plates were used to separate AMPure beads with the DNA attached and remaining supernatant removed. Beads were washed twice in 100µl of 80% ethanol and incubated for 30 seconds. Ethanol was removed by gentle centrifugation and pipetted out. Beads were dried for 2-3 minutes. DNA was resuspended in 30µl of Buffer EB by mixing with pipette and incubated for five minutes. Beads were removed by a magnetic plate and the remaining eluent, containing purified DNA, transferred to a new 1.5ml Eppendorf tube and DNA concentration quantified using qubit (BR).

Each of the 16 pools of digested and ligated product was assigned a unique combination of outer i5 and i7 primers. Amplification was conducted by mixing 50ng of digest, ligated, and cleaned DNA with 20µl of 5x Phusion HF Master Mix, 4µl of outer i5 primer (10µM), 4µl of outer i7 primer (10µM), and ddH_2O to bring the total volume of reactant to 100µl. PCR was conducted with an initial denaturation of 2 minutes at 98°C, followed by 12 annealing cycles of 10 seconds at 98 °C, 30 seconds at 65 °C, and 30 seconds at 72°C. Then held for five minutes at 72°C.

All PCR product (100µl) was purified using AMPure beads. 2.4x of AMPpure XP solution was added to each PCR reaction, mixed by pipette, and incubated at room temperature for five minutes. Magnetic plates were used to separate AMPure beads with the DNA attached and remaining supernatant removed. Beads were washed twice in 100µl of 80% ethanol and incubated for 30 seconds. Ethanol was removed by gentle centrifugation and pipetted out. Beads were dried for 2-3 minutes. DNA was resuspended in 30µl of Buffer EB by mixing with pipette and incubated for five minutes. Beads were removed by a magnetic plate and the remaining eluent, containing purified DNA, transferred to a new 1.5ml Eppendorf tube and DNA concentration quantified using qubit (BR).

The size range was quantified using a Tapestation HS d1000 cassette (Aiglent) to determine the quantity of DNA within the desired fragment length within each of the 16 pools (250-400bp). Each of the 16 pools was pooled equimolarly into a final library.

Size selection was conducted using a pippin prep 2% agarose gel cassette with DF Marker L. 30µl of cleaned pooled PCR product was loaded onto a single lane and

size selected for 250-400bp. 40µl of size selected digested, ligated, and indexed DNA was retrieved from the pippin prep elusion module, DNA concentration was quantified using the qubit high sensitivity and size range was quantified using a Tapestation HS d1000 cassette. This yield 40µl of quaddRAD library at 1.08ng/µl (43.2ng in total) which was sent for paired end 150 sequencing on Illumina NovaSeq 6000 (98 G raw data per sample).

Bioinformatics

Sequencing was conducted on a NovaSeq 6000 (Illumina) within a single lane. Raw sequence files were demultiplex into one of 16 combinations of outer barcodes. Each pool contained on average $16.1x10^6$ paired reads (range $7.3\ x10^6$ to $16.1\ x10^6$) with $294.1x10^6$ paired reads in total. Trimming was conducted using *trimomatic 0.39* to remove low quality bases using a sliding window of 4 and an average base quality of 20. Reads shorter than 15 bases were removed. After filtering, $289.5x10^6$ (98.2%) sequences remained. Sequences were processed with *STACKS v2.60* (Catchen *et al.*, 2013). *clone_filter* identified 17.4% of reads to be PCR clones and were removed, retaining $239.3x10^6$ paired reads.

Sequences were demultiplexed using *process_radtags* which generated 192 individual samples files. In total $215.5x10^6$ paired reads (90.1%) were assigned to a specific sample ranging from 671 to $13.3x10^6$ (mean = $1.12x10^6$) reads per sample.

For all SNP libraries*, samtools v1.13* was used to construct a compressed sequence alignment file (.bam). After aligning the sequence reads to the draft genomes, we excluded samples that had a mean depth of less than 5 (Supplementary Figure 4:2).

Genotype calling was done using *bcftools v1.13* (Li, 2011; Danecek *et al.*, 2021) using the *mpileup* and *call* commands, with a max depth of 10,000 and a prior expected substitution rate of 1e-6. As our samples were collected over a large geographical scale and included multiple species, we did not use Hardy-Weinberg equilibrium calculations for variant calling. After genotyping, variant sites were restricted to SNPs. SNP sites were filtered to remove all SNP calls with a read depth of less than 10, an average read depth across samples greater than 200 per sample, and a quality score less than 20. Further filtering removed SNPs that had a minor allele frequency less than 0.05% (<2 samples), SNPs that were found in less than 80% of samples, and to avoid linkage we randomly selected one SNP from a window of 1000 base pairs using the *prune+*

command in *bcftools* (Danecek *et al.*, 2021). Full bioinformatics pipeline is outlined in Supplementary Figure 4:1

Re-sequencing of highly heterozygous samples

Pre-liminary analysis, using the r package SambaR, identified five samples as having high levels of heterozygosity - one sample from Library One and four samples from Library Two. The high heterozygosity samples from Library Two were processed within the same pool and had the same i5 inner barcode and are likely due to a fault in inner barcode ligation. The likely cause of the high heterozygosity for the sample from Library One could not be determined. To determine whether laboratory error was the cause for the high heterozygosity, we re-extracted DNA (from tissue) for the five identified samples and re-sequenced them in line with the methodology described in Library Two. We attained, $4.7x10^6$ paired reads of sequence data which was trimmed to $4.6\ x10^6$ paired reads, removed clones retaining $4.2\ x10^6$ paired reads, and demultiplexed which retained $4.1\ x10^6$ paired reads using the methodology described in Library Two. All four samples from Library Two did not show high levels of heterozygosity after re-sequencing. The sample from Library One retained high levels of heterozygosity.

Including all sequence data from across of ddRAD libraries, a total of $875x10^6$ reads were mapped (88.7%) with a mean of $2.2x10^6$ reads per sample (range: 422 - $11x10^6$) to the *H. americana* genome. For the *H. titia* genome, $935x10^6$ reads were mapped (94.2%) with a mean of $2.4x10^6$ reads per sample (range: 477 - $11x10^6$).

Species/lineage delimitation

To decrease computation time while running *delimit*R (Smith & Carstens, 2020), we wrote a custom R function called *fastsimcoalsim_sbatch*. Built off the default *delimit*R function *fastsimcoalsim*, *fastsimcoalsim_sbatch* allows each set of fastsimcoal simulations (for each demographic scenario) to be run in parallel using the SLURM HPC management system.

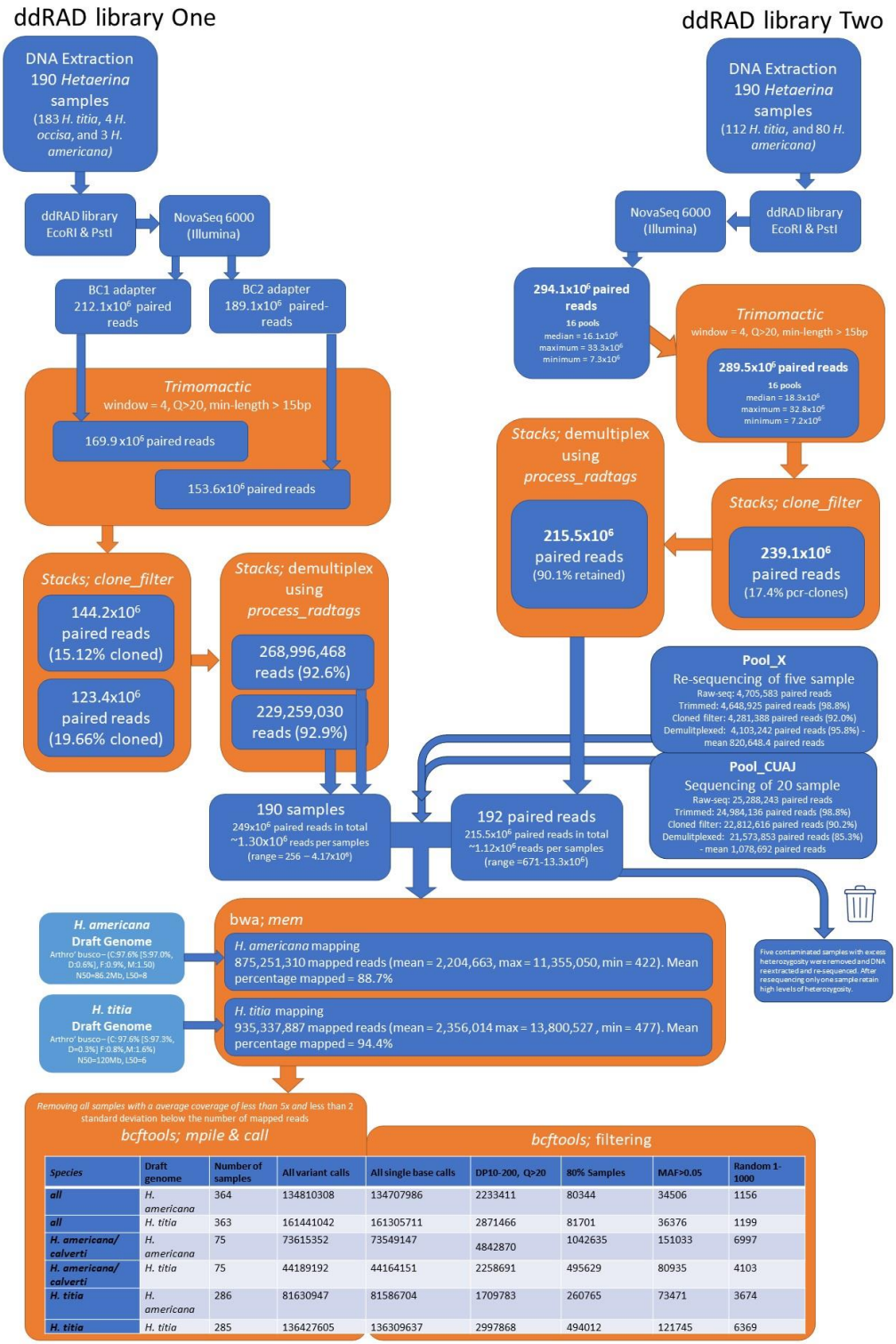

Species	Draft genome	Number of samples	All variant calls	All single base calls	DP10-200, Q>20	80% Samples	MAF>0.05	Random 1-1000
all	H. americana	364	134810308	134707986	2233411	80344	34506	1156
all	H. titia	363	161441042	161305711	2871466	81701	36376	1199
H. americana/ calverti	H. americana	75	73615352	73549147	4842870	1042635	151033	6997
H. americana/ calverti	H. titia	75	44189192	44164151	2258691	495629	80935	4103
H. titia	H. americana	286	81630947	81586704	1709783	260765	73471	3674
H. titia	H. titia	285	136427605	136309637	2997868	494012	121745	6369

Supplementary Figure 4:1: Flow diagram of bioinformatics pipeline for ddRAD libraries. ddRAD one conducted at the NERC environmental omics facility (NEOF) using the ddRAD protocol from DaCosta and Sorenson (2014). Library Two was conducted at Durham University following the methodology from Franchini *et al.* (2017).

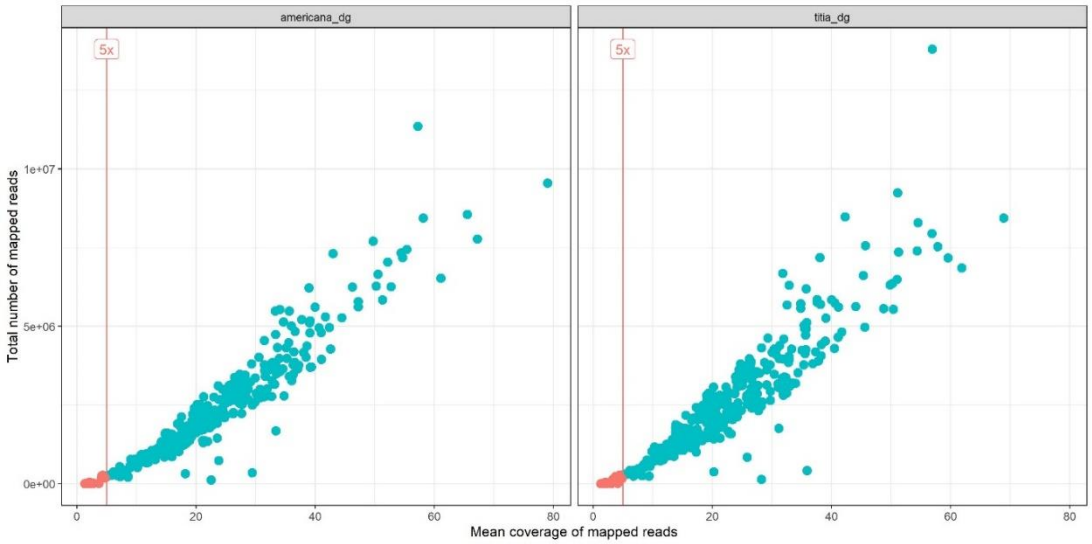

Supplementary Figure 4:2: The total number of mapped reads and the mean coverage for each sample using bwa mem alignment algorithm using *H. americana* draft genome (americana_dg) and the *H. titia* draft genome (titia_dg). Samples that had lower than 5x mean coverage were excluded from downstream analysis. Retained samples are coloured blue, excluded samples are coloured red.

Supplementary Table 4:1: The total number of variants identified in calling and the number of variants remaining after the following filtering steps. Removing indels (All single base calls). Removing all base calls that had read depth of less than 10 and greater than 200, and a quality score less than 20 (DP10-200, Q>20). Removing all SNPs not genotyped for 80% of samples, removing SNPs with a minimum allele frequency less than 0.05, and randomly removing all but one SNP within 1000 base window.

Species	Draft genome	Number of samples	All variant calls	All single base calls	DP10-200, Q>20	80% Samples	MAF>0.05	Random 1-1000
all	*H. americana*	364	134810308	134707986	2233411	80344	34506	1156
all	*H. titia*	363	161441042	161305711	2871466	81701	36376	1199
H. americana/ calverti	*H. americana*	75	73615352	73549147	4842870	1042635	151033	6997
H. americana/ calverti	*H. titia*	75	44189192	44164151	2258691	495629	80935	4103
H. titia	*H. americana*	286	81630947	81586704	1709783	260765	73471	3674
H. titia	*H. titia*	285	136427605	136309637	2997868	494012	121745	6369

Supplementary Results

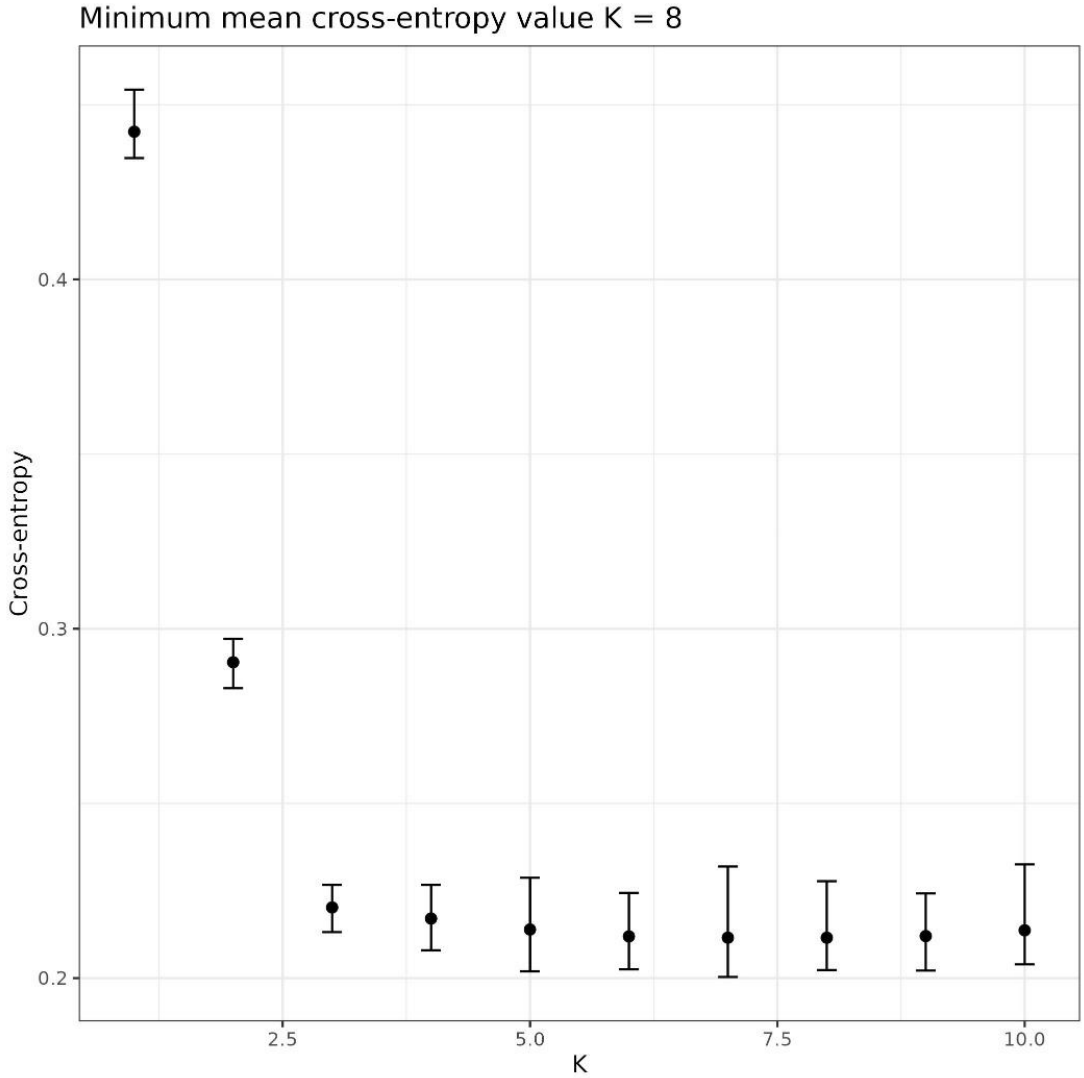

Supplementary Figure 4:3: The cross-entropy values from K = 1-10 and 20 repetition using a data of *Hetaerina titia* samples mapped to the H. titia genome HetTit1.0 (Patterson *et al.*, 2023)

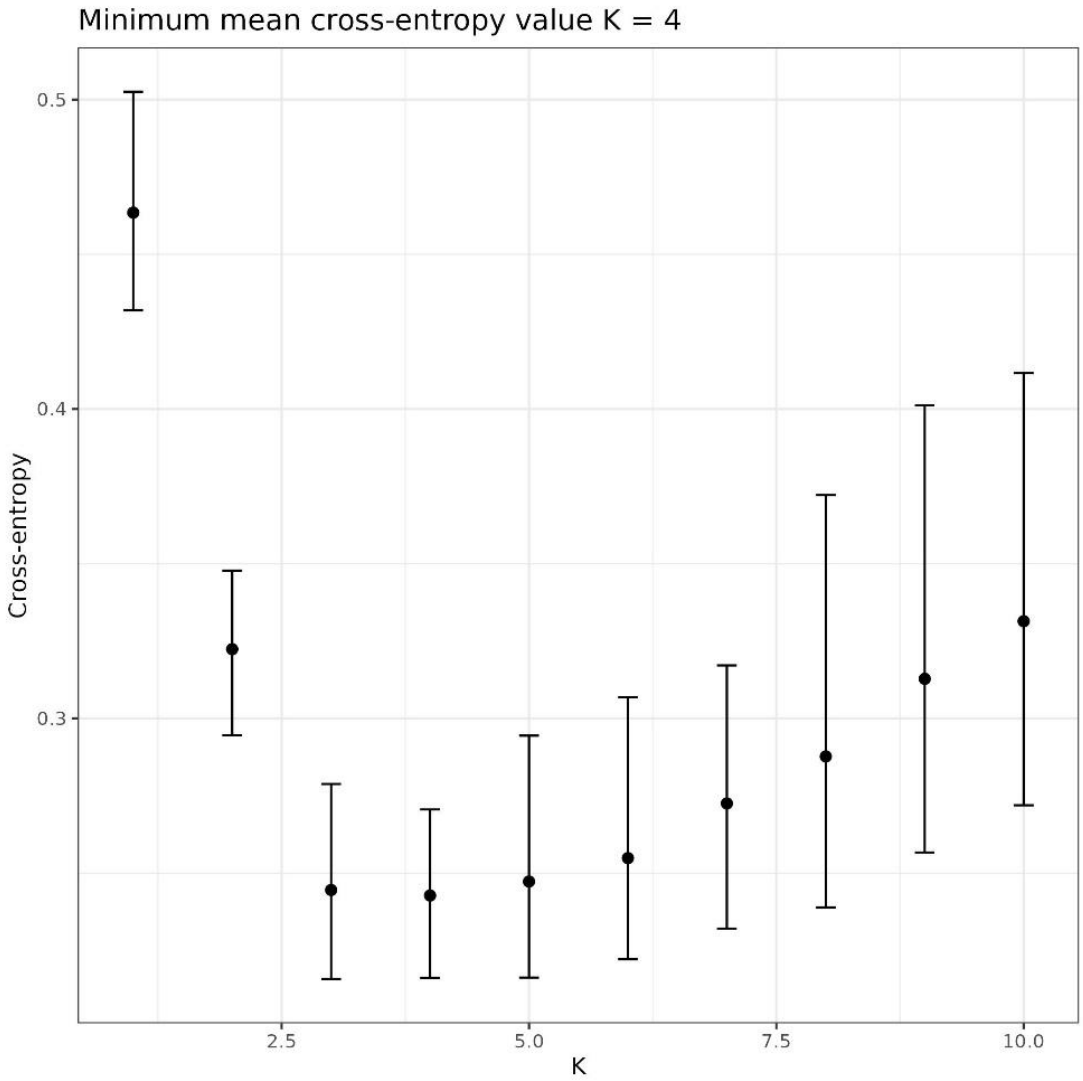

Supplementary Figure 4:4: The cross-entropy values from K = 1-10 and 20 repetition using a data of *Hetaerina americana and H. calverti* samples mapped to the *H. titia* genome HetTit1.0 (Patterson *et al.*, 2023)

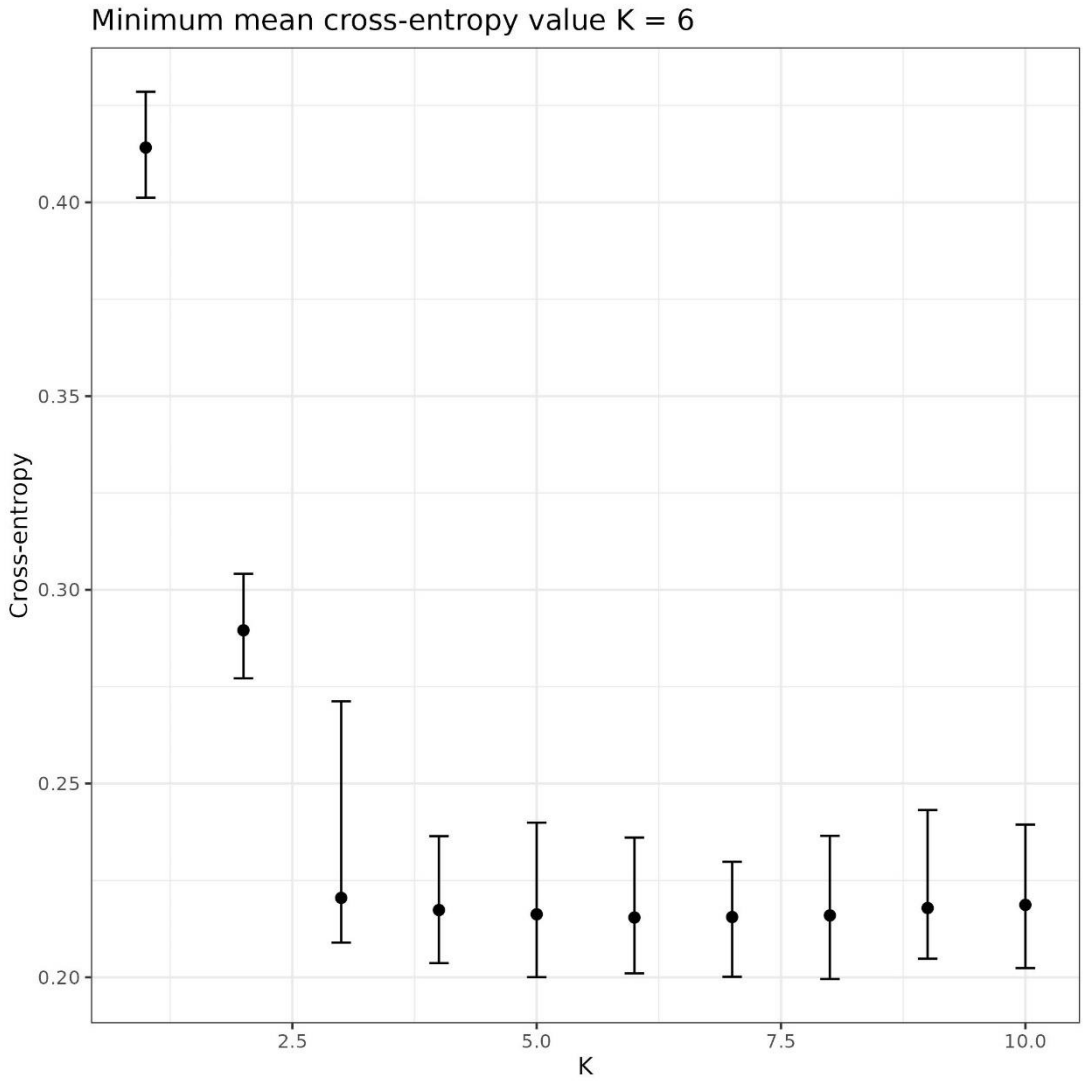

Supplementary Figure 4:5: The cross-entropy values from K = 1-10 and 20 repetition using a data of *Hetaerina titia* samples mapped to the *H. americana* genome HetAmer1.0 (Grether *et al.*, 2023)

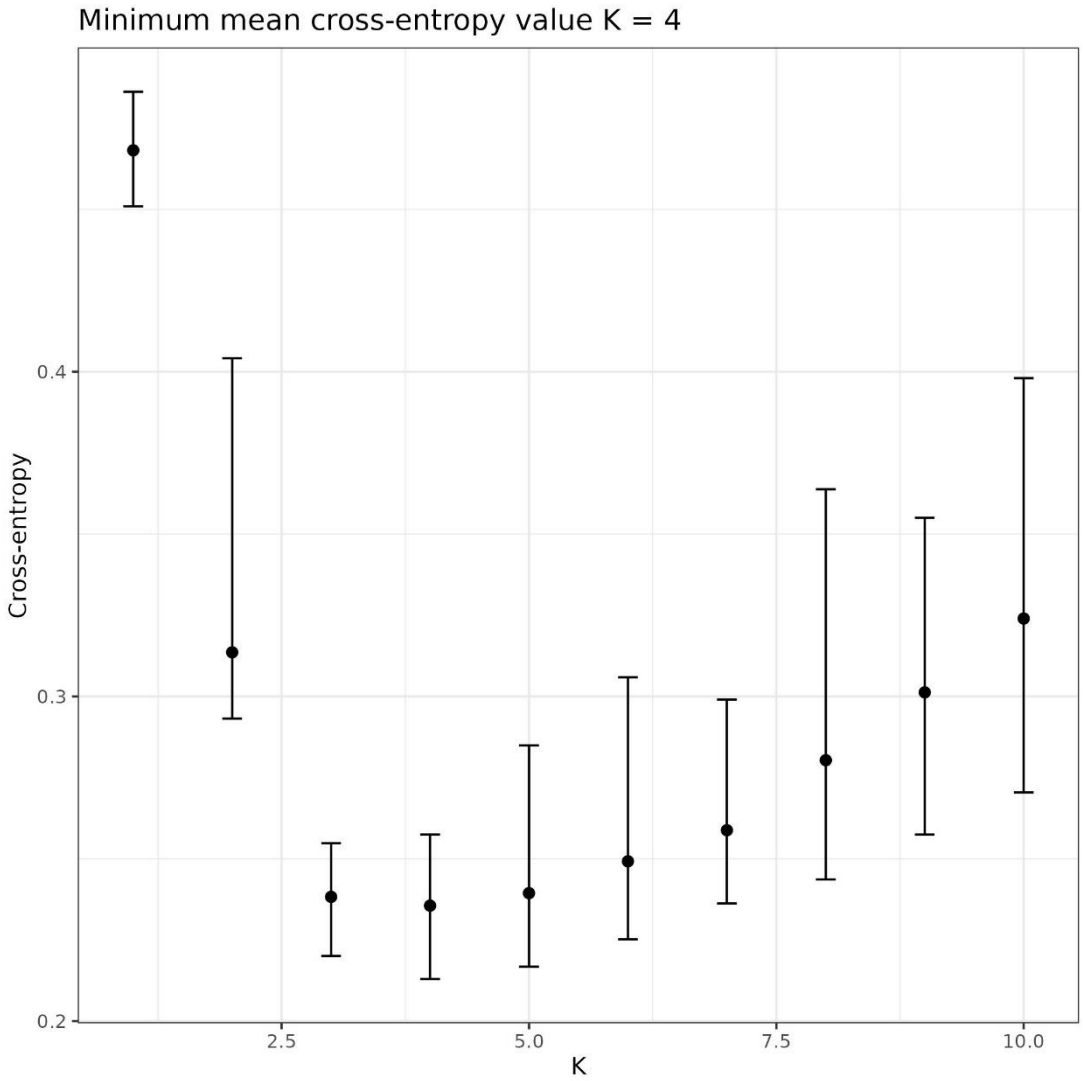

Supplementary Figure 4:6: The cross-entropy values from K = 1-10 and 20 repetition using a data of *Hetaerina americana* and *Hetaerina calverti* samples mapped to the *H. americana* genome HetAmer1.0 (Grether *et al.*, 2023).

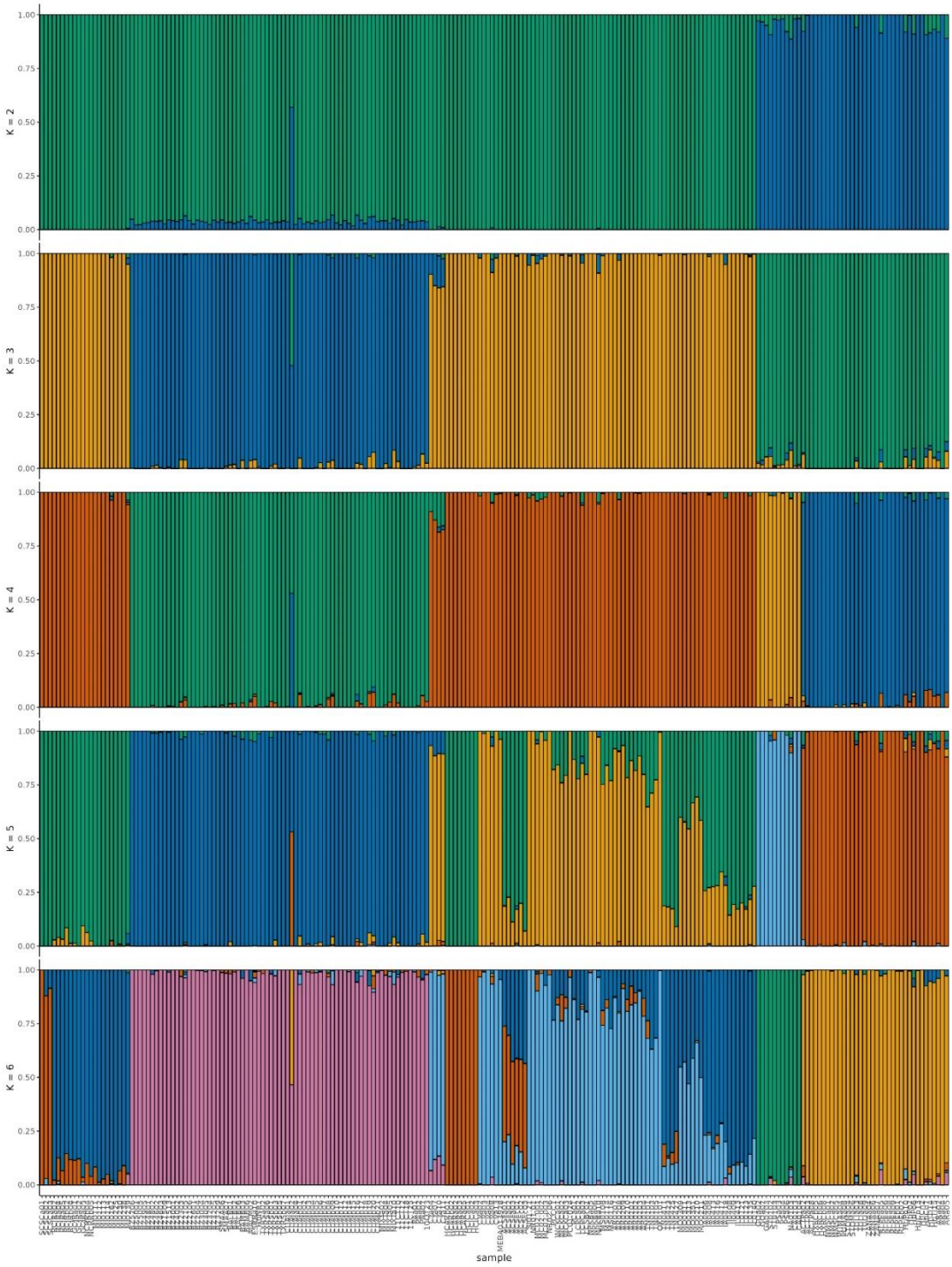

Supplementary Figure 4:7: Estimate of ancestry analysis for each individual using sNMF using K = 2-6 for all *Hetaerina titia* samples using the *Hetaerina titia* draft genome HetTit1.0 from (Patterson *et al.*, 2023) Each value of K was run for 100 times with an alpha value of 100. Samples are ordered by drainage, then country, and then latitude.

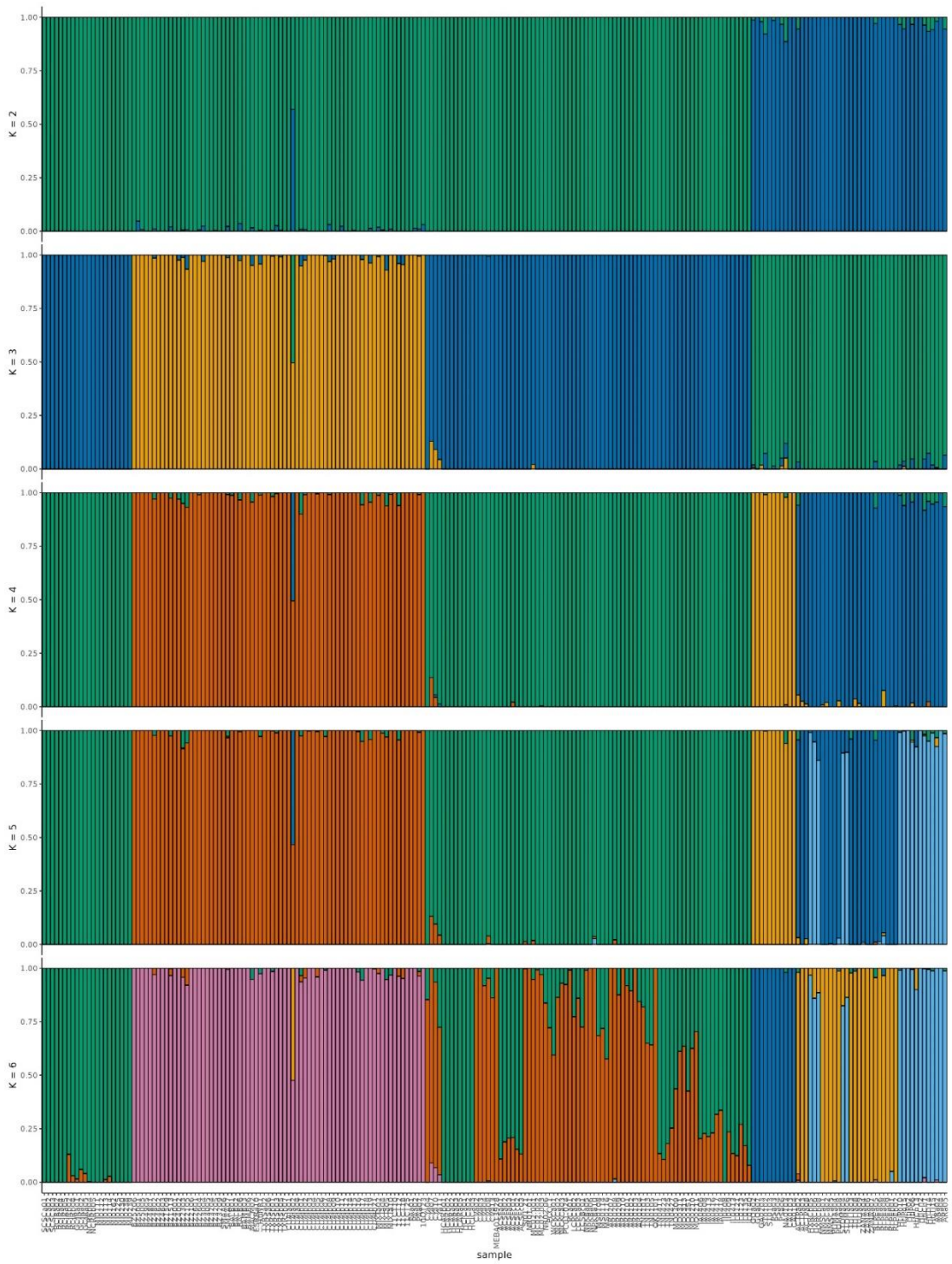

Supplementary Figure 4:8 :Estimate of ancestry analysis for each individual using sNMF using K = 2-6 for all *Hetaerina titia* samples using the *Hetaerina americana* draft genome HetAmer1.0 from (Grether *et al.*, 2023) Each value of K was run for 100 times with an alpha value of 100.

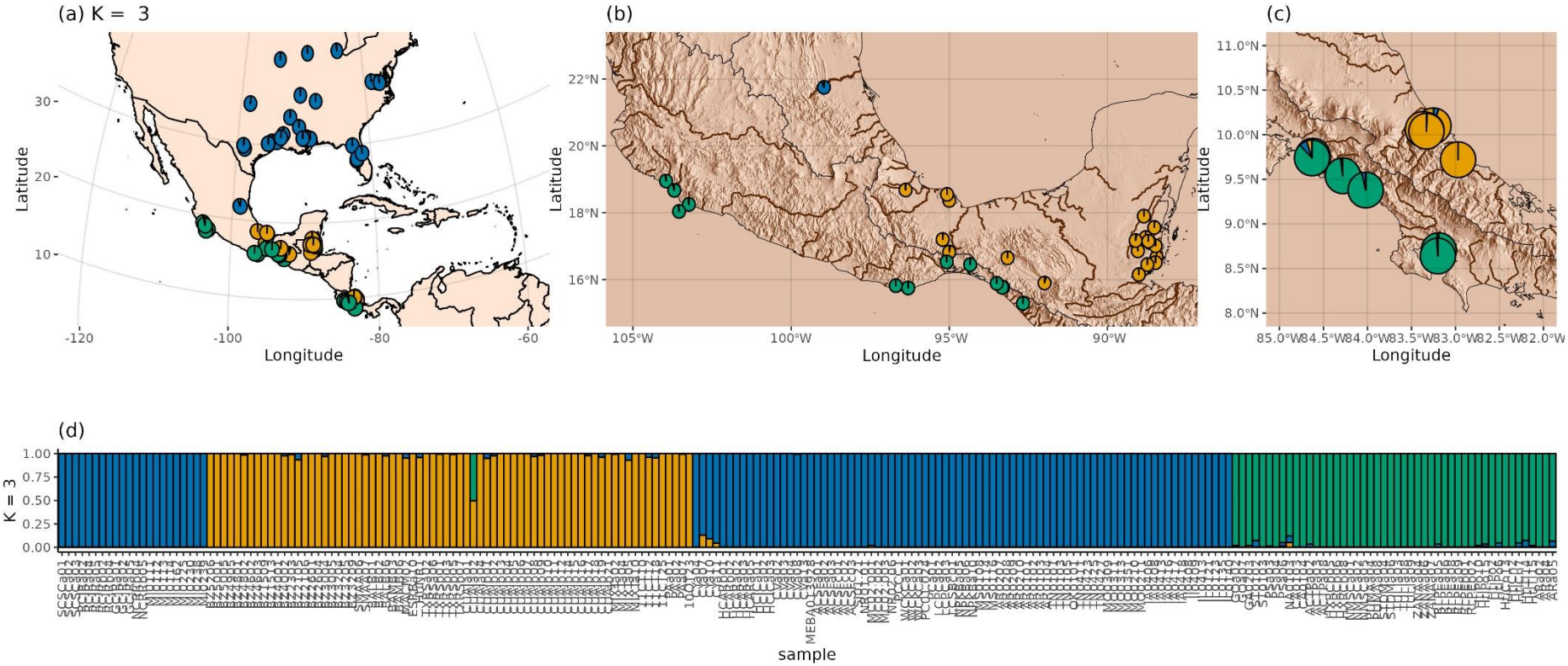

Supplementary Figure 4:9: Ancestry estimates using three ancestral populations for Hetaerina titia. SNPs were generated by mapping ddRAD reads to the draft genome of *H. americana*. LEA was run for 20 repetitions and an alpha value of 100. (a) The mean estimate of ancestry proportion for all samples within each sample site of *Hetaerina titia* across North and Central America, (b) Isthmus of Tehuantepec and Belize, and (c) Costa Rica. (d) Estimate of ancestry analysis for each individual. Samples are ordered by drainage, then country, and then latitude. Rivers and drainage basins from Hydrosheds. Topography data from the R package elevatr.

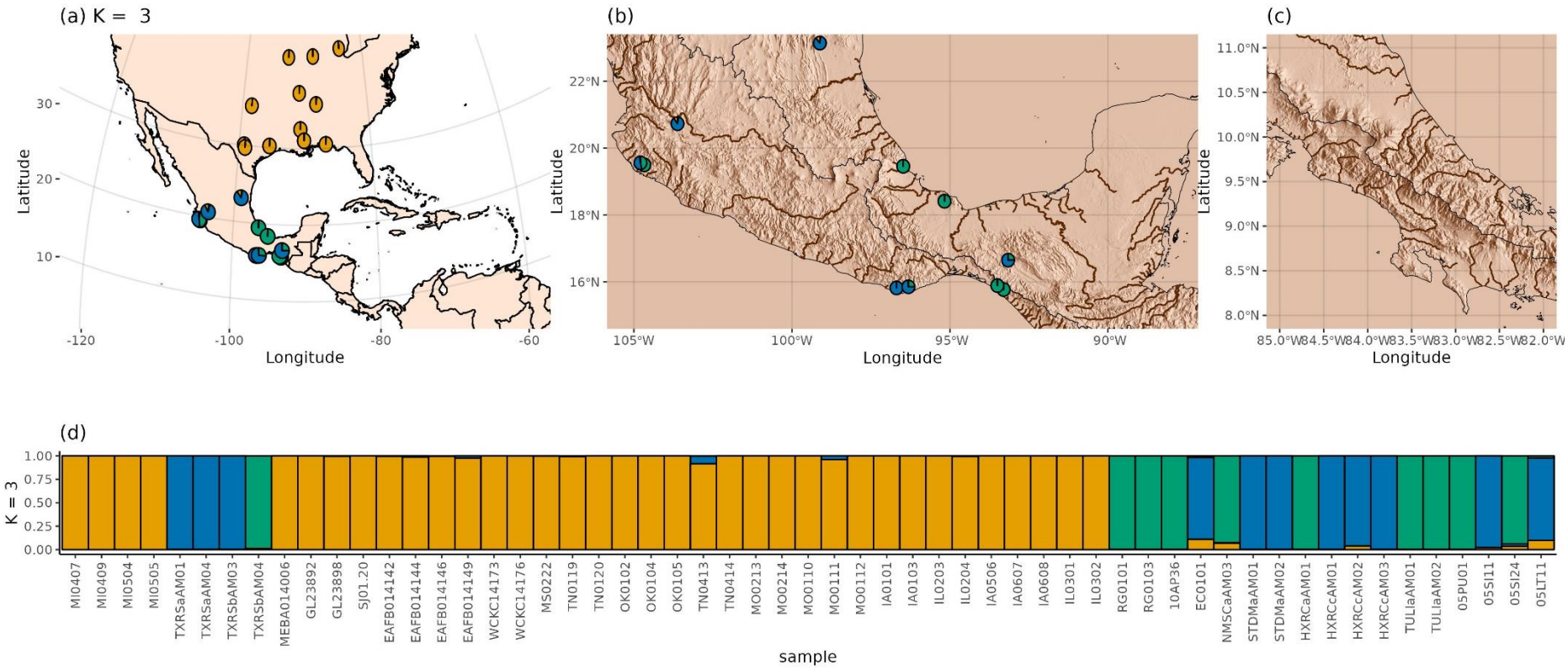

Supplementary Figure 4:10: Ancestry estimates using three ancestral populations for *Hetaerina americana*. SNPs were generated by mapping ddRAD reads to the draft genome of *H. americana*. LEA was run for 20 repetitions and an alpha value of 100. (a) The mean estimate of ancestry proportion for all samples within each sample site of *Hetaerina americana* across North and Central America, (b) Isthmus of Tehuantepec and Belize, and (c) Costa Rica (where there is no *H. americana*). (d) Estimate of ancestry analysis for each individual. Samples are ordered by drainage, then country, and then latitude. Rivers and drainage basins from Hydrosheds. Topography data from the R package elevatr

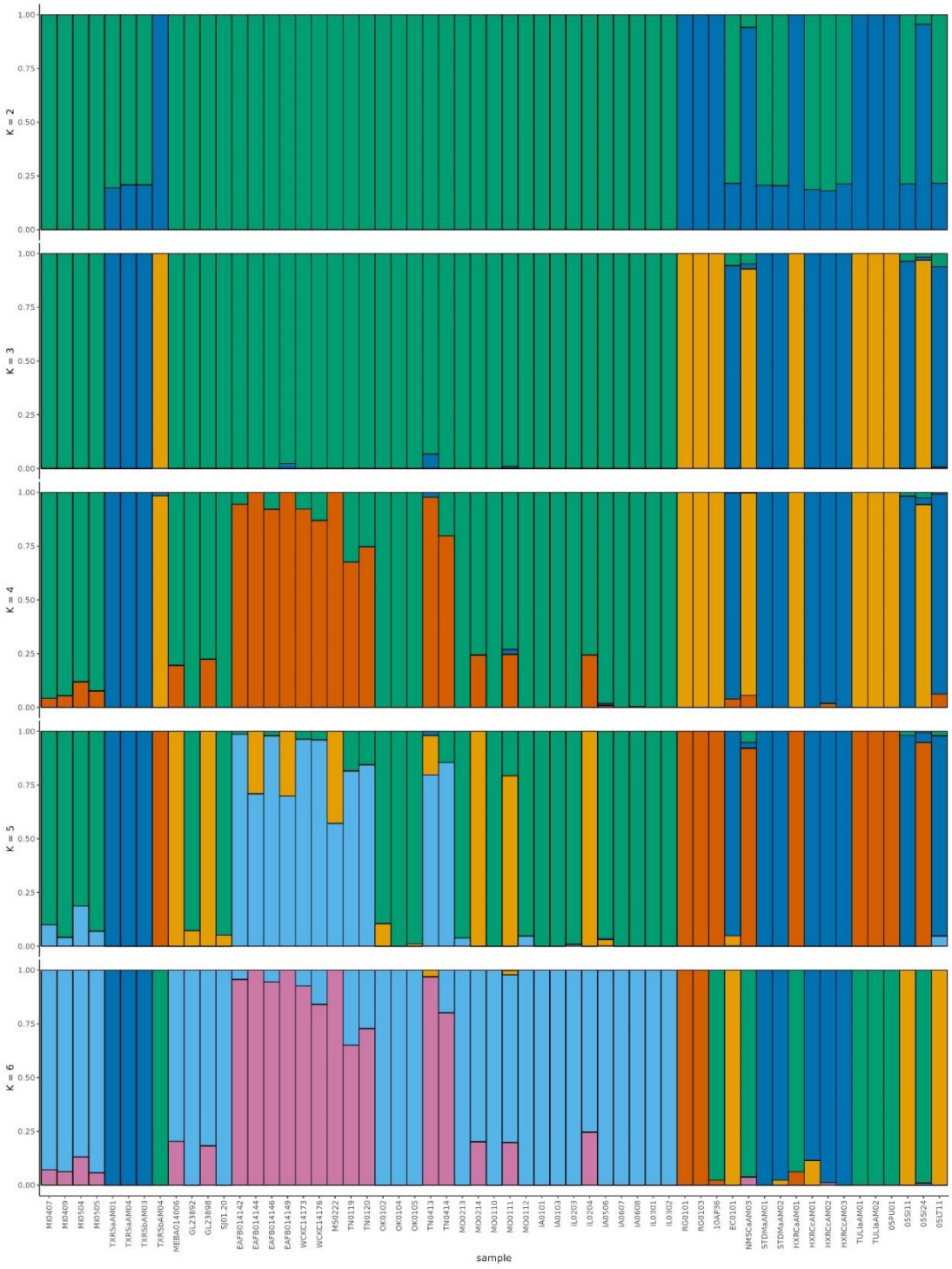

Supplementary Figure 4:11: Estimate of ancestry analysis using sNMF using K = 2-6 for all *Hetaerina americana* samples using the *Hetaerina titia* draft genome HetTit1.0 from (Patterson *et al.*, 2023). Each value of K was run for 100 times with an alpha value of 100.

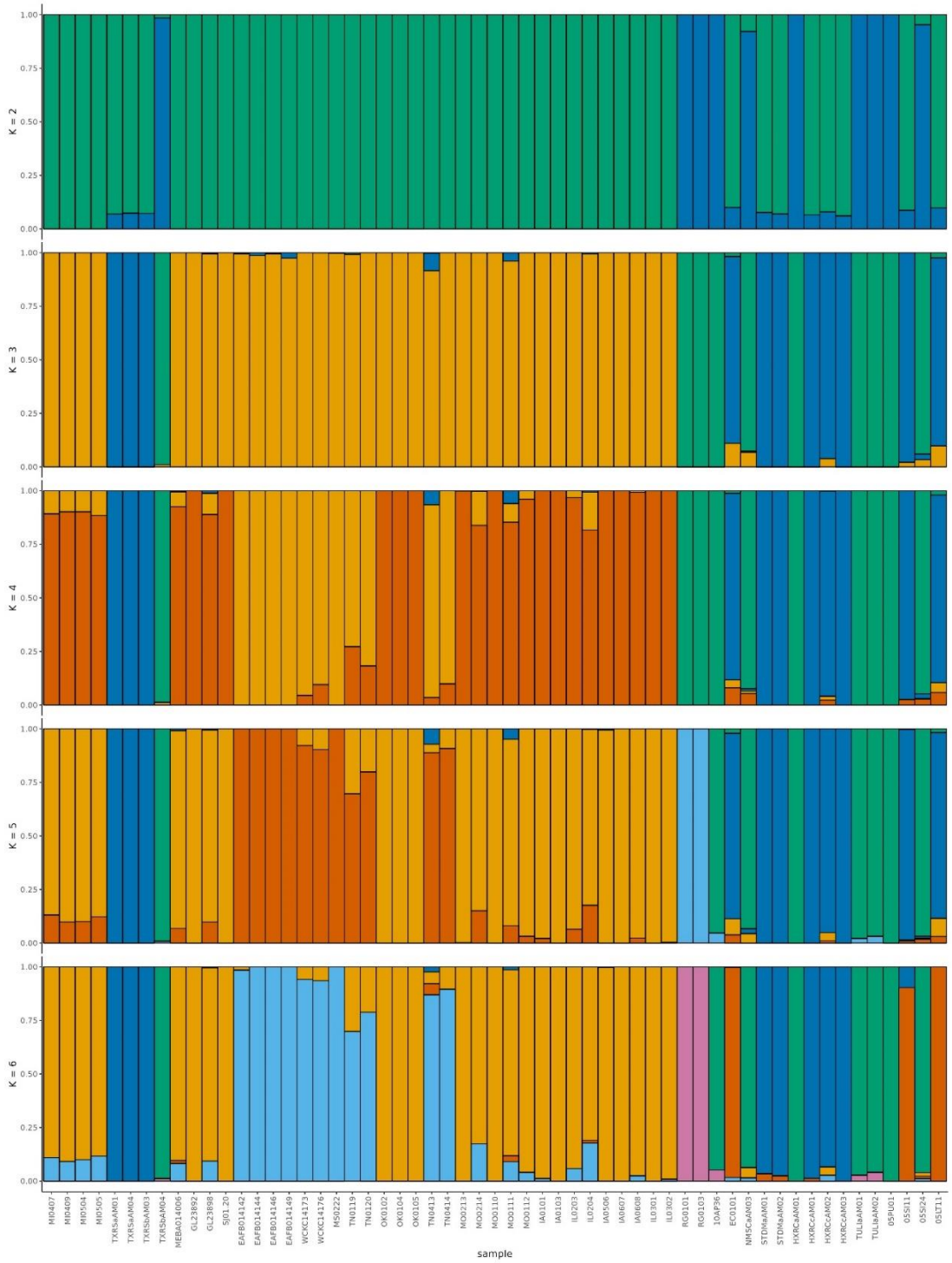

Supplementary Figure 4:12: Estimate of ancestry analysis using sNMF using K = 2-6 for all *Hetaerina americana* samples using the Hetaerina americana draft genome HetAmer1.0 from (Grether *et al.*, 2023) Each value of K was run for 100 times with an alpha value of 100.

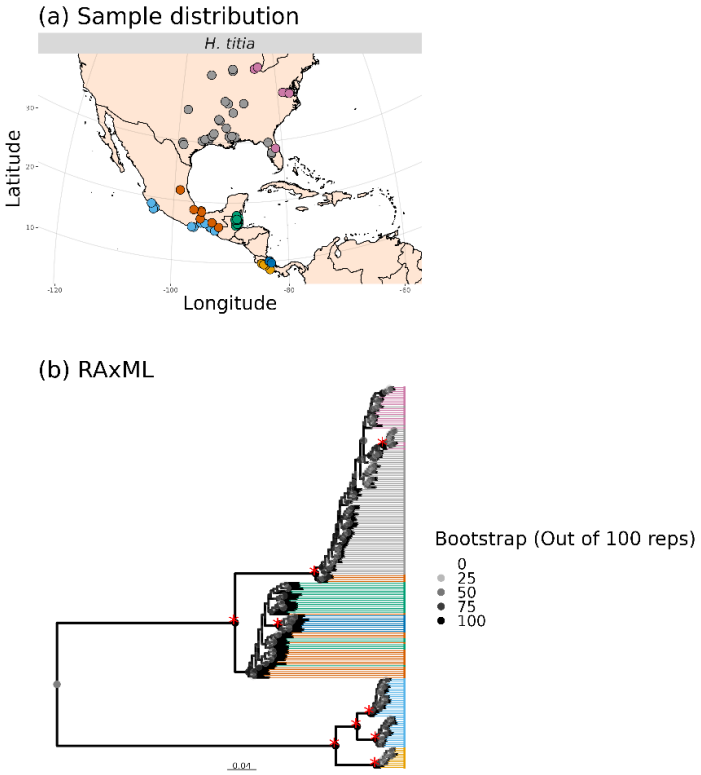

Supplementary Figure 4:13: The maximum likelihood tree for *Hetaerina titia* calculated by RAxML using a SNP library of 3,208 SNPs mapped onto the genome of *H. titia*. The tree is rooted around the midpoint which corresponds the root identified by the multi-species tree. The nodes are coloured by the number of bootstrap support values (out of 100). Nodes with greater than 95% support are marked with a red "*". The tree tips are coloured according to the species, the country, and river drainage of each sample shown in the inset map. Scale bar indicates number of substitutions per SNP site.

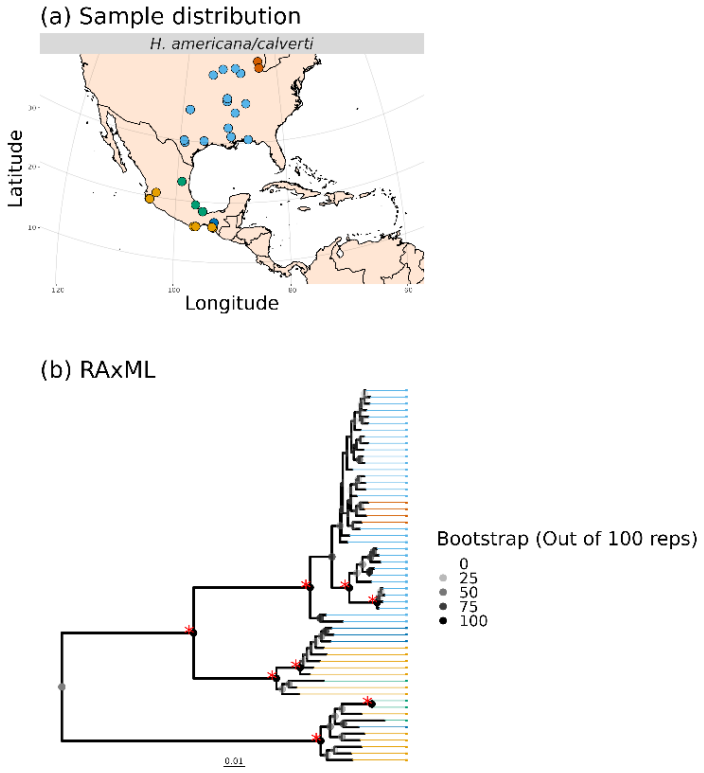

Supplementary Figure 4:14: The maximum likelihood tree for *Hetaerina americana and Hetaerina calverti* calculated by RAxML using a SNP library of 1,382 SNPs mapped onto the genome of *H. titia*. The tree is rooted around the midpoint which corresponds the root identified by the multi-species tree. The nodes are coloured by the number of bootstrap support values (out of 100). Nodes with greater than 95% support are marked with a red "*". The tree tips are coloured according to the species, the country, and river drainage of each sample shown in the inset map. The colour of each tip and geographical position of each sample does not separate *Hetaerina americana* and *Hetaerina calverti*. Scale bar indicates number of substitutions per SNP site.

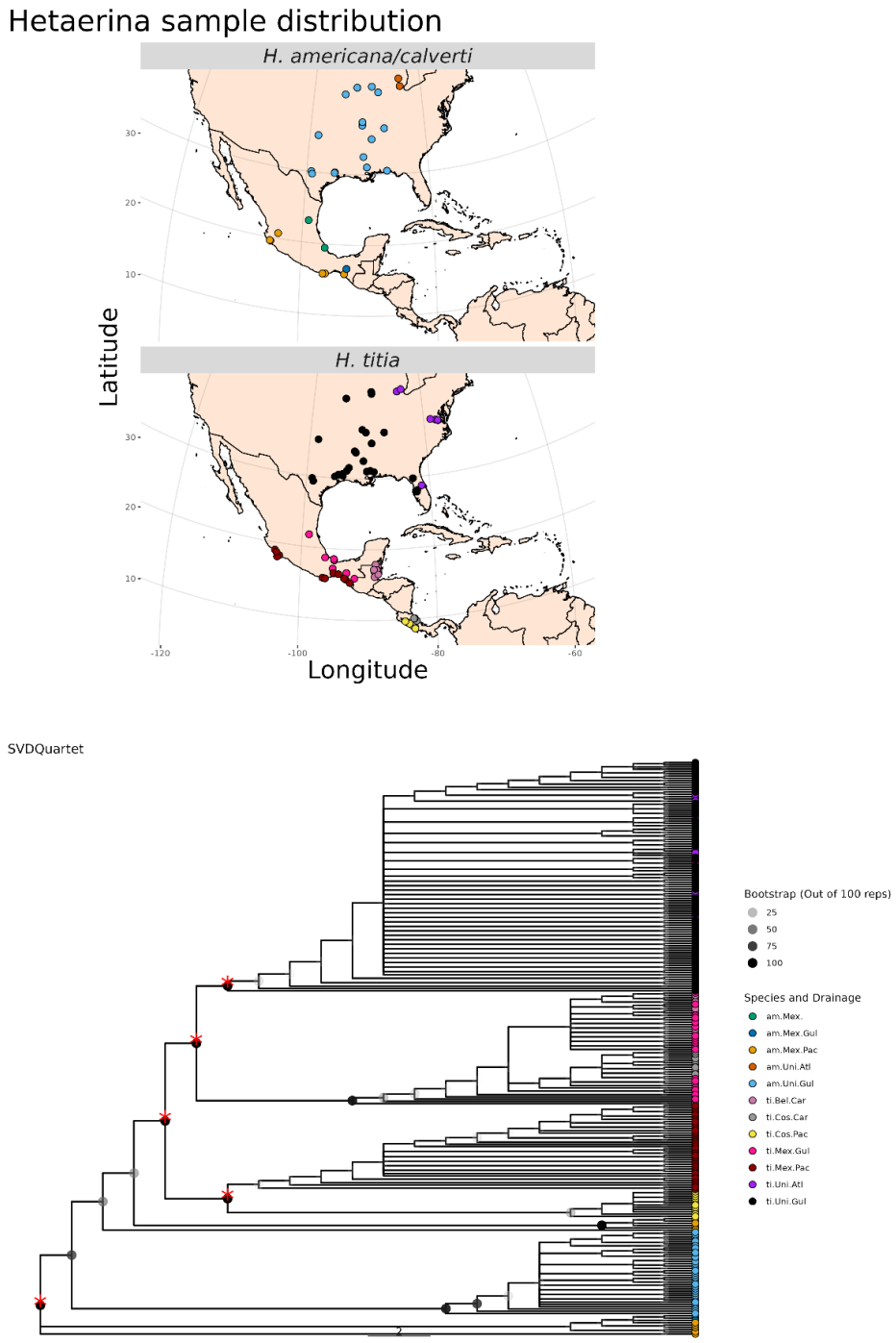

Supplementary Figure 4:15: SVDquartet analysis of *H. tita, H. americana* and *H. calverti* mapped to the draft genome of H. titia. Node with greater than 95% bootstrap support indicated with a read "*".

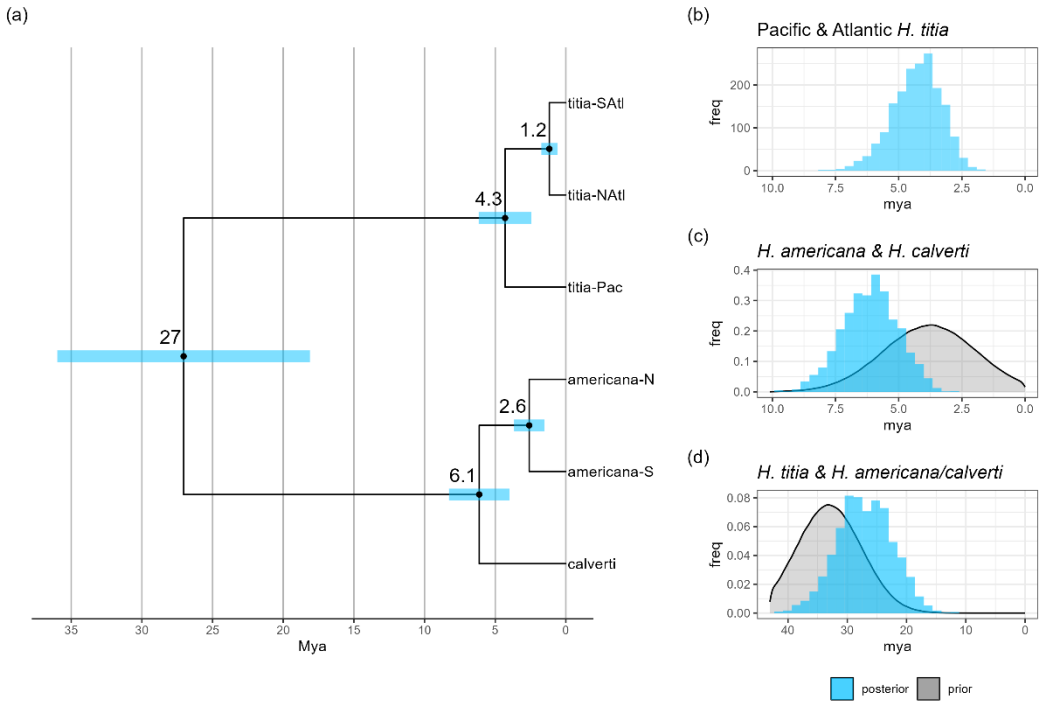

Supplementary Figure 4:16: Estimates of divergence dates between populations of *Hetaerina titia* (titia-NAtl, titia-SAlt, and titia-Pac), *Hetaerina americana* (americana-N americana-S), and *Hetaerina calverti* (calv-1) calculated using SNAPP analysis in beast. Input data was 540 SNPs mapped to the genome of *Hetaerina americana*. Node labels indicate the mean estimated divergence date with 95% highest posterior density in blue. All branches had a posterior distribution of 1.

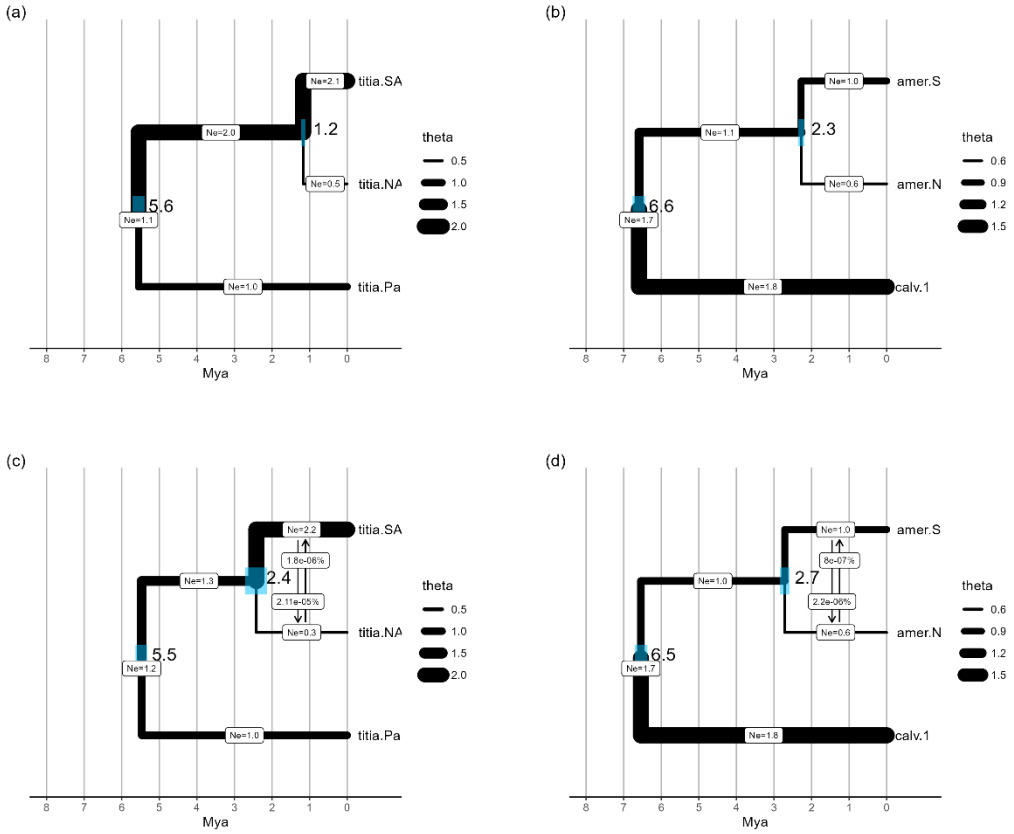

Supplementary Figure 4:17: The estimated divergence times (million years ago) and effective population size (theta – N*e* in millions of individuals) from G-Phocs analysis of *H. titia* and *H. americana*. Migration rate is the number of migrated as a percentage of Ne per generation. All models ran for 1,000,000 interactions with 10% burn in. Blue bars show 95% highest posterior density for each divergence date **(a)** Model estimates for *H. titia* with no migration bands. **(b)** Model estimates for *H. americana* and *H. calverti* with no migration bands. **(c)** Model estimates for *H. titia* demography with migration bands between Northern and Southern Atlantic *H. titia* **(d)** Model estimates for *H. americana* and *H. calverti* with migration bands between North and Southern *H. americana*. G-phocs runs presented here are conducted on the conspecific draft genome. i.e., *H. titia* loci mapped to the *H. titia* draft genome and the *H. americana* loci mapped to the H. americana draft genome.

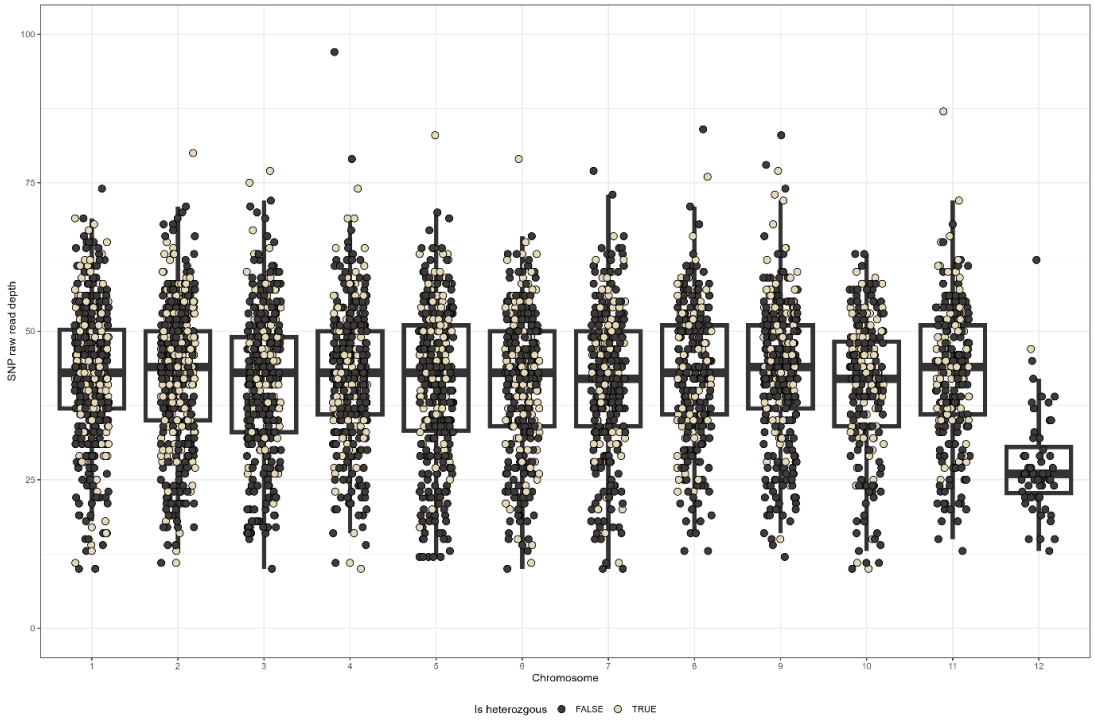

Supplementary Figure 4:18: All genotyped SNPs from individual CUAJa02 from site CUAJ01, Cuajinicuil, Oaxaca (16° 47'24.00"N, 95°0'36.00"W). Each point marks the raw read number used for SNP calling at that specific site, which chromosome the SNP was mapped to and whether site was heterozygous. Chromosome 12 is the X chromosome. The y axis is restricted to a read coverage of 0 to 100 excluding a small number of high coverage autosomal SNPs.

Appendix Chapter 6.

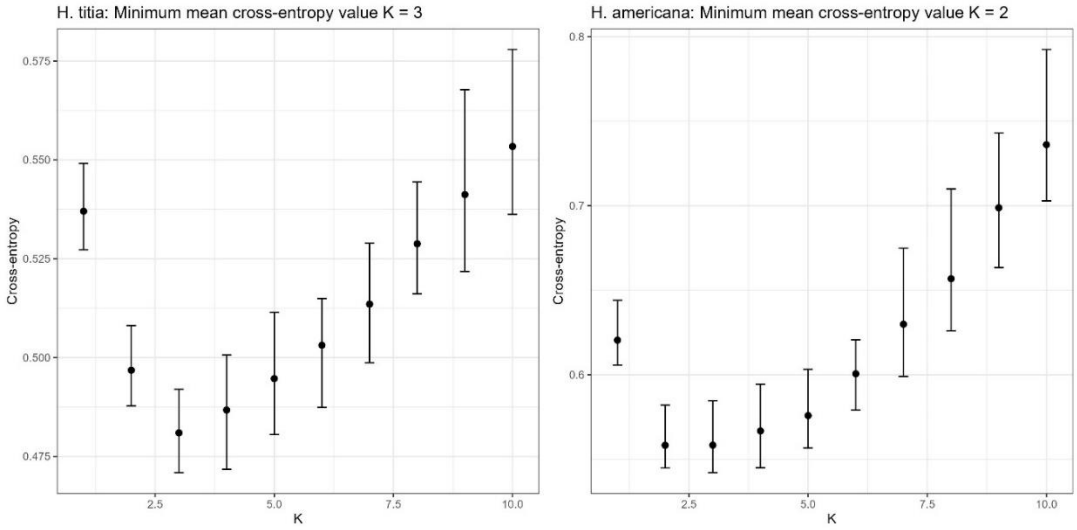

Supplementary Figure 6:1:The cross-entropy values from K = 1-10 and 20 repetition using a data of *Hetaerina titia* and *H. americana* mapped to draft genomes of *H. titia* and *H. americana,* respectively.

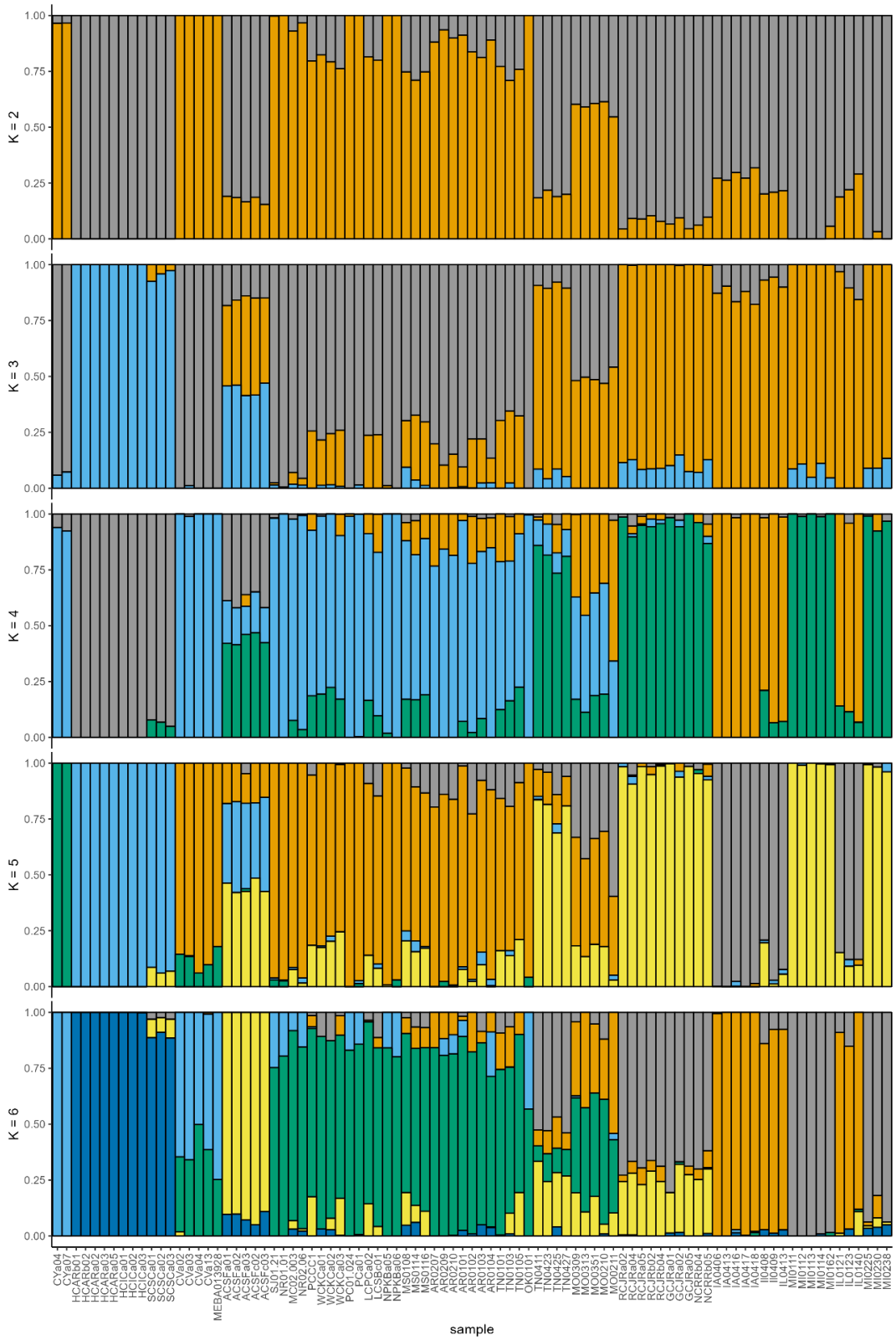

Supplementary Figure 6:2: Estimate of ancestry analysis for each individual using sNMF using K = 2-6 for all *Hetaerina titia* samples using the *Hetaerina titia* draft genome HetTit1.0 from (Patterson *et al.*, 2023). Each value of K was run for 20 times with an alpha value of 100.

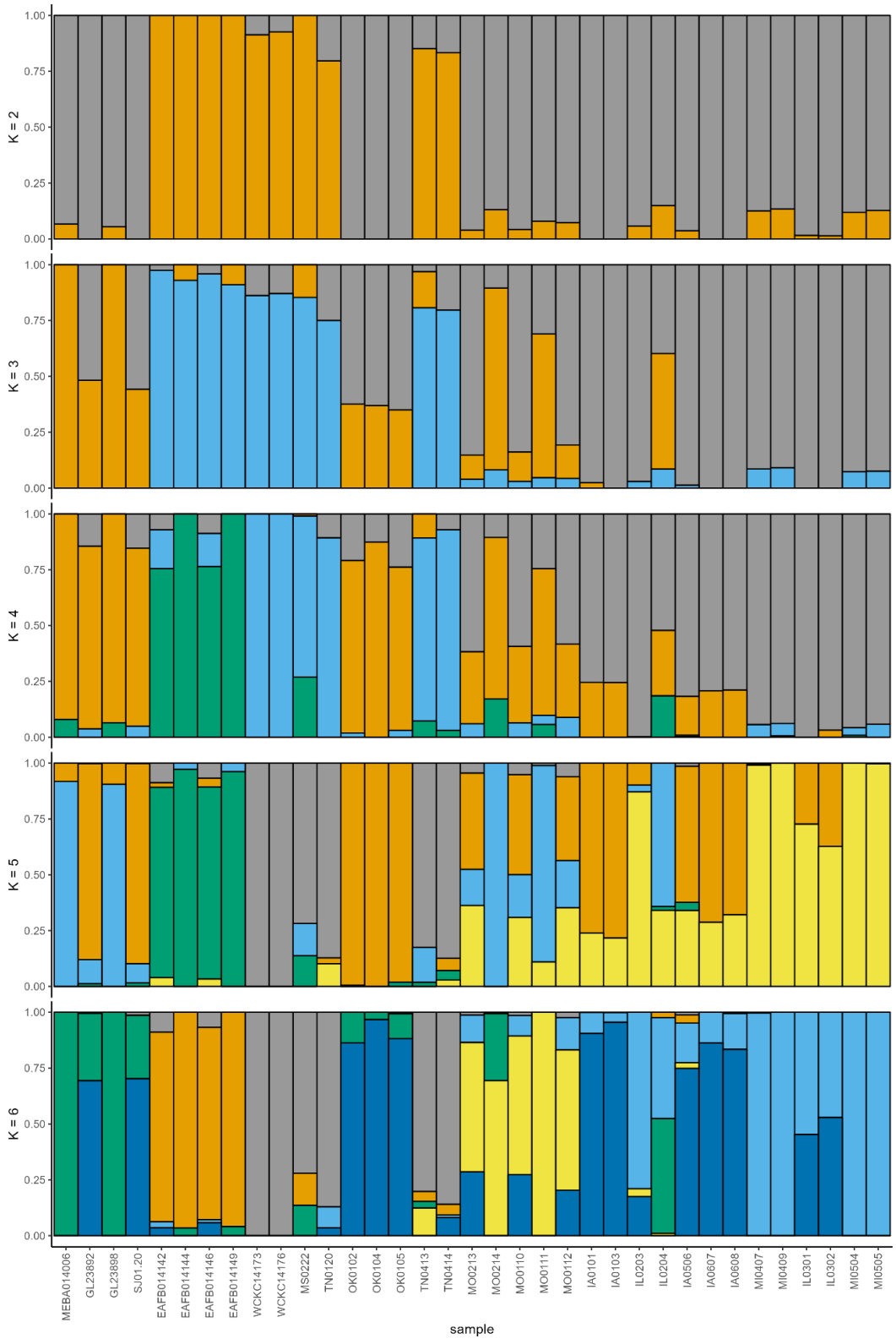

Supplementary Figure 6:3: Estimate of ancestry analysis for each individual using sNMF using K = 2-6 for all *Hetaerina americana* samples using the *Hetaerina americana* draft genome from (Grether *et al.*, 2023) Each value of K was run for 20 times with an alpha value of 100.

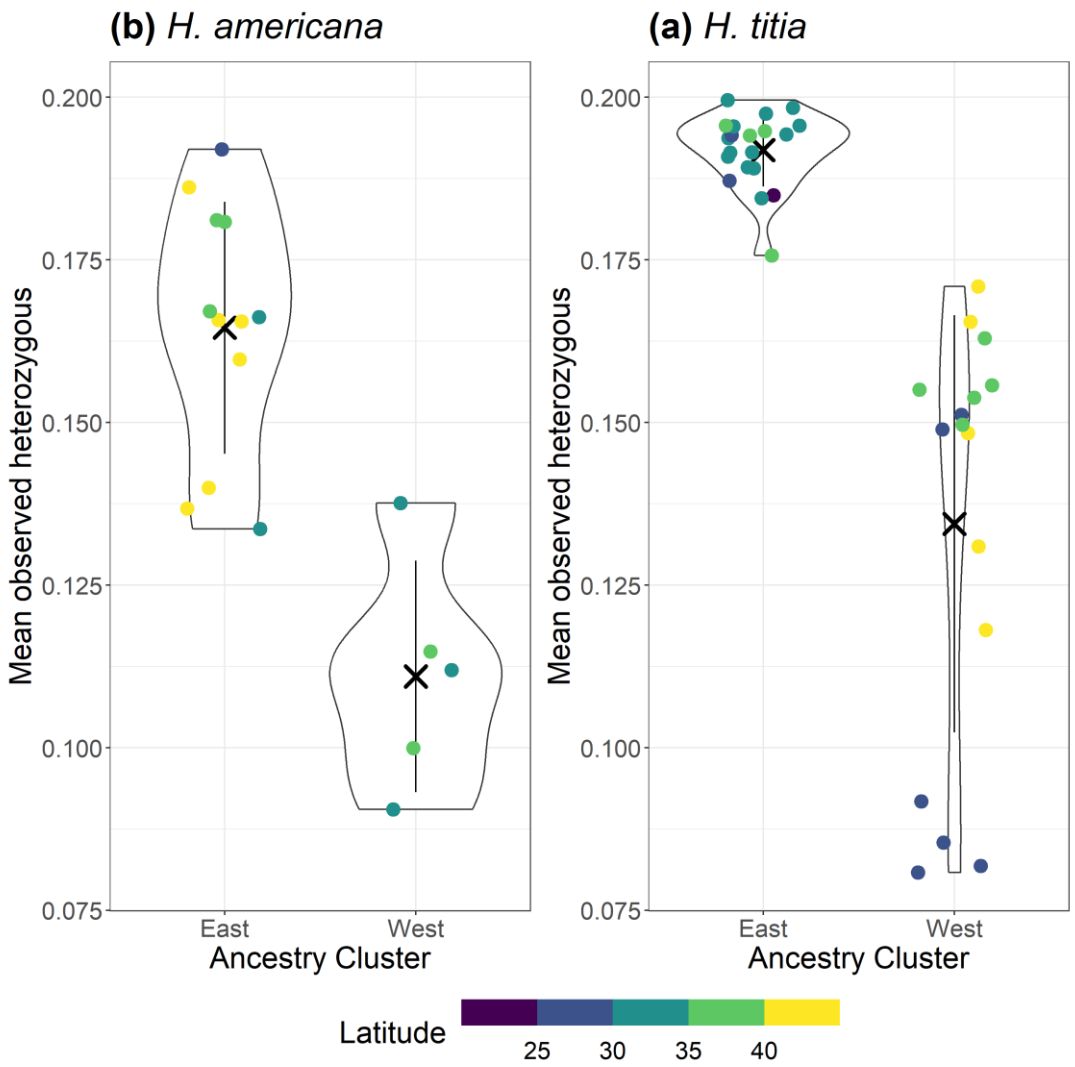

Supplementary Figure 6:4: The mean observed heterozygosity for each population of *H. americana* and *H. titia*. Populations are divided into the eastern and Western ancestor clusters identified by sNMF analysis. The mean level of observed heterozygosity for each ancestral group is mark by an X with the standard deviation marked a vertical line. Populations are coloured by latitude.

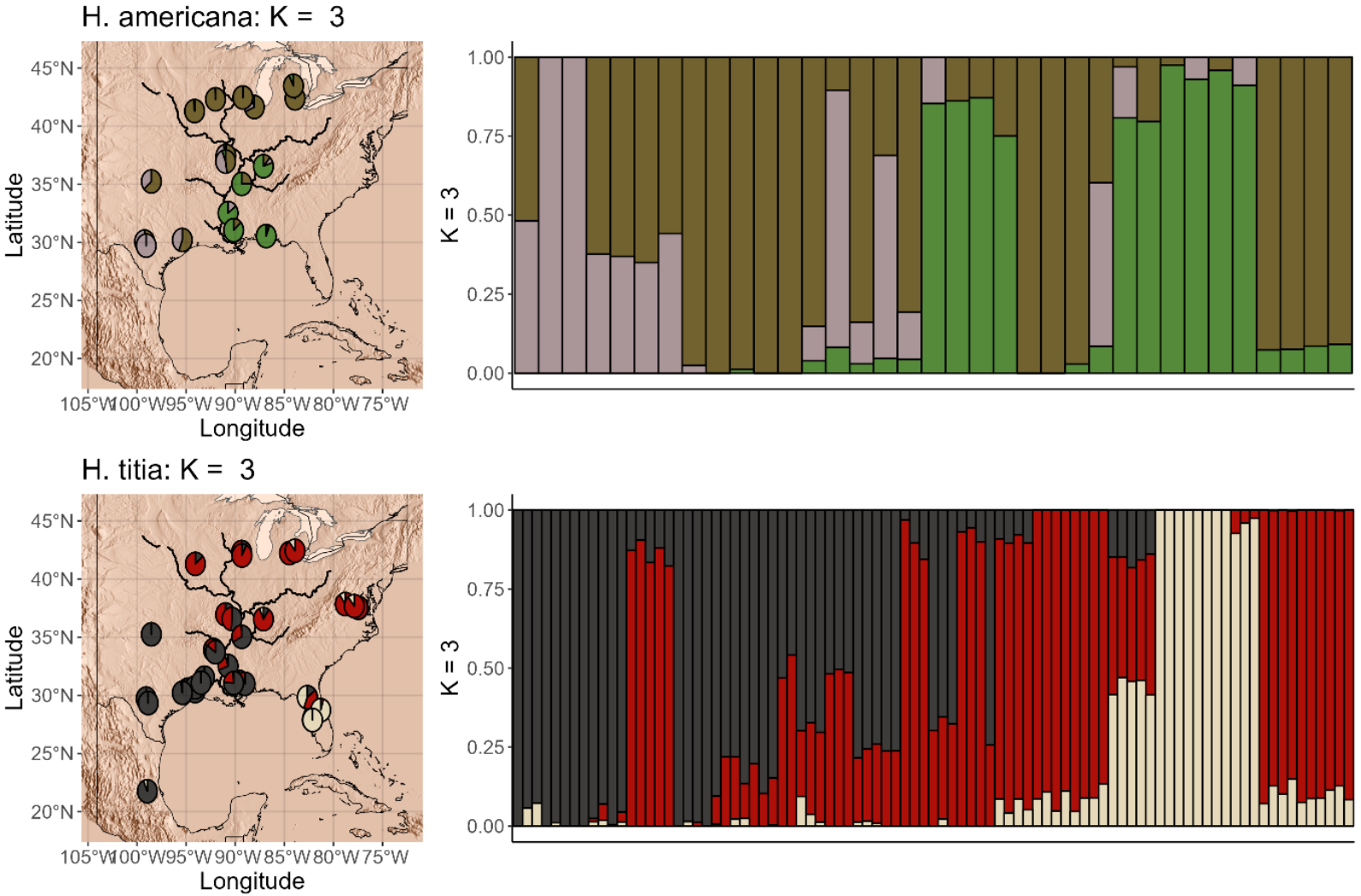
H. americana: K = 3
45°N
40°N
35°N
30°N
25°N
20°N
Latitude
105°W
100°W
95°W
90°W
85°W
80°W
75°W
Longitude
1.00
0.75
0.50
0.25
0.00
K = 3
H. titia: K = 3
45°N
40°N
35°N
30°N
25°N
20°N
Latitude
105°W
100°W
95°W
90°W
85°W
80°W
75°W
Longitude
1.00
0.75
0.50
0.25
0.00
K = 3

Supplementary Figure 6:5: Ancestry estimates using two ancestral populations for 35 *H. americana* (top row)and 89 *Hetaerina titia* (bottom row) using a dataset of 12, 639 and 5,675 unlinked biallelic autosomal SNPs. SNPs were generated by mapping ddRAD reads to the draft genome of *H. titia*. LEA was run for 20 repetitions and an alpha value of 100. **Top left,** the mean estimate of ancestry proportion for all samples within each sample site of *Hetaerina americana* across North America. **Bottom left,** the mean estimate of ancestry proportion for all samples within each sample site of *H. titia* across North America. sNMF plots include a shaded relief map using the package elevatoR (Hollister *et al.*, 2023) and the main tributaries of the Mississippi river from the HydroBasins/v2 river dataset (Lehner *et al.*, 2008). Estimate of ancestry analysis for each individual for *H. americana* (top right) and *H. titia* (bottom right). Estimates of ancestry analysis for each individual for *H. americana* (top right) and *H. titia* (bottom right).

Bibliography

AGUILERA, M.A. & NAVARRETE, S.A. (2012) Interspecific Competition for Shelters in Territorial and Gregarious Intertidal Grazers: Consequences for Individual Behaviour. *PLOS ONE* **7**, e46205. Public Library of Science.

AH-KING, M., KVARNEMO, C. & TULLBERG, B.S. (2005) The influence of territoriality and mating system on the evolution of male care: a phylogenetic study on fish. *Journal of Evolutionary Biology* **18**, 371–382.

AL-ASADI, H., PETKOVA, D., STEPHENS, M. & NOVEMBRE, J. (2019) Estimating recent migration and population-size surfaces. *PLoS Genetics* **15**, e1007908. Public Library of Science San Francisco, CA USA.

ALEXANDER, D.H., NOVEMBRE, J. & LANGE, K. (2009) Fast model-based estimation of ancestry in unrelated individuals. *Genome Research* **19**, 1655–1664.

ALEXANDER, J.M., DIEZ, J.M. & LEVINE, J.M. (2015) Novel competitors shape species' responses to climate change. *Nature* **525**, 515–518.

AMARASEKARE, P. (2002) Interference competition and species coexistence. *Proc. R. Soc. B* **269**, 2541–2550.

ANDERSON, C.N. & GRETHER, G.F. (2010a) Interspecific aggression and character displacement of competitor recognition in Hetaerina damselflies. *Proceedings of the Royal Society B: Biological Sciences* **277**, 549–555.

ANDERSON, C.N. & GRETHER, G.F. (2010b) Character displacement in the fighting colours of *Hetaerina* damselflies. *Proceedings of the Royal Society Biological Sciences Series B* **277**, 3669–3675.

ANDERSON, C.N. & GRETHER, G.F. (2011) Multiple routes to reduced interspecific territorial fighting in Hetaerina damselflies. *Behavioral Ecology* **22**, 527–534.

ANDERSSON, S. (1989) Sexual selection and cues for female choice in leks of Jackson's widowbird Euplectes jacksoni. *Behavioral Ecology and Sociobiology* **25**, 403–410.

ANON. (undated) iNaturalist. https://www.inaturalist.org. https://www.inaturalist.org [accessed 17 January 2024].

ARDILA-GARCIA, A.M. & GREGORY, T.R. (2009) An exploration of genome size diversity in dragonflies and damselflies (Insecta: Odonata). *Journal of Zoology* **278**, 163–173.

ARMBRUSTER, W.S., PÉLABON, C., BOLSTAD, G.H. & HANSEN, T.F. (2014) Integrated phenotypes: understanding trait covariation in plants and animals. *Philosophical Transactions of the Royal Society B: Biological Sciences* **369**, 20130245. Royal Society.

ARMBRUSTER, W.S. & SCHWAEGERLE, K.E. (1996) Causes of covariation of phenotypic traits among populations. *Journal of Evolutionary Biology* **9**, 261–276.

ARNEGARD, M.E., MCINTYRE, P.B., HARMON, L.J., ZELDITCH, M.L., CRAMPTON, W.G.R., DAVIS, J.K., SULLIVAN, J.P., LAVOUÉ, S. & HOPKINS, C.D. (2010) Sexual Signal Evolution Outpaces Ecological Divergence during Electric Fish Species Radiation. *The American Naturalist* **176**, 335–356. The University of Chicago Press.

ASENSIO, N., JOSÉ-DOMÍNGUEZ, J.M., KONGRIT, C. & BROCKELMAN, W.Y. (2017) The ecology of white-handed and pileated gibbons in a zone of overlap and hybridization in Thailand. *American Journal of Physical Anthropology* **163**, 716–728.

AULD, J., EVERINGHAM, S.E., HEMMINGS, F.A. & MOLES, A.T. (2022) Alpine plants are on the move: Quantifying distribution shifts of Australian alpine plants through time. *Diversity and Distributions* **28**, 943–955.

BAGCHI, R., CROSBY, M., HUNTLEY, B., HOLE, D.G., BUTCHART, S.H.M., COLLINGHAM, Y., KALRA, M., RAJKUMAR, J., RAHMANI, A., PANDEY, M., GURUNG, H., TRAI, L.T., VAN QUANG, N. & WILLIS, S.G. (2013) Evaluating the effectiveness of conservation site networks under climate change: accounting for uncertainty. *Global Change Biology* **19**, 1236–1248.

BAKER, D.J., HARTLEY, A.J., BURGESS, N.D., BUTCHART, S.H.M., CARR, J.A., SMITH, R.J., BELLE, E. & WILLIS, S.G. (2015) Assessing climate change impacts for vertebrate fauna across the West African protected area network using regionally appropriate climate projections. *Diversity and Distributions* **21**, 991–1003.

BARGIELOWSKI, I., BLOSSER, E. & LOUNIBOS, L.P. (2015) The Effects of Interspecific Courtship on the Mating Success of Aedes aegypti and Aedes albopictus (Diptera: Culicidae) Males. *Annals of the Entomological Society of America* **108**, 513–518.

BARGIELOWSKI, I.E. & LOUNIBOS, L.P. (2016) Satyrization and satyrization-resistance in competitive displacements of invasive mosquito species. In *Insect Science* pp. 162–174. Blackwell Publishing Ltd.

BARGIELOWSKI, I.E., LOUNIBOS, L.P. & CARRASQUILLA, M.C. (2013) Evolution of resistance to satyrization through reproductive character displacement in populations of invasive dengue vectors. *Proceedings of the National Academy of Sciences* **110**, 2888–2892. Proceedings of the National Academy of Sciences.

BARLEY, A.J., NIETO-MONTES DE OCA, A., MANRÍQUEZ-MORÁN, N.L. & THOMSON, R.C. (2022) The evolutionary network of whiptail lizards reveals predictable outcomes of hybridization. *Science* **377**, 773–777. American Association for the Advancement of Science.

BARTON, N.H. (1979) The dynamics of hybrid zones. *Heredity* **43**, 341–359. Nature Publishing Group.

BARTON, N.H. & HEWITT, G.M. (1989) Adaptation, speciation and hybrid zones. *Nature* **341**, 497–503. Nature Publishing Group UK London.

BARTOSZEK, K., PIENAAR, J., MOSTAD, P., ANDERSSON, S. & HANSEN, T.F. (2012) A phylogenetic comparative method for studying multivariate adaptation. *Journal of Theoretical Biology* **314**, 204–215.

BASTIANELLI, G., WINTLE, B.A., MARTIN, E.H., SEOANE, J. & LAIOLO, P. (2017) Species partitioning in a temperate mountain chain: Segregation by habitat vs. interspecific competition. *Ecology and evolution* **7**, 2685–2696. Ecol Evol.

BAUDACH, A. & VILCINSKAS, A. (2021) The European Map Butterfly Araschnia levana as a Model to Study the Molecular Basis and Evolutionary Ecology of Seasonal Polyphenism. *Insects* **12**, 325. Multidisciplinary Digital Publishing Institute.

BAY, L.K., JONES, G.P. & MCCORMICK, M.I. (2001) Habitat selection and aggression as determinants of spatial segregation among damselfish on a coral reef. *Coral Reefs* **20**, 289–298.

BERGSTROM, B.J. (1992) Parapatry and Encounter Competition between Chipmunk (Tamias) Species and the Hypothesized Role of Parasitism. *American Midland Naturalist* **128**, 168.

BEYER, R.M., KRAPP, M. & MANICA, A. (2020) High-resolution terrestrial climate, bioclimate and vegetation for the last 120,000 years. *Scientific Data* **7**, 236. Nature Publishing Group.

BIZWELL, E.A. & MATTINGLY, H.T. (2010) Aggressive interactions of the endangered Nashville Crayfish, Orconectes shoupi. *Southeastern Naturalist* **9**, 359–372.

BLOIS, J.L., ZARNETSKE, P.L., FITZPATRICK, M.C. & FINNEGAN, S. (2013) Climate change and the past, present, and future of biotic interactions. In *Science* pp. 499–504.

BLONDER, B., WEY, T.W., DORNHAUS, A., JAMES, R. & SIH, A. (2012) Temporal dynamics and network analysis. *Methods in Ecology and Evolution* **3**, 958–972. Wiley Online Library.

BOLGER, D.T. & CASE, T.J. (1992) Intra- and interspecific interference behaviour among sexual and asexual geckos. *Animal Behaviour* **44**, 21–30.

BOUCKAERT, R., VAUGHAN, T.G., BARIDO-SOTTANI, J., DUCHÊNE, S., FOURMENT, M., GAVRYUSHKINA, A., HELED, J., JONES, G., KÜHNERT, D., MAIO, N.D., MATSCHINER, M., MENDES, F.K., MÜLLER, N.F., OGILVIE, H.A., PLESSIS, L. DU, ET AL. (2019) BEAST 2.5: An advanced software platform for Bayesian evolutionary analysis. *PLOS Computational Biology* **15**, e1006650. Public Library of Science.

BOURNEZ, L., CANGI, N., LANCELOT, R., PLEYDELL, D.R.J., STACHURSKI, F., BOUYER, J., MARTINEZ, D., LEFRANÇOIS, T., NEVES, L. & PRADEL, J. (2015) Parapatric distribution and sexual competition between two tick species, Amblyomma variegatum and A. hebraeum (Acari, Ixodidae), in Mozambique. *Parasites and Vectors* **8**, 1–14. BioMed Central Ltd.

BOYCE, A.J. & MARTIN, T.E. (2019) Interspecific aggression among parapatric and sympatric songbirds on a tropical elevational gradient. *Behavioral Ecology* **30**, 541–547. Oxford Academic.

BRADSKI, G. (2000) The OpenCV Library. *Dr. Dobb's Journal of Software Tools*.

BRAKEFIELD, P.M., GATES, J., KEYS, D., KESBEKE, F., WIJNGAARDEN, P.J., MONTELRO, A., FRENCH, V. & CARROLL, S.B. (1996) Development, plasticity and evolution of butterfly eyespot patterns. *Nature* **384**, 236–242. Nature Publishing Group.

BRAKEFIELD, P.M. & LARSEN, T.B. (1984) The evolutionary significance of wet and dry season forms in some tropical butterflies. *Biological Journal of the Linnean Society* **22**, 1–12.

BRONSON, C.L., GRUBB, T.C., SATTLER, G.D. & BRAUN, M.J. (2003) Mate preference: a possible causal mechanism for a moving hybrid zone. *Animal Behaviour* **65**, 489–500.

BROWN, W.L. & WILSON, E.O. (1956) Character displacement. *Systematic Zoology* **5**, 49–64.

BRYANT, D., BOUCKAERT, R., FELSENSTEIN, J., ROSENBERG, N.A. & ROYCHOUDHURY, A. (2012) Inferring species trees directly from biallelic genetic markers: bypassing gene trees in a full coalescent analysis. *Molecular Biology and Evolution* **29**, 1917–1932.

BUBB, D.H., O'MALLEY, O.J., GOODERHAM, A.C. & LUCAS, M.C. (2009) Relative impacts of native and non-native crayfish on shelter use by an indigenous benthic fish. *Aquatic Conservation: Marine and Freshwater Ecosystems* **19**, 448–455. John Wiley & Sons, Ltd.

BUGGS, R. (2007) Empirical study of hybrid zone movement. *Heredity* **99**, 301–312. Nature Publishing Group.

BULL, C.M. & BURZACOTT, D. (1994) Reproductive interactions between two Australian reptile tick species. *Experimental and Applied Acarology* **18**, 555–565.

BURDFIELD-STEEL, E.R. & SHUKER, D.M. (2011) Reproductive interference. *Current Biology* **21**, R450–R451.

BURNER, R.C., BOYCE, A.J., BERNASCONI, D., STYRING, A.R., SHAKYA, S.B., BOER, C., RAHMAN, M.A., MARTIN, T.E. & SHELDON, F.H. (2020) Biotic interactions help explain variation in elevational range limits of birds among Bornean mountains. *Journal of Biogeography* **47**, 760–771. John Wiley & Sons, Ltd.

BURROWS, M.T., HAWKINS, S.J., MOORE, J.J., ADAMS, L., SUGDEN, H., FIRTH, L. & MIESZKOWSKA, N. (2020) Global-scale species distributions predict temperature-related changes in species composition of rocky shore communities in Britain. *Global Change Biology* **26**, 2093–2105. Blackwell Publishing Ltd.

BURROWS, M.T., SCHOEMAN, D.S., RICHARDSON, A.J., MOLINOS, J.G., HOFFMANN, A., BUCKLEY, L.B., MOORE, P.J., BROWN, C.J., BRUNO, J.F., DUARTE, C.M., HALPERN, B.S., HOEGH-GULDBERG, O., KAPPEL, C.V., KIESSLING, W., O'CONNOR, M.I., ET AL. (2014) Geographical limits to species-range shifts are suggested by climate velocity. *Nature* **507**, 492–495. Nature Publishing Group.

BUTLER, M.J. & STEIN, R.A. (1985) An analysis of the mechanisms governing species replacements in crayfish. *Oecologia* **66**, 168–177.

BUZATTO, B.A., CLARK, H.L. & TOMKINS, J.L. (2018) Morph-specific artificial selection reveals a constraint on the evolution of polyphenisms. *Proceedings of the Royal Society B: Biological Sciences* **285**, 20180335. Royal Society.

CAMACHO, C., COULOURIS, G., AVAGYAN, V., MA, N., PAPADOPOULOS, J. & BEALER, K. (2009) BLAST+: architecture and applications. *BMC Bioinformatics* **10**, 1–9.

CANTAREL, B.L., KORF, I., ROBB, S.M.C., PARRA, G., ROSS, E., MOORE, B., HOLT, C., ALVARADO, A.S. & YANDELL, M. (2008) MAKER: An easy-to-use annotation pipeline designed for emerging model organism genomes. *Genome Research* **18**, 188–196.

CASASA, S., BIDDLE, J.F., KOUTSOVOULOS, G.D. & RAGSDALE, E.J. (2021) Polyphenism of a Novel Trait Integrated Rapidly Evolving Genes into Ancestrally Plastic Networks. *Molecular Biology and Evolution* **38**, 331–343.

CASE, T.J., BOLGER, D.T. & PETREN, K. (1994) Invasions and Competitive Displacement among House Geckos in the Tropical Pacific. *Ecology* **75**, 464–477. Ecological Society of America.

CASE, T.J. & GILPIN, M.E. (1974) Interference competition and niche theory. *Proceedings of the National Academy of Sciences of the United States of America* **71**, 3073–3077. National Acad Sciences.

CATCHEN, J., HOHENLOHE, P.A., BASSHAM, S., AMORES, A. & CRESKO, W.A. (2013) Stacks: an analysis tool set for population genomics. *Molecular ecology* **22**, 3124–3140. Mol Ecol.

CHALLIS, R., RICHARDS, E., RAJAN, J., COCHRANE, G. & BLAXTER, M. (2020) BlobToolKit – Interactive Quality Assessment of Genome Assemblies. *G3 Genes|Genomes|Genetics* **10**, 1361–1374.

CHAPPELL, M.A. (1978) Behavioral Factors in the Altitudinal Zonation of Chipmunks (Eutamias). *Ecology* **59**, 565–579. Ecological Society of America.

CHENG, H., CONCEPCION, G.T., FENG, X., ZHANG, H. & LI, H. (2021) Haplotype-resolved de novo assembly using phased assembly graphs with hifiasm. *Nature Methods* **18**, 170–175.

CHENG, H., JARVIS, E.D., FEDRIGO, O., KOEPFLI, K.-P., URBAN, L. & GEMMELL, N.J. (2022) Haplotype-resolved assembly of diploid genomes without parental data. *Nature Biotechnology* **40**, 1332–1335.

CHIFMAN, J. & KUBATKO, L. (2014) Quartet Inference from SNP Data Under the Coalescent Model. *Bioinformatics* **30**, 3317–3324.

CHRISTE, P., KELLER, L. & ROULIN, A. (2006) The predation cost of being a male: implications for sex-specific rates of ageing. *Oikos* **114**, 381–384.

CHU, J. (2018) Jupiter Plot: A Circos-based tool to visualize genome assembly consistency. Zenodo. https://zenodo.org/records/1241235.

CISTERNE, A., SCHWARZKOPF, L. & PIKE, D.A. (2019) Australian house geckos are more aggressive than a globally successful invasive Asian house gecko. *Behavioral Ecology* **30**, 107–113. Oxford Academic.

CLAVEL, J., ESCARGUEL, G. & MERCERON, G. (2015) mvMORPH: An R package for fitting multivariate evolutionary models to morphometric data. *Methods in Ecology and Evolution* **6**, 1311–1319.

CORBET, P.S. (1999) *Dragonflies: Behavior and ecology of Odonata*. In *Dragonflies: Behavior and Ecology of Odonata* p. Cornell Univ. Press, Ithaca, N.Y.

CÓRDOBA-AGUILAR, A. (1994) Adult Survival and Movement in Males of the Damselfly Hetaerina cruentata (Odonata: Calopterygidae). *The Florida Entomologist* **77**, 256–264. Florida Entomological Society.

CORDOBA-AGUILAR, A., BEATTY, C. & BRIED, J. (2022) *Dragonflies and Damselflies: Model Organisms for Ecological and Evolutionary Research*. Oxford University Press.

CÓRDOBA-AGUILAR, A., RAIHANI, G., SERRANO-MENESES, M.A. & CONTRERAS-GARDUÑO, J. (2009) The lek mating system of Hetaerina damselflies (Insecta: Calopterygidae. *Behaviour* **146**, 189–207.

COWEN, M.C., DRURY, J.P. & GRETHER, G.F. (2020) Multiple routes to interspecific territoriality in sister species of North American perching birds. *Evolution* **74**, 2134–2148.

CROWDER, D.W., HOROWITZ, A.R., BRESLAUER, H., RIPPA, M., KONTSEDALOV, S., GHANIM, M. & CARRIÈRE, Y. (2011) Niche partitioning and stochastic processes shape community structure following whitefly invasions. *Basic and Applied Ecology* **12**, 685–694. Elsevier.

CROWLEY, L., PRICE, B., ALLAN, E. & EAGLES, M. (2023) The genome sequence of the Common Darter, Sympetrum striolatum (Charpentier, 1840) [version 1; peer review: awaiting peer review]. *Wellcome Open Research* **8**.

CULUMBER, Z.W., ANAYA-ROJAS, J.M., BOOKER, W.W., HOOKS, A.P., LANGE, E.C., PLUER, B., RAMÍREZ-BULLÓN, N. & TRAVIS, J. (2019) Widespread Biases in Ecological and Evolutionary Studies. *BioScience* **69**, 631–640.

CZEKANSKI-MOIR, J.E. & RUNDELL, R.J. (2019) The Ecology of Nonecological Speciation and Nonadaptive Radiations. *Trends in Ecology & Evolution* **34**, 400–415. Elsevier.

DaCosta, J.M. & Sorenson, M.D. (2014) Amplification Biases and Consistent Recovery of Loci in a Double-Digest RAD-seq Protocol. *PLOS ONE* **9**, e106713. Public Library of Science.

Dalton, A.S., Dulfer, H.E., Margold, M., Heyman, J., Clague, J.J., Froese, D.G., Gauthier, M.S., Hughes, A.L.C., Jennings, C.E., Norris, S.L. & Stoker, B.J. (2023) Deglaciation of the north American ice sheet complex in calendar years based on a comprehensive database of chronological data: NADI-1. *Quaternary Science Reviews* **321**, 108345.

Dame, E.A. & Petren, K. (2006) Behavioural mechanisms of invasion and displacement in Pacific island geckos (Hemidactylus). *Animal Behaviour* **71**, 1165–1173.

Danecek, P., Bonfield, J.K., Liddle, J., Marshall, J., Ohan, V., Pollard, M.O., Whitwham, A., Keane, T., McCarthy, S.A., Davies, R.M. & Li, H. (2021) Twelve years of SAMtools and BCFtools. *GigaScience* **10**, giab008.

Decaestecker, E., Gaba, S., Raeymaekers, J.A.M., Stoks, R., Van Kerckhoven, L., Ebert, D. & De Meester, L. (2007) Host–parasite 'Red Queen' dynamics archived in pond sediment. *Nature* **450**, 870–873. Nature Publishing Group.

DeRaad, D.A., McCormack, J.E., Chen, N., Peterson, A.T. & Moyle, R.G. (2022) Combining Species Delimitation, Species Trees, and Tests for Gene Flow Clarifies Complex Speciation in Scrub-Jays. *Systematic Biology* **71**, 1453–1470.

Devitt, T.J., Wright, A.M., Cannatella, D.C. & Hillis, D.M. (2019) Species delimitation in endangered groundwater salamanders: implications for aquifer management and biodiversity conservation. *Proceedings of the National Academy of Sciences of the United States of America* **116**, 2624–2633.

Dion-Côté, A.-M. & Barbash, D.A. (2017) Beyond speciation genes: an overview of genome stability in evolution and speciation. *Current Opinion in Genetics & Development* **47**, 17–23.

Donath, A., Jühling, F., Al-Arab, M., Bernhart, S.H., Reinhardt, F., Stadler, P.F., Middendorf, M. & Bernt, M. (2019) Improved annotation of protein-coding genes boundaries in metazoan mitochondrial genomes. *Nucleic Acids Research* **47**, 10543–10552.

Dorková, M., Krištín, A., Jarčuška, B. & Kaňuch, P. (2020) The mosaic distribution pattern of two sister bush-cricket species and the possible role of reproductive interference. *Ecology and Evolution* **10**, 2570–2578. John Wiley & Sons, Ltd.

Drury, J.P., Anderson, C.N., Castillo, M.B.C., Fisher, J., McEachin, S. & Grether, G.F. (2019a) A general explanation for the persistence of reproductive interference. *American Naturalist* **194**, 268–275.

Drury, J.P., Anderson, C.N. & Grether, G.F. (2015a) Seasonal polyphenism in wing coloration affects species recognition in rubyspot damselflies (Hetaerina spp.). *Journal of Evolutionary Biology* **28**, 1439–1452.

DRURY, J.P., BARNES, M., FINNERAN, A.E., HARRIS, M. & GRETHER, G.F. (2019b) Continent-scale phenotype mapping using citizen scientists' photographs. *Ecography* **42**, 1436–1445.

DRURY, J.P., COWEN, M. & GRETHER, G.F. (2020) Competition and hybridization drive interspecific territoriality in birds. *Proceedings of the National Academy of Sciences*.

DRURY, J.P. & GRETHER, G.F. (2014) Interspecific aggression, not interspecific mating, drives character displacement in the wing coloration of male rubyspot damselflies (Hetaerina). *Proceedings of the Royal Society B: Biological Sciences* **281**.

DRURY, J.P., OKAMOTO, K.W., ANDERSON, C.N. & GRETHER, G.F. (2015b) Reproductive interference explains persistence of aggression between species. *Proceedings of the Royal Society B: Biological Sciences* **282**.

DUCKWORTH, R.A. (2013) Human-induced changes in the dynamics of species coexistence: An example with two sister species. *Avian Urban Ecology*. Oxford University Press.

DUCKWORTH, R.A. & BADYAEV, A.V. (2007) Coupling of dispersal and aggression facilitates the rapid range expansion of a passerine bird. *Proceedings of the National Academy of Sciences of the United States of America* **104**, 15017–15022. National Academy of Sciences.

DUCKWORTH, R.A., BELLONI, V. & ANDERSON, S.R. (2015) Cycles of species replacement emerge from locally induced maternal effects on offspring behavior in a passerine bird. *Science* **347**, 875–877. American Association for the Advancement of Science.

EARLY, R. & KEITH, S.A. (2019) Geographically variable biotic interactions and implications for species ranges. *Global Ecology and Biogeography* **28**, 42–53. Blackwell Publishing Ltd.

EARLY, R. & SAX, D.F. (2014) Climatic niche shifts between species' native and naturalized ranges raise concern for ecological forecasts during invasions and climate change. *Global Ecology and Biogeography* **23**, 1356–1365.

EDELMAN, N.B. & MALLET, J. (2021) Prevalence and Adaptive Impact of Introgression. *Annual Review of Genetics* **55**, 265–283. Annual Reviews.

ELITH, J. & LEATHWICK, J.R. (2009) Species Distribution Models: Ecological Explanation and Prediction Across Space and Time. *Annual Review of Ecology, Evolution, and Systematics* **40**, 677–697. Annual Reviews.

ELLEGREN, H. (2014) Genome sequencing and population genomics in non-model organisms. *Trends in Ecology & Evolution* **29**, 51–63. Elsevier.

ELO, M., KAJANUS, M.H., TOLVANEN, J., DEVICTOR, V., FORSMAN, J.T., LEHIKOINEN, A., MÖNKKÖNEN, M., THORSON, J.T., VOLLSTÄDT, M.G.R. & KIVELÄ, S.M. (2023) Do large-scale associations in birds imply biotic interactions or environmental filtering? *Journal of Biogeography* **50**, 169–182.

EME, D., ZAGMAJSTER, M., DELIĆ, T., FIŠER, C., FLOT, J.-F., KONECNY-DUPRÉ, L., PÁLSSON, S., STOCH, F., ZAKŠEK, V., DOUADY, C.J. & MALARD, F. (2018) Do cryptic species matter in macroecology? Sequencing European groundwater crustaceans yields smaller ranges but does not challenge biodiversity determinants. *Ecography* **41**, 424–436.

ENBODY, E.D., SENDELL-PRICE, A.T., SPREHN, C.G., RUBIN, C.-J., VISSCHER, P.M., GRANT, B.R., GRANT, P.R. & ANDERSSON, L. (2023) Community-wide genome sequencing reveals 30 years of Darwin's finch evolution. *Science* **381**, eadf6218. American Association for the Advancement of Science.

ENGLER, J.O., RÖDDER, D., ELLE, O., HOCHKIRCH, A. & SECONDI, J. (2013) Species distribution models contribute to determine the effect of climate and interspecific interactions in moving hybrid zones. *Journal of Evolutionary Biology* **26**, 2487–2496.

ERLINGE, S. & SANDELL, M. (1988) Coexistence of Stoat, Mustela Erminea, and Weasel, M. Nivalis: Social Dominance, Scent Communication, and Reciprocal Distribution. *Oikos* **53**, 242–246. [Nordic Society Oikos, Wiley].

ESCAMILLA MOLGORA, J.M., SEDDA, L., DIGGLE, P. & ATKINSON, P.M. (2022) A joint distribution framework to improve presence-only species distribution models by exploiting opportunistic surveys. *Journal of Biogeography* **49**, 1176–1192.

EURICH, J.G., MCCORMICK, M.I. & JONES, G.P. (2018) Direct and indirect effects of interspecific competition in a highly partitioned guild of reef fishes. *Ecosphere* **9**, e02389. John Wiley & Sons, Ltd.

EXCOFFIER, L., DUPANLOUP, I., HUERTA-SÁNCHEZ, E., SOUSA, V.C. & FOLL, M. (2013) Robust demographic inference from genomic and SNP data. *PLoS Genetics* **9**, pgen.1003905.

EXCOFFIER, L., MARCHI, N., MARQUES, D.A., MATTHEY-DORET, R., GOUY, A. & SOUSA, V.C. (2021) Fastsimcoal2: Demographic inference under complex evolutionary scenarios. *Bioinformatics* **37**, 4882–4885. Oxford University Press.

FERNANDES, A.F.A., DÓREA, J.R.R. & ROSA, G.J. DE M. (2020) Image Analysis and Computer Vision Applications in Animal Sciences: An Overview. *Frontiers in Veterinary Science* **7**.

FERRETTI, F. & MORI, E. (2020) Displacement interference between wild ungulate species: does it occur? *Ethology Ecology & Evolution* **32**, 2–15. Taylor & Francis.

FIŠER, C., ROBINSON, C.T. & MALARD, F. (2018) Cryptic species as a window into the paradigm shift of the species concept. *Molecular Ecology* **27**, 613–635.

FITZPATRICK, B.M. (2012) Estimating ancestry and heterozygosity of hybrids using molecular markers. *BMC Evolutionary Biology* **12**, 131.

FORDHAM, D.A., JACKSON, S.T., BROWN, S.C., HUNTLEY, B., BROOK, B.W., DAHL-JENSEN, D., GILBERT, M.T.P., OTTO-BLIESNER, B.L., SVENSSON, A., THEODORIDIS, S., WILMSHURST, J.M., BUETTEL, J.C., CANTERI, E., MCDOWELL,

M., ORLANDO, L., ET AL. (2020) Using paleo-archives to safeguard biodiversity under climate change. *Science* **369**, eabc5654. American Association for the Advancement of Science.

FRANCHINI, P., MONNÉ PARERA, D., KAUTT, A.F. & MEYER, A. (2017) quaddRAD: a new high-multiplexing and PCR duplicate removal ddRAD protocol produces novel evolutionary insights in a nonradiating cichlid lineage. *Molecular Ecology* **26**, 2783–2795.

FREEMAN, B.G. (2020) Lower elevation animal species do not tend to be better competitors than their higher elevation relatives. *Global ecology and biogeography* **29**, 171–181. Wiley Online Library.

FREEMAN, B.G., CLASS FREEMAN, A.M. & HOCHACHKA, W.M. (2016) Asymmetric interspecific aggression in New Guinean songbirds that replace one another along an elevational gradient. *Ibis* **158**, 726–737. Blackwell Publishing Ltd.

FREEMAN, B.G. & MONTGOMERY, G. (2015) Interspecific aggression by the Swainson's Thrush (Catharus ustulatus) may limit the distribution of the threatened Bicknell's Thrush (Catharus bicknelli) in the Adirondack Mountains. *Condor* **118**, 169–178. University of California Press.

FREEMAN, B.G., SCHOLER, M.N., RUIZ-GUTIERREZ, V. & FITZPATRICK, J.W. (2018) Climate change causes upslope shifts and mountaintop extirpations in a tropical bird community. *Proceedings of the National Academy of Sciences of the United States of America* **115**, 11982–11987. National Academy of Sciences.

FRESHWATER, C., GHALAMBOR, C.K. & MARTIN, P.R. (2014) Repeated patterns of trait divergence between closely related dominant and subordinate bird species. *Ecology* **95**, 2334–2345.

FRICHOT, E. & FRANÇOIS, O. (2015) LEA: An R package for landscape and ecological association studies. *Methods in Ecology and Evolution* **6**, 925–929. John Wiley & Sons, Ltd.

FRICHOT, E., MATHIEU, F., TROUILLON, T., BOUCHARD, G. & FRANÇOIS, O. (2014) Fast and efficient estimation of individual ancestry coefficients. *Genetics* **196**, 973–983. Genetics.

FU, K., PENG, J., HE, Q. & ZHANG, H. (2021) Single image 3D object reconstruction based on deep learning: A review. *Multimedia Tools and Applications* **80**, 463–498.

GALLESI, M.M., MOBILI, S., CIGOGNINI, R., HARDERSEN, S. & SACCHI, R. (2016) Season matters: differential variation of wing shape between sexes of Calopteryx splendens (Odonata: Calopterygidae). *Zoomorphology* **135**, 313–322.

GARCÍA, Y., CALLAWAY, R.M., DIACONU, A. & MONTESINOS, D. (2013) Invasive and Non-Invasive Congeners Show Similar Trait Shifts between Their Same Native and Non-Native Ranges. *PLOS ONE* **8**, e82281. Public Library of Science.

GARRISON, R.W. (1990) A synopsis of the genus Hetaerina with descriptions of four new species. *Transactions of the American Entomological Society* **116**, 175–259.

GIFFORD, M.E. & KOZAK, K.H. (2012) Islands in the sky or squeezed at the top? Ecological causes of elevational range limits in montane salamanders. *Ecography* **35**, 193–203.

GITTENBERGER, E. (1991) What about non-adaptive radiation? *Biological Journal of the Linnean Society* **43**, 263–272.

GÓMEZ-LLANO, M., BOYS, W.A., PING, T., TYE, S.P. & SIEPIELSKI, A.M. (2023) Interactions between fitness components across the life cycle constrain competitor coexistence. *Journal of Animal Ecology* **00**, 1–12. Wiley Online Library.

GOMEZ-MESTRE, I. & BUCHHOLZ, D.R. (2006) Developmental plasticity mirrors differences among taxa in spadefoot toads linking plasticity and diversity. *Proceedings of the National Academy of Sciences of the United States of America* **103**, 19021–19026.

GOMPERT, Z. & BUERKLE, A.C. (2010) introgress: a software package for mapping components of isolation in hybrids. *Molecular Ecology Resources* **10**, 378–384.

GONZÁLEZ-TOKMAN, D.M., GONZÁLEZ-SANTOYO, I. & CÓRDOBA-AGUILAR, A. (2013) Mating success and energetic condition effects driven by terminal investment in territorial males of a short-lived invertebrate. *Functional Ecology* **27**, 739–747.

GOOLSBY, E.W. (2015) Phylogenetic Comparative Methods for Evaluating the Evolutionary History of Function-Valued Traits. *Systematic Biology* **64**, 568–578.

GOUDET, J. (2005) hierfstat, a package for r to compute and test hierarchical F-statistics. *Molecular Ecology Notes* **5**, 184–186.

GRETHER, G.F. (1996) Intrasexual competition alone favors a sexually dimorphic ornament in the rubyspot damselfly *Hetaerina americana*. *Evolution* **50**, 1949–1957.

GRETHER, G.F., BENINDE, J., BERAUT, E., CHUMCHIM, N., ESCALONA, M., MACDONALD, Z.G., MILLER, C., SAHASRABUDHE, R., SHEDLOCK, A.M., TOFFELMIER, E. & SHAFFER, H.B. (2023) Reference genome for the American rubyspot damselfly, Hetaerina americana. *Journal of Heredity* **114**, 385–394.

GRETHER, G.F., DRURY, J.P., OKAMOTO, K.W., MCEACHIN, S. & ANDERSON, C.N. (2020) Predicting evolutionary responses to interspecific interference in the wild. *Ecology Letters* **23**, 221–230.

GRETHER, G.F., FINNERAN, A.E. & DRURY, J.P. (2024) Niche differentiation, reproductive interference, and range expansion. *Ecology Letters* **00**.

GRETHER, G.F. & GREY, R.M. (1996) Novel cost of a sexually selected trait in the rubyspot damselfly Hetaerina americana: conspicuousness to prey. *Behavioral Ecology* **7**, 465–473.

GRETHER, G.F., LOSIN, N., ANDERSON, C.N. & OKAMOTO, K. (2009) The role of interspecific interference competition in character displacement and the evolution of competitor recognition. *Biological Reviews* **84**, 617–635.

GRETHER, G.F. & OKAMOTO, K.W. (2022) Eco-evolutionary dynamics of interference competition. *Ecology Letters* **25**, 2167–2176.

GRETHER, G.F., PEIMAN, K.S., TOBIAS, J.A. & ROBINSON, B.W. (2017) Causes and Consequences of Behavioral Interference between Species. *Trends in Ecology & Evolution* **32**, 760–772.

GRONAU, I., HUBISZ, M.J., GULKO, B., DANKO, C.G. & SIEPEL, A. (2011) Bayesian inference of ancient human demography from individual genome sequences. *Nature Genetics* **43**, 1031–1035.

GRÖNING, J. & HOCHKIRCH, A. (2008) Reproductive interference between animal species. *The Quarterly Review of Biology* **83**, 257–282.

GRÖNING, J., LÜCKE, N., FINGER, A. & HOCHKIRCH, A. (2007) Reproductive interference in two ground-hopper species: Testing hypotheses of coexistence in the field. *Oikos* **116**, 1449–1460.

GU, Z., GU, L., EILS, R., SCHLESNER, M. & BRORS, B. (2014) circlize implements and enhances circular visualization in R. *Bioinformatics* **30**, 2811–2812.

GUAN, D., MCCARTHY, S.A., WOOD, J., HOWE, K., WANG, Y. & DURBIN, R. (2020) Identifying and removing haplotypic duplication in primary genome assemblies. *Bioinformatics* **36**, 2896–2898.

GUTENKUNST, R.N., HERNANDEZ, R.D., WILLIAMSON, S.H. & BUSTAMANTE, C.D. (2009) Inferring the joint demographic history of multiple populations from multidimensional SNP frequency data. *PLoS Genetics* **5**, e1000695. Public Library of Science San Francisco, USA.

GUTIÉRREZ, R.J., CODY, M., COURTNEY, S. & FRANKLIN, A.B. (2007) The Invasion of Barred Owls and its Potential Effect on the Spotted Owl: a Conservation Conundrum. *Biological Invasions* **9**, 181–196.

HAERING, R. & FOX, B.J. (1987) Short-Term Coexistence and Long-Term Competitive Displacement of Two Dominant Species of Iridomyrmex: The Successional Response of Ants to Regenerating Habitats. *Journal of Animal Ecology* **56**, 495–507. [Wiley, British Ecological Society].

HAIRSTON, N.G., NISHIKAWA, K.C. & STENHOUSE, S.L. (1987) The evolution of competing species of terrestrial salamanders: niche partitioning or interference? *Evolutionary Ecology* **1**, 247–262.

HALALI, S., HALALI, D., BARLOW, H.S., MOLLEMAN, F., KODANDARAMAIAH, U., BRAKEFIELD, P.M. & BRATTSTRÖM, O. (2021) Predictability of temporal variation in climate and the evolution of seasonal polyphenism in tropical butterfly communities. *Journal of Evolutionary Biology* **34**, 1362–1375.

HANLEY, J.A. & MCNEIL, B.J. (1983) A method of comparing the areas under receiver operating characteristic curves derived from the same cases. *Radiology* **148**, 839–843.

HARRIS, R.S. (2007) Improved pairwise alignment of genomic DNA. The Pennsylvania State University.

HASEGAWA, K. & MAEKAWA, K. (2009) Role of visual barriers on mitigation of interspecific interference competition between native and non-native salmonid species. *Canadian Journal of Zoology* **87**, 781–786. NRC Research Press.

HASEGAWA, K., YAMAMOTO, T., MURAKAMI, M. & MAEKAWA, K. (2004) Comparison of competitive ability between native and introduced salmonids: evidence from pairwise contests. *Ichthyological Research* **51**, 191–194.

HAWKINS, S.J., MOORE, P.J.P., BURROWS, M.T., POLOCZANSKA, E., MIESZKOWSKA, N., HERBERT, R.J.H., JENKINS, S.R.S., THOMPSON, R.C.R., GENNER, M.J. & SOUTHWARD, A.J. (2008) Complex interactions in a rapidly changing world: Responses of rocky shore communities to recent climate change. *Climate Research* **37**, 123–133.

HE, Q., PRADO, J.R. & KNOWLES, L.L. (2017) Inferring the geographic origin of a range expansion: Latitudinal and longitudinal coordinates inferred from genomic data in an ABC framework with the program x-origin. *Molecular Ecology* **26**, 6908–6920.

HELLER, H.C. (1971) Altitudinal Zonation of Chipmunks (eutamias): Interspecific Aggression, Water Balance, and Energy Budgets. Ph.D., Yale University, United States -- Connecticut.

HERNÁNDEZ-BRITO, D., CARRETE, M., POPA-LISSEANU, A.G., IBÁÑEZ, C. & TELLA, J.L. (2014) Crowding in the City: Losing and Winning Competitors of an Invasive Bird. *PLOS ONE* **9**, e100593. Public Library of Science.

HIBBINS, M.S. & HAHN, M.W. (2021) The effects of introgression across thousands of quantitative traits revealed by gene expression in wild tomatoes. *PLOS Genetics* **17**, e1009892. Public Library of Science.

HOBBS, W.H. (1950) The Pleistocene History of the Mississippi River. *Science* **111**, 260–262. American Association for the Advancement of Science.

HOCHKIRCH, A. & GRÖNING, J. (2012) Niche overlap in allotopic and syntopic populations of sexually interacting ground-hopper species. *Insect Science* **19**, 391–402.

HOCHKIRCH, A., GRÖNING, J. & BÜCKER, A. (2007) Sympatry with the devil: reproductive interference could hamper species coexistence. *Journal of Animal Ecology* **76**, 633–642. John Wiley & Sons, Ltd.

HOLLISTER, J., SHAH, T., NOWOSAD, J., ROBITAILLE, A.L., BECK, M.W. & JOHNSON, M. (2023) *elevatr: Access Elevation Data from Various APIs*.

HOOD, G.R., POWELL, T.H.Q., DOELLMAN, M.M., SIM, S.B., GLOVER, M., YEE, W.L., GOUGHNOUR, R.B., MATTSSON, M., SCHWARZ, D. & FEDER, J.L. (2020) Rapid and repeatable host plant shifts drive reproductive isolation following a recent

human-mediated introduction of the apple maggot fly, Rhagoletis pomonella. *Evolution* **74**, 156–168.

HOTALING, S., KELLEY, J.L. & FRANDSEN, P.B. (2020) Aquatic insects are dramatically underrepresented in genomic research. *Insects* **11**, 601.

HOUSER, J.D., GINSBERG, H. & JAKOB, E.M. (2014) Competition between introduced and native spiders (Araneae: Linyphiidae). *Biological Invasions* **16**, 2479–2488. Kluwer Academic Publishers.

HUBISZ, M.J., FALUSH, D., STEPHENS, M. & PRITCHARD, J.K. (2009) Inferring weak population structure with the assistance of sample group information. *Molecular Ecology Resources* **9**, 1322–1332.

IOANNIDIS, P., SIMAO, F.A., WATERHOUSE, R.M., MANNI, M., SEPPEY, M., ROBERTSON, H.M., MISOF, B., NIEHUIS, O. & ZDOBNOV, E.M. (2017) Genomic Features of the Damselfly Calopteryx splendens Representing a Sister Clade to Most Insect Orders. *Genome Biology and Evolution* **9**, 415–430. Oxford Academic.

IRITANI, R. & NORIYUKI, S. (2021) Reproductive interference hampers species coexistence despite conspecific sperm precedence. *Ecology and Evolution* **11**, 1957–1969. Wiley Online Library.

IRWIN, D. & SCHLUTER, D. (2022) Hybridization and the Coexistence of Species. *The American Naturalist*. Cold Spring Harbor Laboratory.

JACKSON, S.T. & BLOIS, J.L. (2015) Community ecology in a changing environment: Perspectives from the Quaternary. *Proceedings of the National Academy of Sciences* **112**, 4915–4921. Proceedings of the National Academy of Sciences.

JANKOWSKI, J.E., ROBINSON, S.K. & LEVEY, D.J. (2010) Squeezed at the top: Interspecific aggression may constrain elevational ranges in tropical birds. *Ecology* **91**, 1877–1884. John Wiley & Sons, Ltd.

JIEYU (2023) An Automated Approach to Wing Spot Identification and Analysis in Smoky Rubyspot Damselflies. Master of Data Science, Durham University.

JOHNSON, C. (1963) Interspecific territoriality in Hetaerina americana (Fabricius) and H. titia (Drury)(Odonata: Calopterygidae) with a preliminary analysis of the wing color pattern variation. *The Canadian Entomologist* **95**, 575–582.

JOMBART, T. (2008) adegenet: a R package for the multivariate analysis of genetic markers. *Bioinformatics* **24**, 1403–1405.

JONES, S.E.I., TOBIAS, J.A., FREEMAN, R. & PORTUGAL, S.J. (2020) Weak asymmetric interspecific aggression and divergent habitat preferences at an elevational contact zone between tropical songbirds. *Ibis* **162**, 814–826. John Wiley & Sons, Ltd.

DE JONG, M.J., DE JONG, J.F., HOELZEL, A.R. & JANKE, A. (2021) SambaR: An R package for fast, easy and reproducible population-genetic analyses of biallelic SNP data sets. *Molecular Ecology Resources* **21**, 1369–1379.

KAMVAR, Z.N., TABIMA, J.F. & GRÜNWALD, N.J. (2014) Poppr: an R package for genetic analysis of populations with clonal, partially clonal, and/or sexual reproduction. *PeerJ* **2**, e281. PeerJ Inc.

KEIGHTLEY, P.D., NESS, R.W., HALLIGAN, D.L. & HADDRILL, P.R. (2014) Estimation of the Spontaneous Mutation Rate per Nucleotide Site in a Drosophila melanogaster Full-Sib Family. *Genetics* **196**, 313–320.

KEITH, S., HOBBS, J.A., BOSTRÖM-EINARSSON, L., HARTLEY, I. & SANDERS, N. (2023) Rapid resource depletion on coral reefs disrupts competitor recognition processes among butterflyfish species. *Proceedings of the Royal Society B* **290**, 20222158. The Royal Society.

KINGSOLVER, J.G. & WIERNASZ, D.C. (1991) Seasonal Polyphenism in Wing-Melanin Pattern and Thermoregulatory Adaptation in Pieris Butterflies. *The American Naturalist*. University of Chicago Press.

KIRITANI, K. (2011) Impacts of global warming on Nezara viridula and its native congeneric species. *Journal of Asia-Pacific Entomology* **14**, 221–226.

KISHI, S. & NAKAZAWA, T. (2013) Analysis of species coexistence co-mediated by resource competition and reproductive interference. *Population Ecology* **55**, 305–313.

KLAUS, K.V. & MATZKE, N.J. (2020) Statistical Comparison of Trait-Dependent Biogeographical Models Indicates That Podocarpaceae Dispersal Is Influenced by Both Seed Cone Traits and Geographical Distance. *Systematic Biology* **69**, 61–75.

KNAUS, B.J. & GRÜNWALD, N.J. (2017) vcfr: a package to manipulate and visualize variant call format data in R. *Molecular Ecology Resources* **17**, 44–53. John Wiley & Sons, Ltd.

KOCH, E.L., NEIBER, M.T., WALTHER, F. & HAUSDORF, B. (2020) Patterns and processes in a non-adaptive radiation: Alopia (Gastropoda, Clausiliidae) in the Bucegi Mountains. *Zoologica Scripta* **49**, 280–294.

KOHLI, M., LETSCH, H., GREVE, C., BÉTHOUX, O., DEREGNAUCOURT, I., LIU, S., ZHOU, X., DONATH, A., MAYER, C., PODSIADLOWSKI, L., GUNKEL, S., MACHIDA, R., NIEHUIS, O., RUST, J., WAPPLER, T., ET AL. (2021) Evolutionary history and divergence times of Odonata (dragonflies and damselflies) revealed through transcriptomics. *iScience* **24**, 103324.

DE KORT, S.R. & TEN CATE, C. (2001) Response to interspecific vocalizations is affected by degree of phylogenetic relatedness in *Streptopelia* doves. *Animal Behaviour* **61**, 239–247.

KOZAK, K.H., WEISROCK, D.W. & LARSON, A. (2005) Rapid lineage accumulation in a non-adaptive radiation: phylogenetic analysis of diversification rates in eastern North American woodland salamanders (Plethodontidae: Plethodon). *Proceedings of the Royal Society B: Biological Sciences* **273**, 539–546. Royal Society.

KUMAR, S., SULESKI, M., CRAIG, J.M., KASPROWICZ, A.E., SANDERFORD, M., LI, M., STECHER, G. & HEDGES, S.B. (2022) TimeTree 5: An Expanded Resource for Species Divergence Times. *Molecular Biology and Evolution* **39**, msac174.

KUNO, E. (1992) Competitive exclusion through reproductive interference. *Researches on Population Ecology* **34**, 275–284.

KUZNETSOVA, V. & GOLUB, N.V. (2020) A checklist of chromosome numbers and a review of karyotype variation in Odonata of the world. *Comparative Cytogenetics* **14**, 501–540.

KUZNETSOVA, V., MARYAŃSKA-NADACHOWSKA, A., ANOKHIN, B., SHAPOVAL, N. & SHAPOVAL, A. (2021) Chromosomal analysis of eight species of dragonflies (Anisoptera) and damselflies (Zygoptera) using conventional cytogenetics and fluorescence in situ hybridization: Insights into the karyotype evolution of the ancient insect order Odonata. *Journal of Zoological Systematics and Evolutionary Research* **59**, 387–399.

KYOGOKU, D. & NISHIDA, T. (2012) The presence of heterospecific males causes an Allee effect. *Population Ecology* **54**, 391–395. Springer.

KYOGOKU, D. & SOTA, T. (2017) A generalized population dynamics model for reproductive interference with absolute density dependence. *Scientific Reports* **7**, 1–8. Nature Publishing Group.

LAMBERT, J.W., REICHARD, M. & PINCHEIRA-DONOSO, D. (2019) Live fast, diversify non-adaptively: evolutionary diversification of exceptionally short-lived annual killifishes. *BMC Evolutionary Biology* **19**, 10.

LARSON, R.J. (1980) Competition, Habitat Selection, and the Bathymetric Segregation of Two Rockfish (Sebastes) Species. *Ecological Monographs* **50**, 221–239. Ecological Society of America.

LEGAULT, G., BITTERS, M.E., HASTINGS, A. & MELBOURNE, B.A. (2020) Interspecific competition slows range expansion and shapes range boundaries. *Proceedings of the National Academy of Sciences of the United States of America* **117**, 26854–26860.

LEHNER, B. & GRILL, G. (2013) Global river hydrography and network routing: baseline data and new approaches to study the world's large river systems. *Hydrological Processes* **27**, 2171–2186.

LEHNER, B., VERDIN, K. & JARVIS, A. (2008) New Global Hydrography Derived From Spaceborne Elevation Data. *Eos, Transactions American Geophysical Union* **89**, 93–94.

LEHTINEN, R.M., CARLSON, B.M., HAMM, A.R., RILEY, A.G., MULLIN, M.M. & GRAY, W.J. (2020) Dispatches from the neighborhood watch: Using citizen science and field survey data to document color morph frequency in space and time. *Ecology and Evolution* **10**, 1526–1538.

LEIGHTON, G.M., LAMOUR, D., MALCOLM, K. & MILLER, E.T. (2023) Both morphological and behavioral traits predict interspecific social dominance in birds. *Journal of Ornithology* **164**, 163–169.

LEPONCE, M., ROISIN, Y. & PASTEELS, J. (1997) Structure and Dynamics of the Arboreal Termite Community in New Guinean Coconut Plantations. *Tropical Biology* **29**, 193–203.

LEWIN, H.A., RICHARDS, S., LIEBERMAN AIDEN, E., ALLENDE, M.L., ARCHIBALD, J.M., BÁLINT, M., BARKER, K.B., BAUMGARTNER, B., BELOV, K., BERTORELLE, G., BLAXTER, M.L., CAI, J., CAPERELLO, N.D., CARLSON, K., CASTILLA-RUBIO, J.C., ET AL. (2022) The Earth BioGenome Project 2020: Starting the clock. *Proceedings of the National Academy of Sciences* **119**, e2115635118. Proceedings of the National Academy of Sciences.

LEWIN, H.A., ROBINSON, G.E., KRESS, W.J., BAKER, W.J., CODDINGTON, J., CRANDALL, K.A., DURBIN, R., EDWARDS, S.V., FOREST, F., GILBERT, M.T.P., GOLDSTEIN, M.M., GRIGORIEV, I.V., HACKETT, K.J., HAUSSLER, D., JARVIS, E.D., ET AL. (2018) Earth BioGenome Project: Sequencing life for the future of life. *Proceedings of the National Academy of Sciences* **115**, 4325–4333. Proceedings of the National Academy of Sciences.

LI, H. (2011) A statistical framework for SNP calling, mutation discovery, association mapping and population genetical parameter estimation from sequencing data. *Bioinformatics* **27**, 2987–2993.

LI, H. & DURBIN, R. (2009) Fast and accurate short read alignment with Burrows-Wheeler transform. *Bioinformatics* **25**, 1754–1760.

LI, Z., GUO, R., LI, M., CHEN, Y. & LI, G. (2020) A review of computer vision technologies for plant phenotyping. *Computers and Electronics in Agriculture* **176**, 105672.

LIAW, A. & WIENER, M. (2002) Classification and Regression by randomForest. *R News* **2**, 18–22.

LILL, A. & MUSCAT, I. (2015) Importance of Inherent Suitability, Behavioural Flexibility and Competitiveness in Occupancy of Urban Parks by an Endemic Honeyeater. *Avian Biology Research* **8**, 227–236. SAGE Publications Ltd.

LIOU, L.W. & PRICE, T.D. (1994) Speciation By Reinforcement of Premating Isolation. *Evolution* **48**, 1451–1459. Wiley Online Library.

LIU, H., JIANG, F., WANG, S., WANG, H., WANG, A., ZHAO, H., XU, D., YANG, B. & FAN, W. (2022) Chromosome-level genome of the globe skimmer dragonfly (Pantala flavescens). *GigaScience* **11**, giac009.

LIU, S.-S., DE BARRO, P.J., XU, J., LUAN, J.-B., ZANG, L.-S., RUAN, Y.-M. & WAN, F.-H. (2007) Asymmetric Mating Interactions Drive Widespread Invasion and Displacement in a Whitefly. *Science* **318**, 1769–1772. American Association for the Advancement of Science.

LOUNIBOS, L.P. & JULIANO, S.A. (2018) Where vectors collide: the importance of mechanisms shaping the realized niche for modeling ranges of invasive Aedes mosquitoes. *Biological Invasions* **20**, 1913–1929. NIH Public Access.

LOUTHAN, A.M., DOAK, D.F. & ANGERT, A.L. (2015) Where and When do Species Interactions Set Range Limits? *Trends in Ecology and Evolution* **30**, 780–792. Elsevier Ltd.

LOZIER, J.D., JACKSON, J.M., DILLON, M.E. & STRANGE, J.P. (2016) Population genomics of divergence among extreme and intermediate color forms in a polymorphic insect. *Ecology and Evolution* **6**, 1075–1091.

LYMAN, R.A. & EDWARDS, C.E. (2022) Revisiting the comparative phylogeography of unglaciated eastern North America: 15 years of patterns and progress. *Ecology and Evolution* **12**, e8827.

LYONS, M.P., SHEPARD, D.B. & KOZAK, K.H. (2016) Determinants of Range Limits in Montane Woodland Salamanders (Genus Plethodon). *https://doi.org/10.1643/OT-14-222* **104**, 101–110. The American Society of Ichthyologists and Herpetologists.

LYYTINEN, A., BRAKEFIELD, P.M., LINDSTRÖM, L. & MAPPES, J. (2004) Does predation maintain eyespot plasticity in Bicyclus anynana? *Proceedings of the Royal Society of London. Series B: Biological Sciences* **271**, 279–283. Royal Society.

MAC NALLY, R., BOWEN, M., HOWES, A., MCALPINE, C.A. & MARON, M. (2012) Despotic, high-impact species and the subcontinental scale control of avian assemblage structure. *Ecology* **93**, 668–678. John Wiley & Sons, Ltd.

MACARTHUR, R.H. (1958) Population Ecology of Some Warblers of Northeastern Coniferous Forests. *Ecology* **39**, 599–619.

MAGGS, C.A., CASTILHO, R., FOLTZ, D., HENZLER, C., JOLLY, M.T., KELLY, J., OLSEN, J., PEREZ, K.E., STAM, W., VÄINÖLÄ, R., VIARD, F. & WARES, J. (2008) Evaluating signatures of glacial refugia for north atlantic benthic marine taxa. *Ecology* **89**, S108–S122. Wiley-Blackwell.

MAGUIRE, K.C., NIETO-LUGILDE, D., BLOIS, J.L., FITZPATRICK, M.C., WILLIAMS, J.W., FERRIER, S. & LORENZ, D.J. (2016) Controlled comparison of species- and community-level models across novel climates and communities. *Proceedings of the Royal Society B: Biological Sciences* **283**, 20152817. Royal Society.

MAGUIRE, K.C., NIETO-LUGILDE, D., FITZPATRICK, M.C., WILLIAMS, J.W. & BLOIS, J.L. (2015) Modeling Species and Community Responses to Past, Present, and Future Episodes of Climatic and Ecological Change. *Annual Review of Ecology, Evolution, and Systematics* **46**, 343–368. Annual Reviews.

MAIR, L., HILL, J.K., FOX, R., BOTHAM, M., BRERETON, T. & THOMAS, C.D. (2014) Abundance changes and habitat availability drive species' responses to climate change. *Nature Climate Change* **4**, 127–131. Nature Publishing Group.

MALDONADO-COELHO, M., MARINI, M.Â., DO AMARAL, F.R. & RIBON, R. (2017) The invasive species rules: competitive exclusion in forest avian mixed-species flocks in a fragmented landscape. *Revista Brasileira de Ornitologia 2017 25:1* **25**, 54–59. Springer.

MANNI, M., BERKELEY, M.R., SEPPEY, M., SIMÃO, F.A. & ZDOBNOV, E.M. (2021) BUSCO Update: Novel and Streamlined Workflows along with Broader and Deeper Phylogenetic Coverage for Scoring of Eukaryotic, Prokaryotic, and Viral Genomes. *Molecular Biology and Evolution* **38**, 4647–4654.

MARÇAIS, G. & KINGSFORD, C. (2011) A fast, lock-free approach for efficient parallel counting of occurrences of k-mers. *Bioinformatics* **27**, 764–770.

MARTIN, P.R. & BONIER, F. (2018) Species interactions limit the occurrence of urban-adapted birds in cities. *Proceedings of the National Academy of Sciences of the United States of America* **115**, E11495–E11504.

MARTIN, P.R., BURKE, K.W. & BONIER, F. (2021) Plasticity versus Evolutionary Divergence: What Causes Habitat Partitioning in Urban-Adapted Birds? *The American Naturalist* **197**, 60–74. The University of Chicago Press.

MASON, T.H., APOLLONIO, M., CHIRICHELLA, R., WILLIS, S.G. & STEPHENS, P.A. (2014) Environmental change and long-term body mass declines in an alpine mammal. *Frontiers in Zoology* **11**, 69.

MATUTE, D.R. & COOPER, B.S. (2021) Comparative studies on speciation: 30 years since Coyne and Orr. *Evolution* **75**, 764–778.

MCEACHIN, S., DRURY, J.P., ANDERSON, C.N. & GRETHER, G.F. (2022) Mechanisms of reduced interspecific interference between territorial species. *Behavioral Ecology* **33**, 126–136.

MCLAIN, D.K. & SHURE, D.J. (1987) Pseudocompetition: Interspecific Displacement of Insect Species through Misdirected Courtship. *Oikos* **49**, 291–296. [Nordic Society Oikos, Wiley].

MCPEEK, M.A. & BROWN, J.M. (2000) Building a Regional Species Pool: Diversification of the Enallagma Damselflies in Eastern North America. *Ecology* **81**, 904–920.

MCQUILLAN, M.A. & RICE, A.M. (2015) Differential effects of climate and species interactions on range limits at a hybrid zone: potential direct and indirect impacts of climate change. *Ecology and Evolution* **5**, 5120–5137. Wiley Online Library.

MIKAMI, O.K. & KAWATA, M. (2004) Does interspecific territoriality reflect the intensity of ecological interactions? a theoretical model for interspecific territoriality. *Evolutionary Ecology Research* **6**, 765–775. Evolutionary Ecology, Ltd.

MIKHEENKO, A., PRJIBELSKI, A., SAVELIEV, V., ANTIPOV, D. & GUREVICH, A. (2018) Versatile genome assembly evaluation with QUAST-LG. *Bioinformatics* **34**, i142–i150.

MIKKELSEN, E.K. & IRWIN, D. (2021) Ongoing production of low-fitness hybrids limits range overlap between divergent cryptic species. *Molecular Ecology* **30**, 4090–4102.

MILLS, L.S., BRAGINA, E.V., KUMAR, A.V., ZIMOVA, M., LAFFERTY, D.J.R., FELTNER, J., DAVIS, B.M., HACKLÄNDER, K., ALVES, P.C., GOOD, J.M., MELO-FERREIRA, J., DIETZ, A., ABRAMOV, A.V., LOPATINA, N. & FAY, K. (2018) Winter color polymorphisms identify global hot spots for evolutionary rescue from climate change. *Science* **359**, 1033–1036.

MILLS, L.S., ZIMOVA, M., OYLER, J., RUNNING, S., ABATZOGLOU, J.T. & LUKACS, P.M. (2013) Camouflage mismatch in seasonal coat color due to decreased snow duration. *Proceedings of the National Academy of Sciences* **110**, 7360–7365. Proceedings of the National Academy of Sciences.

MISOF, B., LIU, S., MEUSEMANN, K., PETERS, R.S., DONATH, A., MAYER, C., FRANDSEN, P.B., WARE, J., FLOURI, T., BEUTEL, R.G., NIEHUIS, O., PETERSEN, M., IZQUIERDO-CARRASCO, F., WAPPLER, T., RUST, J., ET AL. (2014) Phylogenomics resolves the timing and pattern of insect evolution. *Science* **346**, 763–767. American Association for the Advancement of Science.

MOCZEK, A.P. (2010) Phenotypic plasticity and diversity in insects. *Philosophical Transactions of the Royal Society B: Biological Sciences* **365**, 593–603.

MORAN, E.V. & ALEXANDER, J.M. (2014) Evolutionary responses to global change: lessons from invasive species. *Ecology Letters* **17**, 637–649.

MOTTL, O., YOMBAI, J., NOVOTNÝ, V., LEPONCE, M., WEIBLEN, G.D. & KLIMEŠ, P. (2021) Inter-specific aggression generates ant mosaics in canopies of primary tropical rainforest. *Oikos* **130**, 1087–1099.

MURREN, C.J., AULD, J.R., CALLAHAN, H., GHALAMBOR, C.K., HANDELSMAN, C.A., HESKEL, M.A., KINGSOLVER, J.G., MACLEAN, H.J., MASEL, J., MAUGHAN, H., PFENNIG, D.W., RELYEA, R.A., SEITER, S., SNELL-ROOD, E., STEINER, U.K., ET AL. (2015) Constraints on the evolution of phenotypic plasticity: limits and costs of phenotype and plasticity. *Heredity* **115**, 293–301. Nature Publishing Group.

NASCI, R.S., HARE, S.G. & WILLIS, F.S. (1989) Interspecific mating between Louisiana strains of Aedes albopictus and Aedes aegypti in the field and laboratory. *Journal of the American Mosquito Control Association* **5**, 416–421.

NESBIT, D.A., COWEN, M.C., GRETHER, G.F. & DRURY, J.P. (2023) Interspecific territoriality has facilitated recent increases in the breeding habitat overlap of North American passerines. *Ecography* **2023**, e06573.

NISHIDA, T., TAKAKURA, K. & IWAO, K. (2015) Host specialization by reproductive interference between closely related herbivorous insects. *Population Ecology* **57**, 273–281. Springer.

NOVELLA-FERNANDEZ, R., JUSTE, J., IBÁÑEZ, C., REBELO, H., RUSSO, D., ALBERDI, A., KIEFER, A., GRAHAM, L., PAUL, H., DONCASTER, C.P. & RAZGOUR, O. (2021) Broad-scale patterns of geographic avoidance between species emerge in the

absence of fine-scale mechanisms of coexistence. *Diversity and Distributions* **27**, 1606–1618. John Wiley & Sons, Ltd.

OCKENDON, N., BAKER, D.J., CARR, J.A., WHITE, E.C., ALMOND, R.E.A., AMANO, T., BERTRAM, E., BRADBURY, R.B., BRADLEY, C., BUTCHART, S.H.M., DOSWALD, N., FODEN, W., GILL, D.J.C., GREEN, R.E., SUTHERLAND, W.J., ET AL. (2014) Mechanisms underpinning climatic impacts on natural populations: Altered species interactions are more important than direct effects. *Global Change Biology* **20**, 2221–2229. Wiley Online Library.

OKAMOTO, K.W. & GRETHER, G.F. (2013) The evolution of species recognition in competitive and mating contexts: the relative efficacy of alternative mechanisms of character displacement. *Ecology letters* **16**, 670–678.

ORIANS, G. & WILLSON, M. (1964) Interspecific Territories of Birds. *Ecology* **45**, 736–745.

ORTEGO, J. & KNOWLES, L.L. (2020) Incorporating interspecific interactions into phylogeographic models: A case study with Californian oaks. *Molecular Ecology* **29**, 4510–4524. Wiley Online Library.

PAINE, R.T. (1966) Food web complexity and species diversity. *The American Naturalist* **100**, 65–75. Science Press.

PARADIS, E. & SCHLIEP, K. (2019) ape 5.0: an environment for modern phylogenetics and evolutionary analyses in R. *Bioinformatics* **35**, 526–528.

PARMESAN, C., RYRHOLM, N., STEFANESCU, C., HILL, J.K., THOMAS, C.D., DESCIMON, H., HUNTLEY, B., KAILA, L., KULLBERG, J., TAMMARU, T., TENNENT, W.J., THOMAS, J.A. & WARREN, M. (1999) Poleward shifts in geographical ranges of butterfly species associated with regional warming. *Nature* **399**, 579–583. Nature Publishing Group.

PARMESAN, C. & YOHE, G. (2003) A globally coherent fingerprint of climate change impacts across natural systems. *Nature* **421**, 37–42. Nature Publishing Group.

PASCH, B., BOLKER, B.M. & PHELPS, S.M. (2013) Interspecific dominance via vocal interactions mediates altitudinal zonation in neotropical singing mice. *American Naturalist* **182**.

PATTERSON, C.W., BONILLAS-MONGE, E., BRENNAN, A., GRETHER, G.F., MENDOZA-CUENCA, L., TUCKER, R., VEGA-SÁNCHEZ, Y.M. & DRURY, J. (2023) A chromosome-level genome assembly for the smoky rubyspot damselfly (Hetaerina titia). *Journal of Heredity*, esad070.

PATTERSON, C.W. & DRURY, J.P. (2023) Interspecific behavioural interference and range dynamics: current insights and future directions. *Biological Reviews* **98**, 2012–2027.

PAULSON, D. (2011) *Dragonflies and Damselflies of the East*. Princeton University Press.

PAYNE, R.B. (1980) Behavior and Songs of Hybrid Parasitic Finches. *The Auk* **97**, 118–134.

PEARSON, S.F. (2000) Behavioral asymmetries in a moving hybrid zone. *Behavioral Ecology* **11**, 84–92.

PEARSON, S.F. & ROHWER, S. (2000) Asymmetries in male aggression across an avian hybrid zone. *Behavioral Ecology* **11**, 93–101.

PEBESMA, E. (2018) Simple Features for R: Standardized Support for Spatial Vector Data. *The R Journal* **10**, 439–446.

PEIMAN, K.S. & ROBINSON, B.W. (2010) Ecology and evolution of resource-related heterospecific aggression. *Quarterly Review of Biology* **85**, 133–158.

PERDEREAU, E., DEDEINE, F., CHRISTIDÈS, J.-P., DUPONT, S. & BAGNÈRES, A.-G. (2011) Competition between invasive and indigenous species: an insular case study of subterranean termites. *Biological Invasions* **13**, 1457–1470.

PEREIRA, P.F., LOURENÇO, R. & MOTA, P.G. (2020) Two songbird species show subordinate responses to simulated territorial intrusions of an exotic competitor. *Acta Ethologica* **23**, 143–154. acta ethologica.

PEREIRA, R.J., MARTÍNEZ-SOLANO, I. & BUCKLEY, D. (2016) Hybridization during altitudinal range shifts: nuclear introgression leads to extensive cyto-nuclear discordance in the fire salamander. *Molecular Ecology* **25**, 1551–1565. John Wiley & Sons, Ltd.

PESSINO, M., CHABOT, E.T., GIORDANO, R. & DEWALT, R.E. (2014) Refugia and postglacial expansion of Acroneuria frisoni Stark & Brown (Plecoptera:Perlidae) in North America. *Freshwater Science* **33**, 232–249. [The University of Chicago Press, Society for Freshwater Science].

PETER, B.M. & SLATKIN, M. (2013) Detecting range expansions from genetic data. *Evolution* **67**, 3274–3289.

PETERSON, B.K., WEBER, J.N., KAY, E.H., FISHER, H.S. & HOEKSTRA, H.E. (2012) Double Digest RADseq: An Inexpensive Method for De Novo SNP Discovery and Genotyping in Model and Non-Model Species. *PLOS ONE* **7**, 1–11. Public Library of Science.

PETKOVA, D., NOVEMBRE, J. & STEPHENS, M. (2015) Visualizing spatial population structure with estimated effective migration surfaces. *Nature Genetics* **48**, 94–100. Nature Publishing Group.

PETREN, K., BOLGER, D.T. & CASE, T.J. (1993) Mechanisms in the Competitive Success of an Invading Sexual Gecko over an Asexual Native. *Science* **259**, 354–358. American Association for the Advancement of Science.

PFENNIG, D.W. & PFENNIG, K.S. (2012) *Evolution's Wedge: Competition and the Origins of Diversity*. University of California Press.

PFENNIG, K.S. & PFENNIG, D.W. (2009) Character displacement: ecological and reproductive responses to a common evolutionary problem. *Quarterly Review of Biology* **84**, 253–276.

PICHLER, M. & HARTIG, F. (2021) A new joint species distribution model for faster and more accurate inference of species associations from big community data. *Methods in Ecology and Evolution* **12**, 2159–2173.

POGGIATO, G., MÜNKEMÜLLER, T., BYSTROVA, D., ARBEL, J., CLARK, J.S. & THUILLER, W. (2021) On the Interpretations of Joint Modeling in Community Ecology. *Trends in Ecology & Evolution* **36**, 391–401. Elsevier Current Trends.

POLOCZANSKA, E.S., BURROWS, M.T., BROWN, C.J., MOLINOS, J.G., HALPERN, B.S., HOEGH-GULDBERG, O., KAPPEL, C.V., MOORE, P.J., RICHARDSON, A.J., SCHOEMAN, D.S. & SYDEMAN, W.J. (2016) Responses of marine organisms to climate change across oceans. *Frontiers in Marine Science* **3**, 62. Frontiers Media S. A.

PRATES, I., PENNA, A., RODRIGUES, M.T. & CARNAVAL, A.C. (2018) Local adaptation in mainland anole lizards: Integrating population history and genome–environment associations. *Ecology and Evolution* **8**, 11932–11944.

PRICE, B. & ALLAN, E. (2023) The genome sequence of the White-legged damselfly, Platycnemis pennipes (Pallas, 1771) [version 1; peer review: awaiting peer review]. *Wellcome Open Research* **8**.

PRICE, B., WINTER, M. & BROOKS, S. (2022) The genome sequence of the blue-tailed damselfly, Ischnura elegans (Vander Linden, 1820). *Wellcome Open Research* **7**.

PUTNAM, N.H., O'CONNELL, B.L., STITES, J.C., RICE, B.J., BLANCHETTE, M., CALEF, R., TROLL, C.J., FIELDS, A., HARTLEY, P.D., SUGNET, C.W., HAUSSLER, D., ROKHSAR, D.S. & GREEN, R.E. (2016) Chromosome-scale shotgun assembly using an in vitro method for long-range linkage. *Genome Research* **26**, 342–350.

QUINTERO, I., LANDIS, M.J. & HAHN, M. (2020) Interdependent Phenotypic and Biogeographic Evolution Driven by Biotic Interactions. *Systematic Biology* **69**, 739–755. Oxford University Press.

RAINFORD, J.L., HOFREITER, M., NICHOLSON, D.B. & MAYHEW, P.J. (2014) Phylogenetic Distribution of Extant Richness Suggests Metamorphosis Is a Key Innovation Driving Diversification in Insects. *PLOS ONE* **9**, e109085. Public Library of Science.

RANALLO-BENAVIDEZ, T.R., JARON, K.S. & SCHATZ, M.C. (2020) GenomeScope 2.0 and Smudgeplot for reference-free profiling of polyploid genomes. *Nature Communications* **11**, 1432.

RAVINET, M., FARIA, R., BUTLIN, R.K., GALINDO, J., BIERNE, N., RAFAJLOVIĆ, M., NOOR, M. A. F., MEHLIG, B. & WESTRAM, A.M. (2017) Interpreting the genomic landscape of speciation: a road map for finding barriers to gene flow. *Journal of Evolutionary Biology* **30**, 1450–1477.

REAZ, R., BAYZID, M.S. & RAHMAN, M.S. (2014) Accurate Phylogenetic Tree Reconstruction from Quartets: A Heuristic Approach. *PLOS ONE* **9**, e104008. Public Library of Science.

REHFELDT, G. (1992) Impact of predation by spiders on a territorial damselfly (Odonata: Calopterygidae). *Oecologia* **89**, 550–556.

REIF, J., JIRAN, M., REIFOVÁ, R., VOKURKOVÁ, J., DOLATA, P.T., PETRUSEK, A. & PETRUSKOVÁ, T. (2015) Interspecific territoriality in two songbird species: potential role of song convergence in male aggressive interactions. *Animal Behaviour* **104**, 131–136.

REIF, J., REIFOVÁ, R., SKORACKA, A. & KUCZYŃSKI, L. (2018) Competition-driven niche segregation on a landscape scale: Evidence for escaping from syntopy towards allotopy in two coexisting sibling passerine species. *Journal of Animal Ecology* **87**, 774–789.

REIMCHEN, T.E. (1994) Predators and Morphological Evolution in Threespine Stickleback. In *The Evolutionary Biology of the Threespine Stickleback* (eds M.A. BELL & S. A. FOSTER), p. 0. Oxford University Press.

RELYEA, R.A., STEPHENS, P.R., BARROW, L.N., BLAUSTEIN, A.R., BRADLEY, P.W., BUCK, J.C., CHANG, A., COLLINS, J.P., CROTHER, B., EARL, J., GERVASI, S.S., HOVERMAN, J.T., HYMAN, O., LEMMON, E.M., LUHRING, T.M., ET AL. (2018) Phylogenetic patterns of trait and trait plasticity evolution: Insights from amphibian embryos. *Evolution* **72**, 663–678.

RELYEA, R.A., STEPHENS, P.R. & HAMMOND, J.I. (2021) Phylogenetic patterns of trait and trait plasticity evolution: Insights from tadpoles. *Evolution* **75**, 2568–2588.

RIBEIRO, J.M.C. & SPIELMAN, A. (1986) The satyr effect: A model predicting parapatry and species extinction. *American Naturalist* **128**, 513–528. University of Chicago Press.

ROBINSON, D. (1992) Habitat use and foraging behaviour of the scarlet robin and the flame robin at a site of breeding-season sympatry. *Wildlife Research* **19**, 377–395.

ROCHA, J., SILVA, P., SANTOS, N., NAKAMURA, M., AFONSO, S., QNINBA, A., BORATYNSKI, Z., SUDMANT, P.H., BRITO, J.C., NIELSEN, R. & GODINHO, R. (2023) North African fox genomes show signatures of repeated introgression and adaptation to life in deserts. *Nature Ecology & Evolution* **7**, 1267–1286. Nature Publishing Group.

ROLANDO, A. & PALESTRINI, C. (1989) Habitat selection and interspecific territoriality in sympatric warblers at two Italian marshland areas. *Ethology Ecology & Evolution* **1**, 169–183. Taylor & Francis.

RONQUIST, F. (2011) Phylogenetic methods in historical biogeography. *Annual Review of Ecology, Evolution, and Systematics* **42**, 441–464. Annual Reviews.

ROSENBERG, K.V., DOKTER, A.M., BLANCHER, P.J., SAUER, J.R., SMITH, A.C., SMITH, P.A., STANTON, J.C., PANJABI, A., HELFT, L., PARR, M. & MARRA, P.P. (2019)

Decline of the North American avifauna. *Science* **366**, 120–124. American Association for the Advancement of Science.

ROWLES, A.D. & O'DOWD, D.J. (2007) Interference competition by Argentine ants displaces native ants: Implications for biotic resistance to invasion. *Biological Invasions* **9**, 73–85. Springer.

RUNDELL, R.J. & PRICE, T.D. (2009) Adaptive radiation, nonadaptive radiation, ecological speciation and nonecological speciation. *Trends in Ecology & Evolution* **24**, 394–399.

RUOKOLAINEN, L. & HANSKI, I. (2016) Stable coexistence of ecologically identical species: Caonspecific aggregation via reproductive interference. *Journal of Animal Ecology* **85**, 638–647. Wiley Online Library.

RYBINSKI, J., SIRKIÄ, P.M., MCFARLANE, S.E., VALLIN, N., WHEATCROFT, D., ÅLUND, M. & QVARNSTRÖM, A. (2016) Competition-driven build-up of habitat isolation and selection favoring modified dispersal patterns in a young avian hybrid zone. *Evolution* **70**, 2226–2238.

SÁNCHEZ-GUILLÉN, R.A., CÓRDOBA-AGUILAR, A., CORDERO-RIVERA, A. & WELLENREUTHER, M. (2014) Genetic divergence predicts reproductive isolation in damselflies. *Journal of Evolutionary Biology* **27**, 76–87.

SÁNCHEZ-GUILLÉN, R.A., VAN GOSSUM, H. & CORDERO RIVERA, A. (2005) Hybridization and the inheritance of female colour polymorphism in two ischnurid damselflies (Odonata: Coenagrionidae). *Biological Journal of the Linnean Society* **85**, 471–481.

SÁNCHEZ-HERRERA, M., BEATTY, C.D., NUNES, R., SALAZAR, C. & WARE, J.L. (2020) An exploration of the complex biogeographical history of the Neotropical banner-wing damselflies (Odonata: Polythoridae). *BMC Evolutionary Biology* **20**, 74.

SANCHEZ-HERRERA, M., VEGA-SÁNCHEZ, Y.M., BEATTY, C. & KOHLI, M. (2022) Phylogeography: A spatiotemporal perspective on Odonata distributions. In *Dragonflies and Damselflies: Model Organisms for Ecological and Evolutionary Research* (eds A. CORDOBA-AGUILAR, C. BEATTY & J. BRIED), p. 0. Oxford University Press.

SAUNDERS, S.P., MEEHAN, T.D., MICHEL, N.L., BATEMAN, B.L., DELUCA, W., DEPPE, J.L., GRAND, J., LEBARON, G.S., TAYLOR, L., WESTERKAM, H., WU, J.X. & WILSEY, C.B. (2022) Unraveling a century of global change impacts on winter bird distributions in the eastern United States. *Global Change Biology* **28**, 2221–2235. Wiley Online Library.

SAVIDGE, J.A. (1987) Extinction of an island forest avifauna by an introduced snake. *Ecology* **68**, 660–668. Wiley Online Library.

SCHLUTER, D. (2000) *The Ecology of Adaptive Radiation*. OUP Oxford.

SCHNEIDER, C.A., RASBAND, W.S. & ELICEIRI, K.W. (2012) NIH Image to ImageJ: 25 years of image analysis. *Nature Methods* **9**, 671–675.

SEKERCIOGLU, C.H., SCHNEIDER, S.H., FAY, J.P. & LOARIE, S.R. (2008) Climate change, elevational range shifts, and bird extinctions. *Conservation Biology* **22**, 140–150. John Wiley & Sons, Ltd.

SHAFFER, H.B., TOFFELMIER, E., CORBETT-DETIG, R.B., ESCALONA, M., ERICKSON, B., FIEDLER, P., GOLD, M., HARRIGAN, R.J., HODGES, S., LUCKAU, T.K., MILLER, C., OLIVEIRA, D.R., SHAFFER, K.E., SHAPIRO, B., SORK, V.L., ET AL. (2022) Landscape Genomics to Enable Conservation Actions: The California Conservation Genomics Project. *The Journal of Heredity* **113**, 577–588.

SHAPIRO, A.M. (1976) Seasonal polyphenism. *Evolutionary Biology* **9**, 259–333.

SHERRATT, E., SANDERS, K.L., WATSON, A., HUTCHINSON, M.N., LEE, M.S.Y. & PALCI, A. (2019) Heterochronic shifts mediate ecomorphological convergence in skull shape of microcephalic sea snakes. *Integrative and Comparative Biology* **59**, 616–624.

SILVERTOWN, J., COOK, L., CAMERON, R., DODD, M., MCCONWAY, K., WORTHINGTON, J., SKELTON, P., ANTON, C., BOSSDORF, O., BAUR, B., SCHILTHUIZEN, M., FONTAINE, B., SATTMANN, H., BERTORELLE, G., CORREIA, M., ET AL. (2011) Citizen Science Reveals Unexpected Continental-Scale Evolutionary Change in a Model Organism. *PLOS ONE* **6**, e18927. Public Library of Science.

SIM, S.B., CORPUZ, R.L., SIMMONDS, T.J. & GEIB, S.M. (2022) HiFiAdapterFilt, a memory efficient read processing pipeline, prevents occurrence of adapter sequence in PacBio HiFi reads and their negative impacts on genome assembly. *BMC Genomics* **23**, 157.

SIMÃO, F.A., WATERHOUSE, R.M., IOANNIDIS, P., KRIVENTSEVA, E.V. & ZDOBNOV, E.M. (2015) BUSCO: assessing genome assembly and annotation completeness with single-copy orthologs. *Bioinformatics* **31**, 3210–3212. Oxford Academic.

SIMPSON, S.J., SWORD, G.A. & LO, N. (2011) Polyphenism in Insects. *Current Biology* **21**, R738–R749.

SIRÉN, A.P.K. & MORELLI, T.L. (2020) Interactive range-limit theory (iRLT): An extension for predicting range shifts. *Journal of Animal Ecology* **89**, 940–954. Blackwell Publishing Ltd.

SMITH, M.L. & CARSTENS, B.C. (2020) Process-based species delimitation leads to identification of more biologically relevant species. *Evolution* **74**, 216–229.

SNELL-ROOD, E.C., CASH, A., HAN, M.V., KIJIMOTO, T., ANDREWS, J. & MOCZEK, A.P. (2011) Developmental decoupling of alternative phenotypes: insights from the transcriptomes of horn-polyphenic beetles. *Evolution* **65**, 231–245.

SOBROZA, T.V., GORDO, M., BARNETT, A.P.A., BOUBLI, J.P. & SPIRONELLO, W.R. (2021) Parapatric pied and red-handed tamarin responses to congeneric and conspecific calls. *Acta Oecologica* **110**, 103688. Elsevier Masson.

SÖDERBÄCK, B. (1994) Interactions among Juveniles of Two Freshwater Crayfish Species and a Predatory Fish. *Oecologia* **100**, 229–235. Springer.

SÖDERBÄCK, B. (1995) Replacement of the native crayfish Astacus-astacus by the introduced species Pacifastacus leniusculus in a Swedish lake - possible causes and mechanisms. *Freshwater Biology* **33**, 291–304. BLACKWELL SCIENCE LTD.

SONG, H., FOQUET, B., MARIÑO-PÉREZ, R. & WOLLER, D.A. (2017) Phylogeny of locusts and grasshoppers reveals complex evolution of density-dependent phenotypic plasticity. *Scientific Reports* **7**, 6606. Nature Publishing Group.

SORJONEN, J. (1986) Mixed Singing and Interspecific Territoriality - Consequences of Secondary Contact of Two Ecologically and Morphologically Similar Nightingale Species in Europe. *Ornis Scandinavica (Scandinavian Journal of Ornithology)* **17**, 53–67. [Nordic Society Oikos, Wiley].

STAMATAKIS, A. (2014) RAxML version 8: A tool for phylogenetic analysis and post-analysis of large phylogenies. *Bioinformatics* **30**. Oxford Academic.

STANDRING, S., SÁNCHEZ-HERRERA, M., GUILLERMO-FERREIRA, R., WARE, J.L., VEGA-SÁNCHEZ, Y.M., CLEMENT, R., DRURY, J.P., GRETHER, G.F., GONZÁLEZ-RODRÍGUEZ, A., MENDOZA-CUENCA, L., BOTA-SIERRA, C.A. & BYBEE, S. (2022) Evolution and Biogeographic History of Rubyspot Damselflies (Hetaerininae: Calopterygidae: Odonata). *Diversity* **14**.

STELKENS, R.B., SCHMID, C. & SEEHAUSEN, O. (2015) Hybrid Breakdown in Cichlid Fish. *PLOS ONE* **10**, e0127207. Public Library of Science.

STILLER, J., DA FONSECA, R.R., ALFARO, M.E., FAIRCLOTH, B.C., WILSON, N.G. & ROUSE, G.W. (2021) Using ultraconserved elements to track the influence of sea-level change on leafy seadragon populations. *Molecular Ecology* **30**, 1364–1380.

STRUCK, T.H., FEDER, J.L., BENDIKSBY, M., BIRKELAND, S., CERCA, J., GUSAROV, V.I., KISTENICH, S., LARSSON, K.-H., LIOW, L.H., NOWAK, M.D., STEDJE, B., BACHMANN, L. & DIMITROV, D. (2018) Finding Evolutionary Processes Hidden in Cryptic Species. *Trends in Ecology & Evolution* **33**, 153–163.

SUHLING, F., SAHLÉN, G., GORB, S., KALKMAN, V.J., DIJKSTRA, K.-D.B. & TOL, J. VAN (2015) Chapter 35 - Order Odonata. In *Thorp and Covich's Freshwater Invertebrates (Fourth Edition)* (eds J.H. THORP & D.C. ROGERS), pp. 893–932Fourth Edition. Academic Press, Boston.

SUKUMARAN, J. & KNOWLES, L.L. (2018) Trait-Dependent Biogeography: (Re)Integrating Biology into Probabilistic Historical Biogeographical Models. *Trends in Ecology and Evolution* **33**, 390–398. Elsevier.

SUTHERST, R.W. (1987) The dynamics of hybrid zones between tick (Acari) species. *International Journal for Parasitology* **17**, 921–926.

SUWANVECHO, U. & BROCKELMAN, W.Y. (2012) Interspecific territoriality in gibbons (Hylobates lar and H. pileatus) and its effects on the dynamics of interspecies contact zones. *Primates; Journal of Primatology* **53**, 97–108.

SVÄRDSON, G., FÜRST, M. & FJÄLLING, A. (1991) Population resilience of Pacifastacus leniusculus in Sweden. *Finnish Fisheries Research* **12**, 165–177.

SVENNING, J.C., GRAVEL, D., HOLT, R.D., SCHURR, F.M., THUILLER, W., MÜNKEMÜLLER, T., SCHIFFERS, K.H., DULLINGER, S., EDWARDS, T.C., HICKLER, T., HIGGINS, S.I., NABEL, J.E.M.S., PAGEL, J. & NORMAND, S. (2014) The influence of interspecific interactions on species range expansion rates. *Ecography* **37**, 1198–1209.

SVENSSON, E.I., EROUKHMANOFF, F., KARLSSON, K., RUNEMARK, A. & BRODIN, A. (2010) A Role for Learning in Population Divergence of Mate Preferences. *Evolution* **64**, 3101–3113.

SVENSSON, E.I., GÓMEZ-LLANO, M.A., TORRES, A.R. & BENSCH, H.M. (2018) Frequency Dependence and Ecological Drift Shape Coexistence of Species with Similar Niches. *The American Naturalist* **191**, 691–703. The University of Chicago Press.

SVENSSON, E.I., RUNEMARK, A., VERZIJDEN, M.N. & WELLENREUTHER, M. (2014) Sex differences in developmental plasticity and canalization shape population divergence in mate preferences. *Proceedings of the Royal Society B: Biological Sciences* **281**, 20141636. Royal Society.

TAKAKURA, K.-I., NISHIDA, T. & IWAO, K. (2015) Conflicting intersexual mate choices maintain interspecific sexual interactions. *Population Ecology* **57**, 261–271.

TAKAMI, T., YOSHIHARA, T., MIYAKOSHI, Y. & KUWABARA, R. (2002) Replacement of white-spotted charr Salvelinus leucomaenis by brown trout Salmo trutta in a branch of the Chitose River, Hokkaido [Japan]. *Bulletin of the Japanese Society of Scientific Fisheries (Japan)* **68**, 24–28.

THE DARWIN TREE OF LIFE PROJECT CONSORTIUM (2022) Sequence locally, think globally: The Darwin Tree of Life Project. *Proceedings of the National Academy of Sciences* **119**, e2115642118. Proceedings of the National Academy of Sciences.

THOMAS, C.D. (2010) Climate, climate change and range boundaries. *Diversity and Distributions* **16**, 488–495. Wiley/Blackwell (10.1111).

THOMAS, J.A., TRUEMAN, J.W.H., RAMBAUT, A. & WELCH, J.J. (2013) Relaxed Phylogenetics and the Palaeoptera Problem: Resolving Deep Ancestral Splits in the Insect Phylogeny. *Systematic Biology* **62**, 285–297.

THORSON, J.T., PINSKY, M.L. & WARD, E.J. (2016) Model-based inference for estimating shifts in species distribution, area occupied and centre of gravity. *Methods in Ecology and Evolution* **7**, 990–1002.

THUM, R.A. (2007) Reproductive interference, priority effects and the maintenance of parapatry in Skistodiaptomus copepods. *Oikos* **116**, 759–768. Blackwell Publishing Ltd.

TIKHONOV, G., ABREGO, N., DUNSON, D. & OVASKAINEN, O. (2017) Using joint species distribution models for evaluating how species-to-species associations depend on the environmental context. *Methods in Ecology and Evolution* **8**, 443–452. John Wiley & Sons, Ltd.

TITLEY, M.A., BUTCHART, S.H., JONES, V.R., WHITTINGHAM, M.J. & WILLIS, S.G. (2021) Global inequities and political borders challenge nature conservation under climate change. *Proceedings of the National Academy of Sciences* **118**, e2011204118. National Acad Sciences.

TOBIAS, J.A., OTTENBURGHS, J. & PIGOT, A.L. (2020) Avian Diversity: Speciation, Macroevolution, and Ecological Function. *Annual Review of Ecology, Evolution, and Systematics* **51**, 533–560.

TOLMAN, E.R., BEATTY, C.D., BUSH, J., KOHLI, M., MORENO, C.M., WARE, J.L., WEBER, K.S., KHAN, R., MAHESHWARI, C., WEISZ, D., DUDCHENKO, O., AIDEN, E.L. & FRANDSEN, P.B. (2023) A Chromosome-length Assembly of the Black Petaltail (Tanypteryx hageni) Dragonfly. *Genome Biology and Evolution* **15**, evad024.

TØNNESEN, M.H., PENZHORN, B.L., BRYSON, N.R., STOLTSZ, W.H. & MASIBIGIRI, T. (2004) Displacement of Boophilus decoloratus by Boophilus microplus in the Soutpansberg region, Limpopo Province, South Africa. *Experimental and Applied Acarology* **32**, 199–208. Exp Appl Acarol.

TRAVIS, J.M.J., DELGADO, M., BOCEDI, G., BAGUETTE, M., BARTOŃ, K., BONTE, D., BOULANGEAT, I., HODGSON, J.A., KUBISCH, A., PENTERIANI, V., SAASTAMOINEN, M., STEVENS, V.M. & BULLOCK, J.M. (2013) Dispersal and species' responses to climate change. *Oikos* **122**, 1532–1540. Wiley/Blackwell (10.1111).

TROMBULAK, S.C. (1985) The Influence of Interspecific Competition on Home Range Size in Chipmunks (Eutamias). *Journal of Mammalogy* **66**, 329–337.

TSUCHIDA, K., YAMAGUCHI, A., KANBE, Y. & GOKA, K. (2019) Reproductive interference in an introduced bumblebee: Polyandry may mitigate negative reproductive impact. *Insects* **10**, 59. MDPI AG.

TSURUI-SATO, K., FUJIMOTO, S., DEKI, O., SUZUKI, T., TATSUTA, H. & TSUJI, K. (2019) Reproductive interference in live-bearing fish: the male guppy is a potential biological agent for eradicating invasive mosquitofish. *Scientific Reports 2019 9:1* **9**, 1–9. Nature Publishing Group.

TURGEON, J. & MCPEEK, M.A. (2002) Phylogeographic analysis of a recent radiation of Enallagma damselflies (Odonata: Coenagrionidae). *Molecular Ecology* **11**, 1989–2001.

ULIANO-SILVA, M., FERREIRA, J.G.R.N., KRASHENINNIKOVA, K., BLAXTER, M., MIESZKOWSKA, N., HALL, N., HOLLAND, P., DURBIN, R., RICHARDS, T., KERSEY, P., HOLLINGSWORTH, P., WILSON, W., TWYFORD, A., GAYA, E., LAWNICZAK, M., ET AL. (2023) MitoHiFi: a python pipeline for mitochondrial genome assembly from PacBio high fidelity reads. *BMC Bioinformatics* **24**, 288.

VAN DER VALK, T., PEČNEROVÁ, P., DÍEZ-DEL-MOLINO, D., BERGSTRÖM, A., OPPENHEIMER, J., HARTMANN, S., XENIKOUDAKIS, G., THOMAS, J.A., DEHASQUE, M., SAĞLICAN, E., FIDAN, F.R., BARNES, I., LIU, S., SOMEL, M., HEINTZMAN, P.D., ET AL. (2021) Million-year-old DNA sheds light on the genomic history of mammoths. *Nature* **591**, 265–269. Nature Publishing Group.

VALLIN, N., RICE, A.M., ARNTSEN, H., KULMA, K. & QVARNSTRÖM, A. (2012) Combined effects of interspecific competition and hybridization impede local coexistence of Ficedula flycatchers. *Evolutionary Ecology* **26**, 927–942.

VAN BELLEGHEM, S.M., PAPA, R., ORTIZ-ZUAZAGA, H., HENDRICKX, F., JIGGINS, C.D., OWEN MCMILLAN, W. & COUNTERMAN, B.A. (2018) patternize: An R package for quantifying colour pattern variation. *Methods in Ecology and Evolution* **9**, 390–398.

VAN LANEN, N.J., FRANKLIN, A.B., HUYVAERT, K.P., REISER, R.F. & CARLSON, P.C. (2011) Who hits and hoots at whom? Potential for interference competition between barred and northern spotted owls. *Biological Conservation* **144**, 2194–2201.

VEGA-SÁNCHEZ, Y.M., MENDOZA-CUENCA, L.F. & GONZÁLEZ-RODRÍGUEZ, A. (2020) Hetaerina calverti (Odonata: Zygoptera: Calopterygidae) sp. nov., a new cryptic species of the American Rubyspot complex. *Zootaxa* **4766**, zootaxa.4766.3.7.

VEGA-SÁNCHEZ, Y.M., OYAMA, K., MENDOZA-CUENCA, L.F., GAYTÁN-LEGARIA, R. & GONZÁLEZ-RODRÍGUEZ, A. (2024) Genomic differentiation and niche divergence in the Hetaerina americana (Odonata) cryptic species complex. *Molecular Ecology* **33**, e17207.

WANG, P., CROWDER, D.W. & LIU, S.S. (2012) Roles of mating behavioural interactions and life history traits in the competition between alien and indigenous whiteflies. *Bulletin of Entomological Research* **102**, 395–405.

WANG, Y., CAO, Z., OGILVIE, H.A. & NAKHLEH, L. (2021) Phylogenomic assessment of the role of hybridization and introgression in trait evolution. *PLoS Genetics* **17**, e1009701.

WEIR, B.S. & COCKERHAM, C.C. (1984) Estimating F-Statistics for the Analysis of Population Structure. *Evolution* **38**, 1358–1370. Oxford University Press.

WELLENREUTHER, M. & SÁNCHEZ-GUILLÉN, R.A. (2016) Nonadaptive radiation in damselflies. *Evolutionary Applications* **9**, 103–118.

WELLER, H.I., HILLER, A.E., LORD, N.P. & VAN BELLEGHEM, S.M. (2024) recolorize: An R package for flexible colour segmentation of biological images. *Ecology Letters* **27**, e14378.

WENGER, A.M., PELUSO, P., ROWELL, W.J., CHANG, P.-C., HALL, R.J., CONCEPCION, G.T., EBLER, J., FUNGTAMMASAN, A., KOLESNIKOV, A., OLSON, N.D., TÖPFER, A., ALONGE, M., MAHMOUD, M., QIAN, Y., CHIN, C.-S., ET AL. (2019) Accurate circular consensus long-read sequencing improves variant detection and assembly of a human genome. *Nature Biotechnology* **37**, 1155–1162. Nature Publishing Group.

WESTMAN, K. & SAVOLAINEN, R. (2001) Long term study of competition between two co-occurring crayfish species, the native Astacus astacus l. And the introduced Pacifastacus leniusculus dana, in a Finnish lake. *Bulletin Français de la Pêche et de la Pisciculture*, 613–627. EDP Sciences.

WESTMAN, K., SAVOLAINEN, R. & JULKUNEN, M. (2002) Replacement of the native crayfish Astacus astacus by the introduced species Pacifastacus leniusculus in a small, enclosed Finnish lake: a 30-year study. *Ecography* **25**, 53–73. John Wiley & Sons, Ltd.

WESTRAM, A.M., STANKOWSKI, S., SURENDRANADH, P. & BARTON, N. (2022) What is reproductive isolation? *Journal of Evolutionary Biology* **35**, 1143–1164.

WHEAT, C.W. & WAHLBERG, N. (2013) Phylogenomic Insights into the Cambrian Explosion, the Colonization of Land and the Evolution of Flight in Arthropoda. *Systematic Biology* **62**, 93–109.

WIENS, J.D., ANTHONY, R.G. & FORSMAN, E.D. (2014) Competitive interactions and resource partitioning between northern spotted owls and barred owls in western Oregon. *Wildlife Monographs* **185**, 1–50.

WILEY, R.H. (1978) The Lek Mating System of the Sage Grouse. *Scientific American* **238**, 114–125. Scientific American, a division of Nature America, Inc.

WILGENBUSCH, J.C. & SWOFFORD, D. (2003) Inferring Evolutionary Trees with PAUP*. *Current Protocols in Bioinformatics* **00**, 6.4.1-6.4.28.

WILKINSON, D.P., GOLDING, N., GUILLERA-ARROITA, G., TINGLEY, R. & MCCARTHY, M.A. (2019) A comparison of joint species distribution models for presence–absence data. *Methods in Ecology and Evolution* **10**, 198–211. John Wiley & Sons, Ltd.

WILKINSON, D.P., GOLDING, N., GUILLERA-ARROITA, G., TINGLEY, R. & MCCARTHY, M.A. (2021) Defining and evaluating predictions of joint species distribution models. *Methods in Ecology and Evolution* **12**, 394–404. Wiley Online Library.

WILLIAMS, J.W. & JACKSON, S.T. (2007) Novel climates, no-analog communities, and ecological surprises. *Frontiers in Ecology and the Environment* **5**, 475–482.

WISZ, M.S., POTTIER, J., KISSLING, W.D., PELLISSIER, L., LENOIR, J., DAMGAARD, C.F., DORMANN, C.F., FORCHHAMMER, M.C., GRYTNES, J.A., GUISAN, A., HEIKKINEN, R.K., HØYE, T.T., KÜHN, I., LUOTO, M., MAIORANO, L., ET AL. (2013) The role of biotic interactions in shaping distributions and realised assemblages of species: Implications for species distribution modelling. *Biological Reviews* **88**, 15–30. John Wiley & Sons, Ltd.

WOOD, S.N. (2011) Fast stable restricted maximum likelihood and marginal likelihood estimation of semiparametric generalized linear models. *Journal of the Royal Statistical Society (B)* **73**, 3–36.

WU, Y., KIRILLOV, A., MASSA, F., LO, W.-Y. & GIRSHICK, R. (2019) Detectron2. https://github.com/facebookresearch/detectron2.

XIONG, T., TARIKERE, S., ROSSER, N., LI, X., YAGO, M. & MALLET, J. (2023) A polygenic explanation for Haldane's rule in butterflies. *Proceedings of the National Academy of Sciences* **120**, e2300959120. Proceedings of the National Academy of Sciences.

YAMANO, H., SUGIHARA, K. & NOMURA, K. (2011) Rapid poleward range expansion of tropical reef corals in response to rising sea surface temperatures. *Geophysical Research Letters* **38**.

ŽAGAR, A., CARRETERO, M.A., OSOJNIK, N., SILLERO, N. & VREZEC, A. (2015) A place in the sun: interspecific interference affects thermoregulation in coexisting lizards. *Behavioral Ecology and Sociobiology* **69**, 1127–1137. Springer Verlag.

ZALASIEWICZ, J. & WILLIAMS, M. (2021) 3 - Climate change through Earth history. In *Climate Change (Third Edition)* (ed T.M. LETCHER), pp. 49–65. Elsevier.

ZHANG, J., NAIK, H.S., ASSEFA, T., SARKAR, S., REDDY, R.V.C., SINGH, A., GANAPATHYSUBRAMANIAN, B. & SINGH, A.K. (2017) Computer vision and machine learning for robust phenotyping in genome-wide studies. *Scientific Reports* **7**, 44048. Nature Publishing Group.

ZHOU, J., LIU, S., LIU, H., XIE, Z., LIU, L., LIN, L., JIANG, J., YANG, M., ZHOU, G., GU, J., ZHOU, X., YAN, G., JAMES, A.A. & CHEN, X.-G. (2022) Interspecific mating bias may drive Aedes albopictus displacement of Aedes aegypti during its range expansion. *PNAS Nexus* **1**, pgac041.

ZOU, T., KUANG, W., YIN, T., FRANTZ, L., ZHANG, C., LIU, J., WU, H. & YU, L. (2022) Uncovering the enigmatic evolution of bears in greater depth: The hybrid origin of the Asiatic black bear. *Proceedings of the National Academy of Sciences* **119**, e2120307119. Proceedings of the National Academy of Sciences.